

Barren-ground caribou in a rapidly changing Arctic: Effects
of lake ice phenology and monitoring methods on
movement behaviour

Xavier Giroux-Bougard
Doctor of Philosophy

Department of Natural Resource Sciences
McGill University
Montréal, Québec, Canada

April, 2024

A thesis submitted to McGill University in partial
fulfillment of the requirements of the degree of
Doctor of Philosophy

© Xavier Giroux-Bougard, 2024

Table of contents

Table of contents	i
List of tables	iv
List of figures	v
List of abbreviations	x
Abstract	xii
Résumé	xiii
Acknowledgements	xv
Contribution to original knowledge	xvii
Contribution of authors	xxii
Chapter 1 - General introduction and literature review	1
1.1 General introduction	1
1.2 Literature review	4
1.2.1 What are migratory caribou?	4
1.2.2 Why do caribou migrate, and why are these migrations important?	6
1.2.3 What is the current status of migratory caribou herd populations?	8
1.2.4 Why are migratory caribou herds declining?	10
1.2.5 How can remote sensing contribute to caribou research?	16
1.2.6 How can remote sensing contribute to monitoring freshwater ice phenology?	21
1.2.7 How do we monitor caribou movement?	24
1.2.8 How can capture and collaring affect caribou movement and survival?	25
Chapter 2 - Multi-sensor detection of spring breakup phenology of Canada's lakes	29
2.0 Abstract	29
2.1 Introduction	30
2.2 Data	35
2.2.1 High-resolution optical imagery	35
2.2.2 Canadian Ice Service lake ice data	37
2.2.3 Water mask	38
2.2.4 HydroLAKES polygons	38
2.3 Methods	39
2.3.1 Training ice-water classifiers for OPEN-ICE	39
2.3.2 Implementing the OPEN-ICE algorithm	43
2.3.3 Evaluating the OPEN-ICE algorithm	47
2.3.4 Lake size and breakup timing across Canada	50
2.4 Results	51
2.4.1 Decision tree performance	51
2.4.2 Lake-based validation of breakup events	53

2.4.3 Lake-based validation of breakup profiles	54
2.4.4 Evaluating OPEN-ICE's temporal filter	56
2.4.5 Spatial coverage and resolution of OPEN-ICE	57
2.5 Discussion.....	59
2.5.1 Sensor-specific decision trees developed for OPEN-ICE.....	59
2.5.2 OPEN-ICE approach and quality assessment metrics	61
2.5.3 OPEN-ICE accuracy.....	63
2.5.4 OPEN-ICE data product resolution and coverage	65
2.5.5 Variation in lake breakup dates across Canada	68
2.6 Conclusion	72
2.7 Data availability	73
2.8 References.....	74
2.9 Linking statement.....	83
Chapter 3 - Lake ice phenology and the spring migration of barren-ground caribou (<i>Rangifer tarandus groenlandicus</i>) in a rapidly changing North.....	
3.0 Abstract	85
3.1 Introduction	86
3.2 Methods	90
3.2.1 Study area and caribou herds	90
3.2.2 Caribou migration telemetry data	91
3.2.3 Used-available migration paths	93
3.2.4 Environmental covariates	94
3.2.5 Path selection analysis.....	97
3.2.6 Migration duration	101
3.3 Results.....	102
3.3.1 Migration events.....	102
3.3.2 Timing of spring migration and breakup periods.....	105
3.3.3 Path selection analysis.....	106
3.3.4 Migration duration	110
3.4 Discussion.....	112
3.4.1 Small, ice-covered lakes are selected by migrating caribou but large, ice- covered lakes are avoided	113
3.4.2 Breaking ice is strongly avoided by migrating caribou and avoidance increases with lake size	116
3.4.3 Open water is avoided by migrating caribou but not as strongly as breaking ice	118
3.4.4 The ice phenology of small lakes and rivers.....	119
3.4.5 Ice phenology and the timing of spring migration	120
3.4.6 The connectivity of landscapes	123
3.5 Conclusion	124
3.6 References.....	125
3.7 Linking statement.....	134
Chapter 4 - Post-capture survival and movements of barren-ground caribou (<i>Rangifer tarandus groenlandicus</i>).....	
4.0 Abstract.....	136
4.1 Introduction	137

4.2 Methods	144
4.2.1 Study area and caribou herds	144
4.2.2 Capture and serology data	146
4.2.3 Daily movement rates.....	148
4.2.4 Post-capture daily movement rates.....	150
4.2.5 Capture myopathy survival analysis	153
4.3 Results	155
4.3.1 Capture and collar data	155
4.3.2 Post-capture movements	156
4.3.3 Post-capture survival.....	162
4.4 Discussion.....	164
4.4.1 Short-term effects on movement rates	165
4.4.2 Statistical tools for estimating baselines and divergences from baselines ..	169
4.4.3 Stress response and post-capture survival	172
4.4.4 Overall implications and recommendations.....	176
4.5 Conclusion	177
4.6 References.....	178
5. General discussion.....	187
5.1 Big data approaches to remote sensing and wildlife ecology.....	188
5.2 Broad-scale high-resolution freshwater ice phenology data product.....	190
5.3 The spatio-temporal dynamics of caribou spring migration in a warming Arctic ..	193
5.4 Estimating short-term effects on behaviour and survival in single-capture studies	
.....	195
6. Conclusion	199
7. Supplementary materials.....	200
7.1 Supplementary materials for Chapter 2.....	200
7.2 Supplementary materials for Chapter 3.....	207
7.3 Supplementary materials for Chapter 4.....	210
8. Literature cited	211

List of tables

Table 2.1 Comparing accuracy and similarity metrics between Canadian Ice Service observations and the OPEN-ICE algorithm implemented with and without the pixel-wise logistic temporal filter (see Fig. 2.2E).	56
Table 3.1 Model comparison metrics for the three candidate path selection models. The environmental covariates of interest for each model are indicated along with their relative support by the data as estimated by Bayesian model weights, the K-fold cross-validation information criterion (KFCV-IC \pm standard error), the corresponding expected log predictive densities (ELPD \pm standard error), and the differences in ELPD (Δ ELPD \pm standard error) relative to the best model.....	106
Table 4.1 Model comparison metrics for the three candidate hierarchical generalized additive models. The Akaike Information Criterion (AIC) for each model is presented along with the AIC difference (Δ AIC) relative to the best model.	156
Table 4.2 Model summary output for parametric and smooth terms in the selected candidate model that best describes daily movement rates of barren-ground caribou. Model was fit using a hierarchical generalized additive model. Parametric terms include factor-level intercepts for combinations of sex and herd relative to the intercept for the model's reference level ("Intercept", Bluenose-East Female), in units of the response variable (<i>km/h</i>). Smooth terms include cyclic cubic spline regressions for day of year ("s(doy)"), factor-level smooths for day of year for each individual each year ("s(doy, id/year)"), and thin-plate spline regressions for days since capture up to 30 days following a capture event ("s(dsc30)").	158
Table 4.3 Model summary output for generalized additive Cox proportional hazard model implemented with shrinkage on thin plate regression smooth and tensor terms.	163
Supplementary Table 2.1 Names, HydroLAKES IDs, surface area, and centroid geographical coordinates of the 24 lakes from which spectral data was randomly sampled from scenes captured by Landsat 7, Landsat 8, and Sentinel-2.	200
Supplementary Table 2.2 Currently available large-scale data products used for monitoring sea ice, snow cover, and lake ice.	201
Supplementary Table 3.1 Model comparison metrics for the three candidate path selection models. The environmental covariates of interest for each model are indicated along with their relative support by the data as estimated by the widely-applicable information criterion (WAIC \pm standard error), the corresponding expected log predictive densities (ELPD \pm standard error), and the differences in ELPD (Δ ELPD \pm standard error) relative to the best model.	207

List of figures

Figure 2.1 Map illustrating the spatial extent of the study area, lake polygons from the HydroLAKES database (Messenger et al., 2016), the 24 lakes sampled for training data to build decision trees, and the 105 lakes monitored by the Canadian Ice Service and used for validating OPEN-ICE observations.....	37
Figure 2.2 The OPEN-ICE algorithm estimates breakup dates in each pixel by: (A) identifying the images captured over an area of interest by the Landsat 7 ETM+, Landsat 8 OLI, and Sentinel-2 MSI optical sensors, (B) classifying images into water, ice, and clouds using previously trained and tuned sensor-specific CART models, (C) combining the classified images into a denser multi-sensor time series, (D) using a pixel-wise breakup time series to (E) compute a logistic temporal filter that removes erroneous classifications outside the putative ice breakup period (i.e., observations with a very large difference to the predicted probability of ice presence/ absence), and (F) estimating the breakup date using a sliding window to detect the breakup sequence in each pixel.	44
Figure 2.3 Methodology employed to compare OPEN-ICE outputs with Canadian Ice Service (CIS) lake ice fractions. (A) OPEN-ICE pixel breakup dates were extracted from a given lake’s HydroLAKES polygon (here Baker Lake, Nunavut) and relative frequencies were used to construct (B) a breakup profile, composed of a time series of lake ice fractions, for comparison with CIS observations. OPEN-ICE was compared to CIS observations based on the timing of breakup events (breakup start and end) and the similarity of the breakup profiles (maximum Fréchet distance).....	48
Figure 2.4 Structure and accuracy of tuned decision tree classifiers for Landsat 7 ETM+, Landsat 8 OLI, and Sentinel-2 MSI. The scatterplots (A, B, C) depict the thresholds that optimally classify the train set observations into water, ice, and clouds using sensor bands (Blue and Shortwave Infrared 2) or index (Normalized Difference Snow Index). Scales for each axis are displayed in the original range of each band (0 to 1) and index (–1 to 1). The confusion matrices (D, E, F) depict the percentage of test set observations accurately or erroneously classified by the tuned decision trees. Each diagonal tile includes producer’s and user’s accuracy at the bottom and on the right, respectively. The overall accuracy and kappa metrics are presented above each confusion matrix.	53
Figure 2.5 Comparison of spring (A) breakup start and (B) breakup end dates as observed by the OPEN-ICE algorithm and the Canadian Ice Service over 105 freshwater lakes between 2013 and 2021. The 1:1 ratio line is included alongside three model comparison metrics: the mean absolute error (MAE), the mean bias error (MBE), and Pearson’s correlation coefficient (r).	54
Figure 2.6 Maximum Fréchet distance between OPEN-ICE and CIS lake breakup profiles as a function of (A) the mean daily lag (in days) observed in CIS relative to OPEN-ICE throughout a lake’s breakup period, and (B) OPEN-ICE’s sequence detection gap (in days) averaged over all pixels of a lake.	55

Figure 2.7 Map illustrating the pixel breakup (day of year a pixel transitioned from ice to water) estimated by the OPEN-ICE algorithm for all freshwater pixels of Canada during the spring of 2020 at a 30-m resolution. 58

Figure 2.8 Map illustrating the spatial coverage and resolution of OPEN-ICE pixel breakup estimates (in day of year) over a 30-day period in 2020 across different lakes spanning five orders of magnitude in surface area. The lakes are: (A) Lake Nipigon which covers 4505.95 km², (B) Onaman Lake which covers 111.44 km², (C) Treptow Lake which covers 10.64 km², (D) Elwood Lake which covers 0.12 km², and (E) Little Lake which covers 0.03 km². All lakes are situated in the immediate region around Lake Nipigon in Northwestern Ontario. 59

Figure 2.9 (A) Map of Canada’s 15 ecozones with (B) the distribution of annual breakup end dates between 2013 and 2021 in randomly selected lakes (n = 4000) categorized into small (0.1-1 km²), medium (1-10 km²), and large (>10 km²) size classes. The lettering above each boxplot indicates similarities (shared letters) or statistically significant differences (different letters) between the distribution means of each lake size class within a given ecozone as indicated by the Tukey honest significant difference tests (see Section 2.3.4). The number of lakes for a given size class in each ecozone is displayed below each boxplot. 70

Figure 2.10 Scatterplot of (A) breakup start and (B) breakup end dates of randomly-sampled lakes (n = 4000) across 9 spring seasons (2013-2021) as a function of the day of year the spring 0° C isotherm reached each lake. Point colour represents the ecozone of each lake. Dotted, dashed, and full lines represent the trendlines for small (0.1-1 km²), medium (1-10 km²), and large (> 10 km²), respectively. 72

Figure 3.1 Map illustrating the observed spring migration paths during the study period. Spatial data for the annual ranges and calving grounds of each herd are provided by the Government of the Northwest Territories. 91

Figure 3.2 Temporal interactions between female caribou spring migration and lake ice breakup between 2013 and 2022. (A) The overlap in the periods of spring migration and breakup start. The spring migration period for each herd is shown by date intervals illustrated in red for Bathurst and blue for Bluenose-East, with progressive colour shading indicating the total proportion of collared females within each interval. The black-lined boxplots show the distribution of lake breakup start dates for 260 randomly selected lakes ranging from 0.1 to 1000 km² in size and distributed across the entire study area. (B) The relationship between the start of lake breakup and the median start of spring migration for each herd across years. The dotted trendline illustrates a non-significant linear model (p = 0.95). (C) The proportion of observed migration paths that encountered breaking ice or open water each year is shown by blue and red bars alongside their corresponding fractions of observed paths. 104

Figure 3.3 Distribution of posterior estimates for each coefficient in the path selection model with the most support, where step distance was included to reduce bias associated to movement speed. The vertical band illustrates each distribution's median value along with a shaded area representing 50% of the posterior distribution. The distributions are truncated at 95% and bold typeface indicates covariates and

interactions that do not overlap with zero, illustrated in red. Interactions between terms are denoted by “x” 109

Figure 3.4 Conditional effects of mean waterbody size class and proportion of ice, breaking ice, and open water on female caribou path selection during spring migration. The estimated relative probability of selection (\pm 95% CI) varies as a function of the (A) mean within-step waterbody size and its interaction with the proportion of the landscape covered by (B) ice, (C) breaking ice, and (D) open water. Dashed lines depict low confidence in each interaction level’s differentiation from the reference level of small mean waterbody size (i.e., coefficient’s 95% confidence interval includes zero, see Fig. 3.3). Note the variation in x-axis limits, which reflect the full range of proportions of ice, breaking ice, and open water encountered in used/available paths throughout the study period. 110

Figure 3.5 Partial effects of migration start date, distance to calving ground, and ice phenology on the duration of female caribou spring migration events. The duration of a migration event varies as a function of (A) the day of year a female initiated migration, (B) the geographic distance to the calving ground at the start of migration, and (C) the rate (proportion of steps in migration path) of encounters with breakup conditions including both breaking ice and open water. The three population-level smooth terms (black lines) and corresponding 95% confidence interval (grey ribbons) are fitted to observations (blue points) with an HGAM. 112

Figure 4.1 Map illustrating the region of each herd’s range in which capture and collaring efforts were concentrated throughout the study period. Spatial data for annual and calving ranges were provided by the Government of the Northwest Territories. Regions of captures for each herd were drawn using a 95% minimum convex polygon around all capture locations. Projection: NWT Lambert, NAD83. 146

Figure 4.2 Partial effects of the smooth terms on daily movement rates of caribou fit with a hierarchical generalized additive model (HGAM). (ABCD) Seasonal patterns unique to each sex and each herd are modelled by a cyclic cubic regression of caribou daily movement rates as a function of day of year. (EF) Post-capture movement behaviours are modelled by a cubic regression spline of daily movement rates as a function of days since capture. Solid lines and shaded ribbons represent smooth term estimates and their corresponding confidence intervals. Dotted lines indicate trends in which confidence intervals overlap with zero. Strips in the margin of each plot indicate distinct levels for interacting terms for sex and herd. Bathurst herd estimates are illustrated in red while Bluenose-East estimates are illustrated in blue. Y-axis scale is the square-root-transformed daily movement rate (km/h). 159

Figure 4.3 Comparison of predicted daily movement rates (DMR) of caribou in the 30-day period following capture and handling (i.e., post capture) relative to population baseline. DMR for both female (AC) and male (BD) caribou in the Bathurst (AB) and Bluenose-East (CD) herds as predicted by a hierarchical generalized additive model (see Fig. 4.2). Capture events (red diamonds) are evaluated as having occurred on the 80th day of the year (~ March 20th), the mean capture date. Predicted post-capture DMR (solid red line, \pm 95% confidence interval) and baseline DMR (black dashed line) are evaluated for the 30-day period thereafter. 161

Figure 4.4 Predicted probability of female caribou survival 30 days post-capture as a function of significant capture and stress indicators. The probability of survival is predicted by: (A) the combined effects of capture event duration (minutes) and cortisol concentration (mmol/L) modelled by a tensor smooth (2-dimensional response surface illustrated with stretched colour scale) and (B) the effects of natural log-transformed aspartate aminotransferase concentration (units/L) modelled using a thin-plate regression smooth (black line, grey ribbon for \pm 95% confidence intervals). The probability of survival was predicted using a generalized additive Cox proportional hazards model implemented with shrinkage smooths to identify important predictors. See Table 4.3 and Supplementary Figure 4.1 for all model terms and corresponding partial effects. Note that colour scale is bound by the limits of predicted values for survival (0.23 to 1)..... 164

Supplementary Figure 2.1 Individual and combined coverage of top-of-atmosphere reflectance image collections captured by open-access high-resolution optical sensors over Canada between 1999 and 2022. Coverage is illustrated by (A) the total area of all scenes captured by each sensor and (B) the mean revisit time of each sensor over 10,000 randomly selected water pixels across Canada. Coverage was assessed annually specifically within the window used by OPEN-ICE to estimate spring breakup (February 15th to September 30th). The area of the timeline highlighted in red corresponds to the period currently covered by the OPEN-ICE data product. Coverage was assessed using Collection 2 Tier 1 images for Landsat sensors and Level 1-C for Sentinel-2. 202

Supplementary Figure 2.2 Individual and combined coverage of top-of-atmosphere reflectance image collections captured by open-access high-resolution optical sensors over Canada between 1999 and 2022. Coverage is illustrated by (A) the total area of all scenes captured by each sensor and (B) the mean revisit time of each sensor over 10,000 randomly selected water pixels across Canada. Coverage was assessed annually specifically within the window used by OPEN-ICE to estimate spring breakup (February 15th to September 30th). The area of the timeline highlighted in red corresponds to the period currently covered by the OPEN-ICE data product. Coverage was assessed using Collection 2 Tier 1 images for Landsat sensors and Level 1-C for Sentinel-2. 203

Supplementary Figure 2.3 Maps illustrating a (A) Sentinel-2 RGB composite of two lakes alongside the four layers provided by the OPEN-ICE data product for the year 2020. For each pixel, OPEN-ICE provides (B) the breakup date (day of year), (C) the R^2 of the logistic temporal filter (see Fig. 2.2E), (D) the total number of observations used to detect the breakup sequence, and (E) the breakup gap (in days) between the last observed ice and the first observed water (see Fig. 2.2F). Talbot Lake (54.02° N, 99.92° W) was chosen to illustrate a case of extreme turbidity where OPEN-ICE performs poorly. In this case, OPEN-ICE quality metrics indicate that the logistic filter's R^2 is low, that the number of observations is low, and that the breakup gaps are large relative to the neighbouring Moose Lake (53.91° N, 99.76° W). 204

Supplementary Figure 2.4 Distribution of per lake means of pixel quality metrics associated with OPEN-ICE breakup estimates between 2013 and 2021. For each of the 105 lakes monitored by the Canadian Ice Service (see Fig. 2.1), per lake means were

computed for (A) the R² of the logistic temporal filter (see Fig. 2.2E), (B) the total number of observations used to detect the breakup sequence (between February 15th and September 30th), and (C) the breakup gap (in days) between the last observed ice and the first observed water (see Fig. 2.2F)..... 205

Supplementary Figure 2.5 Trends of OPEN-ICE quality metrics extracted from 4000 random lakes annually between 2013 and 2021. Per lake means were computed for (A) the R² of the logistic temporal filter (see Fig. 2.2E) and (B) the breakup gap (in days) between the last observed ice and the first observed water (see Fig. 2.2F). These two metrics are presented as a function of the mean lake observations per pixel to assess their trends as the data density of time series increases. The presented trends are fit using a generalized additive model. 206

Supplementary Figure 3.1 Bayesian estimate trace plots depicting the estimated values of each population-level parameter included in model 3 (most supported model) sampled over 500 post-warmup iterations in each of the 10 Markov chains. 208

Supplementary Figure 3.2 Distribution of posterior estimates for each coefficient in the path selection model with the most support, where step time was included to reduce bias associated to sampling frequency. The vertical band illustrates each distribution's median value along with a shaded area representing 50% of the posterior distribution. The distributions are truncated at 95% and bold typeface indicates covariates and interactions that do not overlap with zero, illustrated in red. Interactions between terms are denoted by "x". 209

Supplementary Figure 4.1 Partial effects of stress-related covariates on the log-hazards function of a Cox proportional hazards model. Panel lettering in bold typeface indicates terms with significant (C) and marginally significant (D) contributions to the survival model (see Table 4.3 and Fig. 4.4)..... 210

List of abbreviations

API: Application Programming Interface
ARLIE: Aggregated River and Lake Ice Extent
AST: Acetate aminotransferase
AVHRR: Advanced Very High Resolution Radiometer
AWEI: Automated Water Extraction Index
BUE: Breakup end
BUS: Breakup start
CART: Classification and regression tree
CIS: Canadian Ice Service
CK: Creatine phosphokinase
CV: Cross-validation
CLMS: Copernicus Land Monitoring Services
ELPD: Expected log predictive density
ESA: European Space Agency
ETM+: Enhanced Thematic Mapper +
GAM: Generalized Additive Model
GEE: Google Earth Engine
GLMM: Generalized Linear Mixed Model
GNWT: Government of the Northwest Territories
GPS: Global Positioning System
HGAM: Hierarchical Generalized Additive Model
IMS: Interactive Multisensor Snow and Ice Mapping System
JRC: Joint Research Centre of the European Commission
KFCV-IC: K-fold cross-validation information criterion
L7: Landsat 7
L8: Landsat 8
MAE: Mean absolute error
MBE: Mean bias error
MFD: Maximum Fréchet distance
MODIS: Moderate Resolution Imaging Spectroradiometer
MSI: MultiSpectral Instrument
NDSI: Normalized Difference Snow Index
NDVI: Normalized Difference Vegetation Index
NDWI: Normalized Difference Water Index
NIR: Near infrared
NSD: Net square displacement
NWT: Northwest Territories
OLI: Operational Land Imager
OPEN-ICE: Open Pixel-based Earth eNginE Ice
PSA: Path Selection Analysis
S2: Sentinel-2
SAR: Synthetic Aperture Radar
SSF: Step Selection Function

SWIR: Short-wave infrared
TOA: Top-of-Atmosphere reflectance
USGS: United States Geological Survey
USNIC: United States National Ice Center
WAIC: Widely-applicable information criterion
WSI: Water-resistant Snow Index

Abstract

Caribou (*Rangifer tarandus*) are vital to terrestrial ecosystems and central to traditional economies throughout their circumpolar distribution. Migratory tundra caribou undertake the longest known terrestrial migrations, and they do so annually through some of the Arctic and Boreal regions that have undergone the most rapid warming on Earth. Movement behaviour, such as migration, is critical to survival and reproduction in variable environments. This thesis investigates how environmental change focused on lake ice phenology and monitoring tools focused on GPS collars, influence caribou movement behaviour and, potentially, survival. In Chapter 1, I synthesize current knowledge linking caribou survival and movement ecology to: (i) broader environmental changes occurring in the Arctic, (ii) shifts in spring lake ice phenology and the remote sensing tools currently available for monitoring environmental change, and (iii) short-term effects of captures required for GPS collar monitoring programs. In Chapter 2, I produce fine-scale large extent maps of spring lake ice phenology by developing an Open Pixel-based Earth eNginE Ice (OPEN-ICE) remote sensing algorithm implemented in Google Earth Engine's (GEE) cloud computing platform. OPEN-ICE combines imagery from 3 different optical sensors to enable monitoring of freshwater lake ice phenology in both small and large waterbodies over the large geographical expanses typical of migratory caribou ranges. I evaluated the accuracy of the OPEN-ICE data product over a 9-year period by comparing breakup start and end dates in 105 lakes monitored by the Canadian Ice Service and found a mean bias error of -1.10 and -0.69 days, respectively. In Chapter 3, I used the OPEN-ICE data product to evaluate the behavioural responses of female barren-ground caribou to shifting lake ice conditions during their spring migration. Caribou selection or avoidance varied with the phenological state (open water, breaking ice, ice) and size of encountered waterbodies. Specifically, during spring migration females exhibited strong avoidance of areas with breaking ice in small and especially in large waterbodies, and to a lesser extent, avoidance of open water areas. Instead, they selected migration paths through areas with smaller ice-covered lakes, while tending to avoid exposed crossings of very large ice-covered lakes. In Chapter 4, I investigated the effects of GPS collar capture events on post-release movement and survival of barren-ground caribou. To assess capture impacts within a single-capture study design, I developed statistical modelling strategies that allow comparisons of recently captured individuals to population baselines accounting for seasonal patterns, sex, inter-annual and inter-individual differences. Captures impacted caribou movement for up to 4 days after capture and capture event duration combined with blood cortisol concentration predicted suspected cases of capture-related mortality. This research provides important remote sensing tools and statistical strategies for monitoring lake ice, studying movement patterns of migratory caribou, and evaluating the impacts of environmental change and handling stress on an ecological and cultural keystone species that faces an uncertain future.

Résumé

Dans l'ensemble de son aire de répartition circumpolaire, le caribou (*Rangifer tarandus*) est vital pour les écosystèmes terrestres et central aux économies traditionnelles. Les caribous de la toundra entreprennent les plus longues migrations observées dans les habitats terrestres, et ils le font chaque année à travers les régions arctiques et boréales qui ont subi le réchauffement le plus rapide de la planète. Le comportement de déplacement, y compris la migration, est essentiel à la survie et à la reproduction dans des environnements variables. Cette thèse étudie comment les changements environnementaux, en particulier les changements dans la phénologie de la glace de lac, et les outils de surveillance, en particulier les colliers GPS, influencent le comportement de déplacement des caribous et, potentiellement, leur survie. Dans le chapitre 1, je fais une synthèse de nos connaissances actuelles liant la survie du caribou et l'écologie du mouvement: (i) aux changements environnementaux plus généraux qui se produisent dans l'Arctique, (ii) aux changements dans la phénologie des glaces de lac au printemps et aux outils de télédétection actuellement disponibles pour surveiller les changements environnementaux, et (iii) aux effets à court terme des captures effectuées dans le cadre des programmes de surveillance par collier GPS. Dans le chapitre 2, je produis des cartes à échelle fine de la phénologie de la glace des lacs de printemps en développant un algorithme de télédétection Open Pixel-based Earth eNgin Ice (OPEN-ICE) mis en œuvre dans la plateforme informatique en nuage de Google Earth Engine (GEE). OPEN-ICE combine des images provenant de trois capteurs optiques différents pour permettre la surveillance de la phénologie de la glace des lacs d'eau douce dans les petites et grandes masses d'eau sur les grandes étendues géographiques typiques des aires de répartition du caribou migrateur. J'ai évalué la précision du produit de données OPEN-ICE sur une période de 9 ans en comparant les dates de début et de fin de la fonte des glaces dans 105 lacs surveillés par le Service canadien des glaces et j'ai trouvé un biais systématique moyen de -1,10 et -0,69 jours, respectivement. Dans le chapitre 3, j'ai utilisé le produit de données OPEN-ICE pour évaluer les réponses comportementales des caribous de la toundra femelles aux conditions transitoires de la glace de lac pendant leur migration printanière. J'ai constaté que la sélection ou l'évitement des caribous variait en fonction de l'état phénologique (eau libre, glace en fonte, glace) et de la taille des plans d'eau rencontrés. Plus précisément, au cours de la migration printanière, les femelles évitaient fortement les zones où la glace se brisait dans les petits et surtout dans les grands plans d'eau et, dans une moindre mesure, les zones d'eau libre. Elles ont plutôt choisi des chemins de migration à travers des zones avec des petits lacs couverts de glace, tout en ayant tendance à éviter les traversées exposées des très grands lacs couverts de glace. Dans le chapitre 4, j'ai étudié les effets de la capture et des colliers GPS sur les déplacements et la survie des caribous de la toundra après leur remise en liberté. Pour évaluer les impacts de la capture dans le cadre d'une étude à capture unique, j'ai développé des stratégies statistiques qui permettent de comparer les individus récemment capturés aux niveaux de référence de la population en tenant compte des tendances saisonnières et des différences sexuelles, interindividuelles et interannuelles. Les captures ont un impact sur les déplacements des caribous jusqu'à

quatre jours après la capture et la durée de la capture combinée à la concentration de cortisol dans le sang permettent de prédire les cas présumés de mortalité liée à la capture. Cette recherche fournit des outils de télédétection et des stratégies statistiques importants pour la surveillance des glaces de lac, l'étude des déplacements des caribous migrateurs et l'évaluation des impacts des changements environnementaux et du stress lié à la manipulation sur une espèce clé au niveau écologique et culturelle et dont l'avenir demeure incertain.

Acknowledgements

As one does at many important crossroads in life, I reflect on the journey behind me and the journey that lies ahead. I'm frankly overwhelmed by gratitude at recalling all the people who have led me here. To all the people who have shared their encouragement, their time, their knowledge, their friendship, and their love.

To my supervisor Murray, who taught me that when things are easy, it's time to swim toward bigger waters. As I set sail, I hope that the journey ahead will reveal others with your particular set of talents: painting the bigger picture, asking the coolest (incidentally also the hardest) questions, and citing song lyrics in scientific articles.

To Manu, our emotional rock, whose sincere willingness to help kept myself and everyone in the lab grounded. *Quel honneur de te compter parmi mes amis.*

To my friends Jeremy, Emily, Ally, Laurence, Gwyneth, Mélanie, and countless others in the Northern Wildlife Knowledge Lab. I can say without a doubt there is no other place I've encountered a collection of ecologists with such a diverse set of skills and interests, from wildlife energetics and genetics to traditional knowledge research, our discussions will truly be missed. It has been and will continue to be a privilege to call you my friends and watch you thrive in all your endeavours.

To muskrat man, with whom I saw my very first caribou on the Porcupine River, standing on a chunk of ice floating downstream. Given the subject of this thesis, that was perhaps a more profound moment than I realized. I cherish the tales of our adventures canoeing around Old Crow Flats, sometimes with or without food and sometimes with or without overly curious bears tearing through our tent.

To the countless people I've met in Old Crow, Yellowknife, Lutsel K'e, and Pangnirtung. Your stories have taught me more about the North than I could ever learn in a book or a classroom.

To Terry, Kenny, Jam, Marcel, Sam, Terra, Claire and Ross, my Kwench friends who not only regularly checked in and cheered me on in these last few months but have truly inspired me by the breadth of their interests, knowledge, entrepreneurship, talents, and all-round awesomeness.

To the family I was given and the family I've made along the way, you have made me who I am today. You have supported me every step of the way, carried me through countless trials and tribulations, and have been there to cheer me on even when my inner voice was not. Each of you is a constant reminder that our greatest and most lasting impact on Earth is our love. To Mom, Dad, Katou (+ Minz), Vanessa, Uros, Sue, Zoe, Jaya, Peter, and Noah-Xavier, my first and second families. To my chosen family Paul, Dalal, Louis-Philippe, Jesse, Marie-Aimée, Raphael, Étienne, Mélissa, Thomas, and many others with whom I have grown up, and with whom I wish to grow old. As

Carole King said: "Winter, spring, summer, or fall, all you gotta do is call... and I'll be there!". This one's for you!

To my partner Vanessa and that fateful day we met on the corner of McTavish and Sherbrooke. You have believed in me every step of the way. Our shared lives and our adventures have been an endless source of joy and laughter. By piano, sailboat, or canoe, home is wherever I'm with you. Je t'aime!

Contribution to original knowledge

Throughout this thesis, I have endeavoured to: (i) create a high-resolution freshwater ice data product to track spring breakup in small and large lakes across broad spatial scales, (ii) investigate the impacts of shifts in freshwater ice phenology on barren-ground caribou migratory behaviour, and (iii) assess the effects of capture and GPS collars on short-term movements and survival of caribou. As part of pursuing these avenues of investigation, I have made several original contributions to knowledge across different fields of study.

1) Big data approaches to remote sensing and movement ecology

We have entered an era defined by data abundance, an era in which advances in scientific inquiry increasingly rely on methods and strategies to distil, aggregate, and summarize massive datasets into usable and insightful products. Migratory caribou roam far and wide, and studying the spatio-temporal relationship between their movement behaviour and the remote landscapes they inhabit exemplifies the need for large datasets and commensurate analytical strategies. As such, this thesis has contributed to big data approaches in remote sensing and movement ecology (Chapter 2, 3, and 4) by developing and describing tools to distil unfathomably large datasets into useful aggregate products and easily interpretable visualizations and results. In Chapter 2, I capitalized on the abundance of open-access high resolution optical satellite imagery and the availability of cloud computing platforms to develop the OPEN-ICE algorithm with which I have successfully processed almost a petabyte of satellite imagery into a data product that provides continental-scale pixel-based estimates for

freshwater breakup dates. In Chapter 3, I studied the effects of lake ice phenology on spring migration by comparing the size and phenology states of waterbodies encountered along 274 spring migration paths (followed by 153 collared females) and 8,220 random paths between winter ranges and calving grounds for two barren-ground caribou herds. Using a cloud computing platform, I summarized phenological data from the OPEN-ICE product in over 2 million caribou steps representing a combined area of over 100 million square kilometres. Overall, I have described methodologies capable of handling and analyzing the large Earth observation and GPS collar datasets that will become increasingly common in wildlife studies.

2) Phenology of lake ice in a period of climate change

Lakes are important sentinels of environmental and climate change. While ice phenology in larger and culturally significant lakes have been recorded in written archives and, more recently, by satellite imagery archives, the study of ice phenology in small, remote lakes is often limited, despite accounting for the majority of Earth's freshwater surface area. In this thesis, I provide the first high-resolution (30-metre), large extent product that provides freshwater spring ice phenology observations for lakes spanning many orders of magnitude in size across all of Canada, the most lake-dense region of the world (Chapter 2). This provides an important contribution to many fields, effectively allowing the inclusion of lake ice phenology in broad-scale studies in limnology, weather and climate science (including biogeochemical, water, and carbon cycles), and terrestrial (e.g., Chapter 3) and aquatic ecology. In addition, spring lake ice phenology records across a range of lake sizes can also contribute tools to inform ice

safety in winter with implications for ice road networks and safe access to traditional territories.

3) Migratory caribou movement ecology in a period of population decline

While migratory caribou are the Arctic's most abundant large mammal, several herds have undergone drastic population declines in recent decades. This thesis provides original contributions to our understanding of this ecological and cultural keystone species that faces an uncertain future in a period of unprecedented environmental change. In Chapter 1, I provide an in-depth overview of movement behaviour and key periods in migratory caribou's annual cycle that have important implications for their survival, reproductive success, and population dynamics. Because spring migration immediately precedes calving, delayed timing of spring migration can have important effects on calf survival. In Chapter 3, I contribute original knowledge to our understanding of how environmental changes linked to climate and lake ice phenology impact caribou spring migrations. Showing that migrating females strongly avoid breaking ice and to a lesser extent open water, that avoidance increases with water body size, and that migration duration increases by more than a week when females encountered more breakup conditions offers new insight into caribou vulnerability to environmental change. One such insight is the importance of protecting terrestrial corridors between lakes that will become more important as the availability of lake ice declines during the spring migration season. In Chapter 4, I further investigate the impacts of tools that caribou monitoring programs rely on to study population movements and dynamics, contributing the first estimates of short-term effects of

capture stress on barren-ground caribou movement rates and the first documented link between a female caribou's capture-related stress response and her survival outcomes.

4) Strategies to evaluate impacts of wildlife captures and biologging

Wildlife ecology has entered a new era in which the ubiquity of biologgers has provided new insights into energetics, nutrition, ecology, behaviour, and movement of many species. Technological advances are improving biologging devices over time, for example by reducing their mass and increasing the quality and frequency of recorded data. However, it remains poorly understood for most species-biologger combinations how biologgers and the capture and handling required to deploy (and in some cases recover) them affect the energetics, behaviour, and survival of monitored individuals. Indeed, across many wildlife monitoring studies, the effects of an initial capture are hard to estimate because there exists no individual behavioural baseline. In Chapter 4, I explore this problem and describe some statistical strategies that enable comparisons of recently capture individuals to population-level baselines of previously captured individuals. The approaches I develop compare the duration and magnitude of any post-release behavioural discrepancies, while accounting for large sources of variability in biologging datasets such as highly non-linear seasonal or daily cycles and inter-annual or inter-individual differences. I also describe some statistical strategies to evaluate the impacts of capture-related stress on survival outcomes in the period following release, using data that can be readily recorded (e.g., handling time) and sampled (e.g., stress indicators in blood serum) within the constraints of single-capture study designs. Together, these two methods contribute important methods to provide continuous information to researchers conducting biologging studies and stakeholders concerned

about the impacts of these approaches about the extent of impacts and how to reduce bias in sampled observations and improve health and survival outcomes for studied individuals.

Contribution of authors

Chapter 2 (published)

Citation: Giroux-Bougard, X., Fluet-Chouinard, E., Crowley, M.A., Cardille, J.A., Humphries, M.M., 2023. Multi-sensor detection of spring breakup phenology of Canada's lakes. *Remote Sens. Environ.* 295, 113656. <https://doi.org/10.1016/j.rse.2023.113656>

XGB conceived the study, designed the OPEN-ICE algorithm and its computational framework, and analyzed and validated the output data. EFC contributed analyses of lake breakup trends across ecozones. XGB wrote the manuscript with help from EFC, MAC, and MMH. MMH and JAC co-supervised the study. All authors provided critical feedback and various stages of the study and helped shape the manuscript.

Chapter 3 (in preparation for publication)

Citation: Giroux-Bougard, X., Humphries, M.M. Lake ice phenology and the spring migration of barren-ground caribou (*Rangifer tarandus groenlandicus*) in a rapidly changing North

XGB conceived the study and its methodology, conducted the analyses and visualizations, and wrote the manuscript. MMH helped with study conceptualization, contributed to writing the original draft and provided reviews and edits, and supervised the research.

Chapter 4 (in preparation for publication)

Citation: Giroux-Bougard, X., Adamczewski, J.Z., Humphries, M.M. Post-capture survival and movements of barren-ground caribou (*Rangifer tarandus groenlandicus*)

XGB conceived the study and its methodology, conducted the analyses and visualizations, and wrote the manuscript. JZA conceptualized the study, provided investigation and data curation, reviewed and edited, and co-supervised. MMH helped with study conceptualization, contributed to writing the original draft and provided reviews and edits, and supervised the research.

Chapter 1 - General introduction and literature review

1.1 General introduction

In the past decades, many barren-ground caribou (*Rangifer tarandus groenlandicus*) herds have undergone stark population declines (Gunn, 2016; Uboni et al., 2016; Vors and Boyce, 2009). Migratory caribou are, in many ways, emblematic of Canada's North (Hummel and Ray, 2008). During this period of caribou decline, the regions caribou inhabit have warmed at an alarming rate, casting additional uncertainty on how they will cope and adapt to the rapid environmental changes unfolding in their habitats. Some of these changes have directly observable consequences, such as shifts in plant phenology (Post & Forchhammer 2008) or increased insect harassment (Witter et al. 2012), which result in reduced foraging opportunities. Many other changes, however, can be difficult to understand because their influence on caribou herds are indirect or occur at spatial and temporal scales that are harder to observe given current remote sensing technologies.

Freshwater lakes in Canada's North, as well as throughout the Northern Hemisphere, can serve as accurate sentinels of the rapid changes unfolding in these regions. However, freshwater lakes are many and varied and we need to be able to detect what they are telling us. Over the past few decades, warmer air temperatures in the North have accelerated ice break up in spring and delayed freeze-up in autumn, resulting in a longer ice-free season (Duguay et al. 2006; Latifovic & Pouliot 2007). The prevalence of freshwater systems in many northern regions means that these changes in ice phenology have important effects beyond the aquatic ecosystems they shelter

(Prowse et al. 2011). Namely, barren-ground caribou undertake the longest terrestrial migrations in the world through these regions, where freshwater lakes typically cover 15-40% of the landscape (Duguay et al. 2003). Even for a highly vagile species like caribou, movement can be facilitated or impeded by the presence of ice or open water over the abundant hydrological features characteristic of the North (Leblond et al. 2016). During migration, lake ice offers caribou an easier surface for travelling than the deeper snow typically covering the surrounding landscape during winter and spring (Fancy & White 1987). In contrast, even though caribou are excellent swimmers, the thin ice or large expanses of open water present between melt onset in spring and freeze-up in autumn can prove to be formidable obstacles, and can potentially lead to exhaustion, injury, or death (Miller & Gunn 1986). Throughout their yearly cycle, caribou's dynamic use of space determines how they experience environmental conditions and acquire resources in their seasonal ranges. As ice phenology shifts and the ice-free season gradually encroaches into caribou migration periods, herds may be required to adapt the timing of migration and the predominant routes travelled to successfully relocate between calving grounds, summer ranges, and winter ranges.

GPS collars provide information crucial to studying animal movement, effectively allowing us to explore spatial processes and habitat selection. Nonetheless, capturing and collaring wildlife is not without risk (Arnemo et al. 2006) and can produce bias in the acquired data (Dechen Quinn et al. 2012). As caribou herds rapidly decline throughout the North, wildlife management agencies in several jurisdictions have expanded their collar deployment programs to track changes in behaviour and survival. Understanding

and quantifying the effects of GPS collars on their movement and post-capture survival is a crucial component of caribou research and management.

This thesis focuses on the movement ecology of two migratory barren-ground caribou herds – the Bluenose-East and Bathurst herds – in northern Canada, including an evaluation of the impacts of freshwater ice phenology and the effects of capture and collaring events on their movement and migratory patterns. This thesis' objectives are to: (i) improve temporal and spatial resolution of classifying spring breakup in both small and large lakes at continental scales by developing sensor-specific ice-water classifications for multiple open-access optical satellite imagery repositories and fusing them into a coherent freshwater ice phenology time series (Chapter 2), (ii) to use this ice phenology time series to examine the fine-scale movement of caribou in response to ice, breaking ice, and open water conditions in the thousands of lakes traversed during their spring migration (Chapter 3), and (iii) to evaluate how capturing and collaring barren-ground caribou impacts their movement and survival (Chapter 4).

In the following sections of this chapter, I review literature focused on migratory tundra caribou and, more specifically, barren-ground caribou populations trends, their seasonal cycles and movement ecology, and the unprecedented environmental changes unfolding in their ranges. I then provide an overview of current literature on the remote sensing techniques and data products, which are essential to studying species with ranges as massive as those of migratory caribou. Particular attention is dedicated to the challenges of monitoring freshwater ice phenology. Finally, I review literature on wildlife monitoring techniques, and how the impacts of these techniques can influence the behaviour and survival scientists wish to study.

1.2 Literature review

1.2.1 What are migratory caribou?

Caribou and reindeer are, respectively, North American and Eurasian representatives of *Rangifer tarandus*, a single, circumpolar species within the deer family *Cervidae* and the even-toed ungulate order *Artiodactyla* (Harding, 2022). In North America, caribou are divided into three main ecotypes based on distinctive habitats and calving behaviours: the migratory tundra ecotype, the mountain ecotype, and the boreal woodland ecotype (Mallory and Hillis, 1998). The main distinction between them are their respective habitats and calving behaviour (Bergerud et al., 2008). In spring, migratory tundra migrate to higher latitudes to calve on the tundra in the safety of larger aggregations (COSEWIC, 2016). In contrast, woodland boreal caribou are generally sedentary and spread apart to calve alone in secluded and sheltered areas of the boreal forest (COSEWIC, 2002). Mountain caribou herds may, depending on the region, either calve together in alpine zones or spread apart in subalpine zones. Migratory tundra caribou form massive herds, sometimes numbering more than half a million individuals, that roam vast expanses from the northernmost reaches of subarctic taiga to arctic tundra, including even the islands of Canada's High Arctic. Migratory caribou herds are composed of multiple social groupings that are bound together by the fidelity of females to a common traditional annual calving ground (Skoog, 1968). Migratory tundra herds of Canada are generally classified into: (i) the eastern migratory herds (e.g., George and Leaf River herds of Quebec) belonging to the woodland subspecies *Rangifer tarandus tarandus*, (ii) the barren-ground caribou herds of the Northwest Territories and Nunavut (e.g., Bluenose-East and Bathurst herds) that form their own distinct subspecies

Rangifer tarandus groenlandicus, (iii) the subspecies *Rangifer tarandus granti* that calf on the coastal plains of Alaska (e.g., Porcupine herd of Yukon and Alaska), and (iv) the Peary Island caribou herds of the High Arctic of the subspecies *Rangifer tarandus pearyi*. Given the diversity of *Rangifer sp.*, understanding the distinctions between ecotypes, subspecies, and herds is tedious and complex (Harding, 2022), and indeed has been the subject of much research and debate on the morphological (Banfield, 1961), genetic (Klüttsch et al., 2016), behavioural (Nagy et al., 2011), and demographic (Adamczewski et al., 2015; Gunn et al., 2011b) differences between groups. However, delineating ecotypes, subspecies, and herds remains an essential exercise that allows wildlife co-management partners to assess the demographic trends for well-defined conservation units (COSEWIC, 2011), implement conservation strategies (Serrouya et al., 2019) and land-use planning at appropriate spatial scales (Government of the Northwest Territories, 2019), and assess the similarities and differences in the challenges faced across herds and regions (COSEWIC, 2016). As such, while this thesis focuses on barren-ground caribou, and more specifically the Bluenose-East and Bathurst herds of the NWT and Nunavut, I frequently draw from broader knowledge and research on caribou and reindeer from other herds and subspecies, and inversely, I draw conclusions from my own research with broader implications for other herds. Throughout this thesis, I may refer to migratory caribou, migratory tundra caribou, and barren-ground caribou interchangeably. As I will soon discuss, the threats faced by many migratory herds and the challenges associated with studying them are shared in being defined by their massive annual ranges, spanning thousands of square kilometres

in remote regions, and the movement and migratory behaviours that connect individuals to these ranges.

1.2.2 Why do caribou migrate, and why are these migrations important?

Throughout the planet, long-distance migrations are an important adaptation to seasonality (Alerstam et al., 2003) and predation (Kubelka et al., 2022; McKinnon et al., 2010) and migratory caribou epitomize the evolution of this life history trait in terrestrial habitats (Joly et al., 2019). Migratory caribou typically overwinter in the northern reaches of the boreal forest where they dig for their preferred source of winter food, lichens buried in the snow (Webber et al., 2022). In fact, their North American name is most likely derived from “xalibu”, their name in the Mi'kmaq language which describes their pawing behaviour when digging in snow, a winter behaviour observed in all *Rangifer* subspecies and ecotypes. As the spring approaches, females migrate hundreds of kilometres northward to coastal areas in the tundra of the Arctic (Bergerud et al., 2008), aggregating in the thousands at calving grounds distinct to each herd (Gunn and Miller, 1986). Migratory tundra caribou distinguish themselves from other ecotypes by gathering into large groups instead of spreading apart during calving season, as is more typical of their woodland ecotype counterparts. This gregarious reproductive strategy serves two main purposes: it reduces predation pressure on neonates (Bergerud, 1996) and, if timed correctly with the northward march of the arctic spring's “green wave” (Myrsterud, 2013), it provides fresh and abundant high-quality forage during lactation, both of which ultimately promote calf health and survival in their first few weeks of life (Bergerud et al., 2008). In the post-calving period and during the following summer months, caribou slowly spread out into smaller groups while seeking

forage in tundra south of their calving grounds. However, their grazing may be interrupted several times by periods of severe insect harassment, typical of short arctic summers, which drive them into large social aggregations in higher exposed rocky terrain as they seek wind and refuge in numbers (Johnson et al., 2022). As the fall commences, caribou gather once again for the rut season. During the fall and rut period, caribou migrate southward on their return journey to their wintering grounds, a more gradual and less synchronous migration relative to spring migration. Annual round trips often cover thousands of kilometres and constitute the longest terrestrial migration in the world (Fancy et al., 1989; Joly et al., 2019).

As the most abundant large mammal in Arctic terrestrial ecosystems, caribou are not only an ecological keystone species (Mills et al., 1993), but also a cultural keystone species (Garibaldi and Turner, 2004). Caribou migrations and cycles and have been a central part of life, language, culture, and spirituality for Indigenous peoples of the Arctic for thousands of years (Bourgeon et al., 2017; Jacobsen, 2011; Zoe, 2012). Caribou meat remains one of the main sources of protein and an important contributor to food security for both Inuit (Kenny et al., 2018) and First Nation (Schuster et al., 2011) communities in Canada's North. In addition to its close relationship with Indigenous peoples, migratory caribou are an important part of Arctic food webs, providing an important source of nutrition for many predators and scavengers, including grey wolves (*Canis lupus*), grizzly bears (*Ursus arctos*), black bears (*Ursus americanus*), Arctic fox (*Vulpes lagopus*), wolverines (*Gulo gulo*), lynx (*Lynx canadensis*), golden eagles (*Aquila chrysaetos*), and bald eagles (*Haliaeetus leucocephalus*) (COSEWIC, 2016). Like many large herbivores, migratory caribou and wild reindeer herds play an important role in

shaping tundra and taiga through trampling, grazing, and nitrogen cycling (Henry and Gunn, 1991; Joly et al., 2007; Olofsson et al., 2001). They also play an important role in aquatic ecosystems, whereby the larvae of biting insects, whose productivity heavily depends on caribou blood (Joly et al., 2020), form important trophic links in freshwater food webs, and fecal pellets that accumulate on lake ice during winter form important influxes of nitrogen into freshwater ecosystems (COSEWIC, 2016). As such, the future of the Arctic and its First Peoples are closely intertwined with the future of migratory caribou herds and the rhythms of their seasonal migrations (Hummel and Ray, 2008).

1.2.3 What is the current status of migratory caribou herd populations?

Important population declines have been observed across several large migratory caribou and wild reindeer herds in recent decades (Gunn, 2016; Uboni et al., 2016; Vors and Boyce, 2009). Since aerial surveys and photo census methods became more widely adopted for monitoring large caribou herds in the 1970s, wildlife biologists have counted individuals during calving or post-calving aggregations and observed population peaks and subsequent crashes. For example, an aerial photocensus conducted during post-calving of the aggregations of the George River herd, an eastern migratory herd in Quebec and Labrador, suggest it was composed of more than 823,000 individuals in 1993 (Couturier et al., 1996), while the latest photocensus in 2022 estimates the population to be 7200, a staggering population drop of 99% over 29 years (Brodeur et al., 2021). Over the same period, several large barren-ground caribou herds of the Northwest Territories and Nunavut have declined at a similar pace. As of the last survey in 2021, the Bathurst herd has declined by approximately 98% since its population peaked in 1984 at 472,000 (Adamczewski et al., 2022). Surveys of the

Bluenose-East herd suggest it peaked in 2010 at approximately 114,000 individuals and has since plummeted by approximately 70% (Boulanger et al., 2022). Further westward, the Porcupine caribou herd is currently the only population that seems to have stabilized and continued to increase, with the latest survey in 2017 estimating the population at 218,000, an increase of almost 94,000 individuals relative to its previous low in 2001 (Porcupine Caribou Technical Committee, 2022).

Migratory caribou population dynamics are characterized by important population cycles, so while these declines are dramatic, they have been observed before. Prior to the adoption of aerial surveys for management in the 1970s and 1980s, periods of extended population crashes were documented across several herds (Bongelli et al., 2022). Because these cycles are central to life in the Arctic, they are well documented in traditional knowledge accounts of the Indigenous peoples that have depended on migratory caribou for millennia (Dokis-Jansen et al., 2021; Ferguson et al., 1998). Dendrochronological methods have also been used to date these cycles back 120 years using the scarring patterns created by trampling the roots of spruce trees as a proxy for caribou abundance along important migration corridors (Morneau and Payette, 2000; Zalatan et al., 2006).

In the light of current declines, territorial and federal governments of Canada have designated barren-ground caribou herds as threatened (COSEWIC, 2016; NWT Species at Risk Committee, 2017), although no official status has yet been designated for eastern migratory caribou. Unlike their woodland and mountain ecotype counterparts, whose declines are driven primarily by habitat loss and degradation from mining and forestry activities (Hervieux et al., 2013), there remains some uncertainty as

to the exact drivers of population declines in migratory caribou herds. This uncertainty is further compounded by the unprecedented rates of climate warming and landscape changes observed in the Arctic (Rantanen et al., 2022). The precautionary principle justifies adequate protections and prioritization of research to adequately inform conservation efforts and range planning.

1.2.4 Why are migratory caribou herds declining?

The relative synchrony of population cycles suggests drivers operating at broad spatial scales (Elton, 1924; Gunn, 2003; Hansen et al., 2020; Moran, 1953), although research increasingly points to a variety of mechanisms at various spatial scales which synergistically impose cumulative effects on migratory caribou, effectively increasing their vulnerability when a herd's population is low (Bongelli et al., 2022; Gunn et al., 2011a). Finding sufficient food to satisfy energy requirements is crucial throughout the year, but in caribou, the calving, post-calving, and summer seasons have been identified as significant energetic bottlenecks that either promote or hinder calf survival and female reproductive success. Therefore, experts have identified anthropogenic disturbances and seasonal conditions on the summer range, the calving grounds, and during spring migration as key to the conservation and protection of migratory caribou (Bongelli et al., 2022).

1.2.4.1 Summer season

As capital breeders (Taillon et al., 2013), the body condition and reproductive success of migratory caribou pivots on the nutritional uptake by females during summer being sufficient to not only sustain themselves but to bring a foetus to term over the

winter months when food is scarcer and not as nutritious (Gerhart et al., 1996). In the nitrogen-limited terrestrial ecosystems of the Arctic, the preferred summer forage species for migratory caribou typically consist of fresh graminoids such as sedges (e.g., *Carex spp.*, *Eriophorum spp.*), lichens, fresh foliage of some shrub species such as birch (*Betula spp.*) and willow (*Salix spp.*), as well mushrooms later in the summer (Béland et al., 2023; Webber et al., 2022). The short Arctic summers impose a race against time to consume as much of this fresh forage as possible before its quality degrades in late summer and early fall, and missed foraging opportunities during summer can reduce the body fat and resources available to sustain females through to the following spring. Missed opportunities are the consequence of many different processes which vary by year and by herd (Bongelli et al., 2022). For example, when the population of some large herds reached their peak in the 90s, deterioration of forage on summer ranges was observed and thus density dependence partly contributed to the subsequently observed declines (Bergerud et al., 2008; Messier et al., 1988). Climate change has caused increased temperatures and regional shifts in precipitation patterns that can be linked to changes in food seasonality, availability, and quality. With the longer growing seasons throughout the Sub-Arctic and Arctic, the structure and composition of vegetation communities are shifting, with shrubs such as willow, birch, and alder (*Alnus spp.*) becoming more prevalent in many regions of the Arctic (Tape et al., 2006; Tremblay et al., 2012) and reducing overall species richness (Pajunen et al., 2012). Although this represents an overall increase in vegetation biomass (Yu et al., 2017), these shrub species lock more proteins into indigestible woody tissue and their leaves contain higher concentrations of phenols and other metabolites that curtail

browsing in late summer (Thompson and Barboza, 2014). Consequently, the increased dominance of these species likely reduces overall availability of nutrients relative to sedges and grasses dominated communities (Bryant et al., 2014), and may increase apparent competition as other large herbivores that prefer shrubs expand northward (Joly et al., 2012). However, the effects of reduced nutritional availability may be mitigated by a longer and more productive growing season, which has been related to reproductive success in some populations (Albon et al., 2017). However, climate change has also been linked to increased parasitism and insect harassment. In the short Arctic summer, when temperatures peak and wind dies down, insect harassment by mosquitoes (*Aedes spp.*), warble flies (*Hypoderma tarandi*), and bot flies (*Cephenemyia trompe*) can be so severe that it drives massive aggregations of caribou to higher, cooler, and more wind-exposed areas with less foraging opportunities (Witter et al., 2012). Because insect avoidance limits foraging time, summers with particularly intense levels of insect harassment are typically followed by a decrease in the body-condition of females and calf weights the following spring, which has been directly linked to survival and reproductive success in some populations (Johnson et al., 2022; Joly et al., 2020).

1.2.4.2 Calving and post-calving season

Many migratory species congregate as spring arrives in the Arctic to raise their offspring, a behaviour which has evolved to reduce predation on vulnerable young and to capitalize on the seasonal abundance of highly nutritious food sources (Williams et al., 2017). In addition to recovering from the nutritional stress of the winter season and the energetic cost of gestation, female migratory caribou must contend with the high

energetic cost of lactation in the period immediately following parturition. Consequently, the synchrony of calving with spring vegetation phenology has been linked to calf condition, survival, and recruitment. For example, recent research on the George River herd suggests that the single most important determinant of calf survival is its date of birth, with later births linked to increased mortality (Vuillaume et al., 2023). While maternal body condition is important (Taillon et al., 2012), the availability of fresh forage in the period immediately following parturition likely outweighs the energetic capital accumulated from the previous summers, although reduced predator density earlier in the season may also be a factor (Vuillaume et al., 2023).

Climate change has caused widespread advances in Arctic spring vegetation phenology (Høye et al., 2007), and it is unclear that the environmental cues that prompt spring migration and calving have adjusted. Consequently, some herds have experienced a trophic mismatch between the energetic demands of lactation in the period immediately following parturition and the peak availability of nitrogen during spring green-up (Paoli et al., 2018), in some cases with direct consequences to calf survival (Eikelenboom et al., 2021; Post and Forchhammer, 2008). In other herds there is evidence that the migratory behaviour of caribou is sufficiently flexible to conserve the synchrony of parturition and lactation with earlier spring green-up (Mallory et al., 2020). However, in some regions of the Arctic, phenological trends of the last decade suggest that advancing green-up has gradually slowed and been overshadowed by important increases in the variability of spring green-up dates (Schmidt et al., 2023). While the behavioural flexibility of migratory caribou should not be underestimated, it is likely that trophic mismatches will become more important as the climate continues to change.

1.2.4.3 *Spring migration*

With the arrival of spring, migratory caribou undertake a long journey north, an especially urgent one for parturient females trying to reach their traditional calving ground. As previously discussed, the timing of parturition with spring green-up is extremely important to calf survival, even more so if a female is nutritionally stressed due to poor summer range conditions or a difficult winter (Taillon et al., 2012; Vuillaume et al., 2023). Consequently, the ability of females to initiate spring migration at the right moment and the environmental factors that hinder or facilitate their movements play an extremely important role in determining reproductive success. The initiation of spring migration seems to be synchronous across many herds (Gurarie et al., 2019), and mounting evidence suggests that one of the main environmental cues is the onset of snowmelt (Gurarie et al., 2019; Laforge et al., 2021) which both facilitates movement (Leclerc et al., 2021) and is closely related to spring green-up (Laforge et al., 2023). Milder winters typically advance departure and periods of heavier snowfall in late winter typically retard it (Gurarie et al., 2019; Le Corre et al., 2016). Notably, because females compensate for late departures by moving faster to the calving ground, one of the best predictors of movement speed during migration is departure date (Gurarie et al., 2019). Despite flexibility in migration speed and timing, disturbances and environmental conditions encountered during migration can significantly delay arrival to the calving ground and in some extreme examples, cause females to calve before they have reached the relative predator-free safety of their calving ground (Gurarie et al., 2019). With climate change, the amount and density of snow accumulation and the timing of snow melt are expected to undergo important regional shifts. Travelling through deeper

snow, and especially crust-covered snow is extremely costly for locomotion, even for a highly vagile species like caribou (Fancy and White, 1987). Accordingly, deep snow cover and deep wet snow following heavier spring snowfall has been linked to important delays in migration (Leclerc et al., 2021). The availability of freshwater ice during migration is also an important factor, as frozen lakes are typically windswept and characterized by less and more compact snow enabling faster and more efficient travel (Leclerc et al., 2021) and more visibility to avoid ambush by predators (Ferguson and Elkie, 2005). As the climate warms, many of the freshwater lakes in the Northern Hemisphere are breaking up sooner and freezing later (Sharma et al., 2019) and, consequently, migrating females now encounter breaking ice and open water more frequently in spring. This is especially worrisome for the many herds whose range overlaps the Canadian Shield, as freshwater features can cover up to 40% of the landscape. Indeed, in warmer springs the earlier transition of lakes from movement highways to movement barriers has resulted in longer migration routes (Leblond et al., 2016; Leclerc et al., 2021). While caribou are excellent swimmers, there is an increased risk of exhaustion, injury, and mortality when navigating areas with breaking ice (Miller and Gunn, 1986). In the Canadian Arctic Archipelago, migratory herds such as the Dolphin and Union herds and their Peary caribou counterparts further north require sea ice to access different parts of their range, including their winter range on the mainland, and absence of sea ice in some years has already disrupted seasonal migrations and will continue to pose a significant threat to these herds in the future (Jenkins et al., 2016; Miller, 1995; Miller et al., 2005; Poole et al., 2010). Disruptions in spring and fall migrations have also been observed as a direct consequence of anthropogenic

disturbances. Abandoned roads, active roads, and exploration and industrial activities related to mining are typically avoided by caribou and can divert migrating individuals resulting in longer routes and additional delays to reaching the calving ground or winter range (Boulanger et al., 2020; Johnson and Russell, 2014; Panzacchi et al., 2013; Wilson et al., 2016).

1.2.5 How can remote sensing contribute to caribou research?

Because the annual range of migratory caribou covers immense and remote regions, monitoring climate and weather, environmental conditions, and landscape changes at the spatial and temporal scales impacting caribou is extremely challenging. For example, the annual range of the Bathurst herd spans 250,000 km² (Case et al., 1996) while the range of the Leaf River herd covers a staggering 663,810 km², larger than any country within continental Europe. Since the launch of the first Landsat missions in the 1970s, imagery of Earth's surface captured by satellites equipped with various sensors (e.g., optical, hyperspectral, microwave) has increased in abundance, frequency of capture, quality, and overall availability for civil research applications (Malenovský et al., 2012; Wulder et al., 2019). By enabling us to monitor environmental conditions over large and remote regions, remote sensing and Earth observation technologies have emerged as crucial contributors to our understanding of migratory caribou, the environmental drivers of their seasonal movements, and the changes unfolding on their ranges as a result of climate change and human development.

Satellite imagery captured by optical and hyperspectral sensors has provided researchers with the opportunity to track annual vegetation phenology and year to year vegetation changes during key periods of migratory caribou's annual cycle (Dearborn

and Danby, 2022). By exploiting the spectral properties of vegetation, indices such as the Normalized Difference Vegetation Index (NDVI; Rouse Jr et al., 1974) can help track phenological events such as the onset of spring greening, the peak greening observed in summer, and the subsequent browning as senescence progresses through late summer and autumn (e.g., Descals et al., 2020). Research tracking the evolution of nitrogen availability in fresh forage during the Arctic's spring green-up has demonstrated that its peak is typically correlated with the moment an annual NDVI time series reaches half of its maximum value (Doiron et al., 2013). This has allowed researchers to investigate the synchrony of caribou calving events across the Arctic in relation to the peak availability of nutritious forage to assess the incidence and extent of trophic mismatch and its downstream implications for population dynamics (Eikelenboom et al., 2021; Mallory et al., 2020; Paoli et al., 2018; Post and Forchhammer, 2008). Remote sensing technologies can also help distinguish between different types of habitats and vegetation community composition to study how caribou respond to seasonal or long-term changes in food availability throughout the post-calving period and summer months (Campeau et al., 2019; Rickbeil et al., 2018, 2017). In a rapidly warming Arctic, continuing to track the long-term changes in plant communities and the complex interactions that shape them (Kelsey et al., 2021; van der Wal and Stien, 2014) will be key to understanding potential impacts on caribou populations.

Weather monitoring satellites and derived data products have enabled the development of accurate insect harassment indices over large regions that are otherwise impossible to monitor. Predictive models based on insect traps, data from weather stations (including wind, temperature, and relative humidity), and landcover

classifications were used to develop indices enabling researchers to estimate the relative intensity of insect harassment throughout the Arctic summer (Witter et al., 2012). Using satellite-based weather and climate reanalysis datasets provided by NASA (Rienecker et al., 2011), researchers have expanded on these localised indices to provide standardized broad-scale daily mosquito and oestrid (botflies and warble flies) harassment indices over spring and summer ranges of all North American migratory caribou herds as far back as 1980 (Russell et al., 2013). Such insect harassment indices have been instrumental in understanding the spatio-temporal dynamics of caribou movement in summer and the cumulative negative effects on females that carry over into the following year's reproductive success (Johnson et al., 2022). Continued monitoring of these weather-insect-caribou dynamics is extremely important because the intensity and regionality of changes in insect harassment under future climate scenarios and their demographic impacts for caribou is still poorly understood (Koltz and Culler, 2021).

Although snow conditions are a key variable that determine how caribou access winter forage (Fancy and White, 1985), initiate migrations (Gurarie et al., 2019; Leclerc et al., 2021), and expend energy while travelling (Fancy and White, 1987), monitoring snow conditions with remote sensing data products remains extremely difficult. Snowfall and accumulation patterns are changing in many regions of the Arctic due to shifting evaporation and precipitation patterns arising from rapid warming and shorter sea-ice seasons (Lam et al., 2023; Park et al., 2013). While detecting the presence of snow and estimating snow-on and snow-off dates is relatively straightforward (Hall et al., 1995), the depth of the snowpack and its characteristics such as density are extremely difficult

to remotely sense at the fine spatial scales which are required to study caribou movement (Gurarie et al., 2019). Humidity, temperature, and wind action are important determinants of the characteristics of the snowpack (Helfricht et al., 2018), but in a warming Arctic the increased frequency of rain-on-snow events and thaw-freeze cycles (McCrystall et al., 2021) is transforming the density and granular structure of the snow, which requires further refinement of remote sensing methodologies to detect, interpret, and classify a wider range of optical and microwave properties (Dolant et al., 2018). Currently, most snow data products with a high temporal resolution are either derived from coarse optical imagery (Hall et al., 2023) or large-scale weather and climate models (Luoju et al., 2021). Higher-resolution and broader-attribute snowpack data may soon be readily available, given increased in-situ large scale monitoring efforts in the Arctic (e.g., Lam et al., 2023; McGrath et al., 2019) and new air- and space-borne radar sensors (Lemmetyinen et al., 2022; Rott et al., 2012; Tsang et al., 2022), which could greatly enhance understanding of fine-scale movement behaviour of caribou and many other species (Boelman et al., 2019).

The exponential increase in the quantity of satellite images available for analysis (Liu et al., 2018), notably as a result of the advent of open-access satellite image archives (Malenovský et al., 2012; Wulder et al., 2019), represents both a research opportunity and a challenge. Because the environmental drivers of caribou populations and movements operate both at local (individual's immediate surroundings) and landscape spatial scales (herd's entire range), and these local and landscape scales are characterized by relevant daily, seasonal, and multi-annual change, researchers require remote sensing data products with large spatial extents and high spatial

resolutions, as well as long time series with frequent observations. As such, researchers must often negotiate trade offs between spatial and temporal resolution, choosing between: (i) coarse but frequently captured images to account for daily variations in environmental conditions, or (ii) high-resolution images to capture conditions in the immediate landscape that can be related to fine-scale movement and selection. Furthermore, these approaches frequently require prohibitively large image collections that are difficult to analyze with traditional computational resources, a problem now faced across many remote sensing disciplines (Chi et al., 2016). Cloud computing platforms such as Google Earth Engine (Gorelick et al., 2017) and the Sentinel Application Platform (ESA, 2023) have effectively democratized the tools required to access large image archives and perform geospatial analyses at planetary scales. Many recent advances in our understanding of caribou behaviour and dynamics have relied on such tools, including advances in our understanding of the timing of migration and calving (Couriot et al., 2023; Gurarie et al., 2019; John et al., 2020; Laforge et al., 2021) and our ability to map and classify important forage communities over large areas (Macander et al., 2020) or track their change over time (Konkolics et al., 2021). While several knowledge gaps still exist due to the resolution of data products (e.g., snow), in the next section we will discuss how abundant Earth observation data can be harnessed to answer questions about a future with declining availability of freshwater ice, another key form of environmental change known to influence caribou migrations.

1.2.6 How can remote sensing contribute to monitoring freshwater ice phenology?

Because of its cultural, socio-economic, and ecological importance, freshwater ice has been monitored by humans for centuries. For some lakes of particular importance, there exists archives of ice-on and ice-off dates consistently recorded for over 500 years (Sharma et al., 2022). These records, and more recently satellite records, have revealed that freshwater lakes and their seasonal ice-cover are true sentinels of global climate trends (Adrian et al., 2009). As a result of a rapidly warming Arctic (Rantanen et al., 2022), increased air temperatures are causing lakes to freeze later in autumn and breakup earlier in spring (Sharma et al., 2019) and experts estimate that the ice-free season is growing at a rate of 12.3 days/century, a trend which is observed both in historical ice records (Magnuson et al., 2000) and satellite records (Du et al., 2017). These changes are especially alarming in Canada's North as its landscapes are characterized by the highest density of freshwater lakes in the world (Messenger et al., 2016), frequently covering 15%-40% of the landscape by area (Duguay et al., 2003). The decrease in ice-cover duration will have important effects for: (i) transportation and northern economies (Prowse et al., 2009), (ii) regional changes in weather and climate (Prowse et al., 2011), and (iii) terrestrial (Leblond et al., 2016) and freshwater ecosystems (Adrian et al., 2006; Reist et al., 2006). Understanding and tracking changes in lake ice phenology is therefore an important priority for cold-climate research and dedicated government agencies (e.g., United States National Ice Center, Canadian Ice Service) have expended large efforts to monitor both sea ice and freshwater ice using remote sensing technologies.

Detecting the presence or absence of ice with satellite imagery has become a crucial part of tracking lake ice, especially if large areas are being monitored and there are a large number of lakes of interest. Detection of phenological events like spring breakup or fall freeze-up, which need to be defined at day-to-week timescales, typically requires imagery captured by satellites that frequently revisit the same location. As such, current broad scale monitoring efforts have favoured imagery with high temporal resolution and, in an effort to build longer time series of lake ice, have targeted a limited collection of larger lakes which often have complementary historical records that pre-date satellite archives (Latifovic and Pouliot, 2007; Lenormand et al., 2002; Magnuson et al., 2000; Sharma et al., 2019). While satellites such as AVHRR and more recently MODIS are perfect for these applications, their coarse spatial resolution (> 500 m) makes them unsuitable for monitoring smaller lakes. Importantly, most lakes are small (Messenger et al., 2016) and, relative to larger lakes and terrestrial ecosystems, they are likely to be most responsive to environmental change (McCarthy et al., 2023) and have shown to be extremely important contributors to geochemical cycles, including through carbon and greenhouse gas emissions (Holgerson and Raymond, 2016; Pi et al., 2022). Monitoring ice phenology in these smaller lakes is more challenging, as sensors that capture high-resolution images (e.g., < 30 metre pixels) are deployed on satellites that follow low polar orbits and do not frequently revisit the same area (e.g., Landsat 8 ETM+ or Sentinel-2 MSI imagery).

In recent years, efforts to include smaller lakes and rivers in broad scale ice monitoring projects have multiplied. Undoubtedly, the staggering quantity and quality of images collected by the European Space Agency's Sentinel missions have been

instrumental in these efforts. For example, Sentinel-2 MSI optical sensors have a spatial resolution of 10 metres and are deployed on 2 satellites, allowing a combined revisit time of approximately 5 days. As a twin satellite mission, Sentinel-1's active synthetic aperture radar sensors achieve similar revisit times and capture images at a 10- to 40-metre resolution (Torres et al., 2012). Sentinel-1 SAR imagery is especially useful for detecting lake ice in conditions that are limiting to optical sensors, such as periods of heavy cloud cover and short-day winter months, making it an especially powerful tool to track ice phenology at higher latitudes (e.g., Murfitt and Duguay, 2020). Capitalizing on the abundance of imagery captured by Sentinel-1 and Sentinel-2, the Copernicus Land Monitoring Service (CLMS) has developed the Aggregated River and Lake Ice Extent data product which provides daily waterbody-based ice cover statistics from 20-m resolution ice-water classifications over the entire European subcontinent (CLMS, 2023a, 2023b), an unprecedented endeavour. For North America, the only comparable data products are limited to larger lakes as they are typically based on coarser imagery (500 metres) such as the ESA's Lakes Climate Change Initiative product that uses MODIS sensors (e.g., Crétaux et al., 2021) and the Copernicus Global Land Service's (CGLS) Lake Ice Extent product which relies on Sentinel-3 SLSTR (CGLS, 2023).

Monitoring lake ice phenology at a spatial and temporal scale that is relevant for studying caribou migration, and indeed many other applications, highlights the important challenges we have discussed regarding the typical trade-off between spatial and temporal resolution of satellite data products. Migrating caribou movements are mediated by fine-scale responses to the presence of ice and water in the surrounding landscape (Leblond et al., 2016), but due to limitations in spatial resolution of freshwater

ice products we currently lack the ability to: (i) investigate the effects of ice phenology in smaller lakes (< 600 km²) and (ii) identify the transitional states between water and ice (forming or breaking) which can be especially critical for caribou (Miller and Gunn, 1986).

1.2.7 How do we monitor caribou movement?

Humans have carefully studied animal movements for many millennia, essentially for as long as they have relied on hunting as a source of food. Archeological description of, for example, caribou fences (Van Der Sluijs et al., 2020), buffalo jumps (Frison, 1970), and fish weirs (Prince, 2005) highlight the antiquity of First Peoples intimate understanding of animal movement patterns and tendencies. The question of why animals move shows up very early in what we often consider to be the roots of scientific and philosophical inquiry in the Western world, the classical Greek era, with notable works such as Aristotle's *De Motu Animalium* (On the Movement of Animals) (Joo et al., 2022; Nathan et al., 2008). Until relatively recently, animal movements were mainly monitored through direct observation of animals or tracking of their footprints and scat. However, with the wider adoption of mark-recapture methods that began with bird banding efforts in the 19th century (Wood, 1945) and wildlife telemetry methods (e.g. radio and GPS collars, biologgers) that rose to prominence in the latter half of the 20th century (Wilmers et al., 2015), broad-scale analyses of individual and population movement behaviour have become an important area of investigation in understand the spatial and temporal dynamics that mediate population structures (i.e., gene flow) and dynamics (Nathan et al., 2008).

The use of telemetry collars is especially well suited to studying larger and highly vagile species (Hofman et al., 2019; Joo et al., 2022) such as caribou. Since the first deployments of VHF-equipped collars on migratory caribou herds in Alaska in the 1970s (Davis and Valkenburg, 1979) and the later adoption of GPS-equipped collars first deployed on eastern migratory herds in the 1990s (Rodgers, 2001), telemetry collars have been central to research and management of caribou herds (Bergerud et al., 2008), providing incredible insights into their use of space and seasonal cycles (Nagy, 2011), their population dynamics (Rivest et al., 1998), and the effects of environmental changes (Sharma et al., 2009) and disturbances (Boulanger et al., 2021; Wilson et al., 2016). In the last two decades, the deployment of a variety of biologgers on caribou and reindeer, including accelerometers, heart rate monitors, and cameras, have provided unprecedented insights into their daily cycles (Arnold et al., 2018), seasonal energetics (Trondrud et al., 2021), responses to stressors (Ugland, 2021), forage preferences (Béland et al., 2023), and calf survival (Vuillaume et al., 2021). While the contributions of these monitoring methods have been instrumental to caribou research, they require capturing individuals which is not without risk. With new technologies, such as genotyping or biochemical analysis of hair or scat, providing less invasive alternatives to some of these monitoring methods, it is essential to understand and report the overall effects of stress experienced by individuals as a result of capture (McIntyre, 2015).

1.2.8 How can capture and collaring affect caribou movement and survival?

Biologging technologies such as accelerometers and GPS collars have been lauded for reducing observer effects on the behaviour of wildlife (Brown et al., 2013), but they do require the capture and immobilization of individuals which causes stress

that can potentially introduce bias to sampled observations or negatively impact condition, survival, and reproduction (Ugland, 2021). The impacts of capture and collaring can vary widely between species and individuals, ranging from minor (e.g., elevated heart rate) to severe (e.g., mortality) and from immediate (e.g., disorientation) to long-term (e.g., reproductive success) (Rachlow et al., 2014). Some effects, such as stress responses (e.g., increased temperature, combativeness), injuries, or mortalities, can be directly monitored and observed during capture and handling, and have been widely documented for many species (Arnemo et al., 2006). However, other direct (e.g., capture myopathy) or indirect (e.g., vulnerability to predation) effects of capture-related stress may be harder to detect as they only manifest in the days to weeks after an animal is released. For example, capture myopathy can occur in as little as a few minutes and up to 30 days after an individual is released (Beringer et al., 1996). Capture myopathy is an often fatal disease caused by a metabolic shock from stress-induced muscle exertion as a result of chase, capture, handling, and transport (Breed et al., 2019; Paterson, 2014; Spraker, 1993). Capture myopathy is more prevalent in ungulates relative to other mammals (Paterson, 2014) and it remains especially difficult to confirm without close observation or necropsy of muscle tissues, which is usually impossible in most remote wilderness areas. Among ungulates, sub-lethal effects of capture-related stress can include increased or decreased movement rates during a habituation period (Dechen Quinn et al., 2012; Jung et al., 2019; Stabach et al., 2020), permanent changes in movement behaviour as a result of heavier collars (Brooks et al., 2008), deteriorated body condition after repeated recaptures (Borquet, 2020), and shifts in behavioural responses to potential threats (Trondrud et al., 2022; Ugland, 2021).

Capturing large animals like caribou most commonly requires an initial chase by helicopter (sometimes by snowmobile) to separate an individual from its conspecifics and position it safely for either chemical immobilization via dart-delivered anaesthetic or physical immobilization by net-gunning and physical restraints (Cattet, 2018). In the earliest deployments of telemetry collars on migratory caribou in the 1970s and 1980s, capture-related injuries and mortality related to dart or net design were more common (Valkenburg et al., 1999, 1983). However, through the knowledge gained from these early deployments on caribou and indeed many other species (Arnemo et al., 2006), there are now well-established protocols and guidelines for all methods related to capture and chemical or physical immobilization of caribou (Cattet, 2018, 2011; Kreeger et al., 2023). Capture-related mortalities are now much less common, and usually the result of longer interventions and handling such as those required for the reintroduction, relocation, and maternal penning efforts used in support of endangered mountain and boreal woodland caribou conservation (Chisana Caribou Recovery Team, 2010; Compton et al., 1995; Mathieu et al., 2022; St-Laurent and Dussault, 2012). Telemetry technologies have also greatly improved, and while the energetic penalty imposed by the heavy mass of first-generation GPS collars affected survival rates of individuals (Dau, 1997; Haskell and Ballard, 2007; Rasiulis et al., 2014), modern GPS collars are now more accurate and much lighter, improving the quality and frequency of sampled data and greatly reducing potential negative effects imposed by extra weight. Trondrud et al. (2022) conducted a thorough evaluation of the immediate, short- and long-term effects of repeated capture and handling events on Svalbard reindeer. By sampling condition indicators (e.g., mass, back fat), blood serum stress indicators (e.g., cortisol),

and estimates of activity collected with accelerometers and heart rate monitors, the authors demonstrated that recovery and return to baseline activities was typically swift for individuals recaptured yearly and that long-term effects such as reduced reproductive success only occurred in instances of multiple recaptures within the same year. While this intensive recapture study provides invaluable insights into the magnitude of stressors and the short and long-term stress responses of individuals, monitoring these stress responses in migratory caribou herds remains a challenge because their vast ranges constrain monitoring programs to single-capture study designs for which pre-capture activity baselines are extremely difficult to define.

Chapter 2 - Multi-sensor detection of spring breakup phenology of Canada's lakes

2.0 Abstract

The ice phenology of freshwater lakes throughout the Northern Hemisphere has undergone important climate-induced shifts over the past century. In Canada's North, where freshwater lakes and wetlands cover 15 to 40% of the landscape, monitoring ice phenology is vital to understand its impacts on climate, socio-economic, ecological, and hydrological systems. The rapid and dynamic nature of ice phenology events has restricted monitoring efforts to the use of satellite sensors with frequent revisit times (e.g., MODIS, AVHRR), but their low resolution (e.g., >500 m) limits observations to larger water bodies. However, the increased abundance of high-resolution open-access satellite imagery combined with the rise of cloud-computing technologies has provided opportunities to reduce the trade-off between temporal (i.e., revisit time) and spatial (i.e., pixel size) resolution allowing for lake ice monitoring over broad scales. In this study, we present the Open Pixel-based Earth eNginE Ice (OPEN-ICE) algorithm implemented in Google Earth Engine (GEE), which classifies imagery from multiple open-access optical sensors, then combines them to construct dense annual time series of ice-water observations and estimate pixel spring breakup dates at a 30-m resolution. Using Landsat 7 ETM+, Landsat 8 OLI, and Sentinel-2 MSI scenes over lakes spanning northern latitudes, we build reference datasets to train decision trees that discriminate between ice, water, and clouds. We combine ice-water classifications from each sensor into annual time series and remove misclassifications with a temporal filter applied using a pixel-wise logistic regression. We then detect the sequence of

transition from ice to water in each pixel's time series to estimate the occurrence of breakup each year. We deploy the OPEN-ICE algorithm over all freshwater pixels of Canada for the period of 2013 to 2021. Spring ice phenology events estimated by OPEN-ICE show high accuracy when compared to whole-lake breakup dates measured by the Canadian Ice Service in 105 lakes across 9 years, with mean bias errors of -1.10 and -0.69 days for breakup start and end, respectively. We apply the OPEN-ICE algorithm to 4000 lakes across Canada and evaluate differences in breakup dates across ecozones and lake sizes. Our new OPEN-ICE tool provides accurate estimates of annual spring breakup events applicable across all boreal and arctic regions to monitor the rapid changes taking place in these vulnerable ecosystems.

2.1 Introduction

In recent decades, Boreal and Arctic regions have undergone a disproportionately rapid warming compared to other regions of the globe (IPCC, 2014; Post et al., 2019), a trend which is expected to continue well into the next century. While much attention has focused on the impacts of warming on sea ice decline (Post et al., 2013; Stroeve et al., 2007), warming trends in boreal and arctic ecosystems have driven declines in the presence and duration of seasonal lake ice cover (Sharma et al., 2019). A vast majority of the world's freshwater occurs as ice, primarily as glaciers, but also in the form of frozen ground water or permafrost and seasonal ice cover on rivers and lakes (Peterson et al., 2019). Analyses indicate that of the globe's estimated 117 million freshwater lakes, most are situated within boreal and arctic latitudes (45°-75° N; Verpoorter et al., 2014), where annual ice cover is a central driver of lake ecology and biogeochemical processes (Hampton et al., 2017; Rautio et al., 2011; Wrona et al.,

2016). Lakes are particularly abundant in the Boreal and Arctic regions of Canada, where 15 to 40% of the landscape is covered by approximately 880 thousand lakes with a surface $> 0.1 \text{ km}^2$, the highest lake density in the world (Duguay et al., 2003; Messenger et al., 2016). Lakes smaller than 0.1 km^2 are also extremely abundant, as each drop of one order of magnitude in size results in a 10-fold increase in lakes (Messenger et al., 2016). In these systems, warmer air temperature speeds up melt onset and ice breakup in spring and delays freeze up in autumn (Higgins et al., 2021; Weyhenmeyer et al., 2004). Consequently, the length of the ice-free season has been increasing an average of 12.3 days/century (Magnuson et al., 2000) as observed consistently in historical ice records and satellite observations (Du et al., 2017; Sharma et al., 2019).

While the abundant lakes in Boreal and Arctic regions act as sentinels of climate change (Williamson et al., 2009), they also exert great influence on climate, geochemical, socio-economic, and ecological systems. For example, lakes are important contributors to regional and global climate via evaporation (Rouse et al., 2008) and gas exchanges (Woolway et al., 2020) during the ice-free season. Both ponds and small lakes in particular have emerged as important emitters of greenhouse gases in rapidly warming regions (Pi et al., 2022), and contribute more per unit area to the global carbon cycle than large lakes and terrestrial ecosystems (Downing, 2010; Holgerson and Raymond, 2016; Raymond et al., 2014). Northern economies are greatly dependent on lake ice for transportation in water dominated landscapes, be it through networks of ice roads which enable transportation of freight to communities in remote areas, or through trail networks enabling safe access to trap lines and hunting territories

on which Indigenous communities rely for harvesting traditional foods (Knoll et al., 2019; Prowse et al., 2009). Changes in ice phenology and consequently changes in the hydrological and thermal regimes of lakes, rivers, and wetlands have great implications for the seasonal cycles in both freshwater and terrestrial ecosystems. For example, shifts have been observed in species community structures with longer ice-free season (Adrian et al., 2006), earlier breakup has been linked to earlier out-migration of fish species (Reist et al., 2006), and later freeze-up dates have interfered with fall migration of barren-ground caribou (Leblond et al., 2016; Sharma et al., 2009). As a result, lake ice cover and thickness have been designated as two essential climate variables by the Global Climate Observing System (GCOS, 2021). Understanding and tracking changes in lake ice phenology is therefore an important priority for research in northern regions, including in smaller lakes which are more sensitive to climatic shifts (Adrian et al., 2009; Gerten and Adrian, 2001) and which are harder to monitor across large regions.

Considerable effort has been expended to develop sea ice detection methods using satellite sensors (Lyu et al., 2022; Sandven et al., 2023; Shokr and Sinha, 2015), yet most of these methods are not specifically tuned to provide accurate estimates of ice-on and ice-off dates critical to evaluating phenological patterns and trends over freshwater lakes. Because sea ice extent is spatially expansive and multiyear ice remains present during the long daylight conditions of arctic summers, sea ice dynamics can be well-described at monthly, annual, and decadal scales using low-spatial resolution optical or radar sensors (Shokr and Sinha, 2015). Remote sensing of lake ice phenology is more challenging because most lakes are small (Cael and Seekell, 2016; Messenger et al., 2016; Verpoorter et al., 2014), the spectral characteristics of lake water

are very diverse (Kallio et al., 2015), spring breakup and especially autumn freeze-up periods coincide with shorter photoperiods, and their dynamics occur across shorter time frames defined by hours and days rather than months and years (Duguay et al., 2015). As a result, lake ice phenology monitoring is constrained by methodological trade-offs between competing objectives of broad spatial coverage (e.g., the number of lakes or the size of the area assessed), high spatial resolution (i.e., pixel size or unit of observation), long time series duration (e.g., the number of years, decades or centuries monitored), and high temporal resolution (e.g., frequent and gap-free observations intervals). Reflecting the difficulty of achieving all four objectives simultaneously, studies of ice phenology in freshwater systems tend to be either (i) time series analyses focused on detecting change over time among a set of pre-selected, typically large lakes using in situ historical records (Duguay et al., 2006; Magnuson et al., 2000; Sharma et al., 2019) or low resolution but longer duration satellite sensors (Brown and Duguay, 2012; Du et al., 2017; Kropáček et al., 2013; Latifovic and Pouliot, 2007), (ii) spatial analyses of phenological differences observed across a smaller landscape or region (Murfitt and Brown, 2017; Zhang and Pavelsky, 2019), or (iii) using higher-resolution optical or radar satellite sensors over a limited spatial extent and across a handful of years (Antonova et al., 2016; Geldsetzer et al., 2010; Hoekstra et al., 2020; Murfitt and Duguay, 2020; Surdu et al., 2015; Wang et al., 2018).

Advances in Earth observation data collection and cloud-based processing platforms have enabled several monitoring projects to distil massive amounts of imagery into snow cover, sea ice, and lake ice data products with large spatial coverage. For example, analysts from the United States National Ice Center (USNIC)

use data from 13 satellite sensors to produce daily sea ice and terrestrial snow-cover estimates for the Northern Hemisphere at a 1-km spatial resolution using the Interactive Multisensor Snow and Ice Mapping System (IMS) (USNIC, 2008). The European Space Agency's (ESA) Lakes Climate Change Initiative uses MODIS Terra/Aqua imagery to produce lake ice cover maps for over 2000 lakes of the Northern Hemisphere at a 250-m resolution. The increased availability of open-access optical (Bevington et al., 2018; Drusch et al., 2012; Wulder et al., 2019) and radar (Torres et al., 2012) satellite imagery at a resolution of 30 m or less has created new opportunities to study lake ice phenology, allowing monitoring programs to reconcile the gap between high-resolution analyses covering small regions and low-resolution analyses covering large regions. For example, the Copernicus Land Monitoring Services (CLMS) produces the Aggregated River and Lake Ice Extent (ARLIE) data product (CLMS, 2023a), which combines lake ice classifications developed for radar and optical imagery from Sentinel-1 and Sentinel-2, respectively, to monitor lake ice phenology over Europe at a 20-m resolution.

In this study, we develop a fully automated algorithm named OPEN-ICE to monitor lake ice breakup phenology using optical imagery during the spring breakup season. We leverage open-access data and cloud computation tools to develop an algorithm that: (i) increases spatial resolution of lake ice phenology detection products currently available across Canada, (ii) improves temporal resolution relative to high-resolution single sensor methods by fusing observations from multiple sensors into a single time series, and (iii) is scalable to continental scales and easily extended to other regions of the Northern Hemisphere. To demonstrate the spatial resolution and geographical coverage, the accuracy, and the potential applications of OPEN-ICE, (i)

we use it to estimate spring breakup dates in all 30 m freshwater pixels of Canada, (ii) we extract lake-based breakup statistics to validate our data product using an observational dataset of 105 lakes, and (iii) describe regional difference in lake breakup dates in 4000 randomly selection lakes across Canada.

2.2 Data

2.2.1 High-resolution optical imagery

We draw on open-access imagery captured over Canada by the Landsat 7 ETM+, Landsat-8 OLI/TIRS and Sentinel-2 MSI sensors, specifically in the periods when the missions overlapped between 2013 and 2021. Given that parts of our study area (see Fig. 2.1) are situated at high latitudes ($> 60^\circ$ N) where lower sun elevation makes surface reflectance corrections unreliable (Campbell and Aarup, 1989; USGS, 2020), we opted for top-of-atmosphere (TOA) reflectance products. Specifically, for Landsat 7 ETM+ (L7) and Landsat 8 OLI (L8) we used the United States Geological Survey's (USGS) Collection 2 Tier-1 Level-1 TOA reflectance products (USGS, 2022a, 2022b) while for Sentinel-2 MSI (S2) we used the European Space Agency's (ESA) TOA reflectance Collection-1 Level-1C product (ESA, 2022). These datasets are pre-processed by the USGS and ESA and provide the highest standard of radiometric and geometric (i.e., sub-pixel spatial error) corrections available for TOA reflectance products from each sensor, making them the best suited products for time series analysis. L7's Collection 2 Tier-1 product includes a scan-line corrector (SLC) mask that flags valid pixels for individual bands. In our study we only included a pixel if a valid value was available in every spectral band, an approach which left gaps in most scenes. To conserve computational efficiency (Yin et al., 2017), we gap-filled values in a small

buffer up to 60 m (i.e., 2 pixels wide) by iteratively (8 times) computing an empty pixel's focal mean for each band based on values within a circular radius of 60 m. This conservative approach allowed us to reduce missing data in the core regions of scenes where gaps are seldom wider than 1 or 2 pixels, thereby providing denser time series to precisely estimate break-up dates, but not imputing large gaps at the edges of scenes. We accessed and analyzed all L7, L8, and S2 imagery in Google Earth Engine (GEE; Gorelick et al., 2017) using, respectively, the "LANDSAT/LE07/C02/T1_TOA", "LANDSAT/LC08/C02/T1_TOA", and "COPERNICUS/S2_HARMONIZED" image collections. Together these collections contain approximately 0.55 billion square kilometres of scenes captured over Canada in 2013, with combined coverage increasing to approximately 4.20 billion square kilometres by 2021 (see Suppl. Fig. 2.1A). The combined mean revisit time of these 3 collections was approximately 5 days in 2013 and 1 day by the end of our study period in 2021 (see Suppl. Fig. 2.1B), with S2 contributing to approximately 75% of observations used.

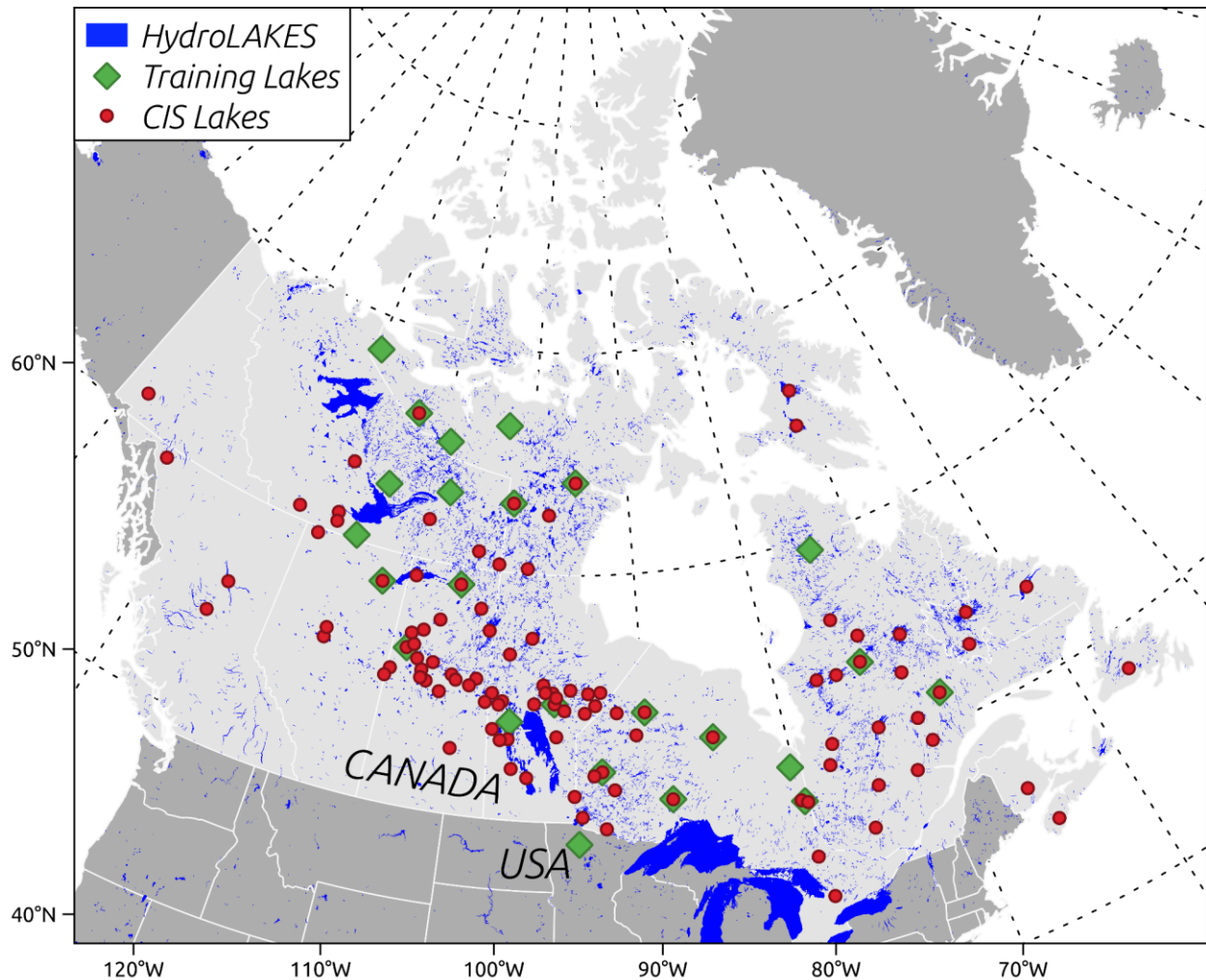


Figure 2.1 Map illustrating the spatial extent of the study area, lake polygons from the HydroLAKES database (Messenger et al., 2016), the 24 lakes sampled for training data to build decision trees, and the 105 lakes monitored by the Canadian Ice Service and used for validating OPEN-ICE observations.

2.2.2 Canadian Ice Service lake ice data

We used the lake ice phenology database (Lenormand et al., 2002) maintained by the Canadian Ice Service (CIS) to compare and validate OPEN-ICE algorithm results. The CIS database is based on both in situ records and imagery acquired by optical and radar sensors (i.e., AVHRR, MODIS, RADARSAT) and subsequently analyzed, inspected, and interpreted by CIS ice experts and analysts in near real-time for operational use. Each week, the database is updated with the fraction (out of 10) of

ice cover in over 130 lakes in both Canada and the northern United States. We used CIS lakes in Canada for which records were available between 2013 and 2021, and we excluded large lakes separated into different zones within the CIS database, leaving a total of 105 lakes for validation (see Fig. 2.1). These 105 lakes span 3 orders of magnitude in size, ranging from 53 to 7167 km² of surface area.

2.2.3 Water mask

We limited all of our analyses to freshwater pixels associated with inland water bodies using a water mask layer derived from the Global Surface Water data product developed by the Joint Research Center (JRC) of the European Commission (Pekel et al., 2016). The JRC's data product provides per-pixel estimates of global surface water occurrence at a 30-m resolution throughout the Landsat archive (1984 to 2022). We defined our freshwater mask using a conservative threshold of 80% occurrence in the JRC data product. This global water mask presents two main advantages: (i) it includes lakes, rivers, and small water bodies sufficiently large to be captured by a 30-m pixel (i.e., > 0.0009 km²), and (ii) its accuracy and availability in Google Earth Engine facilitates the future extension of our methodology beyond our current study area to other regions of the Northern Hemisphere where freshwater ice is also seasonally abundant. Due to methodological constraints, the JRC surface water data product does not cover High Arctic regions north of 78° N.

2.2.4 HydroLAKES polygons

To produce the lake-based statistics outlined in our methodology, we used lake polygons from the HydroLAKES database (Messenger et al., 2016) to extract, aggregate, and summarize pixel values from satellite imagery and OPEN-ICE model outputs. The

HydroLAKES database maps lake area, volume, and other characteristics for lakes and reservoirs $>0.1 \text{ km}^2$ at their maximum historic extent, and it has been manually corrected to exclude rivers and fluvial features. We used these polygons: (i) to randomly sample spectral data from freshwater pixels in 24 lakes to train sensor-specific decision trees (see Section 2.3.1), (ii) to extract pixel breakup dates and other metrics from OPEN-ICE outputs to estimate lake-based breakup events and validate these with CIS records for 105 lakes (see Section 2.3.3), and (iii) to extract pixel breakup dates from OPEN-ICE outputs for 4000 lakes randomly sampled across Canada to describe regional patterns in the timing of breakup events (see Section 2.3.4).

2.3 Methods

2.3.1 Training ice-water classifiers for OPEN-ICE

To incorporate satellite imagery from different sensors as inputs for the OPEN-ICE algorithm, we first trained sensor-specific decision tree classifiers capable of discriminating water, ice, and clouds in optical imagery over freshwater lakes. We used the classification and regression tree (CART) method described by Breiman et al. (1984) which builds decision trees by recursively partitioning data into sub-groups (i.e., classes) using an optimal threshold for each explanatory variable. Henceforth, we refer to decision trees and CART models interchangeably. While not as sophisticated or powerful as more recently developed machine learning algorithms (Lawrence and Moran, 2015), decision tree models are simpler and more computationally efficient when predicting classes on new data (Maxwell et al., 2018), making them easier to interpret and to scale efficiently to large datasets of satellite imagery at continental and even global scales.

To build reference datasets for training classifiers, we visually inspected L7, L8, and S2 scenes acquired between 2013 and 2021 in winter, spring, and summer over 24 freshwater lakes (see Fig. 2.1 & Suppl. Table 2.1) spanning 3 orders of magnitude in surface area (60 to 4500 km²) and regularly distributed across north-american latitudes (48° to 70° N) and longitudes (68° to 120° W). For each sensor, we selected a total of 262, 233, and 245 images, respectively, representative of typical conditions over freshwater lakes in the period prior to, during, and post breakup. In order to streamline sampling, we chose images in which a given lake's surface was entirely covered by either water (including clear and turbid water), ice (including ice and snow-covered ice), or clouds. We attributed each scene its corresponding reference label (i.e., water, ice, clouds), then randomly sampled pixels from the portions of labelled scenes within the polygons of the 24 lakes. We sampled pixels' spectral data from bands in the visible (Blue, Green, Red), near infra-red (NIR) and short-wave infrared (SWIR1, SWIR2) range for each sensor. We also included multispectral indices previously shown to be helpful in discriminating between water, ice, and clouds such as the Normalized Difference Vegetation Index (NDVI; Rouse et al., 1974), the Normalized Difference Water Index (NDWI; McFeeters, 1996), the Normalized Difference Snow Index (NDSI; Kyle et al., 1978), the Automated Water Extraction Index (AWEI; Feyisa et al., 2014), and the Water-resistant Snow Index (WSI; Sharma et al., 2016). While spectral bands are bound between 0 and 1, the possible values for the multi-spectral indices range between -1 and 1 for normalized difference indices (NDVI, NDWI, NDSI, and WSI) and between -4.25 to 6.75 for AWEI. To ensure that indices were evaluated in the same parameter space as spectral bands, we linearly rescaled (i.e., min-max normalization)

each multispectral index's values from their respective minimum-maximum range to a fixed range of 0 to 1. For each sensor's reference dataset, we sampled approximately 2 to 3 scenes over each lake for each label, resulting in approximately 400,000 to 500,000 sampled pixels per label. Prior to model training, we randomly resampled each reference dataset to ensure balance between the three reference classes (He and Garcia, 2009). We randomly split each dataset into a train set (70%) for model training using the method described below and a test set (30%) for evaluating the performance of each final model.

Using the train sets, we developed decision trees for each sensor using a cross-validation (CV) procedure to optimize each tree's split rules (i.e., variables used to partition data) and maximum tree depth (i.e., number of splits used to partition data). While decision trees offer a powerful and simple solution to classification problems, they are prone to overfitting and require careful pruning to ensure their out-of-sample predictions remain accurate and robust to new observation (Pal and Mather, 2003). To train a decision tree robust to the variety of conditions in lakes across the study area, we implemented a spatial CV design (Wu et al., 2021) whereby we grouped all training samples by lake and divided them into 6 folds ($k = 6$) composed of observations from 4 randomly-selected lakes each. Using this grouped 6-fold CV strategy, we fit a decision tree to each unique combination of 5 folds ($k-1$) using the classification and regression tree (CART) method described by Breiman et al. (1984) and computed its predictive accuracy on observations in the remaining 4 lakes in the hold-out fold. Additionally, we tuned the decision tree's maximum tree depth parameter by repeating this CV procedure 10 times for each possible tree depth (ranging from 1 to 10). We chose the

optimal tree for each sensor based on the highest predictive accuracy on out-of-fold lakes. Once this final tuned model was selected for each sensor, we tested its overall predictive ability on the test data we set aside prior to model training. We computed overall model accuracy, Cohen's kappa, producer's accuracy, and user's accuracy (Congalton, 1991; Congalton and Green, 2019) as calculated from the confusion matrix of predicted versus reference classes in the test set. We performed these analyses in R (R Core Team, 2023) using the CART method implemented in the rpart package (Therneau and Atkinson, 2022) and the CV model training and tuning tools implemented in the caret package (Kuhn, 2008).

The performance and accuracy of CART models are sensitive to the quantity and the quality of input training data (Maxwell et al., 2018; Pal and Mather, 2003). To further test the robustness of our final decision trees, we built an additional reference dataset solely for testing the final CART models using scenes with mixed conditions. We selected 73, 88, and 74 images captured by L7, L8, and S2, respectively, which contained mixed conditions (e.g., mix of open water, ice, cloud cover) in the period prior to, during, and after breakup. In each image, we manually digitized polygons and identified them with their corresponding label (i.e., water, ice, clouds). For each sensor, we then sampled approximately 400,000 to 500,000 pixels per class from the labelled polygons. We repeated the testing procedure detailed above, whereby we tested the overall predictive ability of each CART model on the new test set of previously unseen observations sampled from mixed scenes. We computed overall model accuracy, Cohen's kappa, producer's accuracy, and user's accuracy as calculated from the confusion matrix of predicted versus reference classes in the test set.

2.3.2 Implementing the OPEN-ICE algorithm

To monitor spring breakup events, we developed the Open Pixel-based Earth eNgin Ice (hereby named OPEN-ICE) detection algorithm capable of flagging the day of the year at which a given freshwater pixel transitioned from ice to water (see Fig. 2.2). We identified L7, L8, and S2 imagery collections acquired over a given region during spring breakup (see Fig. 2.2A). Using the sensor-specific decision trees trained using the methods described in Section 2.3.1, we classified each image into ice and water (see Fig. 2.2B), and masked out clouds from all downstream analyses. We then combined all the classified imagery into a single cohesive time series to conduct pixel-wise analysis of ice and water presence over all freshwater pixels of Canada at a 30-m resolution (see Fig. 2.2C & D). We then identified the time of breakup for each pixel's time series in two main steps further detailed below: (i) we applied a temporal filter to remove misclassified ice and water in the time series (see Fig. 2.2E), and (ii) we then found the sequence of observations that matched a breakup sequence from ice to water (see Fig. 2.2F).

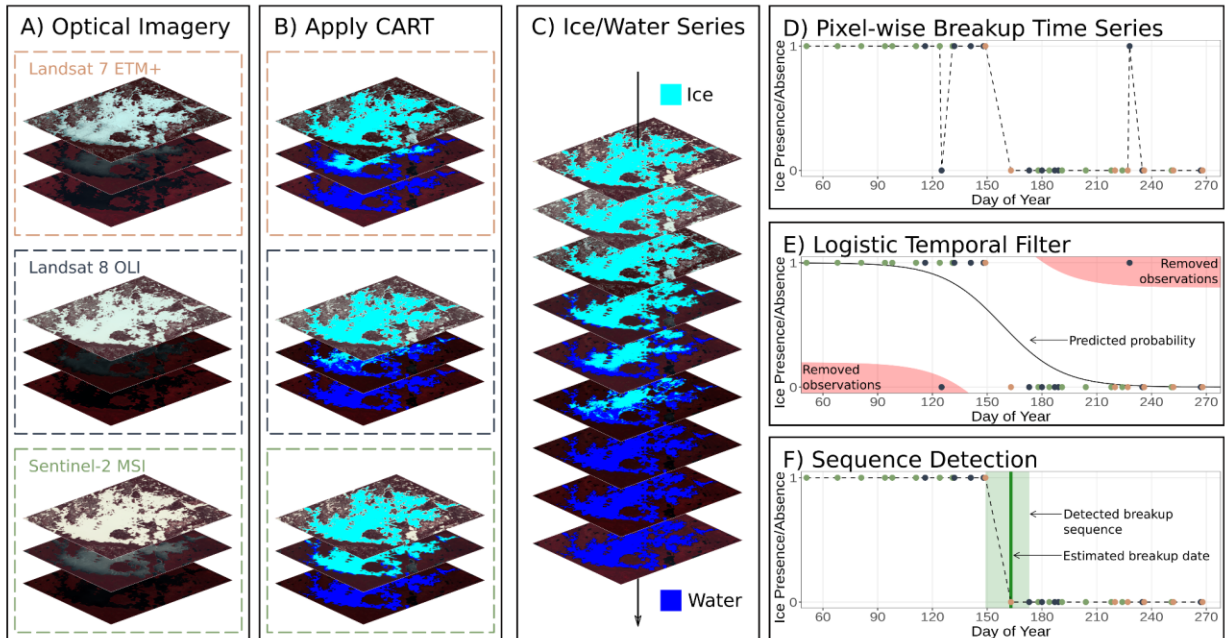


Figure 2.2 The OPEN-ICE algorithm estimates breakup dates in each pixel by: (A) identifying the images captured over an area of interest by the Landsat 7 ETM+, Landsat 8 OLI, and Sentinel-2 MSI optical sensors, (B) classifying images into water, ice, and clouds using previously trained and tuned sensor-specific CART models, (C) combining the classified images into a denser multi-sensor time series, (D) using a pixel-wise breakup time series to (E) compute a logistic temporal filter that removes erroneous classifications outside the putative ice breakup period (i.e., observations with a very large difference to the predicted probability of ice presence/absence), and (F) estimating the breakup date using a sliding window to detect the breakup sequence in each pixel.

We removed misclassified pixels using a temporal filter based on pixel-wise logistic regressions fitted to the whole observation set in each year (see Fig. 2.2E). Logistic regression offers a powerful statistical method (Neter et al., 1996) that can be used to model seasonal processes such as vegetation phenology (Li et al., 2019; Yang et al., 2019). Excluding the Great Lakes, most lakes in Canada usually freeze over completely in winter and thaw in spring or summer (Duguay et al., 2006). Using this prior knowledge, we assumed that within any given year, all pixels should transition from ice to water between February 15th and September 30th following a pattern similar to a logistic function. To fit the logistic regression in each pixel over this period, we used its

linearized form in which we defined the response variable as the log-odds obtained with the logit function, such that:

$$\text{logit } p(t) = \ln\left(\frac{ICE_t}{1-ICE_t}\right) = \beta_0 + \beta_1 t \quad (\text{Equation 2.1})$$

where t is time (i.e., day of year), β_0 and β_1 are the intercept and slope of the regression, ICE_t is the ice presence/absence at time t , and $p(t)$ is the probability of ice presence/absence at time t . To avoid the production of infinite values in the logit function, we added or subtracted a very small value (e.g., 0.0001) to ice presence (1) or absence (0) such that $\{ICE_t \in R \mid ICE_t \in (0,1)\}$. We fit the logistic regression of ice presence/absence over time using linear least squares, then solved for $p(t)$:

$$p(t) = \frac{e^{\beta_0 + \beta_1 t}}{1 + e^{\beta_0 + \beta_1 t}} \quad (\text{Equation 2.2})$$

which is the predicted probability of ice presence/absence (bound between 0 and 1) described by the sigmoidal curve observed in Fig. 2.2E. Using the predicted probability of ice presence/absence, we then filtered out misclassified pixels in the time series based on their residuals. Specifically, we removed values with absolute residuals higher than the conservative threshold of 0.85, which removed conspicuous misclassifications all while preserving any observations around the critical period during which a pixel transitions from ice to water (see Fig. 2.2E).

To estimate a pixel's breakup date, we used a sliding window to identify a sequence of three observations in its time series that matched a predefined breakup sequence. Given that lake breakup events can be highly dynamic (Ariano and Brown, 2019), a pixel may alternate between ice and water multiple times before it is completely

ice free. By design, the temporal filter described above conserves these transitional observations. Consequently, we defined the breakup sequence as the period in which an ice observation was followed by two consecutive water observations in the pixel's time series. When three observations matching this breakup sequence (i.e., ice-water-water) were identified in a pixel time series, we flagged the first water observation in that sequence as the date of breakup (see Fig. 2.2F).

The final output of OPEN-ICE consists of a raster image containing the estimated date of breakup for each 30-m freshwater pixel over a region of interest. In addition to the breakup date, we also recorded 3 metrics as indicators of the relative quality of the breakup date estimated in each pixel: (i) the coefficient of determination (R^2) of the logistic regression used as a temporal filter, (ii) the number of pixels that are ingested by the sequence detection routine after the temporal filter is applied and misclassifications have been removed, and (iii) the "sequence detection gap" (i.e., time elapsed between the last ice observation and the first water observation). Together these allow us to compare pixels and get a relative sense of the quality and quantity of input observations as well as the temporal uncertainty around our estimate of breakup date.

To ensure that OPEN-ICE remains scalable to broad spatial scales and to temporally dense image stacks, each step of the algorithm is implemented in Google Earth Engine (GEE; Gorelick et al., 2017) using its API for Python 3 (Van Rossum and Drake, 2009). As all OPEN-ICE outputs are set to 30-m resolution, GEE automatically resamples S2 imagery to match L7 and L8 prior to classification and ingestion in the algorithm. To estimate regression parameters, we employed GEE's only native parameter estimation function (see "ee.Reducer.linearRegression" in GEE

documentation) which implements a linear least squares method. As a demonstration of its capacity to handle large datasets, we applied the algorithm to every spring season between 2013 and 2021 over our entire study area (see Fig. 2.1) to produce a Canada-wide image with the estimated date of breakup for each 30-m freshwater pixel.

2.3.3 Evaluating the OPEN-ICE algorithm

2.3.3.1 Extracting lake breakup profiles and events from OPEN-ICE outputs

To allow comparison of OPEN-ICE outputs with the lake ice fraction observations of the CIS database, we extracted all pixel breakup dates (i.e., day of year) within a lake of interest's HydroLAKES polygon (see Fig. 2.3A). Using the relative frequencies of pixel breakup days, we constructed a time series of lake ice fractions, hereby referred to as a lake's breakup profile (see Fig. 2.3B). We then identified the lake's breakup events: breakup start and breakup end. Breakup start (BUS) is generally defined as the first day of the year that spring melt is observed in a lake, also known as melt onset (see Kang et al., 2012). Breakup end (BUE) is defined as the first day of the year a lake was free of ice. Following Kropáček et al. (2013), we accounted for false signals in small groups of pixels by flagging BUS and BUE when 5% and 95% of a lake's pixels, respectively, had transitioned from ice to water in the OPEN-ICE breakup profile (see Fig. 2.3B). For CIS breakup profiles, we flagged BUS as the last day of the year that the lake ice fraction was 10/10, and BUE as the first day of the year that the lake ice fraction was 0/10 (see Fig. 2.3B).

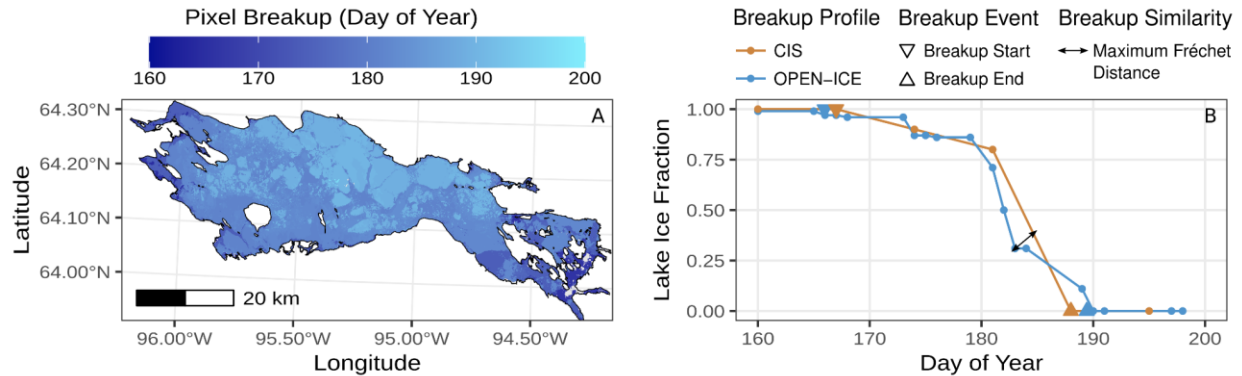


Figure 2.3 Methodology employed to compare OPEN-ICE outputs with Canadian Ice Service (CIS) lake ice fractions. (A) OPEN-ICE pixel breakup dates were extracted from a given lake's HydroLAKES polygon (here Baker Lake, Nunavut) and relative frequencies were used to construct (B) a breakup profile, composed of a time series of lake ice fractions, for comparison with CIS observations. OPEN-ICE was compared to CIS observations based on the timing of breakup events (breakup start and end) and the similarity of the breakup profiles (maximum Fréchet distance).

2.3.3.2 Comparing OPEN-ICE lake breakup events to CIS records

We used three metrics to evaluate the concordance between lake BUS and BUE dates estimated by OPEN-ICE with those recorded in the CIS database of lake ice fractions. We used mean absolute error (MAE) to estimate the overall error between observed dates from each dataset and mean bias error (MBE) to determine if the dates estimated by the OPEN-ICE algorithm systematically fell before or after the dates recorded in the CIS database (Willmott et al., 1985). To compare our results to several other studies, we also used Pearson's r as a metric of the linear correlation between breakup event observations in CIS vs OPEN-ICE.

2.3.3.3 Comparing OPEN-ICE lake breakup profiles to CIS records

We compared OPEN-ICE and CIS lake breakup profiles using two metrics allowing us to describe the similarity and synchrony of the time series of ice fractions and the trajectory of ice decline throughout the breakup period. First, we computed the

maximum Fréchet distance between each lake's OPEN-ICE and CIS breakup profiles (see Fig. 2.3B). The maximum Fréchet distance metric evaluates the similarity between the trajectory of two time series (Fréchet, 1906) and is analogous to the length of the leash required to keep a dog walker and his dog connected while they travel their respective paths. For each lake breakup profile, we take the maximum Fréchet distance as a metric of the difference in timing and profile trajectory for the entire breakup period. Maximum Fréchet distances (MFDs) are unitless and can be compared across profiles with larger distances indicating wider disagreement between the OPEN-ICE and CIS profiles in the period between BUS and BUE. Because all distances are calculated from the lake ice fraction and day of year, the MFD can be compared and provide a relative measure of the fit to the CIS profile. We computed MFDs using the *kmlShape* package (Genolini et al., 2016) implemented in R. Additionally, we computed an indicator, which we named "mean breakup lag", to estimate the temporal synchrony of ice proportions in the OPEN-ICE and CIS breakup profiles of a given lake. For a given lake, we calculated the difference in days at each incremental drop of 1% in ice cover between the OPEN-ICE and CIS breakup profiles and then computed the mean value for the entire period between BUS and BUE. While the MFD provides a relative measure of how closely the OPEN-ICE profile matches the CIS profile, the "mean breakup lag" provides a metric of temporal synchrony that informs us whether the OPEN-ICE breakup profile leads or lags behind the CIS profile in the period between BUS and BUE.

2.3.3.4 Evaluating OPEN-ICE's temporal logistic filter

In order to evaluate the performance of the temporal logistic filter in the OPEN-ICE algorithm (see Fig. 2.2E), we estimated breakup events and profiles for the 105

lakes monitored by the CIS using two implementations of OPEN-ICE, one with and one without the temporal filter. Using the outputs from each implementation of OPEN-ICE, we computed comparative metrics to evaluate their concordance with lake ice fraction data from the CIS database. Specifically, we computed mean bias error and mean absolute error for both BUS and BUE (see Section 2.3.3.2), as well as the maximum Fréchet distances (see Section 2.3.3.3). We checked if the temporal logistic filter improved the performance of OPEN-ICE by testing for significant reductions in mean error rates between metrics for each implementation of OPEN-ICE using a paired observation *t*-test.

2.3.4 Lake size and breakup timing across Canada

Using the OPEN-ICE algorithm's output data product, we investigated Canada-wide patterns of ice breakup dates between 2013 and 2021 over 4000 randomly-selected lakes distributed across 3 size classes and 15 ecozone regions. We separated lakes into 3 size classes according to their surface area as recorded in the HydroLAKES database: small (0.1 to 1 km²), medium (1 to 10 km²), and large (>10 km²) lakes. For each randomly selected lake, we estimated the BUE date (see Section 2.3.3.1) each year. Within each ecoregion, we evaluated differences in the distributions of BUE dates between size classes using pairwise Tukey's honest significant difference test (Tukey, 1949), a method that provides a one-step test of difference in means between multiple groups.

We also used OPEN-ICE outputs to explore the relationship between breakup events and spring air temperatures. Specifically, we studied the relationship between breakup events (BUS and BUE) across the 4000 randomly-selected lakes in 3 different

class sizes and the spring 0° C isotherm across 9 years. For each spring season between 2013 and 2021, we used the daily minimum (t_{min}) and maximum (t_{max}) temperature in 1-km grids available from the Daymet Version 4 dataset (Thornton et al., 2020) and calculated the rolling mean of the daily mean temperature ($\frac{t_{max} - t_{min}}{2}$) within a 31-day window. Within each grid cell, we recorded the first day of the year the mean temperature in the 31-day window rose to 0° C (Bonsal and Prowse, 2003). We used a lake's polygon centroid to extract the corresponding cell value from the grid and recorded it as the day the spring 0° C isotherm reached that lake. We tested the significance of the relationship between spring 0° C isotherm and breakup dates using linear models and used ANOVAs to test for significant differences between linear models with and without the lake size classes.

2.4 Results

2.4.1 Decision tree performance

The decision trees developed separately for L7, L8, and S2 exploit the low reflectance of water in the visible range and the low reflectance of snow and ice in the short-wave infrared range relative to clouds to generate high-accuracy classifications (see Fig. 2.4). In each train set, tuning the tree depth parameter with cross-validation resulted in a decision tree model with only 2 splits with 3 leaves, as each additional split resulted in negligible increases in classification accuracy. The L7 decision tree first uses the SWIR2 band to separate clouds and then Blue band to separate ice and water. Both L8 and S2 trees first use the Blue band to separate water and then NDSI, the normalized difference of Green and SWIR1, to separate snow and ice from clouds. The

overall accuracy and kappa metrics for the L7 decision tree are 96.6% and 94.9%, respectively. The L8 and S2 decision trees performed slightly better when applied to their test sets, with overall accuracies of 99.7% and 98.3% and kappa metrics of 99.6% and 97.4%, respectively. User's accuracy, the complementary metric of errors of commission (i.e., type 1 errors), ranges from 96.1% to 99.9% across all classes in all decision trees. Producer's accuracy, the complementary metric of errors of omission (i.e., type 2 errors), ranges from 93.9% to 100% across all classes in all decision trees. In the L7 decision tree, the producer's accuracy for ice is 93.9%, with the remaining 6.1% errors of omission roughly shared between ice misclassified as water and ice misclassified as clouds. While ice is correctly classified as ice by the L8 decision tree in 99.2% of cases, the producer's accuracy for ice in the S2 tree is 97.2%, with the remaining 2.8% errors of commission mainly due to ice misclassified as clouds. Overall, the decision trees tend to classify water with a higher producer's accuracy relative to ice and clouds, while ice is classified with the lowest producer's accuracy in each decision tree. The overall predictive accuracy of each sensor's decision tree model persists even when tested on a large reference test set sampled separately using different scenes with mixed conditions (see Suppl. Fig. 2.2).

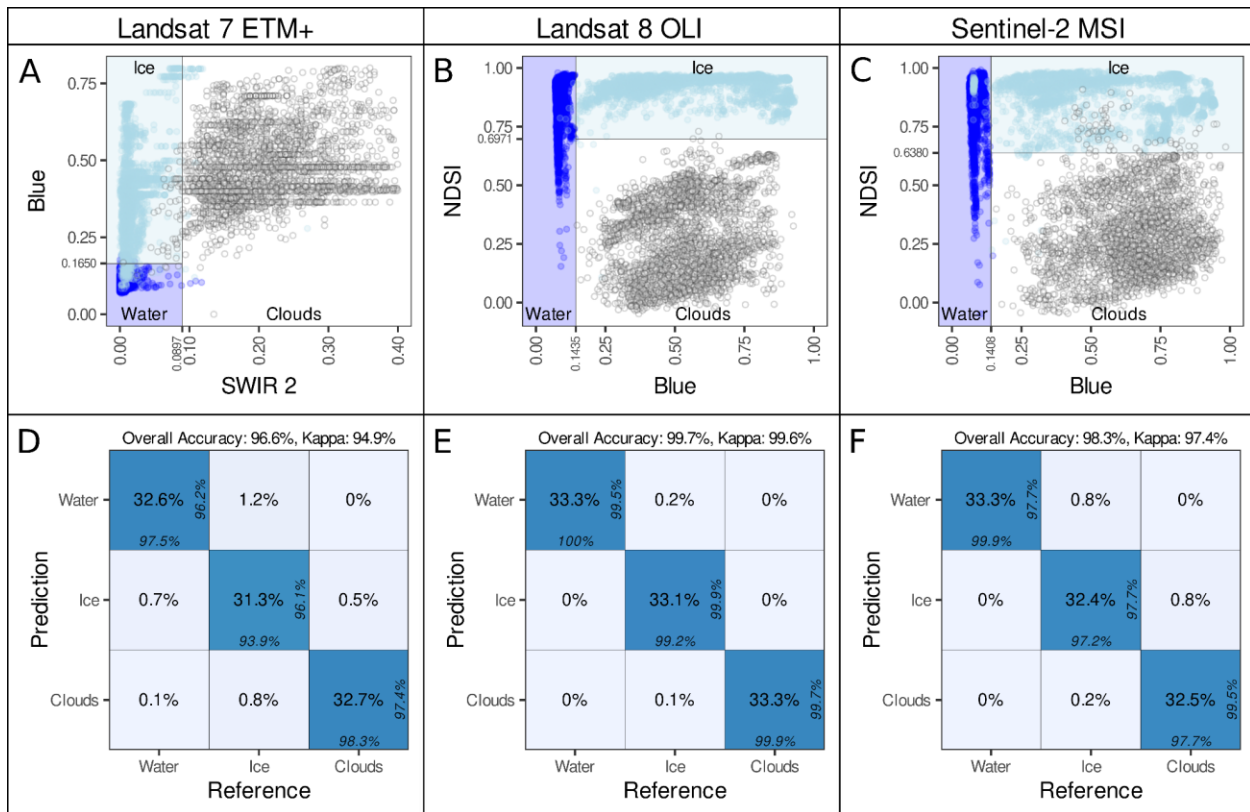


Figure 2.4 Structure and accuracy of tuned decision tree classifiers for Landsat 7 ETM+, Landsat 8 OLI, and Sentinel-2 MSI. The scatterplots (A, B, C) depict the thresholds that optimally classify the train set observations into water, ice, and clouds using sensor bands (Blue and Shortwave Infrared 2) or index (Normalized Difference Snow Index). Scales for each axis are displayed in the original range of each band (0 to 1) and index (-1 to 1). The confusion matrices (D, E, F) depict the percentage of test set observations accurately or erroneously classified by the tuned decision trees. Each diagonal tile includes producer's and user's accuracy at the bottom and on the right, respectively. The overall accuracy and kappa metrics are presented above each confusion matrix.

2.4.2 Lake-based validation of breakup events

The spring breakup start and end dates recorded by the CIS and estimated by the OPEN-ICE algorithm are very similar across all lakes in all years (see Fig. 2.5). In the 105 lakes used for validation, the earliest breakup starts were in late February at lower latitudes, while some lakes at higher latitudes started breakup as late as mid-July. By early August, even lakes at very high latitudes were completely free of ice. Lake ice phenology events observed by the CIS and OPEN-ICE are highly correlated with

Pearson's coefficient of correlation of 0.83 ($P < 0.001$) for BUS and 0.87 ($P < 0.001$) for BUE. Lakes with BUS in February and early March show slightly more divergence between datasets. Despite a temporal resolution of 7 days for CIS observations, the mean absolute errors are only 7.96 days and 7.92 days when compared to OPEN-ICE observations for BUS and BUE, respectively. The OPEN-ICE algorithm systematically observes BUS and BUE about 1 day earlier than the CIS, with mean bias errors of -1.10 days and -0.69 days, respectively.

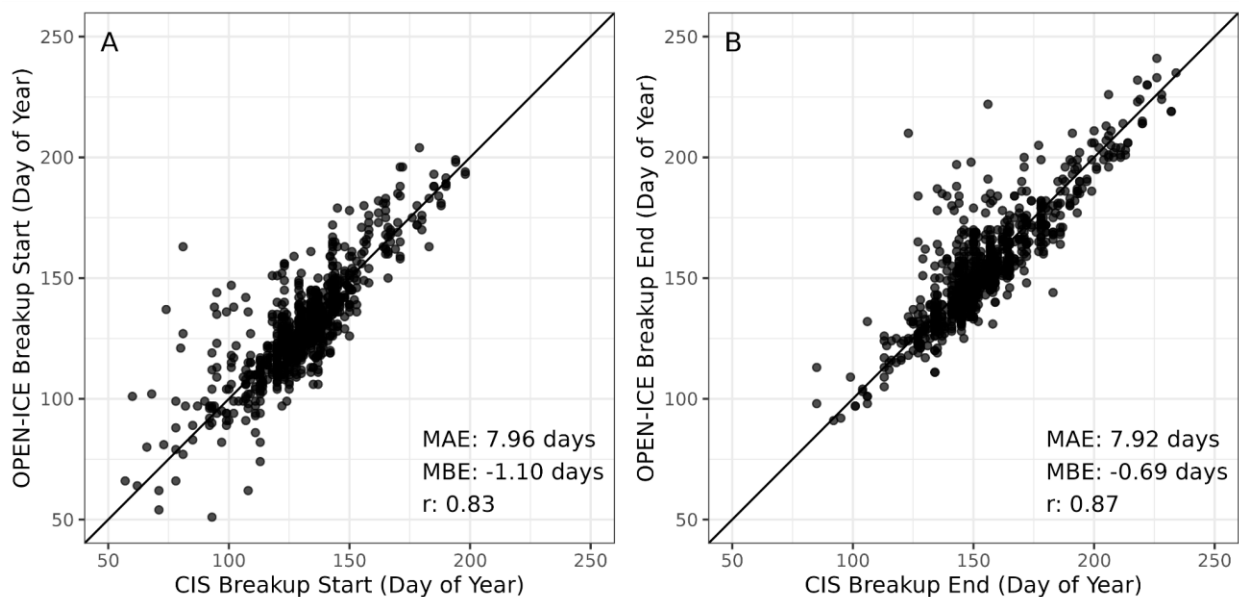


Figure 2.5 Comparison of spring (A) breakup start and (B) breakup end dates as observed by the OPEN-ICE algorithm and the Canadian Ice Service over 105 freshwater lakes between 2013 and 2021. The 1:1 ratio line is included alongside three model comparison metrics: the mean absolute error (MAE), the mean bias error (MBE), and Pearson's correlation coefficient (r).

2.4.3 Lake-based validation of breakup profiles

The breakup profiles extracted from OPEN-ICE outputs are similar to those described by CIS lake ice fractions. The mean of maximum Fréchet distances (MFDs) computed between OPEN-ICE and CIS breakup profiles, across 105 lakes and 9 spring

seasons, is approximately 4.63 (see Fig. 2.6 & Table 2.1). Most lake breakup profiles described by CIS lake ice fractions lag behind OPEN-ICE outputs by 0 to 5 days (see Fig. 2.6A), which aligns with the mean bias errors observed for BUS and BUE (see Fig. 2.5). Lakes with higher MFDs tend to be lakes where the overall CIS breakup profile lags behind OPEN-ICE (see Fig. 2.6A). Larger MFDs also occur in lakes with smaller mean sequence detection gaps (see Fig. 2.6B), which indicates that breakup profiles for lakes in which OPEN-ICE breakup estimates have an overall higher temporal precision tend to systematically lead over CIS breakup profiles. In most lakes, the mean sequence detection gap across all pixels is below 10 days (see Fig. 2.6B), though this varies throughout the study period as satellite observations increase (see Suppl. Fig. 2.4C).

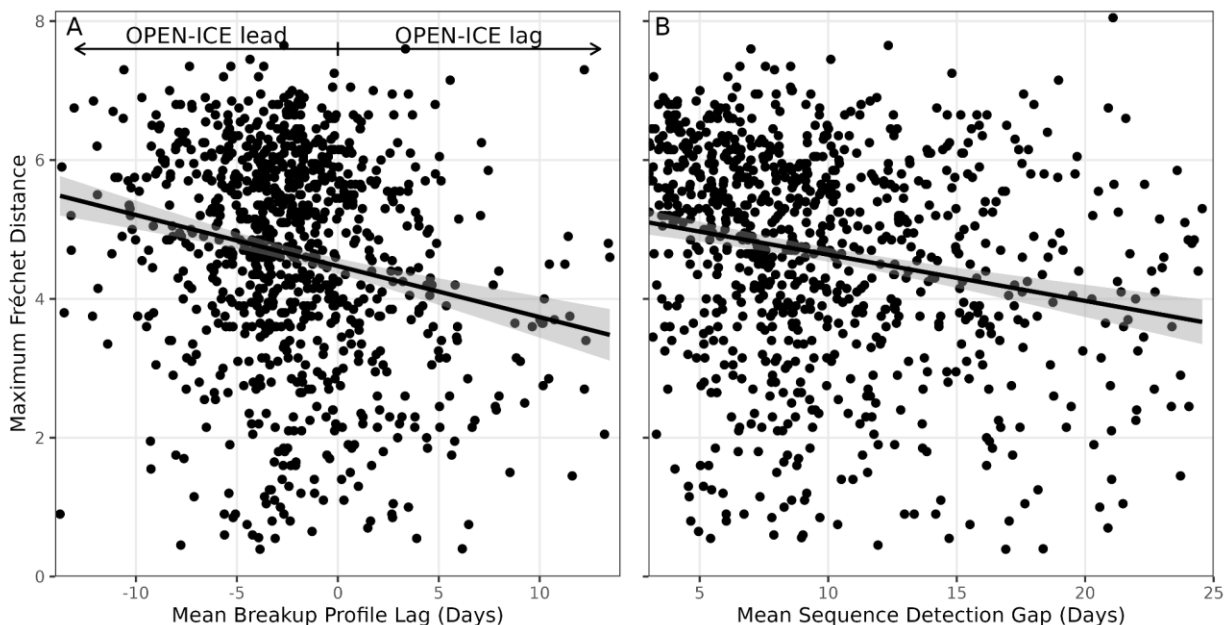


Figure 2.6 Maximum Fréchet distance between OPEN-ICE and CIS lake breakup profiles as a function of (A) the mean daily lag (in days) observed in CIS relative to

OPEN-ICE throughout a lake's breakup period, and (B) OPEN-ICE's sequence detection gap (in days) averaged over all pixels of a lake.

2.4.4 Evaluating OPEN-ICE's temporal filter

Most comparative metrics show increased agreement between CIS and OPEN-ICE breakup events and profiles (see Table 2.1) when OPEN-ICE is implemented with a pixel-wise temporal logistic filter to remove ice and water misclassifications in the time series prior to sequence detection (see Fig. 2.2E). Mean bias error of OPEN-ICE lake breakup events relative to CIS improves with the use of the temporal logistic filter, with BUS and BUE falling on average 0.67 ($P < 0.0001$) and 0.79 ($P < 0.0001$) days closer, respectively, to CIS breakup events. Mean absolute error for BUS is also reduced by 0.3 days ($P < 0.01$) when the temporal logistic filter is used, though no significant reduction occurs for BUE estimates ($P < 0.1$). Maximum Fréchet distances indicate that no significant changes ($P > 0.1$) occur in OPEN-ICE breakup profiles relative to CIS when the temporal logistic filter is used.

Table 2.1 Comparing accuracy and similarity metrics between Canadian Ice Service observations and the OPEN-ICE algorithm implemented with and without the pixel-wise logistic temporal filter (see Fig. 2.2E).

Metric	No Filter	Filter	Significance
BUS Mean Bias Error (days)	-1.47	-1.10	$P < 0.0001$
BUS Mean Absolute Error (days)	8.01	7.96	$P < 0.01$
BUE Mean Bias Error (days)	-1.59	-0.69	$P < 0.0001$
BUE Mean Absolute Error (days)	7.80	7.92	$P > 0.1$
Mean Maximum Fréchet Distance	4.69	4.63	$P < 0.01$

Bold typeface highlights significant ($P < 0.05$) differences in means from a paired observation t -test.

2.4.5 Spatial coverage and resolution of OPEN-ICE

The data product output by OPEN-ICE consists of a raster image with per-pixel estimates of spring breakup for a lake or region of interest any year between 2013 and 2021 (see Fig. 2.7 & Fig. 2.8). As a demonstration of the scalability of OPEN-ICE, we estimate spring ice breakup dates at a 30-m resolution for all freshwater pixels of Canada (see Fig. 2.7), an area spanning almost 10 million km². Despite the massive area analyzed, the OPEN-ICE data product provides sufficiently high resolution to support visual inspection of breakup patterns at small spatial scales. For example, the inspection of breakup dates in five lakes spanning five orders of magnitude in surface area (see Fig. 2.8) helps discern areas in each that are first- and last-to-thaw, with the former often in close proximity to shore and the latter most often in central open portions. Each pixel's breakup estimate is also accompanied by three indices of the relative quality of the breakup estimate (see Suppl. Fig. 2.3). These indices help visually discern areas where: (i) the temporal logistic filter performed adequately or poorly (see Suppl. Fig. 2.3C), (ii) the total observations ingested by the OPEN-ICE sequence detection routine were plentiful or scarce (see Suppl. Fig. 2.3D), and (iii) the sequence detection gap indicates low or high temporal accuracy of the resulting breakup estimate (see Suppl. Fig. 2.3E).

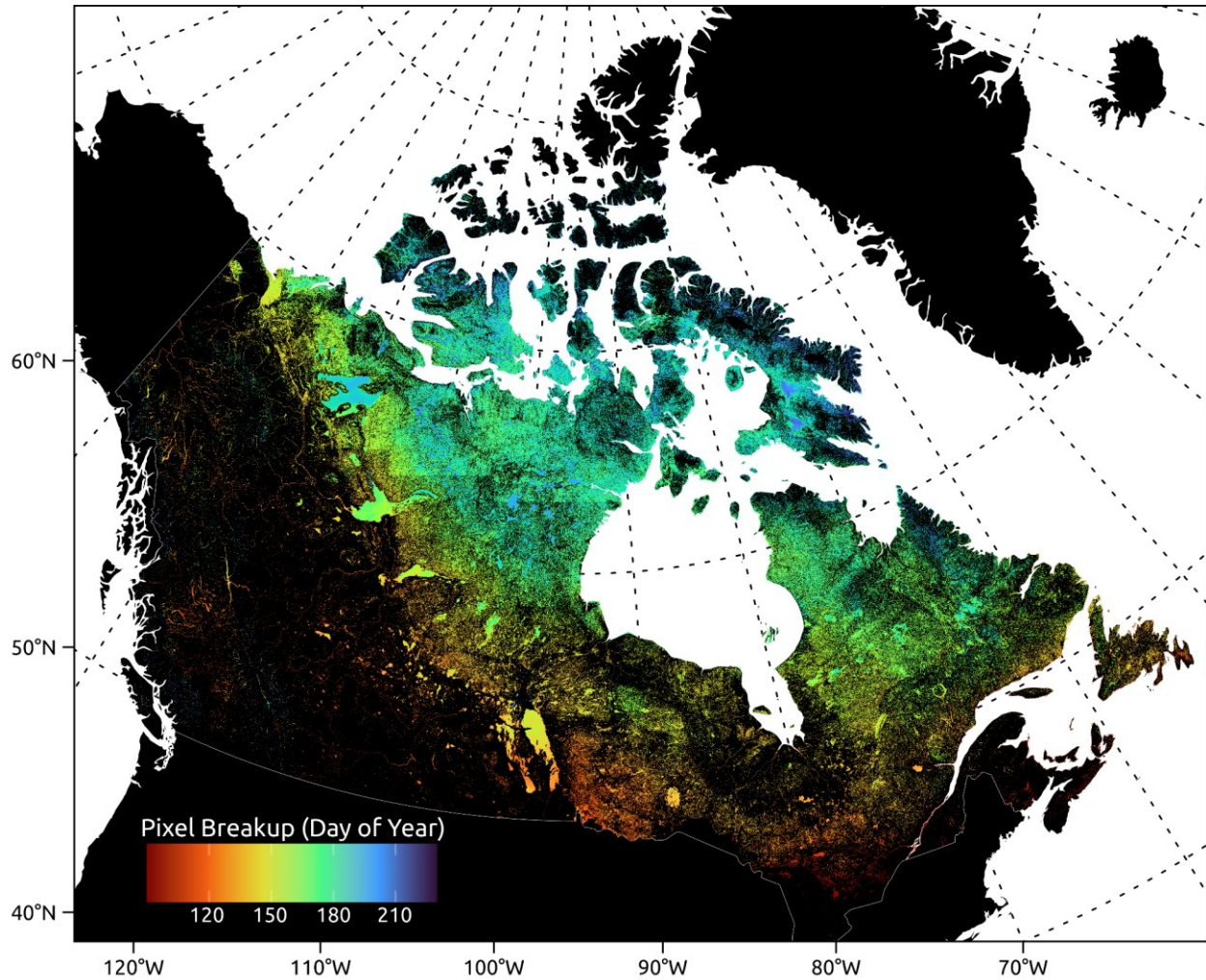


Figure 2.7 Map illustrating the pixel breakup (day of year a pixel transitioned from ice to water) estimated by the OPEN-ICE algorithm for all freshwater pixels of Canada during the spring of 2020 at a 30-m resolution.

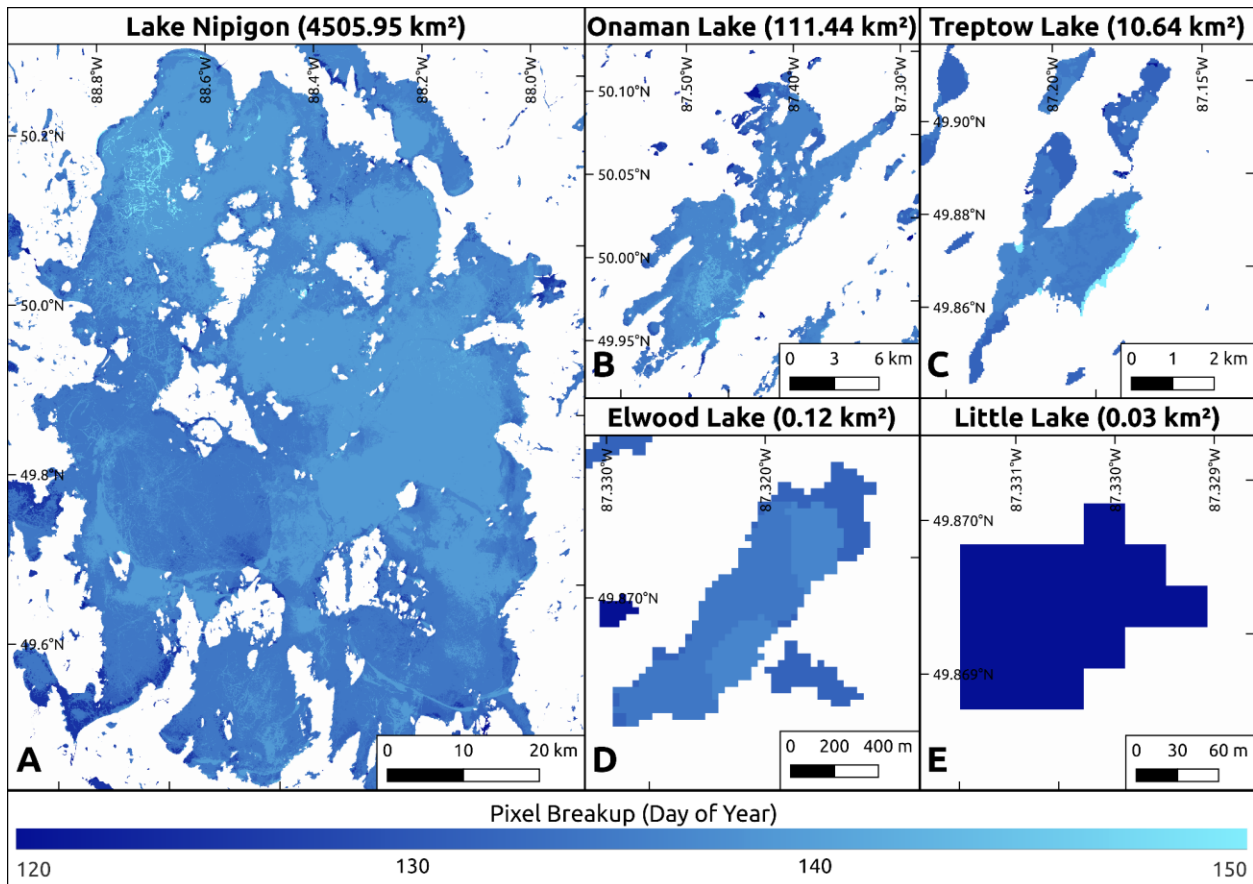


Figure 2.8 Map illustrating the spatial coverage and resolution of OPEN-ICE pixel breakup estimates (in day of year) over a 30-day period in 2020 across different lakes spanning five orders of magnitude in surface area. The lakes are: (A) Lake Nipigon which covers 4505.95 km², (B) Onaman Lake which covers 111.44 km², (C) Treptow Lake which covers 10.64 km², (D) Elwood Lake which covers 0.12 km², and (E) Little Lake which covers 0.03 km². All lakes are situated in the immediate region around Lake Nipigon in Northwestern Ontario.

2.5 Discussion

2.5.1 Sensor-specific decision trees developed for OPEN-ICE

To ensure the scalability of OPEN-ICE, we focused on developing simple decision trees to discriminate between water, ice, and clouds. To achieve this, we built a highly curated reference dataset with abundant observations (~1.5 million pixels per sensor) collected from over 740 unique images capturing prevalent conditions over 24 freshwater lakes (see Section 2.3.1). We trained simple sensor-specific decision trees

which exploited the different reflectance properties of ice, water, and clouds in the visible and shortwave infrared wavelengths (Warren, 2019). One minor difference is that the S2 and L8 decision trees use the NDSI index (Green and Shortwave Infrared). We attribute these different tree structures to: (i) the improved spectral resolution of the Green and Shortwave Infrared wavelengths in the OLI (see Roy et al., 2016) and MSI sensors relative to ETM+ providing improved discrimination of snow and clouds with the NDSI index and (ii) the high sensitivity of CART models to input training data (Pal and Mather, 2003). Given that the optical characteristics of freshwater can vary substantially by region and by season (Kallio et al., 2015), misclassifications may arise when these decision trees encounter uncommon conditions. For example, there is overlap between snow and clouds in the shortwave-infrared range of the spectrum when clouds are in ice phase (Warren, 2019), which explains the lower producer's accuracy for ice in all decision trees (see Fig. 2.4D, E, & F). The turbidity of water (Doxaran et al., 2002) and sun glint caused by waves (Wang and Bailey, 2001) can also increase the reflectance of water and create overlap with the visible wavelength signature of snow. While we included abundant observations from highly turbid lakes in our training data (e.g., see Lake Claire, Cedar Lake, Lake Abitibi, and MacAlpine Lake in Suppl. Table 2.1), we have found that in some cases sediment load (e.g., silt and clay), algal blooms, or whiting events (Effler et al., 1987) can cause extreme turbidity in lakes, which saturates the visible wavelengths (Luo et al., 2018) used by all three decision trees. In these rarer conditions, the consistently misclassified imagery ingested by the OPEN-ICE algorithm results in poor performance. However, the quality metrics included in the OPEN-ICE data product provide a useful tool for users to easily identify problematic water bodies

(e.g., see Lake Talbot in Suppl. Fig. 2.3). Although some rarer edge cases may perform poorly, there is a strong incentive to keep our classifiers as simple as possible. Because decision trees are simple and efficient (Pal and Mather, 2003), they allow us to classify massive quantities of high-resolution images quickly. This gain in computational efficiency (Maxwell et al., 2018) allows the OPEN-ICE algorithm to ingest dense multi-sensor time series of ice-water classifications which provide a temporal context with which to properly discern trends in individual pixels. Indeed, denser time series improve the ability of our temporal filter to identify misclassifications and increase the temporal precision of the estimated breakup events (see Suppl. Fig. 2.4 & Suppl. Fig. 2.5).

2.5.2 OPEN-ICE approach and quality assessment metrics

A key component of the OPEN-ICE algorithm is in its ability to capitalize on data abundance to identify and remove misclassifications using a temporal filter implemented with a logistic function. Logistic models provide an intuitive approach to modelling time series with phenological and seasonal patterns. For example, double logistic functions are used to model time series of vegetation phenology at broad scales using remote sensing data (Li et al., 2019; Yang et al., 2019). In adapting logistic regression as a filter to remove misclassified binary data, we have improved OPEN-ICE's breakup event estimates (see Table 2.1) without the need to filter outliers in time series using visual interpretation, temporal thresholds which may vary geographically according to seasonality (Latifovic and Pouliot, 2007), or regional statistics and temporal segmentation techniques (Du et al., 2017) that may become computationally expensive at broad spatial scales. This approach also avoids the use of weather and climate data products to temporally filter outliers (Zhang and Pavelsky, 2019) which precludes

subsequent independent empirical evaluations of ice-climate relations because air temperature, wind, and precipitation are inherent drivers of lake breakup processes (Gebre et al., 2014). Using an approach strictly based on climate-independent Earth observation data provides downstream users of OPEN-ICE with sufficiently high-resolution data to further investigate interactions between lake ice and climatic and physical processes (Brown and Duguay, 2010) or to validate thermodynamic lake ice models such as CLIMo (Duguay et al., 2003) across a larger distribution of lake sizes than those typically available in observational ice phenology databases like the CIS database (Lenormand et al., 2002) and the Global Lake and River Ice Phenology Database (Benson et al., 2000).

The temporal logistic filter (see Fig. 2.2E) and sequence detection algorithm (see Fig. 2.2F) also include valuable metrics we can provide users as indicators of the relative quality of pixels in the OPEN-ICE data product. The temporal logistic filter provides a coefficient of determination (R^2) which can be used to inform users how closely the time series of a given pixel (or group of pixels) matches our expectation of a clear signal of seasonal transition from ice to water. This tool allows users to assess the relative quality of OPEN-ICE breakup estimates in areas of interest, and helps them identify areas where the time series of spring breakup is noisy due to, for example, consistent ingestion of misclassifications from edge cases (see Suppl. Fig. 2.3). The sequence detection algorithm further provides us with two additional metrics: (i) the number of total observations ingested by the sequence detection algorithm (see Fig. 2.2E) as an indicator of the time series density, and (ii) the sequence detection gap (see Fig. 2.2F) as an indicator of the temporal precision of the breakup date estimate. In

addition to using these 3 metrics to investigate the performance of OPEN-ICE in regions of interest, we can also use them to describe broader patterns in temporal coverage of the algorithm in its current implementation using 3 sensors. Between 2013 and 2021, the combined amount of observations captured over Canada by all 3 sensors more than quadrupled (see Suppl. Fig. 2.1A). Throughout this period, we observe that in the 105 CIS lakes: 1) the mean R^2 of the logistic temporal filter increases (see Suppl. Fig. 2.4A), 2) the temporal density of observations increases (see Suppl. Fig. 2.4B), and 3) the mean pixel breakup gap decreases (see Suppl. Fig. 2.4C). These trends indicate that as OPEN-ICE ingests denser time series of classified imagery, the mean breakup gap decreases and the fit of the temporal filter increases as does, consequently, its ability to discern and remove misclassifications. These trends are further supported if we investigate these relationships across 4000 random lakes, where we observe clear signals that increases in time series density lead to higher temporal filter R^2 (see Suppl. Fig. 2.5A) and improved temporal resolution of breakup estimates (see Suppl. Fig. 2.5B).

2.5.3 OPEN-ICE accuracy

The data product output by the OPEN-ICE algorithm accurately detects the timing of breakup events in 105 lakes spanning all of Canada (see Fig. 2.5), a region containing 62% of the world's freshwater lakes larger than 0.1 km² (Messenger et al., 2016), over the period of 2013 to 2021. Breakup start and end dates observed using the OPEN-ICE data were highly correlated ($r = 0.83$ to 0.87) with those recorded by the CIS, with mean bias errors (MBE) around -1.1 and -0.69 days. In contrast, with literature reporting on lake breakup event extraction, the OPEN-ICE data product (30-m

resolution) was validated using more lakes across a larger area and presents either similar or improved accuracy. For example, Latifovic and Pouliot (2007) used temporal breakpoints of AVHRR (1-km resolution) spectral signatures extracted over the entire area of lakes of interest to predict BUS and BUE dates that were correlated by 0.66 and 0.95 with CIS events in 20 large lakes over a period of 20 years. Šmejkalová et al. (2016) used the MODIS near-infrared band (250-m resolution) to extract lake-wide spectral profiles and estimated BUE dates which had low mean bias errors (-1.38 days) and were correlated by 0.8 with in-situ observation data from 25 Finnish and Swedish lakes. Both these studies also tried to predict freeze-up dates, but the accuracy of their estimates was relatively low given the limited availability of optical imagery during freeze-up. Radar sensors provide a key solution to monitoring breakup events during periods of low light and cloud cover. Howell et al. (2009) used QuikSCAT imagery (10-km resolution) to estimate breakup and freeze-up events to within 8 to 14 days of the CIS records for two large lakes in Canada over a six year period. Du et al. (2017) used lake-wide radiometric profiles extracted from AMSR-E and AMSR2 images (5-km resolution) to produce breakup end and freeze-up end dates that were correlated by 0.86 and 0.69 with dates recorded by the CIS for 12 very large lakes between 2002 and 2015. Murfitt et al. (2018) developed a threshold-based method using RADARSAT-2 (100-m resolution) to estimate lake phenology events in 3 lakes between 2009 and 2017, with MBE relative to MODIS images ranging from -6.1 to 10 for freeze-up and -4.2 to 3.7 days for breakup end. Murfitt and Duguay (2020) used Otsu-threshold image segmentation methods to estimate lake phenology events in a High Arctic lake using the high density time series of Sentinel-1 (40-m resolution) over a 4 year period (2015-

2019), with MBEs ranging from -2 to -7 for breakup end dates and -6 to -10 for freeze-up relative to human interpreted Sentinel-2 images.

2.5.4 OPEN-ICE data product resolution and coverage

The OPEN-ICE data product currently provides users with spring breakup estimates at a 30-m resolution for all freshwater pixels of Canada over a 9 year period (2013-2021). The main advance in providing pixel-based estimates at this resolution is it enables monitoring of ice phenology in water bodies spanning several orders of magnitude in size (see Fig. 2.8) over vast regions (see Fig. 2.7). Small lakes have typically been excluded from large-scale lake ice monitoring efforts due to constraints in spatial resolution, despite their abundance (Messenger et al., 2016), their important combined surface area relative to other lake size classes (Verpoorter et al., 2014), and disproportionate contributions to atmospheric gas exchanges (Pi et al., 2022). Also, while the current study has focused on lakes, the OPEN-ICE data product can be used to monitor other water bodies like rivers. While there are diverse and powerful methods for remote sensing of lake ice, few are made available as data products for downstream operational use or large-scale monitoring efforts. The United States National Ice Center (USNIC) produces the Interactive Multisensor Snow and Ice Mapping System (IMS) (USNIC, 2008), a near real-time data product that tracks sea ice and snow cover at a 1-km resolution using analyst interpreted imagery from 13 different sensors (see Suppl. Table 2.2). In addition, the USNIC provides imagery from NASA's Terra/Aqua MODIS sensors that are processed into various snow cover and sea ice extent products at 250- to 500-m resolutions (Hall et al., 2006). While these two data products can be used and adapted to study lake ice over some large lakes, some data products specifically tuned

for monitoring lake ice over large regions have become available in recent years. For example, the Copernicus Global Land Service (CGLS) provides the Lake Ice Extent (LIE; CGLS, 2023) data product which, provides daily ice-water classifications of imagery from Sentinel-3 SLSTR (500-m resolution) in over 13,000 lakes of the Northern Hemisphere (see Suppl. Table 2.2) since 2021. Spanning 2000 to 2020, the European Space Agency's Lakes Climate Change Initiative (Crétaux et al., 2021) provides a longer time series of dedicated lake ice data products for over 2000 lakes of the Northern Hemisphere based on MODIS imagery (500-m resolution). The Copernicus Land Monitoring Service (CLMS) developed the ICE algorithm which it uses to produce the River and Lake Ice Extent (RLIE) data products for both Sentinel-2 (S2) and Sentinel-1 (S1) imagery, effectively providing dense time series of 20-m resolution ice-water classifications over the entire European subcontinent (see Suppl. Table 2.2; CLMS, 2023a). The CLMS further combines the S1 and S2 RLIE products into the Aggregated RLIE (ARLIE) data product by extracting ice cover statistics for all lakes and sections of some rivers of Europe, effectively monitoring breakup and freeze-up events using high resolution imagery at an unprecedented geographic scale.

In this study, we have exploited the abundance and overlap of L7, L8, and S2 imagery in the spring seasons of 2013 to 2021 (see Suppl. Fig. 2.1) to improve the temporal resolution of our breakup estimates relative to single-sensor approaches. At the beginning of our study period, we estimate that the combined L7 and L8 revisit time was approximately 4 days (see Suppl. Fig. 2.1B). As S2 missions became fully operational, combined revisit times dropped to approximately 1 day in the last 4 years of our study (see Suppl. Fig. 2.1B). Even with this frequency of captured images in the last

4 years, we found that across all 105 CIS lakes, the average lake mean of pixel breakup gaps varied from 6.36 days to 8.99 days (see Suppl. Fig. 2.4C). By design, the temporal resolution of the OPEN-ICE algorithm can be improved by ingesting images from other potential sensors of interest, so long as the imagery is classified into water and ice with a relatively high degree of accuracy prior to being incorporated into the time series analysis (see Fig. 2.2C, D, E, & F). For example, as the imagery from the Landsat 9 mission is currently available on GEE, we are actively developing a dedicated CART model to ingest ice-water classifications and improve the OPEN-ICE data product for the post-2021 period (see Suppl. Fig. 2.1). While abundant high-resolution optical imagery helps monitor spring breakup, the reduced daylight and lack of quality optical imagery in the freeze-up periods at higher latitudes make it very difficult to develop any form of automated algorithm (Duguay et al., 2015) over large geographical areas. To address this limitation, imagery from cloud-penetrating Synthetic Aperture Radar (SAR) sensors such as those deployed on Sentinel-1 (S1; Torres et al., 2012) could be used to fill gaps in the current time series and extend it to the fall freeze-up period. However, discriminating between ice and water in SAR data with high accuracy typically requires more complex classifiers such as random forests (Hoekstra et al., 2020), support vector machines (Wang et al., 2016), and neural networks (Dirscherl et al., 2021; Tom et al., 2020) which are more computationally expensive and harder to scale to massive datasets. Nonetheless, threshold-based methods can provide elegant and computationally efficient solutions to ice-water classifications (Stonevicius et al., 2022), some of which are even currently deployed for operational use. For example, the CLMS's RLIE Sentinel-1 data product provides near real-time ice-water classifications

based on single thresholds for each polarization channel (i.e., VV and VH) yielding an estimated accuracy of 76.7% (CLMS, 2023b). The CLMS further improves this product by fusing it with their S2 classifications to produce the ARLIE data product. Another method to improve the accuracy of threshold-based SAR classifications was explored by Murfitt and Duguay (2020), who applied Otsu-thresholding image segmentation (Otsu, 1979) to find optimal scene specific thresholds for lake ice and water. While this study was limited to a single lake, Otsu-thresholding methods have been successfully used in other applications (e.g., water detection) to analyze high-resolution remote sensing datasets at global scales on platforms like GEE (Donchyts et al., 2016). In the post-2015 period, the increased availability of high resolution open-access Sentinel-1 SAR imagery (Torres et al., 2012) provides unprecedented opportunities to monitor lake ice phenology in both small and large lakes across large regions during the fall freeze-up period and indeed throughout the entire ice phenology cycle. While in the future many other promising imagery datasets may be harnessed to improve the OPEN-ICE data product, we are committed to prioritizing open-access datasets available through the Google Earth Engine platform to ensure the algorithm remains easily reproducible over any area of interest by downstream users.

2.5.5 Variation in lake breakup dates across Canada

As a demonstration of the monitoring applications of the Canada-wide OPEN-ICE data product (see Fig. 2.7), we provide comparisons of breakup event statistics extracted from 4000 random lakes distributed across 15 different ecozones. Breakup end dates vary substantially across the range of lake sizes and ecozones (see Fig. 2.9). For example, lakes in the Arctic (Arctic Cordillera, Northern Arctic, Southern Arctic)

become ice free nearly 100 days later than those located at lower latitudes in Maritime and Mixedwood ecozones. Within Arctic, Taiga, and Boreal ecozones, the end of breakup in larger lakes ($> 10 \text{ km}^2$) is significantly delayed relative to other lake size classes, often by approximately 10-20 days (see Fig. 2.9B), a pattern which is less prominent in ecozones where spring breakup occurs earlier. This is likely because the breakup process of lakes in southern regions are more sensitive to changes in air temperature, while the prolonged exposure to extreme cold in lakes at higher latitudes creates thicker ice cover which withstands melting conditions longer in spring (Weyhenmeyer et al., 2011). Significant differences in breakup timing between lake size classes are not discernible in ecozones where regional climate is mediated by large water bodies (Pacific Maritime, Atlantic Maritime, Hudson Plain, Mixedwood Plain). Altitude is another important factor in lake ice phenology (Livingstone et al., 2010), and we can observe a higher variability of breakup dates in smaller lakes in regions dominated by mountains such as the Montane Cordillera and Pacific Maritime ecozones (see Fig. 2.9B).

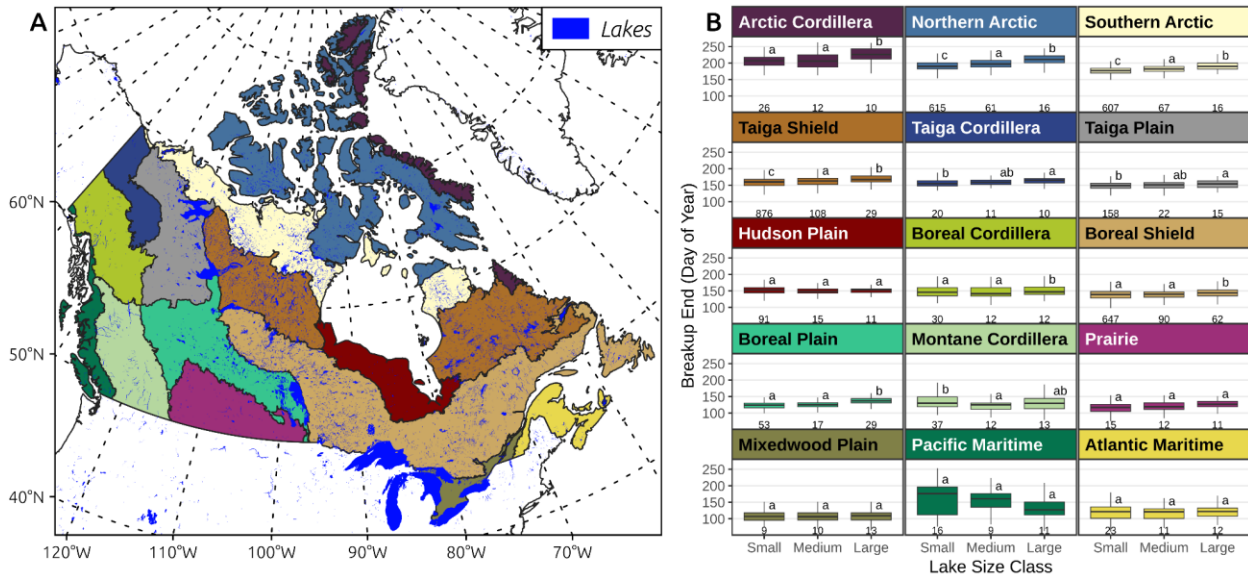


Figure 2.9 (A) Map of Canada's 15 ecozones with (B) the distribution of annual breakup end dates between 2013 and 2021 in randomly selected lakes ($n = 4000$) categorized into small ($0.1-1 \text{ km}^2$), medium ($1-10 \text{ km}^2$), and large ($>10 \text{ km}^2$) size classes. The lettering above each boxplot indicates similarities (shared letters) or statistically significant differences (different letters) between the distribution means of each lake size class within a given ecozone as indicated by the Tukey honest significant difference tests (see Section 2.3.4). The number of lakes for a given size class in each ecozone is displayed below each boxplot.

As previously explored in lake ice phenology literature (Bonsal and Prowse, 2003; Higgins et al., 2021), we found that air temperature provides an effective first-order prediction of both BUS and BUE. This was especially true for BUS dates, where air temperatures (spring 0°C isotherms) explained almost 81% of variability in dates between lakes (adjusted $R^2 = 0.8082$, $P < 0.0001$), across all lakes, ecozones, and years, with no discernible differences between lake size classes ($P = 0.6106$). Breakup typically starts 13.6 days after the air temperature reaches 0°C , regardless of lake class size (see Fig. 2.10A). However, the duration of the breakup period varies much more among lakes. This is because many other factors drive the breakup process, such as solar radiation (Cai et al., 2022), the size and morphometry of a lake, the current in the lake, the wind fetch, and the characteristics of the previous winter's snow pack (Ariano

and Brown, 2019; Jeffries and Morris, 2007). Nonetheless, Livingstone (1997) found that air temperature alone could account for approximately 60-70% of the variability in BUE dates of freshwater lakes. Using the OPEN-ICE data extracted for 4000 lakes, we also explained 69% of the variation in BUE dates (adjusted $R^2 = 0.6865$, $P < 0.0001$), but only once we included both the date of the spring 0°C isotherm and the lake size class as covariates to account for air temperature and lake heat storage, respectively. On average, we found that breakup ends approximately 28.8 days after the air temperature initially reaches 0°C for small lakes ($0.1\text{-}1\text{ km}^2$), while medium ($1\text{-}10\text{ km}^2$) and large ($> 10\text{ km}^2$) lakes become free of ice approximately 33.4 and 39.1 days after, respectively (see Fig. 2.10B). An in-depth empirical analysis of the drivers of BUS and BUE is beyond the scope of this paper but is made possible in the future using the HydroLAKES database (Messenger et al., 2016) to extract breakup statistics from the OPEN-ICE data product in the 880,000 lakes ($>0.1\text{ km}^2$) of Canada. As time series of high temporal density continue to be collected by multiple sensors, OPEN-ICE could be used to evaluate fine- and large-scale changes in the breakup of millions of lakes over longer periods in response to climate change. The strong relationship between breakup events and air temperature also stresses the importance of developing lake ice phenology products based solely on observational data to enable appropriate evaluation of deterministic relationships and feedback between climate and lake ice.

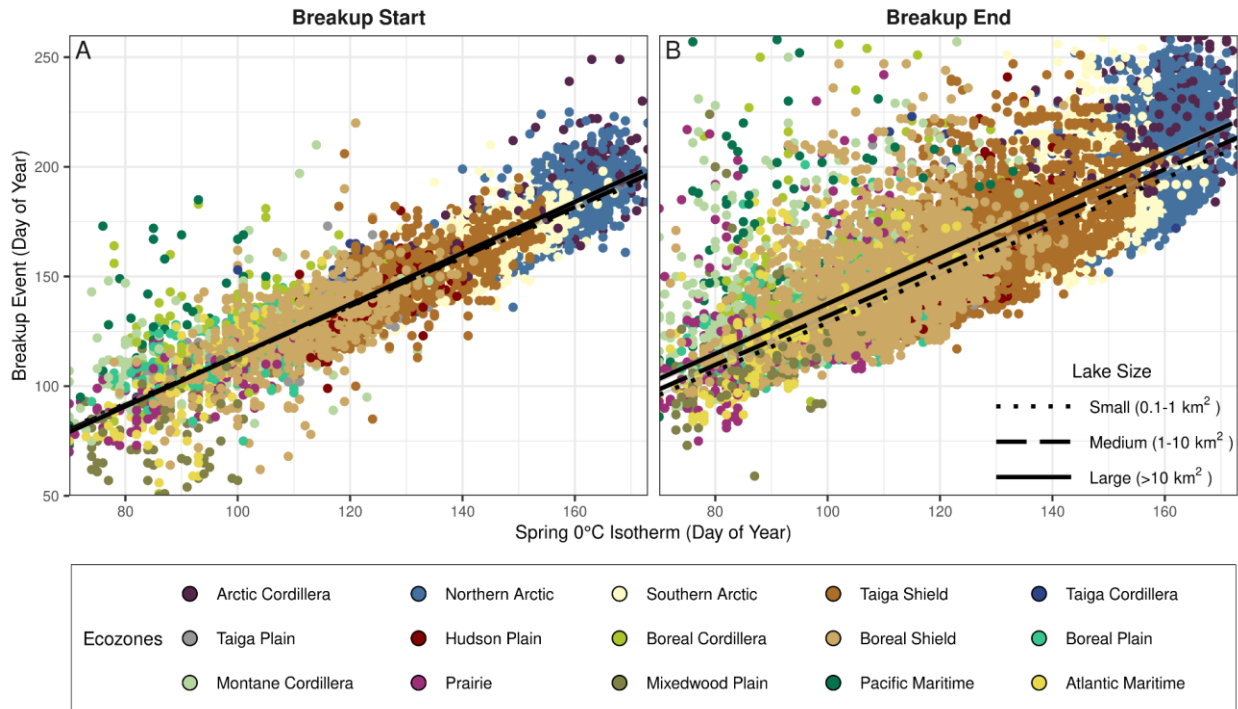


Figure 2.10 Scatterplot of (A) breakup start and (B) breakup end dates of randomly-sampled lakes ($n = 4000$) across 9 spring seasons (2013-2021) as a function of the day of year the spring 0°C isotherm reached each lake. Point colour represents the ecoregion of each lake. Dotted, dashed, and full lines represent the trendlines for small ($0.1\text{-}1\text{ km}^2$), medium ($1\text{-}10\text{ km}^2$), and large ($>10\text{ km}^2$), respectively.

2.6 Conclusion

Here we describe OPEN-ICE, a modular algorithm that can draw on imagery from multiple satellites to produce accurate high-resolution estimates of breakup dates across regions as broad as Canada. We showed how OPEN-ICE closely matches spring breakup events over 9 years in 105 lakes monitored by analysts of the CIS, thus providing a valuable post-hoc data product to complement near real-time CIS observations. OPEN-ICE further provides equal coverage of both very small ($< 0.01\text{ km}^2$) and very large lakes ($>10,000\text{ km}^2$), effectively allowing users to monitor spring breakup events in lakes with sizes ranging many orders of magnitude. The OPEN-ICE tool can provide a high-resolution data product to expand studies of lake ice phenology

across broad scales and further investigate the impacts of lake ice change on climatic feedback, ecosystems, and northern communities. Designed entirely using open-source code and open-access satellite imagery, the OPEN-ICE algorithm is reproducible over any region of interest using freely available data and readily improved by incorporating ice-water classifications derived from other potential sensors of interest.

2.7 Data availability

The OPEN-ICE code repository is published via GitHub under the Apache 2.0 license: https://github.com/xgirouxb/open_ice

2.8 References

- Adrian, R., O'Reilly, C.M., Zagarese, H., Baines, S.B., Hessen, D.O., Keller, W., Livingstone, D.M., Sommaruga, R., Straile, D., Van Donk, E., Weyhenmeyer, G.A., Winder, M., 2009. Lakes as sentinels of climate change. *Limnol. Oceanogr.* 54, 2283–2297. https://doi.org/10.4319/lo.2009.54.6_part_2.2283.
- Adrian, R., Wilhelm, S., Gerten, D., 2006. Life-history traits of lake plankton species may govern their phenological response to climate warming. *Glob. Chang. Biol.* 12, 652–661. <https://doi.org/10.1111/j.1365-2486.2006.01125.x>.
- Antonova, S., Duguay, C., Käab, A., Heim, B., Langer, M., Westermann, S., Boike, J., 2016. Monitoring bedfast ice and ice phenology in lakes of the Lena River Delta using TerraSAR-X backscatter and coherence time series. *Remote Sens.* 8, 903. <https://doi.org/10.3390/rs8110903>.
- Ariano, S.S., Brown, L.C., 2019. Ice processes on medium-sized north-temperate lakes. *Hydrol. Process.* 33, 2434–2448. <https://doi.org/10.1002/hyp.13481>.
- Benson, B., Magnuson, J., Sharma, S., 2000. Global Lake and River Ice Phenology Database, Version 1. National Snow and Ice Data Center, Colorado, United States.
- Bevington, A., Gleason, H., Giroux-Bougard, X., De Jong, J.T., 2018. A review of free optical satellite imagery for watershed-scale landscape analysis. *Confluence: J. Watershed Sci. Manag.* 2, 1–22. <https://doi.org/10.22230/jwsm.2018v2n2a18>.
- Bonsal, B.R., Prowse, T.D., 2003. Trends and variability in spring and autumn 0° C isotherm dates over Canada. *Clim. Chang.* 57, 341–358. <https://doi.org/10.1023/A:1022810531237>.
- Breiman, L., Friedman, J., Stone, C.J., Olshen, R.A., 1984. Classification and regression trees, 1st ed. Taylor & Francis, New York, United States. <https://doi.org/10.1201/9781315139470>.
- Brown, L.C., Duguay, C.R., 2012. Modelling lake ice phenology with an examination of satellite-detected subgrid cell variability. *Adv. Meteorol.* 2012, 1–19. <https://doi.org/10.1155/2012/529064>.
- Brown, L.C., Duguay, C.R., 2010. The response and role of ice cover in lake-climate interactions. *Prog. Phys. Geogr.* 34, 671–704. <https://doi.org/10.1177/0309133310375653>.
- Cael, B.B., Seekell, D.A., 2016. The size-distribution of Earth's lakes. *Sci. Rep.* 6, 29633. <https://doi.org/10.1038/srep29633>.
- Cai, Y., Ke, C.-Q., Xiao, Y., Wu, J., 2022. What caused the spatial heterogeneity of lake ice phenology changes on the Tibetan Plateau? *Sci. Total Environ.* 836, 155517. <https://doi.org/10.1016/j.scitotenv.2022.155517>.
- Campbell, J.W., Aarup, T., 1989. Photosynthetically available radiation at high latitudes. *Limnol. Oceanogr.* 34, 1490–1499. <https://doi.org/10.4319/lo.1989.34.8.1490>.
- Congalton, R.G., 1991. A review of assessing the accuracy of classifications of remotely sensed data. *Remote Sens. Environ.* 37, 35–46. [https://doi.org/10.1016/0034-4257\(91\)90048-B](https://doi.org/10.1016/0034-4257(91)90048-B).
- Congalton, R.G., Green, K., 2019. Assessing the accuracy of remotely sensed data, 3rd ed. Taylor & Francis, Boca Raton, United States. <https://doi.org/10.1201/9780429052729>.

- Copernicus Global Land Service, 2023. Lake Ice Extent - Northern Hemisphere (LIE-NH):500 metre version 1 product.
- Copernicus Land Monitoring Service, 2023a. Pan-European high-resolution snow & ice monitoring of the Copernicus Land Monitoring Service.
- Copernicus Land Monitoring Service, 2023b. Pan-European high-resolution snow & ice monitoring of the Copernicus Land Monitoring Service: Quality assessment report for ice products based on Sentinel-1 and Sentinel-2.
- Crétaux, J.-F., Merchant, C.J., Duguay, C., Simis, S., Calmettes, B., Bergé-Nguyen, M., Wu, Y., Zhang, D., Carrea, L., Liu, X., Selmes, N., Warren, M., 2021. ESA Lakes Climate Change Initiative (Lakes_cci): Lake products, Version 1.1. <https://doi.org/10.5285/EF1627F523764EAE8BBB6B81BF1F7A0A>.
- Dirscherl, M., Dietz, A.J., Kneisel, C., Kuenzer, C., 2021. A novel method for automated supraglacial lake mapping in Antarctica using Sentinel-1 SAR imagery and deep learning. *Remote Sens.* 13, 197. <https://doi.org/10.3390/rs13020197>.
- Donchyts, G., Baart, F., Winsemius, H., Gorelick, N., Kwadijk, J., Van De Giesen, N., 2016. Earth's surface water change over the past 30 years. *Nat. Clim. Chang.* 6, 810–813. <https://doi.org/10.1038/nclimate3111>.
- Downing, J.A., 2010. Emerging global role of small lakes and ponds: Little things mean a lot. *Limnetica* 29, 9–24. <https://doi.org/10.23818/limn.29.02>.
- Doxaran, D., Froidefond, J.-M., Lavender, S., Castaing, P., 2002. Spectral signature of highly turbid waters. *Remote Sens. Environ.* 81, 149–161. [https://doi.org/10.1016/S0034-4257\(01\)00341-8](https://doi.org/10.1016/S0034-4257(01)00341-8).
- Drusch, M., Del Bello, U., Carlier, S., Colin, O., Fernandez, V., Gascon, F., Hoersch, B., Isola, C., Laberinti, P., Martimort, P., Meygret, A., Spoto, F., Sy, O., Marchese, F., Bargellini, P., 2012. Sentinel-2: ESA's optical high-resolution mission for GMES operational services. *Remote Sens. Environ.* 120, 25–36. <https://doi.org/10.1016/j.rse.2011.11.026>.
- Du, J., Kimball, J.S., Duguay, C., Kim, Y., Watts, J.D., 2017. Satellite microwave assessment of northern hemisphere lake ice phenology from 2002 to 2015. *Cryosphere* 11, 47–63. <https://doi.org/10.5194/tc-11-47-2017>.
- Duguay, C.R., Bernier, M., Gauthier, Y., Kouraev, A., 2015. Remote sensing of lake and river ice. In: Tedesco, M. (Ed.), *Remote Sensing of the Cryosphere*. Wiley, Hoboken, United States, pp. 273–306.
- Duguay, C.R., Flato, G.M., Jeffries, M.O., Ménard, P., Morris, K., Rouse, W.R., 2003. Ice-cover variability on shallow lakes at high latitudes: Model simulations and observations. *Hydrol. Process.* 17, 3465–3483. <https://doi.org/10.1002/hyp.1394>.
- Duguay, C.R., Prowse, T.D., Bonsal, B.R., Brown, R.D., Lacroix, M.P., Ménard, P., 2006. Recent trends in Canadian lake ice cover. *Hydrol. Process.* 20, 781–801. <https://doi.org/10.1002/hyp.6131>.
- Effler, S.W., Perkins, M.G., Greer, H., Johnson, D.L., 1987. Effect of “whiting” on optical properties and turbidity in Owasco Lake, New York. *J. Am. Water Resour. Assoc.* 23, 189–196. <https://doi.org/10.1111/j.1752-1688.1987.tb00796.x>.
- European Space Agency, 2022. Copernicus Sentinel-2 MultiSpectral Instrument Collection 1 Level-1C Top-of-Atmosphere reflectance product. https://doi.org/10.5270/S2_-742ikh.

- Feyisa, G.L., Meilby, H., Fensholt, R., Proud, S.R., 2014. Automated water extraction index: A new technique for surface water mapping using landsat imagery. *Remote Sens. Environ.* 140, 23–35. <https://doi.org/10.1016/j.rse.2013.08.029>.
- Fréchet, M.M., 1906. Sur quelques points du calcul fonctionnel. *Rend. Circ. Matem. Palermo* 22, 1–72. <https://doi.org/10.1007/BF03018603>.
- GCOS, 2021. The status of the Global Climate Observing System 2021 (GCOS-240). World Meteorological Organization, Geneva, Switzerland.
- Gebre, S., Boissy, T., Alfredsen, K., 2014. Sensitivity of lake ice regimes to climate change in the Nordic region. *Cryosphere* 8, 1589–1605. <https://doi.org/10.5194/tc-8-1589-2014>.
- Geldsetzer, T., van der Sanden, J., Brisco, B., 2010. Monitoring lake ice during spring melt using RADARSAT-2 SAR. *Can. J. Remote Sens.* 36, 391–400. <https://doi.org/10.5589/m11-001>.
- Genolini, C., Ecochard, R., Benghezal, M., Driss, T., Andrieu, S., Subtil, F., 2016. kmlShape: An efficient method to cluster longitudinal data (time-series) according to their shapes. *PLoS ONE* 11, e0150738. <https://doi.org/10.1371/journal.pone.0150738>.
- Gerten, D., Adrian, R., 2001. Differences in the persistency of the North Atlantic oscillation signal among lakes. *Limnol. Oceanogr.* 46, 448–455. <https://doi.org/10.4319/lo.2001.46.2.0448>.
- Gorelick, N., Hancher, M., Dixon, M., Ilyushchenko, S., Thau, D., Moore, R., 2017. Google Earth Engine: Planetary-scale geospatial analysis for everyone. *Remote Sens. Environ.* 202, 18–27. <https://doi.org/10.1016/j.rse.2017.06.031>.
- He, H., Garcia, E.A., 2009. Learning from imbalanced data. *IEEE Trans. Knowl. Data Eng.* 21, 1263–1284. <https://doi.org/10.1109/TKDE.2008.239>.
- Hall, D.K., Riggs, G.A., Salomonson, V.V., 2006. MODIS snow and sea ice products. In: Qu, J.J., Gao, W., Kafatos, M., Murphy, R.E., Salomonson, V.V. (Eds.), *Earth Science Satellite Remote Sensing*. Springer, New York, United States, pp. 154–181. https://doi.org/10.1007/978-3-540-37293-6_9.
- Hampton, S.E., Galloway, A.W.E., Powers, S.M., Ozersky, T., Woo, K.H., Batt, R.D., Labou, S.G., O'Reilly, C.M., Sharma, S., Lottig, N.R., Stanley, E.H., North, R.L., Stockwell, J.D., Adrian, R., Weyhenmeyer, G.A., Arvola, L., Baulch, H.M., Bertani, I., Bowman, L.L., Carey, C.C., Catalan, J., Colom-Montero, W., Domine, L.M., Filip, M., Granados, I., Gries, C., Grossart, H.-P., Haberman, J., Haldna, M., Hayden, B., Higgins, S.N., Jolley, J.C., Kahilainen, K.K., Kaup, E., Kehoe, M.J., MacIntyre, S., Mackay, A.W., Mariash, H.L., McKay, R.M., Nixdorf, B., Nöges, P., Nöges, T., Palmer, M., Pierson, D.C., Post, D.M., Pruett, M.J., Rautio, M., Read, J.S., Roberts, S.L., Rücker, J., Sadro, S., Silow, E.A., Smith, D.E., Sterner, R.W., Swann, G.E.A., Timofeyev, M.A., Toro, M., Twiss, M.R., Vogt, R.J., Watson, S.B., Whiteford, E.J., Xenopoulos, M.A., 2017. Ecology under lake ice. *Ecol. Lett.* 20, 98–111. <https://doi.org/10.1111/ele.12699>.
- Higgins, S.N., Desjardins, C.M., Drouin, H., Hrenchuk, L.E., van der Sanden, J.J., 2021. The role of climate and lake size in regulating the ice phenology of boreal lakes. *J. Geophys. Res. Biogeosci.* 126, e2020JG005898. <https://doi.org/10.1029/2020JG005898>.

- Hoekstra, M., Jiang, M., Clausi, D.A., Duguay, C., 2020. Lake ice-water classification of RADARSAT-2 images by integrating IRGS segmentation with pixel-based random forest labeling. *Remote Sens.* 12, 1425. <https://doi.org/10.3390/rs12091425>.
- Holgerson, M.A., Raymond, P.A., 2016. Large contribution to inland water CO₂ and CH₄ emissions from very small ponds. *Nat. Geosci.* 9, 222–226. <https://doi.org/10.1038/ngeo2654>.
- Howell, S.E.L., Brown, L.C., Kang, K.K., Duguay, C.R., 2009. Variability in ice phenology on Great Bear Lake and Great Slave Lake, Northwest Territories, Canada, from SeaWinds/QuikSCAT: 2000–2006. *Remote Sens. Environ.* 113, 816–834. <https://doi.org/10.1016/j.rse.2008.12.007>.
- IPCC, 2014. *Climate Change 2014: Synthesis Report*. IPCC (Intergovernmental Panel on Climate Change), Geneva, Switzerland.
- Jeffries, M.O., Morris, K., 2007. Some aspects of ice phenology on ponds in Central Alaska, USA. *Ann. Glaciol.* 46, 397–403. <https://doi.org/10.3189/172756407782871576>.
- Kallio, K., Koponen, S., Ylöstalo, P., Kervinen, M., Pyhälähti, T., Attila, J., 2015. Validation of MERIS spectral inversion processors using reflectance, IOP and water quality measurements in boreal lakes. *Remote Sens. Environ.* 157, 147–157. <https://doi.org/10.1016/j.rse.2014.06.016>.
- Kang, K.-K., Duguay, C.R., Howell, S.E.L., 2012. Estimating ice phenology on large northern lakes from AMSR-E: Algorithm development and application to Great Bear Lake and Great Slave Lake, Canada. *Cryosphere* 6, 235–254. <https://doi.org/10.5194/tc-6-235-2012>.
- Knoll, L.B., Sharma, S., Denfeld, B.A., Flaim, G., Hori, Y., Magnuson, J.J., Straile, D., Weyhenmeyer, G.A., 2019. Consequences of lake and river ice loss on cultural ecosystem services. *Limnol. Oceanogr. Lett.* 4, 119–131. <https://doi.org/10.1002/lol2.10116>.
- Kropáček, J., Maussion, F., Chen, F., Hoerz, S., Hochschild, V., 2013. Analysis of ice phenology of lakes on the Tibetan Plateau from MODIS data. *Cryosphere* 7, 287–301. <https://doi.org/10.5194/tc-7-287-2013>.
- Kuhn, M., 2008. Building predictive models in R using the caret package. *J Stat. Softw.* 28, 1–26. <https://doi.org/10.18637/jss.v028.i05>.
- Kyle, H.L., Curran, R.J., Barnes, W.L., Escoe, D., 1978. A cloud physics radiometer. In: *Third Conference on Atmospheric Radiation*. American Meteorological Society, Davis, United States, pp. 107–109.
- Latifovic, R., Pouliot, D., 2007. Analysis of climate change impacts on lake ice phenology in Canada using the historical satellite data record. *Remote Sens. Environ.* 106, 492–507. <https://doi.org/10.1016/j.rse.2006.09.015>.
- Lawrence, R.L., Moran, C.J., 2015. The AmericaView classification methods accuracy comparison project: A rigorous approach for model selection. *Remote Sens. Environ.* 170, 115–120. <https://doi.org/10.1016/j.rse.2015.09.008>.
- Leblond, M., St-Laurent, M.-H., Côté, S.D., 2016. Caribou, water, and ice – fine-scale movements of a migratory arctic ungulate in the context of climate change. *Movement Ecol.* 4, 14. <https://doi.org/10.1186/s40462-016-0079-4>.

- Lenormand, F., Duguay, C.R., Gauthier, R., 2002. Development of a historical ice database for the study of climate change in Canada. *Hydrol. Process.* 16, 3707–3722. <https://doi.org/10.1002/hyp.1235>.
- Li, X., Zhou, Y., Meng, L., Asrar, G.R., Lu, C., Wu, Q., 2019. A dataset of 30 m annual vegetation phenology indicators (1985–2015) in urban areas of the conterminous United States. *Earth Syst. Sci. Data* 11, 881–894. <https://doi.org/10.5194/essd-11-881-2019>.
- Livingstone, D.M., 1997. Break-up dates of alpine lakes as proxy data for local and regional mean surface air temperatures. *Clim. Chang.* 37, 407–439. <https://doi.org/10.1023/A:1005371925924>.
- Livingstone, D.M., Adrian, R., Blenckner, T., George, G., Weyhenmeyer, G.A., 2010. Lake ice phenology. In: George, G. (Ed.), *The Impact of Climate Change on European Lakes*. Springer, Netherlands, Dordrecht, pp. 51–61.
- Luo, Y., Doxaran, D., Ruddick, K., Shen, F., Gentili, B., Yan, L., Huang, H., 2018. Saturation of water reflectance in extremely turbid media based on field measurements, satellite data and bio-optical modelling. *Opt. Express* 26, 10435. <https://doi.org/10.1364/OE.26.010435>.
- Lyu, H., Huang, W., Mahdianpari, M., 2022. A meta-analysis of sea ice monitoring using spaceborne polarimetric SAR: Advances in the last decade. *IEEE J. Sel. Top. Appl. Earth Obs. Remote Sens.* 15, 6158–6179. <https://doi.org/10.1109/JSTARS.2022.3194324>.
- Magnuson, J.J., Robertson, D.M., Benson, B.J., Wynne, R.H., Livingstone, D.M., Arai, T., Assel, R.A., Barry, R.G., Card, V., Kuusisto, E., Granin, N.G., Prowse, T.D., Stewart, K.M., Vuglinski, V.S., 2000. Historical trends in lake and river ice cover in the northern hemisphere. *Science* 289, 1743–1746. <https://doi.org/10.1126/science.289.5485.1743>.
- Maxwell, A.E., Warner, T.A., Fang, F., 2018. Implementation of machine-learning classification in remote sensing: An applied review. *Int. J. Remote Sens.* 39, 2784–2817. <https://doi.org/10.1080/01431161.2018.1433343>.
- McFeeters, S.K., 1996. The use of the normalized difference water index (NDWI) in the delineation of open water features. *Int. J. Remote Sens.* 17, 1425–1432. <https://doi.org/10.1080/01431169608948714>.
- Messenger, M.L., Lehner, B., Grill, G., Nedeva, I., Schmitt, O., 2016. Estimating the volume and age of water stored in global lakes using a geo-statistical approach. *Nat. Commun.* 7, 13603. <https://doi.org/10.1038/ncomms13603>.
- Murfitt, J., Brown, L., Howell, S., 2018. Evaluating RADARSAT-2 for the monitoring of lake ice phenology events in mid-latitudes. *Remote Sens.* 10, 1641. <https://doi.org/10.3390/rs10101641>.
- Murfitt, J., Brown, L.C., 2017. Lake ice and temperature trends for Ontario and Manitoba: 2001 to 2014. *Hydrol. Process.* 31, 3596–3609. <https://doi.org/10.1002/hyp.11295>.
- Murfitt, J., Duguay, C.R., 2020. Assessing the performance of methods for monitoring ice phenology of the world's largest high Arctic lake using high-density time series analysis of Sentinel-1 data. *Remote Sens.* 12, 382. <https://doi.org/10.3390/rs12030382>.

- Neter, J., Kutner, M.H., Nachtsheim, C.J., Wasserman, W., 1996. Applied linear statistical models, 4th ed. McGraw-Hill, New York, United States.
- Otsu, N., 1979. A threshold selection method from gray-level histograms. *IEEE Trans. Syst. Man Cybern.* 9, 62–66. <https://doi.org/10.1109/TSMC.1979.4310076>.
- Pal, M., Mather, P.M., 2003. An assessment of the effectiveness of decision tree methods for land cover classification. *Remote Sens. Environ.* 86, 554–565. [https://doi.org/10.1016/S0034-4257\(03\)00132-9](https://doi.org/10.1016/S0034-4257(03)00132-9).
- Pekel, J.-F., Cottam, A., Gorelick, N., Belward, A.S., 2016. High-resolution mapping of global surface water and its long-term changes. *Nature* 540, 418–422. <https://doi.org/10.1038/nature20584>.
- Peterson, L., Heynen, M., Pellicciotti, F., 2019. Freshwater resources: Past, present, future. In: Richardson, Douglas, Castree, N., Goodchild, M.F., Kobayashi, A., Liu, W., Marston, R.A. (Eds.), *International Encyclopedia of Geography: People, the Earth, Environment and Technology*. Wiley, Hoboken, United States. <https://doi.org/10.1002/9781118786352.wbieg0712.pub2>.
- Pi, X., Luo, Q., Feng, L., Xu, Y., Tang, J., Liang, X., Ma, E., Cheng, R., Fensholt, R., Brandt, M., Cai, X., Gibson, L., Liu, J., Zheng, C., Li, W., Bryan, B.A., 2022. Mapping global lake dynamics reveals the emerging roles of small lakes. *Nat. Commun.* 13, 5777. <https://doi.org/10.1038/s41467-022-33239-3>.
- Post, E., Alley, R.B., Christensen, T.R., Macias-Fauria, M., Forbes, B.C., Gooseff, M.N., Iler, A., Kerby, J.T., Laidre, K.L., Mann, M.E., Olofsson, J., Stroeve, J.C., Ulmer, F., Virginia, R.A., Wang, M., 2019. The polar regions in a 2° C warmer world. *Sci. Adv.* 5, eaaw9883. <https://doi.org/10.1126/sciadv.aaw9883>.
- Post, E., Bhatt, U.S., Bitz, C.M., Brodie, J.F., Fulton, T.L., Hebblewhite, M., Kerby, J., Kutz, S.J., Stirling, I., Walker, D.A., 2013. Ecological consequences of sea-ice decline. *Science* 341, 519–524. <https://doi.org/10.1126/science.1235225>.
- Prowse, T.D., Furgal, C., Chouinard, R., Melling, H., Milburn, D., Smith, S.L., 2009. Implications of climate change for economic development in northern Canada: Energy, resource, and transportation sectors. *Ambio*. 38, 272–281. <https://doi.org/10.1579/0044-7447-38.5.272>.
- R Core Team, 2023. R: A language and environment for statistical computing. R Foundation for Statistical Computing, Vienna, Austria.
- Rautio, M., Dufresne, F., Laurion, I., Bonilla, S., Vincent, W.F., Christoffersen, K.S., 2011. Shallow freshwater ecosystems of the circumpolar Arctic. *Écoscience* 18, 204–222. <https://doi.org/10.2980/18-3-3463>.
- Raymond, P.A., Hartmann, J., Lauerwald, R., Sobek, S., McDonald, C., Hoover, M., Butman, D., Striagl, R., Mayorga, E., Humborg, C., Kortelainen, P., Dürr, H., Meybeck, M., Ciais, P., Guth, P., 2014. Global carbon dioxide emissions from inland waters. *Nature* 507, 355–359. <https://doi.org/10.1038/nature13142>.
- Reist, J.D., Wrona, F.J., Prowse, T.D., Power, M., Dempson, J.B., King, J.R., Beamish, R.J., 2006. An overview of effects of climate change on selected arctic freshwater and anadromous fishes. *Ambio* 35, 381–387. [https://doi.org/10.1579/0044-7447\(2006\)35](https://doi.org/10.1579/0044-7447(2006)35).
- Rouse Jr., J.W., Haas, R.H., Schell, J.A., Deering, D.W., 1974. Monitoring vegetation systems in the Great Plains with ERTS. In: *Third Earth Resources Technology Satellite-1 Symposium: The Proceedings of a Symposium Held by Goddard*

- Space Flight Center at Washington, DC on December 10-14, 1973. NASA, Washington DC, United States, pp. 309–317.
- Rouse, W.R., Binyamin, J., Blanken, P.D., Bussi eres, N., Duguay, C.R., Oswald, C.J., Schertzer, W.M., Spence, C., 2008. The influence of lakes on the regional energy and water balance of the central Mackenzie River basin. In: Woo, M. (Ed.), *Cold Region Atmospheric and Hydrologic Studies. The Mackenzie GEWEX Experience*. Springer, Berlin, Germany, pp. 309–325. https://doi.org/10.1007/978-3-540-73936-4_18.
- Roy, D.P., Kovalskyy, V., Zhang, H.K., Vermote, E.F., Yan, L., Kumar, S.S., Egorov, A., 2016. Characterization of Landsat-7 to Landsat-8 reflective wavelength and normalized difference vegetation index continuity. *Remote Sens. Environ.* 185, 57–70. <https://doi.org/10.1016/j.rse.2015.12.024>.
- Sandven, S., Spreen, G., Heygster, G., Girard-Ardhuin, F., Farrell, S.L., Dierking, W., Allard, R.A., 2023. Sea ice remote sensing—Recent developments in methods and climate data sets. *Surv. Geophys.* <https://doi.org/10.1007/s10712-023-09781-0>.
- Sharma, R.C., Tateishi, R., Hara, K., 2016. A new water-resistant snow index for the detection and mapping of snow cover on a global scale. *Int. J. Remote Sens.* 37, 2706–2723. <https://doi.org/10.1080/01431161.2016.1183832>.
- Sharma, S., Blagrove, K., O'Reilly, C.M., Samantha, O., Ryan, B., Magee, M.R., Straile, D., Weyhenmeyer, G.A., Winslow, L., Woolway, R., Magnuson, J.J., 2019. Widespread loss of lake ice around the northern hemisphere in a warming world. *Nat. Clim. Chang.* <https://doi.org/10.1038/s41558-018-0393-5>.
- Sharma, S., Couturier, S., C ot e, S.D., 2009. Impacts of climate change on the seasonal distribution of migratory caribou. *Glob. Chang. Biol.* 15, 2549–2562. <https://doi.org/10.1111/j.1365-2486.2009.01945.x>.
- Shokr, M., Sinha, N., 2015. *Sea ice: Physics and remote sensing*. American Geophysical Union; Wiley, Hoboken, United States.
- Šmejkalova, T., Edwards, M.E., Dash, J., 2016. Arctic lakes show strong decadal trend in earlier spring ice-out. *Sci. Rep.* 6, 38449. <https://doi.org/10.1038/srep38449>.
- Stonevicius, E., Uselis, G., Grendaite, D., 2022. Ice detection with Sentinel-1 SAR backscatter threshold in long sections of temperate climate rivers. *Remote Sens.* 14, 1627. <https://doi.org/10.3390/rs14071627>.
- Stroeve, J., Holland, M.M., Meier, W., Scambos, T., Serreze, M., 2007. Arctic sea ice decline: Faster than forecast. *Geophys. Res. Lett.* 34 <https://doi.org/10.1029/2007GL029703>.
- Surdu, C., Duguay, C., Pour, H., Brown, L., 2015. Ice freeze-up and break-up detection of shallow lakes in Northern Alaska with spaceborne SAR. *Remote Sens.* 7, 6133–6159. <https://doi.org/10.3390/rs70506133>.
- Therneau, T., Atkinson, B., 2022. rpart: Recursive partitioning and regression trees, R package version 4.1.19. <https://cran.r-project.org/package=rpart>.
- Thornton, M.M., Shrestha, R., Wei, Y., Thornton, P.E., Kao, S., Wilson, B.E., 2020. Daymet: Daily surface weather data on a 1-km grid for North America. version 4. ORNL Distributed Active Archive Center. <https://doi.org/10.3334/ORNLDAAAC/1840>.

- Tom, M., Aguilar, R., Imhof, P., Leinss, S., Baltasvias, E., Schindler, K., 2020. Lake ice detection from Sentinel-1 SAR with deep learning. *ISPRS Ann. Photogramm. Remote Sens. Spat. Inf. Sci.* 3, 409–416. <https://doi.org/10.5194/isprs-annals-V-3-2020-409-2020>.
- Torres, R., Snoeij, P., Geudtner, D., Bibby, D., Davidson, M., Attema, E., Potin, P., Rommen, B., Flouy, N., Brown, M., Traver, I.N., Deghaye, P., Duesmann, B., Rosich, B., Miranda, N., Bruno, C., L'Abbate, M., Croci, R., Pietropaolo, A., Huchler, M., Rostan, F., 2012. GMES Sentinel-1 mission. *Remote Sens. Environ.* 120, 9–24. <https://doi.org/10.1016/j.rse.2011.05.028>.
- Tukey, J.W., 1949. Comparing individual means in the analysis of variance. *Biometrics* 5, 99. <https://doi.org/10.2307/3001913>.
- U.S. National Ice Center, 2008. IMS daily Northern Hemisphere snow and ice analysis at 1 km, 4 km, and 24 km resolutions, version 1. <https://doi.org/10.7265/N52R3PMC>.
- United States Geological Survey, 2022a. Landsat 7 Enhanced Thematic Mapper Plus (ETM+) Collection 1 Level-1 Tier-1 Top-of-Atmosphere reflectance product. <https://doi.org/10.5066/F7WH2P8G>.
- United States Geological Survey, 2022b. Landsat 8 Operational Land Imager (OLI) and Thermal Infrared Sensor (TIRS) Collection 2 Level-1 Tier-1 Top-of-Atmosphere reflectance product. <https://doi.org/10.5066/P975CC9B>.
- United States Geological Survey, 2020. Landsat 8 Collection 1 (C1) Land surface reflectance code (LaSRC) product guide version 3.0.
- Van Rossum, G., Drake, F.L., 2009. Python 3 Reference Manual. CreateSpace, Scotts Valley, United States.
- Verpoorter, C., Kutser, T., Seekell, D.A., Tranvik, L.J., 2014. A global inventory of lakes based on high-resolution satellite imagery. *Geophys. Res. Lett.* 41, 6396–6402. <https://doi.org/10.1002/2014GL060641>.
- Wang, J., Duguay, C., Clausi, D., Pinard, V., Howell, S., 2018. Semi-automated classification of lake ice cover using dual polarization RADARSAT-2 imagery. *Remote Sens.* 10, 1727. <https://doi.org/10.3390/rs10111727>.
- Wang, L., Scott, K.A., Clausi, D.A., 2016. Improved sea ice concentration estimation through fusing classified SAR imagery and AMSR-E data. *Can. J. Remote. Sens.* 42, 41–52. <https://doi.org/10.1080/07038992.2016.1152547>.
- Wang, M., Bailey, S.W., 2001. Correction of sun glint contamination on the SeaWiFS ocean and atmosphere products. *Appl. Opt.* 40, 4790–4798. <https://doi.org/10.1364/AO.40.004790>.
- Warren, S.G., 2019. Optical properties of ice and snow. *Philos. Trans. R. Soc. A Math. Phys. Eng. Sci.* 377, 20180161. <https://doi.org/10.1098/rsta.2018.0161>.
- Weyhenmeyer, G.A., Livingstone, D.M., Meili, M., Jensen, O., Benson, B., Magnuson, J.J., 2011. Large geographical differences in the sensitivity of ice-covered lakes and rivers in the northern hemisphere to temperature changes. *Glob. Chang. Biol.* 17, 268–275. <https://doi.org/10.1111/j.1365-2486.2010.02249.x>.
- Weyhenmeyer, G.A., Meili, M., Livingstone, D.M., 2004. Nonlinear temperature response of lake ice breakup. *Geophys. Res. Lett.* 31, 6–9. <https://doi.org/10.1029/2004GL019530>.

- Williamson, C.E., Saros, J.E., Vincent, W.F., Smol, J.P., 2009. Lakes and reservoirs as sentinels, integrators, and regulators of climate change. *Limnol. Oceanogr.* 54, 2273–2282. https://doi.org/10.4319/lo.2009.54.6_part_2.2273.
- Willmott, C.J., Ackleson, S.G., Davis, R.E., Feddema, J.J., Klink, K.M., Legates, D.R., O'Donnell, J., Rowe, C.M., 1985. Statistics for the evaluation and comparison of models. *J. Geophys. Res.* 90, 8995–9005. <https://doi.org/10.1029/JC090iC05p08995>.
- Woolway, R.I., Kraemer, B.M., Lenters, J.D., Merchant, C.J., O'Reilly, C.M., Sharma, S., 2020. Global lake responses to climate change. *Nat. Rev. Earth Environ.* 1, 388–403. <https://doi.org/10.1038/s43017-020-0067-5>.
- Wrona, F.J., Johansson, M., Culp, J.M., Jenkins, A., Mård, J., Myers-Smith, I.H., Prowse, T.D., Vincent, W.F., Wookey, P.A., 2016. Transitions in Arctic ecosystems: Ecological implications of a changing hydrological regime. *J. Geophys. Res. Biogeosci.* 121, 650–674. <https://doi.org/10.1002/2015JG003133>.
- Wu, Y., Duguay, C.R., Xu, L., 2021. Assessment of machine learning classifiers for global lake ice cover mapping from MODIS TOA reflectance data. *Remote Sens. Environ.* 253, 112206 <https://doi.org/10.1016/j.rse.2020.112206>.
- Wulder, M.A., Loveland, T.R., Roy, D.P., Crawford, C.J., Masek, J.G., Woodcock, C.E., Allen, R.G., Anderson, M.C., Belward, A.S., Cohen, W.B., Dwyer, J., Erb, A., Gao, F., Griffiths, P., Helder, D., Hermosilla, T., Hipple, J.D., Hostert, P., Hughes, M.J., Huntington, J., Johnson, D.M., Kennedy, R., Kilic, A., Li, Z., Lyburner, L., McCorkel, J., Pahlevan, N., Scambos, T.A., Schaaf, C., Schott, J.R., Sheng, Y., Storey, J., Vermote, E., Vogelmann, J., White, J.C., Wynne, R.H., Zhu, Z., 2019. Current status of Landsat program, science, and applications. *Remote Sens. Environ.* 225, 127–147. <https://doi.org/10.1016/j.rse.2019.02.015>.
- Yang, Luo, Huang, Wu., Sun, 2019. Weighted double-logistic function fitting method for reconstructing the high-quality Sentinel-2 NDVI time series data set. *Remote Sens.* 11, 2342. <https://doi.org/10.3390/rs11202342>.
- Yin, G., Mariethoz, G., Sun, Y., McCabe, M.F., 2017. A comparison of gap-filling approaches for Landsat-7 satellite data. *Int. J. Remote Sens.* 38, 6653–6679. <https://doi.org/10.1080/01431161.2017.1363432>.
- Zhang, S., Pavelsky, T.M., 2019. Remote sensing of lake ice phenology across a range of lakes sizes, ME, USA. *Remote Sens* 11, 1718. <https://doi.org/10.3390/rs11141718>.

2.9 Linking statement

In the previous chapter, I developed the OPEN-ICE algorithm and data product to address the spatio-temporal trade off that researchers often face when monitoring lake ice phenology. Because they are in high polar orbit, optical sensors such as MODIS and AVHRR revisit locations on Earth almost daily, making them particularly well-suited to study phenological events like spring breakup that can happen so rapidly. Despite their higher temporal resolution, these sensors have low spatial resolution, limiting their monitoring ability to larger lakes. To study small lakes, researchers must instead turn to higher resolution imagery which does not revisit each location as often. The OPEN-ICE algorithm was designed to capitalize on the abundance of open-access high-resolution optical imagery to fill in these temporal gaps, effectively allowing researchers to study lake ice phenology patterns in both large and small lakes at continental scales. Small lakes are more abundant and cover more of Earth's surface than large lakes, and the availability of a data product like OPEN-ICE allows researchers to incorporate freshwater ice phenology impacts to investigate broad-scale patterns of the limnological, biogeochemical, and ecological changes occurring in these important ecosystems. One such potential application, the original reason I set out to develop the OPEN-ICE algorithm, is investigating the impacts of shifting lake ice phenology on the spring migration of caribou.

Studying the movement ecology of a migratory species as vagile as barren-ground caribou imposes similar trade offs as studying lake ice. Indeed, the environmental drivers of caribou's annual cycles and movements operate across small-to-large spatio-temporal scales. During spring migration, one of the key periods of their

annual cycle, the speed and mobility of females urgently trying to reach their calving ground is determined by their fine-scale movement responses to snowscapes and the availability of freshwater ice, both of which are in a rapid state of flux. However, the availability of snow and ice Earth observation products at both high temporal and spatial scales have been lacking. While previous research has identified these as key factors to migration, the incorporation of lake ice phenology has been limited to large lakes and ice presence/absence. In this next chapter I use the OPEN-ICE data product to study the migratory behaviour of female caribou in response to water body size and phenological states (including ice, the transition state of breaking ice, and open water) as they traverse one of the most lake dense regions of Earth.

Chapter 3 - Lake ice phenology and the spring migration of barren-ground caribou (*Rangifer tarandus groenlandicus*) in a rapidly changing North

3.0 Abstract

Long-distance migration is an important evolutionary adaptation to reduce predation and access resources in biomes with drastic seasonal cycles. In Canada's North, barren-ground caribou undertake the longest terrestrial migration in the world. In spring, females depart their wintering grounds in the taiga and travel northward to their calving ground in the Arctic's coastal tundra. Females gather in large numbers to reduce predation on calves, and the timing of parturition and lactation is synchronized with the greening of the tundra and availability of fresh and high-quality forage following long winters. On their journey, they traverse regions with the highest density of freshwater lakes in the world. The disproportionately rapid warming occurring in the Arctic relative to the globe is causing important shifts in freshwater ice phenology and, consequently, encounters between migrating caribou and breaking ice or open water are expected to increase. Using high spatial and temporal resolution ice phenology products, we investigated the use and availability of ice, breaking ice, and open water across different waterbody sizes during the spring migration of GPS-collared females in two herds using path selection analysis. Females typically select migration paths over small (0.1 - 10 km²) ice-covered lakes during spring migration but avoid larger ice-covered waterbodies. Migrating females exhibit strong avoidance of areas with breaking ice and to a lesser extent open water, and their avoidance behaviour typically increases around larger waterbodies. When females encountered a greater prevalence of breakup

conditions, the duration of their migration could increase by more than a week. As the availability of freshwater ice declines throughout the North, there is a great deal of uncertainty as to how increased exposure to breakup conditions during migration will influence the connectivity of landscapes, the timing and duration of migration, the safety/survival of migrating females, and their ability to ensure timely arrival to their destination to promote calf survival.

3.1 Introduction

How the phenology of organisms aligns with the seasonality of environments is central to understanding organism-environment interactions and thus the discipline of ecology (Morissette et al., 2009). Schwartz (2013) defines phenology as “the study of periodic biological events [...] as influenced by the environment, especially temperature changes driven by weather and climate” and seasonality as “a related term, referring to similar non-biological events, such as timing of the fall formation and spring breakup of ice on freshwater lakes”. Studies that consider phenology and seasonality in relation to each other often focus on identifying the environmental cues that initiate, and the environmental drivers that cause, phenological responses (Chmura et al., 2019). But given the diversity of organisms and the ubiquity of environmental variation, regardless of how and how well phenology is synchronized with seasonality, a given phenological stage or transition is likely to coincide with a wide range of prevailing environmental conditions. The suitability or incompatibility of environmental conditions that prevail during a given phenological stage or transition can have drastic and direct influence on organismal survival and reproduction, including, for example, weather-related mass-mortality events during bird migration (Newton, 2007), frost or drought-induced

reproductive failure in plants (Schermer et al., 2020), weather-induced winter mortality of diapausing insects (Musolin, 2007), and winter storm impacts on fish spawning and larval drift (Checkley et al., 1988). Prevailing environmental conditions during a particular phenological stage can also lead to carryover effects that alter the timing and success of subsequent life history stages and allocations (Aikens et al., 2021; Marra et al., 2015). Documenting how seasonal progressions and prevailing environmental conditions affect the expression and success of phenological responses helps to reveal the directional, stabilizing, or disruptive selection driving the evolution of phenological traits and the prevalence and consequences of phenological mismatches in an era of environmental change.

Migration is a common phenological response of mobile organisms in seasonal environments (Alerstam et al., 2003). In this context, migration refers to seasonal movement from one region to another, followed by a seasonal return to the starting point, with the direction and timing of movement shared with conspecifics (Fudickar et al., 2021). Migration phenology – the seasonal timing of migration – is an individual and population trait known to be a key determinant of migration success, winter survival, and spring reproduction (Cotton, 2003; Knudsen et al., 2007). Most studies of migration phenology focus on environmental cues and drivers of migration timing (e.g., Haest et al., 2018), migration timing as an indicator of climate change responses (e.g., Van Buskirk et al., 2009), and how migration timing relates to prey abundance and predator vulnerability during, before, and after migration (e.g., Bowers et al., 2016). But, similar to other phenological responses, the environmental conditions that occur during migration can be a key determinant of migration costs and outcomes. Birds are characterized by

the longest distance migrations of all organisms (Fudickar et al., 2021), and environmental conditions encountered during migration, including wind, fog, temperature, ice and snow, cloud cover, precipitation and barometric pressure, have been described to influence migration routes, stopover durations, orientation, and overall migratory success (Newton, 2007). Other non-avian examples of long-distance migration include, monarch butterflies (*Danaus plexippus*) (Reppert and de Roode, 2018), white sharks (*Carcharodon carcharias*) (Bonfil et al., 2005), sockeye salmon (*Oncorhynchus nerka*) (Wood et al., 2008), Atlantic eels (*Anguilla rostrata*) (Wright et al., 2022), loggerhead sea turtles (*Caretta caretta*) (Mansfield et al., 2017), flying foxes (*Pteropus poliocephalus*) (Roberts et al., 2012), and humpback whales (*Megaptera novaeangliae*) (Riekkola et al., 2020). Although all these species are likely to encounter variable environmental conditions during migration, the medium through which they move remains consistent; for those that fly air remains air and for those that swim water remains water. In contrast, for land animals migrating in places and at times of year when snow is melting from land surfaces and ice is melting from water surfaces, environmental variation encountered during migration is likely to define the basic modalities of their movements.

Barren-ground caribou undertake the longest terrestrial migrations on earth and the energetic requirements of such an undertaking mediate their movement behaviours and, consequently, their choice of migratory routes (Alerstam et al., 2003). For example, snow depth has been shown to increase energy expenditure exponentially in caribou (Fancy and White, 1987), and reduce travel rates during winter and migration periods (Bergerud et al., 2008). To reduce energy expenditures during migration, caribou

frequently travel on frozen freshwater bodies because these typically facilitate movement and offer better visibility of predators. However, while the ice-free season on freshwater lakes and rivers of northern Canada continues to increase (Latifovic and Pouliot, 2007), the consequences on caribou migrations remain poorly understood. Despite caribou being excellent swimmers, large lakes may become significant obstacles in the absence of ice, and open rivers with abnormally strong flow have caused massive drowning events in the past (Berkes, 1988). Thin ice also presents significant dangers, as breaking through can lead to exhaustion, injury, hypothermia, and drowning (Miller and Gunn, 1986).

As arctic regions undergo the most drastic climatic changes on our planet (IPCC, 2014; Rantanen et al., 2022), there is much concern on how barren-ground caribou, a species of huge economic and cultural importance, will cope with rapid changes in its environment. Many potential impacts of these changes have already been observed or predicted, such as: increased insect harassment (Witter et al., 2012) and exposure to disease and parasites (Hoberg et al., 2008); changes in plant phenology causing a mismatch between calving and forage availability (Post and Forchhammer, 2008) as well as reduced forage quality on summer ranges (Turunen et al., 2009); wet snow and freezing rain reducing access to ground level forage during winter (Miller and Gunn, 2003); and increasing forest fires (Gillett et al., 2004) reducing potential winter ranging habitat (Rupp et al., 2006). The resilience of caribou to the cumulative effects of these environmental changes depends in part on their dynamic use of space and, consequently, there is much interest in understanding how migratory patterns might be influenced by climate.

Our objective is to assess the impacts of ice phenology on the fine-scale movement behaviours of caribou during migration. We hypothesize that ice presence, absence, or transitional states during spring break-up will influence how caribou respond to hydrological features in the landscape.

3.2 Methods

3.2.1 Study area and caribou herds

The annual ranges of the Bluenose-East and Bathurst herds cover large regions of the Northwest Territories and Nunavut (see Fig. 3.1). Their winter range typically lies in the southern areas of their annual range, below the treeline. In spring, females migrate northward to their respective calving grounds adjacent to the Coronation Gulf and the Bathurst Inlet, typically travelling hundreds of kilometres through three designated ecozones (Ecological Stratification Working Group, 1995): the Taiga Plains, the Taiga Shield, and finally the Tundra Plains (or Barren Ground). The landscapes they encounter during these long-distance travel events are characterized by the highest lake density in the world (Messenger et al., 2016) and typically covered by 15 to 40% freshwater (Duguay et al., 2003). The population of both these herds has declined significantly over the past two decades (Government of the Northwest Territories, 2019, 2016). As a consequence of this decline, annual ranges have contracted to core areas and the winter ranges of each herd have moved northward.

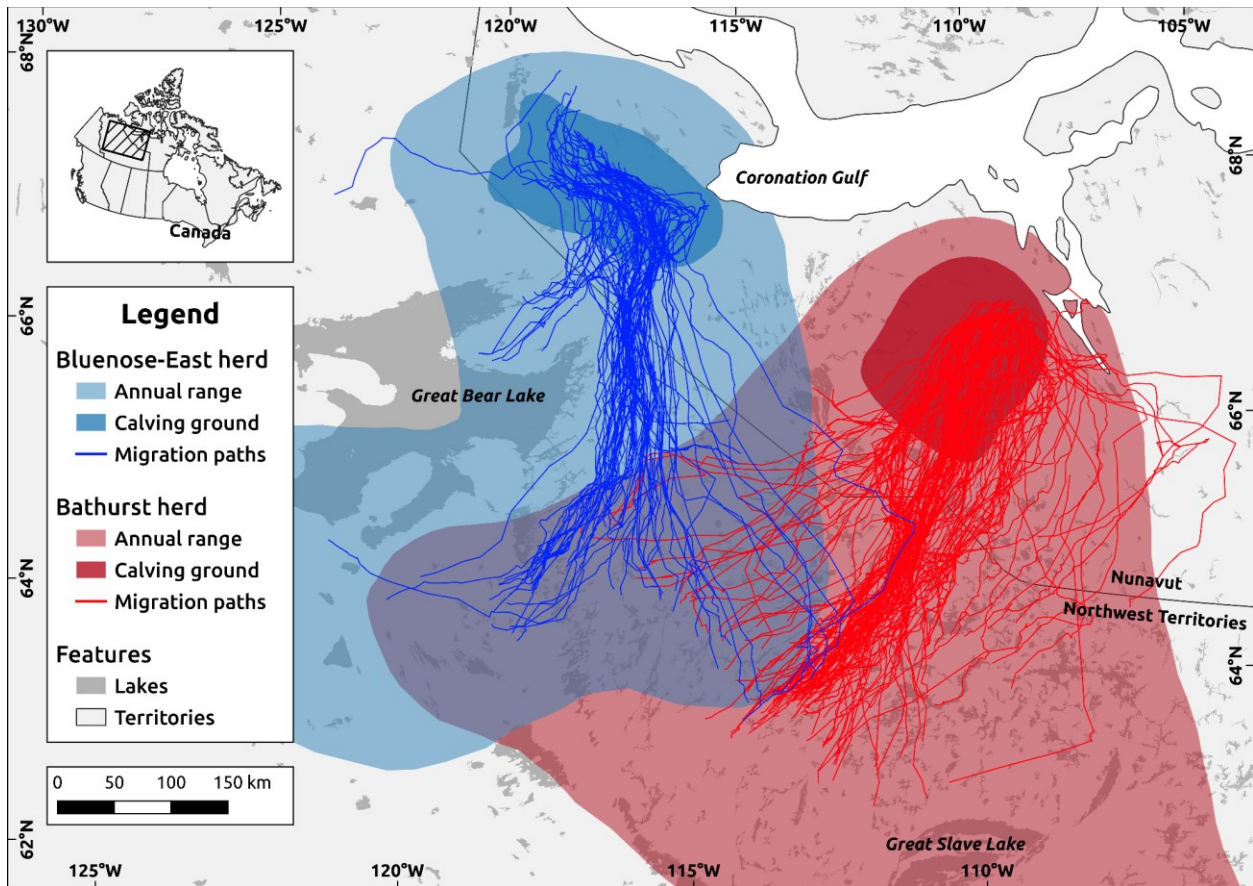


Figure 3.1 Map illustrating the observed spring migration paths during the study period. Spatial data for the annual ranges and calving grounds of each herd are provided by the Government of the Northwest Territories.

3.2.2 Caribou migration telemetry data

We used GPS location data recorded by satellite telemetry collars deployed on female caribou of the Bathurst and Bluenose-East herds. The GPS relocation data is part of an ongoing caribou monitoring program administered by the Government of the Northwest Territories' (GNWT) Wildlife Division (Gunn et al., 2013) following strict ethical guidelines (Cattet, 2011). As part of a data sharing agreement with the GNWT (#8515-05 DR29), we accessed this data via the Movebank repository (Kays et al., 2022). We selected female relocation data recorded between 2013 and 2021, inclusively, as this period overlaps with the availability of freshwater ice phenology data with high spatio-

temporal resolution (see Section 3.2.4.3). We screened all observed locations for duplicates (i.e., identical timestamps/locations for a given ID) and other potential errors such as unlikely speeds (i.e., remarkable outliers in population-wide distribution) and rapid roundtrips (i.e., a rapid departure from and return to the same location indicative of GPS-collar error). The GPS location sampling frequency varied between deployed collars, years, and seasons (e.g., more frequent fixes during calving season, more frequent fixes on collars deployed in recent years), and sampling frequencies were typically every 1, 3, 8, or 24 hours. Within each individual track travelled by a distinct individual in a given year, we resampled the time series with its coarsest fix rate (either 8 or 24h) to ensure consistent intervals between successive observations. We accounted for these different intervals in our downstream analyses by including sampling rates as a covariate in our models (see Section 3.2.5.1).

We identified individual spring migration events by inspecting (i) maps of individual tracks, (ii) time series of movement speed, and (iii) time series of net square displacement (NSD; Singh et al., 2016). To account for individual and annual variation in migration periods, we closely inspected all female tracks in the period starting one month prior to and ending one month after each herd's previously reported spring migration start and end dates (see Nagy, 2011). Specifically, the periods of interest we flagged for inspection spanned from March 20th to July 1st for the Bathurst herd and March 10th to June 27th for the Bluenose-East herd. For each potential individual migration event, we calculated the movement speed between successive relocations and the NSD relative to the initial observed GPS location within the period of interest. To better discern overall trends in the time series, we computed the mean in a 48-hour

moving window centered on each observation. We recorded an individual's migration start date when we observed, concurrently, a sudden increase in mean speed followed by steadily increasing NSD and a trajectory with directional movement. Similarly, we noted the migration end date when the individual's movement speed slowed, the NSD reached a plateau, and the trajectory began slowly meandering within the bounds of a calving ground. Using this approach, we identified a single migration path per female for a given year and we hereby refer to this distinct id-year grouping of location data as a "migration event". We conserved a path even if small observational gaps were present, and only discarded a path if any single time gap was greater than 72 hours or if more than 10% of the observations between the migration start and end date were missing. In total, we discarded 8 paths and conserved 274 identified distinct migration paths composed of, on average, approximately 52 steps each.

We performed all the data manipulations, computations of movement metrics, and visualizations and inspection of tracks required to identify potential migration events using R (R Core Team, 2023) and QGIS (QGIS Development Team, 2022).

3.2.3 Used-available migration paths

We compared observed (used) female migrations paths to randomly generated (available) migration paths using a path selection analysis (PSA) framework. While classical habitat/resource selection analysis methods implement a used-available study design based on location data to assess affinity for or avoidance of certain habitats (Johnson et al., 2006), PSA focuses on the entire trajectory described by multiple successive relocations along a path to understand how the landscape mediates animal movement behaviours. Similarly to step selection functions (SSFs, Fortin et al., 2005;

Thurfjell et al., 2014), PSA models the movement behaviour responses to landscapes but using an entire path as a unit of comparison instead of individual steps (Zeller et al., 2015). Similarly to Leclerc et al. (2021), we found PSA to be the most intuitive method to constrain both observed and random paths to the fixed starting point (i.e., winter range) and end point (i.e., calving ground) which are characteristic of barren-ground caribou spring migrations.

For each observed annual migration path we identified, hereinafter referred to as an “observed migration path”, we generated 20 associated random migration paths. Each random path was bound to the same start and end locations as the observed path, and the steps composing the new path were obtained by randomly sampling pairs of the step distances and bearings, without replacement, from the observed path.

To study the relationship between freshwater ice phenology and migration path use-availability, we sampled environmental covariates within a buffered area around each individual step. Caribou movement responses to landscape features are scale-dependent (Boulanger et al., 2021; Wilson et al., 2016) so we used a 2.5-kilometre buffer to focus on the effect of the immediate landscape experienced by caribou during movement events while accounting for the uncertainty of the exact path an individual may have travelled between two successive GPS locations (Fortin et al., 2005).

3.2.4 Environmental covariates

To investigate the effects of freshwater ice phenology on migration paths, we focused exclusively on environmental covariates related to hydrological features, namely: (i) their prevalence in the landscape, (ii) their relative size, and (iii) the

phenological state of their ice cover. We sampled each of these covariates of interest in the 2.5-kilometre buffer around each step as described below. We accessed, processed, and sampled all the hydrological and ice phenology data using Google Earth Engine's JavaScript API (Gorelick et al., 2017).

3.2.4.1 Hydrological proportion

Within each step's buffer, we computed the proportion of the landscape covered by freshwater, which we hereinafter refer to as "hydrological proportion". We created a freshwater raster layer using the European Commission Joint Research Center (JRC) global water dataset (Pekel et al., 2016). The JRC surface water data product provides an estimate of the persistence of water at a 30-metre resolution, globally, based on the Landsat archive (1984-2022). Within our study area, we defined freshwater as pixels with greater than 80% water occurrence in the Landsat archive thus effectively excluding ephemeral water from our analysis.

3.2.4.2 Lake size class

We assigned each step one of three categorical classes indicative of the mean lake size (i.e., surface area) within its buffer: small (0.1 - 10 km²), large (10 - 1000 km²), and very large (> 1000 km²). We computed mean lake sizes for each step using lake polygons and surface area measurements from the HydroLAKES dataset (Messenger et al., 2016). We calculated the mean size of the lakes within each step, weighted by the proportion of the step occupied by each lake, and assigned the corresponding class (i.e., small, large, very large). During our study period, caribou encountered only three very large lakes (i.e., > 1000 km²) during spring migration: Great Bear Lake, Napaktuliq

Lake, and Contwoyto Lake. We included lake size as a categorical variable in our models to ensure that observed patterns were not uniquely driven by these very large lakes and remained comparable to previous investigations of caribou migration and ice phenology, which focused primarily on lakes or reservoirs larger than 1000 km² (Leblond et al., 2016).

3.2.4.3 Ice, breaking ice, and open water proportions

Within each step's buffer, we computed the proportion of the landscape covered by ice, breaking ice, and open water. While the two previous covariates (hydrological proportion and lake size) were computed from static layers, the ice phenology of freshwater is a highly dynamic process in constant state of flux throughout the annual spring breakup and caribou migration periods. To account for this, we used the OPEN-ICE data product (Giroux-Bougard et al., 2023) which provides annual estimates of spring breakup dates for all freshwater pixels in Canada at a 30-metre resolution between 2013 to 2021, inclusively. Using these spring breakup date estimates, we classified the freshwater within the 2.5-kilometre buffer for each caribou used-available step into "ice", "breaking ice", and "open water" following a two-step procedure: (i) we classified each pixel within the step buffer into ice or water based on the breakup day of year relative to the day of year of the timestamp at the step's end location, and then (ii) we classified each distinct grouping of connected pixels (8-way connected) within a step's buffer as "ice" when 95% or more of the pixels in the group were still ice, as "breaking ice" when less than 95% but more than 10% of the pixels in the group were still ice, and as "open water" when 10% or less of the pixels in the group were still ice. It was then possible to compute the proportion of each step buffer covered by freshwater

in each phenological stage of spring breakup. Note that the sum of the ice, breaking ice, and open water proportions within a step is equal to the hydrological proportion.

3.2.5 Path selection analysis

3.2.5.1 Model parameterization

To evaluate how observed migration paths responded to hydrological features during spring breakup, we used generalized linear mixed models (GLMMs) to implement path selection analysis. We parameterized our mixed models using the form:

$$\omega(\mu_{ij}) = \exp(\alpha_{jt} + x_1\beta_{1ij} + \dots + x_k\beta_{kij} + x_{kj}\gamma_{kj}) \quad (\text{Equation 3.1})$$

where $\omega(\mu_{ij})$ denotes the relative probability that step i will be used during migration event j ; $x_1 \dots x_k$ are the environmental covariates of interest; α_{jt} is the strata level intercept of group j at time t (i.e., group composed of an observed step with 20 associated random steps); $\beta_1 \dots \beta_k$ are the population-level coefficients of interest; and γ_{kj} the random coefficients fitted to environmental covariate x_k associated to migration event j .

Following this mixed model structure, we fit three *a priori* candidate GLMMs to model hypothesized behavioural responses of migrating females to hydrological features during spring breakup (see Table 3.1). In each model, we included steps as individual observations where the binomial responses were either “used” (1) for observed steps or “available” (0) for associated random steps. We included each environmental covariate of interest both as a fixed effect and as a random effect whereby slopes were allowed to vary within groups of used-available paths associated to a distinct migration event (i.e., year-id grouping of observed and associated random

paths). This year-id grouping for each random slope further allowed us to include model terms that control for variation due to individual behavioural differences and sampling regimes (Gillies et al., 2006). We included interactions between environmental covariates as fixed effects. We excluded global intercepts from all three models, instead opting to estimate random intercepts within each stratum (see Equation 3.1). In order of increasing complexity, we constructed the three candidate models using different covariates as follows:

- *Model 1: Caribou select migratory paths based on the prevalence of freshwater features in the landscape.* Consequently, we might expect females to use or avoid areas where the proportion of the landscape covered by freshwater features (i.e., hydrological proportion) is high, regardless of the size of those features or the presence of ice, breaking ice, or open water on those features. In this model, we included the hydrological proportion of the landscape as the only environmental covariate.
- *Model 2: Caribou select migratory paths based on the phenological state of ice cover on hydrological features.* For example, caribou might use freshwater features still covered with ice but avoid those with breaking ice and open water. In this model we included the proportion of ice, breaking ice, and open water as the only environmental covariate.
- *Model 3: Caribou select migratory paths based on both the phenological state of ice cover on hydrological features and their relative sizes.* For example, we might expect migrating caribou to use areas dominated by small lakes regardless of their phenological state but avoid areas with larger lakes where breaking ice or

open water have begun to form. In this model we included mean lake size class and its interaction with the proportion of ice, breaking ice, and open water as environmental covariates.

To reduce potential sources of bias in estimating the fixed-effect parameters of each model (Forester et al., 2009; Muff et al., 2020), we fit each of the three candidate models twice using: (i) the step distance to account for bias due to movement speed, or (ii) the step time to account for variations in sampling rates.

3.2.5.2 Model fitting

We performed model fitting and diagnostics using a Bayesian workflow. To facilitate the fitting of PSA models using a Bayesian approach, we used a Poisson family distribution with a binomial response and fixed variances for strata level intercepts (Muff et al., 2020). We set normally distributed priors with a very large fixed variance (i.e., $N(0, 10^6)$) to avoid shrinkage of the strata intercepts towards the mean, which can bias other parameter estimates (Muff et al., 2020). We specified normally-distributed weakly informative priors (i.e., $N(0, 10)$) for all other parameters included in our models (Lemoine, 2019). To estimate model parameters, we used ten Hamiltonian Monte Carlo chains (Betancourt, 2017) run with 1500 iterations each, including 1000 warmup iterations, for a combined total of 5000 post-warmup iterations. We checked models for divergent transitions and ensured that each model had sufficient iterations for the estimated parameter distributions to stabilize across chains using the R-hat convergence statistic (i.e., $R\text{-hat} < 1.05$). We evaluated individual model fit using graphical posterior predictive checks (Gelman et al., 2020). We performed all model fitting, diagnostics, and visualization using the “brms” (Bürkner, 2017) and “bayesplot”

(Gabry et al., 2019) packages implemented in the R and Stan languages (Stan Development Team, 2022).

3.2.5.3 Model comparison

We evaluated the relative predictive ability of each PSA model using three Bayesian model comparison metrics: the model weights, the k-fold cross-validation information criterion (KFCV-IC; Vehtari et al., 2017), and the widely-applicable information criterion (WAIC; Vehtari et al., 2017). We computed model weights using Bayesian model stacking, which performs model averaging by optimizing the weights accorded to each model in a manner that achieves the best predictive ability (Yao et al., 2018). For each model, we computed KFCV-IC using a 10-fold cross-validation scheme in which each fold (i.e., data partition) was stratified into groups of distinct migration events, effectively allowing us to evaluate the predictive ability of the model when faced with new data (Vehtari et al., 2017). To further inform model comparison, we computed the WAIC for each model (Piiironen and Vehtari, 2017; Watanabe, 2010). Alongside each information criterion, we also included the expected log predictive densities (ELPD) as well as the difference in ELPD (Δ ELPD) between the most supported model and the other two. We computed all model comparison metrics using the “brms” (Bürkner, 2017) and “loo” (Vehtari et al., 2022) packages implemented in R (R Core Team, 2023). We further investigated the coefficients and conditional effects of the model with the most support using the “bayesplot” package (Gabry et al., 2019) implemented in R (R Core Team, 2023).

3.2.6 Migration duration

We further investigated the effects of ice phenology on the duration of spring migration events using a hierarchical generalized additive model (HGAM). While the start date of spring migration varies considerably between individuals and between herds, the plasticity of migration behaviours is such that females with delayed departures typically migrate faster to reach the calving grounds in time (Gurarie et al., 2019). We accounted for variability of departures in our HGAM by including the start day (day of year) of each migration event ($n = 274$). To account for differences in departure periods between herds and years, we added a factor smooth whereby the migration start smooth term was further allowed to vary by groupings of herd/year with the same wiggleness factor, an approach analogous to random slopes in a GLMM (Pedersen et al., 2019). We also included random intercepts for each female to account for behavioural differences in the initiation and duration of migration events. Even within the same herd, individual winter ranges can be far apart, and population winter ranges shift significantly over time (Bergerud et al., 2008). We therefore accounted for the different distances required for each individual to reach its calving ground by including a smooth term for the straight-line geographical distance between the start and end locations of migration. Finally, to account for the potential effects of ice phenology on the duration of migration we included a smooth term for the breakup condition encounter rate of each migration event, which we estimated as the proportion of steps within each migration path that encountered breaking ice or open water. We used thin plate regression splines to model smooth terms (Wood, 2003), fitted the HGAM, and conducted model

diagnostics and visualization using the “mgcv” (Wood, 2017) and “gratia” (Simpson, 2024) packages implemented in R (R Core Team, 2023).

3.3 Results

3.3.1 Migration events

Throughout the study period, we identified a total of 274 distinct spring migration events undertaken by a total of 153 collared females that reached either the Bathurst or Bluenose-East calving grounds. For 82% of collared females, we only identified one or two migration events. For most of the remaining 18% of females, we identified three or four migration events, and for two females we successfully identified five.

For the Bathurst herd, we identified 187 distinct migration paths travelled by 115 females. Throughout the study period, migrations typically started in mid-April and ended in early June (see Fig. 3.2A), departing from overwintering grounds in the region immediately north of Great Slave Lake and arriving at their calving grounds near Bathurst Inlet (see Fig. 3.1). Specifically, the annual median departure dates ranged from April 20th in 2021 to May 21st in 2018, while the median departure date across all Bathurst female migration events during the study period was April 30th. In contrast, the median arrival dates ranged from May 16th in 2021 to June 1st in 2018, with the median arrival date across all migration events being May 24th. Many of the migratory paths cross large lakes (see Fig. 3.1), most frequently Contwoyto Lake (1054 km², 65°39'0" N, 110°43'0" W) and Lac de Gras (700 km², 65°39'0" N, 110°43'0" W), as well as some sections or tributaries of the upper Coppermine River system, such as Point Lake (977 km², 65°14'0" N, 113°9'0" W) and Mackay Lake (967 km², 63°55'0" N, 111°2'0" W).

For the Bluenose-East herd, we identified 87 migration paths undertaken by 38 females. Throughout the study period, migrations predominantly began in late April (see Fig. 3.2A) in the regions south and south-east of Great Bear Lake, although some females overwintered on the westernmost peninsula of the Great Bear Lake prior to undertaking a shorter spring migration than their counterparts (see Fig. 3.1). The annual median departure date ranged from April 23rd in 2014 to May 12th in 2013, while the median departure across all migration events throughout the study period was May 2nd. Migration typically ended in early to mid-June (see Fig. 3.2A) in the calving grounds stretching between Bluenose Lake and the Coronation Gulf (see Fig. 3.1). The annual median arrival date ranged from May 30th in 2016 to June 5th in 2013 and 2018, while the median arrival date across all migration events throughout the study period was June 2nd. None of the migration paths travelled by Bluenose-East crossed Great Bear Lake (31,153 km², 65°50'0" N, 120°45'0" W), the largest lake in their annual range. Bluenose-East herd migration paths did interact with one large lake, Hottah Lake (951 km², 65°30'0" N, 118°29'0" W), but unlike their Bathurst counterparts, they did not cross very large lakes.

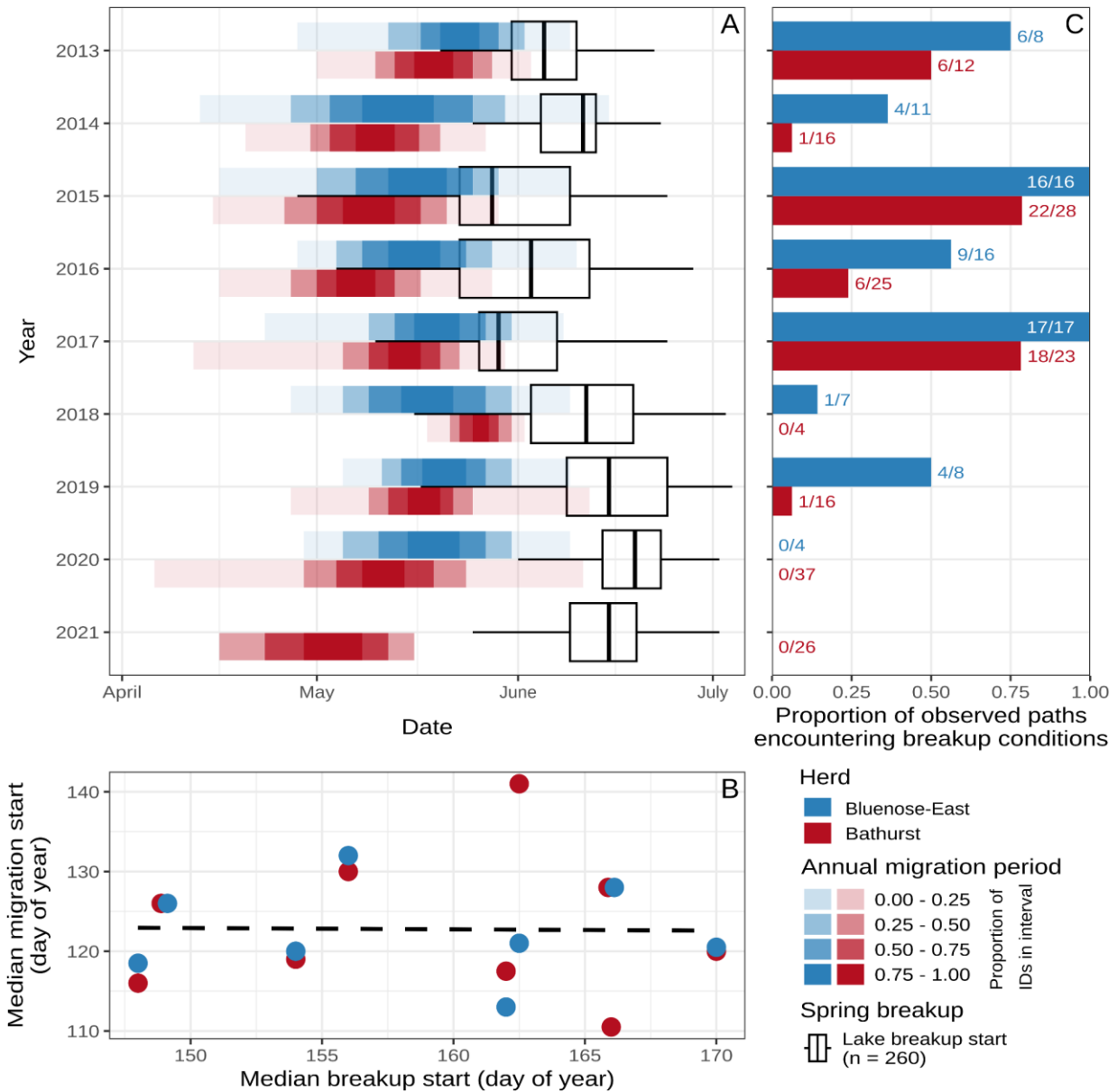


Figure 3.2 Temporal interactions between female caribou spring migration and lake ice breakup between 2013 and 2022. (A) The overlap in the periods of spring migration and breakup start. The spring migration period for each herd is shown by date intervals illustrated in red for Bathurst and blue for Bluenose-East, with progressive colour shading indicating the total proportion of collared females within each interval. The black-lined boxplots show the distribution of lake breakup start dates for 260 randomly selected lakes ranging from 0.1 to 1000 km² in size and distributed across the entire study area. (B) The relationship between the start of lake breakup and the median start of spring migration for each herd across years. The dotted trendline illustrates a non-significant linear model ($p = 0.95$). (C) The proportion of observed migration paths that encountered breaking ice or open water each year is shown by blue and red bars alongside their corresponding fractions of observed paths.

3.3.2 Timing of spring migration and breakup periods

The beginning of spring migration and the start of the lake breakup period vary among years (see Fig. 3.2A), but there is no relationship or correlation between their respective annual timing (see Fig. 3.2B). In some years, the overlap between the period of lake ice breakup and spring migration is more pronounced. For example, between 2013 and 2017 when 25%–50% of sampled lakes ($n = 260$) began to break up before the end of the Bathurst herd migration (see Fig. 3.2A) and approximately 75% of lakes began to break up before the end of spring migration for the Bluenose-East herd. Between 2013 and 2017, inclusively, 6%–78% of collared Bathurst females encountered breaking ice or open water (see Fig. 3.2C) in at least one step along their migration paths. For Bluenose-East females, 36%–100% of observed annual migration paths encountered breakup conditions in at least one step (see Fig. 3.2C). In both herds, the proportion of paths encountering breaking ice or open water was highest in 2015 and 2017 when 100% of Bluenose-East and 78% of Bathurst migration paths encountered these conditions (see Fig. 3.2B). In contrast, the post-2017 period is characterized by smaller periods of overlap between spring breakup and migration. Between 2018 and 2020, spring migration for both herds typically came to an end as approximately only 25% of the sampled lakes had begun breaking up. In 2021, none of the lakes had begun to break up before the end of the Bathurst spring migration. For the Bathurst herd, only 1 of the 83 paths observed between 2018 and 2021 encountered breaking ice or open water. In 2019, half of the observed migration paths (4 of 8 paths) for the Bluenose-East herd encountered breaking ice or open water, whereas only one in 2018

(1 of 4 paths) and none in 2020 (0 of 4 paths) encountered these conditions (see Fig. 3.2B).

3.3.3 Path selection analysis

3.3.3.1 Model comparison

Path selection model 3, incorporating the phenological states of freshwater ice and water body size, is the model with the most support (Table 3.1). While run time varied with model complexity, we detected no chains with divergent transitions and all models successfully converged to stable posterior distributions (see Suppl. Fig. 3.1). The information criteria and associated expected log predictive densities (ELPD) computed using both the KFCV-IC (Table 3.1) and WAIC (Suppl. Table 3.1) methods reveal large differences between the candidate path selection models in favour of model 3. Model 1, which only included the proportion of each step's area covered by hydrological features, has the lowest support with a KFCV-IC of 198,012.7 (± 998.8) and corresponding a ELPD difference of -20,309.6 (± 122.6) relative to model 3. Model 2, which incorporated the phenological state of freshwater, has marginally better support than model 1, with an ELPD difference of -20,051.2 (± 121.1) relative to model 3. Bayesian model weights attribute full support to model 3 (weight of 1) relative to model 1 and 2 (weights of 0; Table 3.1).

Table 3.1 Model comparison metrics for the three candidate path selection models. The environmental covariates of interest for each model are indicated along with their relative support by the data as estimated by Bayesian model weights, the K-fold cross-validation information criterion (KFCV-IC \pm standard error), the corresponding expected log predictive densities (ELPD \pm standard error), and the differences in ELPD (Δ ELPD \pm standard error) relative to the best model.

Model	Environmental covariates	Model weights	KFCV-IC (± SE)	ELPD (± SE)	ΔELPD (± SE)
3	Mean waterbody size (Small, Large, Very large) Proportion of ice x Mean waterbody size Proportion of breaking ice x Mean waterbody size Proportion of open water x Mean waterbody size	1	157,393.6 (814.5)	-78,696.8 (407.3)	0 (0)
2	Proportion of ice Proportion of breaking ice Proportion of open water	0	197,496.0 (994.9)	-98,748.0 (497.4)	-20,051.2 (121.1)
1	Proportion of hydrological features	0	198,012.7 (998.8)	-99,006.4 (499.4)	-20,309.6 (122.6)

x Denotes interactions between variables

Bold typeface indicates the model and associated variables with the most support.

3.3.3.2 Effects of waterbody state and size on migration

Relative to associated random paths, typical females select migration paths characterized by the prevalence of land or small ice-covered lakes and avoid paths which encounter larger waterbodies, breaking ice, and/or open water (see Fig. 3.3 & 3.4). The inclusion of step distance ($\beta = 0.006$ [-0.010 – 0.023]; Fig. 3.3) or step time ($\beta = -0.001$ [-0.003 – 0.002]; Suppl. Fig. 3.2) has no influence on these selection/avoidance patterns.

The estimated population-level coefficients and their 95% confidence intervals for small ($\beta = -3.01$ [-3.04 – -2.97]), large ($\beta = -3.05$ [-3.12 – -2.98]) and very large ($\beta = -3.10$ [-4.01 – -2.19]) lakes indicate increased avoidance of hydrological features with increased waterbody size in observed paths relative to associated random paths (see Fig. 3.3). Conditional effects indicate that, all other covariates being held constant, the relative probability of females selecting paths encountering small waterbodies is 1.2 and 8.2 times higher, respectively, than paths encountering large and very large waterbodies (see Fig. 3.4A).

During spring migration, females typically show a weak selection of ice-covered waterbodies ($\beta = 0.62$ [0.33 – 0.90]) relative to other parts of the landscape, but a strong avoidance of open water ($\beta = -11.44$ [-24.78 – -0.20]) and an extreme avoidance of breaking ice ($\beta = -22.37$ [-29.88 – -15.77]; Fig. 3.3). Conditional effects reveal that the relative selection or avoidance of lakes based on the state of spring breakup is further mediated by an interaction with their size, with avoidance increasing as waterbody size increases (see Fig. 3.3 & 3.4). The relative probability of a path being selected by typical migrating females increases in areas of the landscape dominated by small ice-covered lakes (see Fig. 3.4B). In contrast, paths over large ice-covered lakes are less likely to be selected and paths over very large ice-covered lakes are avoided altogether (see Fig. 3.4B). Once spring breakup begins, the relative probability of selection abruptly drops to 0 as the proportion of breaking ice increases to 20% in the landscape within around paths, even when the corresponding lakes are small (see Fig. 3.4C). This drop is more pronounced for steps encountering large lakes, where the relative probability of selection drops to 0 when the proportion of breaking ice increases to 10% (see Fig. 3.4C). Breaking ice conditions over very large lakes were exceedingly rare and only occurred in a single observed step, so there is low support ($\beta = -1.34$ [-20.38 – 17.58]; Fig. 3.3 & 3.4C) for this term in the path selection model. Observed paths rarely encountered open water in large lakes (16 steps) and did not encounter open water in very large lakes (0 steps) during the study period, so these interaction terms also have low support in the model. Typical females actively avoided paths that encountered small lakes with open water, with the relative probability of selection dropping to near 0 as the proportion of open water increased to 30% (see Fig. 3.4D). All other terms being held

constant at their means, the relative probability of selection is 8.9 times higher for areas with 20% open water than for areas with 20% breaking ice in small lakes (see Fig. 3.4C & D).

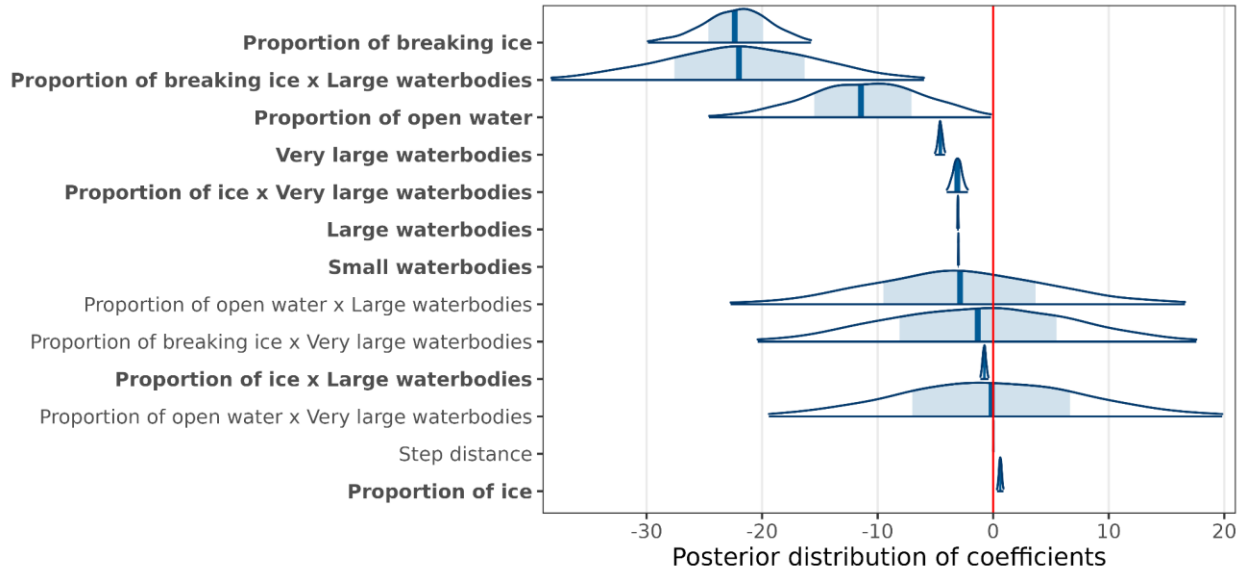


Figure 3.3 Distribution of posterior estimates for each coefficient in the path selection model with the most support, where step distance was included to reduce bias associated to movement speed. The vertical band illustrates each distribution's median value along with a shaded area representing 50% of the posterior distribution. The distributions are truncated at 95% and bold typeface indicates covariates and interactions that do not overlap with zero, illustrated in red. Interactions between terms are denoted by "x".

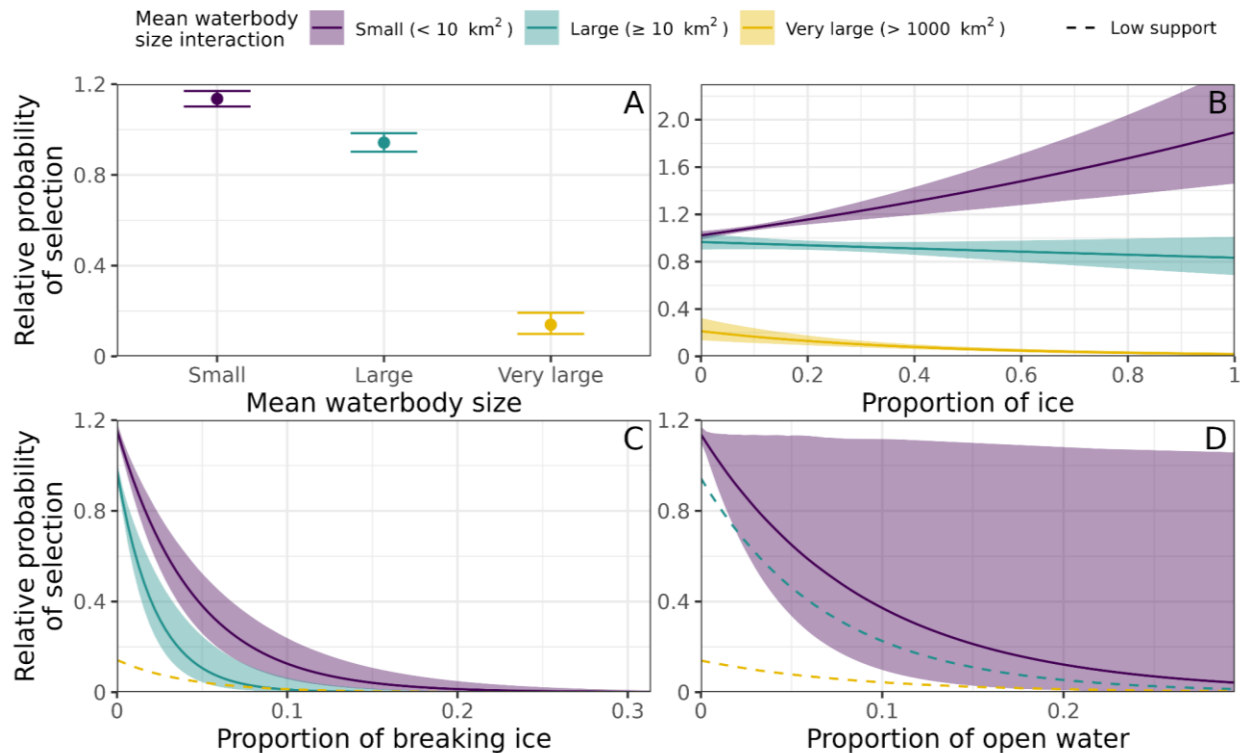


Figure 3.4 Conditional effects of mean waterbody size class and proportion of ice, breaking ice, and open water on female caribou path selection during spring migration. The estimated relative probability of selection (\pm 95% CI) varies as a function of the (A) mean within-step waterbody size and its interaction with the proportion of the landscape covered by (B) ice, (C) breaking ice, and (D) open water. Dashed lines depict low confidence in each interaction level's differentiation from the reference level of small mean waterbody size (i.e., coefficient's 95% confidence interval includes zero, see Fig. 3.3). Note the variation in x-axis limits, which reflect the full range of proportions of ice, breaking ice, and open water encountered in used/available paths throughout the study period.

3.3.4 Migration duration

All the behavioural and environmental covariates included in the HGAM, including lake ice phenology, are significant contributors to the duration of migration events (Adjusted $R^2 = 0.891$, Deviance explained = 92,6%). Once we account for inter-group differences in typical departure dates across herd/year as well as for inter-individual behavioural differences, the duration of migration varies as a function of population-level smooth terms including departure dates of individual migration events

(see Fig. 3.5A), the geographic distances between wintering grounds and calving (see Fig. 3.5B), and the rate of encounters with breakup conditions during the migration (see Fig. 3.5C). The most important determinant of spring migration duration was a female's departure date, with late departures resulting in significantly shorter migrations. The partial effects uniquely attributable to migration start date are such that the latest departures result in migration events that are 15 days shorter than the population mean while, inversely, the earliest departures result in migration events that are almost 25 days longer. Across individual migration events, the geographic distance to the calving ground at the start of migration varied between 116 and 516 km. Despite this range, the partial effect of distance is limited to an approximately 7-day difference in duration between the shortest and longest observed geographic distance at the start of migration (see Fig. 3.5B). In contrast, the state of lake ice phenology is a more important determinant of migration duration than geographic distance. As the rate of encounter with breakup conditions along each migration path climbs to 30%, a typical migration is delayed by approximately 8 days relative to migrations which only encounter ice (see Fig. 3.5C). This delay increases to almost 2 weeks when the breakup encounter rate doubles to 60%, but the confidence intervals become much wider given the rarity of such observations during our study period (<5% of observations between 30% and 60%).

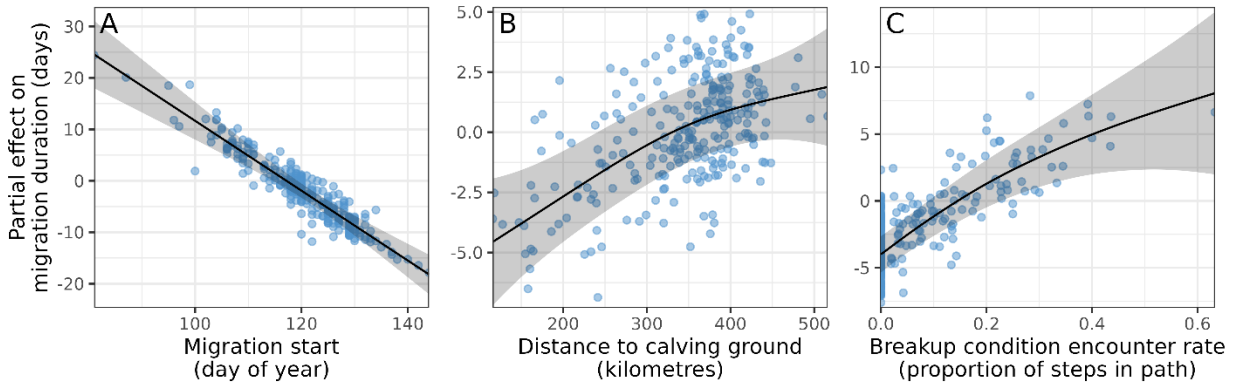


Figure 3.5 Partial effects of migration start date, distance to calving ground, and ice phenology on the duration of female caribou spring migration events. The duration of a migration event varies as a function of (A) the day of year a female initiated migration, (B) the geographic distance to the calving ground at the start of migration, and (C) the rate (proportion of steps in migration path) of encounters with breakup conditions including both breaking ice and open water. The three population-level smooth terms (black lines) and corresponding 95% confidence interval (grey ribbons) are fitted to observations (blue points) with an HGAM.

3.4 Discussion

By incorporating a freshwater ice phenology data product (OPEN-ICE) with high spatial and temporal resolution, our study provides unique insights into female caribou movement behaviour during spring migration across the full breadth of waterbody sizes (i.e., 0.1 to 31,153 km²) and ice phenological states (i.e., ice, breaking ice, and open water). Our main findings highlight that female caribou tend to select migratory paths through parts of the landscape composed mainly of terrestrial habitats or small frozen lakes and avoid larger lakes even if these remain ice-covered. As spring progresses and freshwater ice begins to melt, caribou exhibit strong avoidance of open water and extreme avoidance of breaking ice, with avoidance intensifying as the size of encountered waterbodies increases. These results show that breaking ice and to a lesser extent open water present important obstacles to migration, and that the

phenological states of lake and river ice are important determinants of migratory routes and, consequently, migration duration.

3.4.1 Small, ice-covered lakes are selected by migrating caribou but large, ice-covered lakes are avoided

Our study demonstrates that females from the Bathurst and Bluenose-East herds select ice-covered waterbodies during their spring migration, though this selection behaviour was only observed in areas of the landscape dominated by smaller waterbodies (< 10 km²; Fig. 3.4B). Due to the small size of these waterbodies and the relatively coarse sampling frequency of GPS locations (8h or 24h) in our study, in some areas it is difficult to ascertain if the exact path travelled by an individual between two successive GPS locations crossed water or land. Nonetheless, the high proportion of observed steps in regions with smaller lakes (~68%) combined with the strong signal of the probability of selection increasing with the proportion of small ice-covered waterbodies (see Fig. 3.4B) provides high confidence that caribou are preferentially crossing small ice-covered lakes. Previous investigations have also reported that caribou select routes along ice-covered waterbodies when these are available during migration (Leblond et al., 2016; Leclerc et al., 2021). For example, Leclerc et al. (2021) found that waterbodies were avoided relative to other open habitats such as tundra and shrub tundra habitats, although no distinctions were made between ice and water states over lakes. However, they did note a relatively high probability of selection of presumably frozen waterbodies during higher speed migratory movements. Similarly, waterbodies were avoided altogether when phenological states were not included as covariates (see Model 1, Table 3.1). However, by distinguishing ice from other

phenological states, our most supported model reveals a high probability of selection for smaller ice-covered waterbodies and relatively weak avoidance of ice-covered larger waterbodies. By distinguishing ice from water in 10 very large lakes and reservoirs during spring and fall migrations, Leblond et al. (2016) also found evidence of selection for routes travelling over ice-covered lakes and noted that selection strength increased in the years when the ice-availability season was shorter.

Caribou avoidance of larger ice-covered lakes is indicated by no migratory paths over the study region's two largest lakes (e.g., Great Bear Lake and Great Slave Lake), which remained ice-covered throughout every spring migration period. However, the years prior to and during our study were characterized by significant population declines resulting in the Bathurst herd's range retracting to core areas north of Great Slave Lake. In previous decades when the Bathurst herd overwintered in the regions south of Great Slave Lake, migrating individuals were known to cross the East Arm of Great Slave Lake where there are many islands to minimize exposed crossings over large expanses (Gunn et al., 2013). Similar behaviour was observed in migratory caribou in Québec, where an individual travelled 60 km over ice on the Robert-Bourassa reservoir (Leblond et al., 2016), a very large waterbody (2,835 km²) with thousands of small islands. Although, to our knowledge, there are no documented crossings of the larger exposed portions of Great Slave Lake and Great Bear Lake by barren-ground caribou, other migratory caribou and reindeer are known to undertake crossings between High Arctic islands, sometimes travelling distances exceeding 100 km over extremely exposed areas of sea ice (Miller et al., 2005). This contrast suggests that while caribou have the ability to travel great distances over ice, they are more likely to do so in regions where it

is required to access crucial parts of their range (e.g., Miller et al., 2005) or provides considerable time and energy savings (e.g., Joly, 2013). The landscape structures unique to each region likely explain the differences we observed in each herd's migratory behaviour in response to larger lakes. For example, the northward spring migration of the George River herd requires paths to traverse an important East-West freshwater barrier imposed by a series of large reservoirs from massive hydro-electric complexes. In contrast, the Bluenose-East herd's migration circumvents Great Bear Lake, and individuals from the Bathurst herd frequently cross Contwoyto Lake which, while very large, is long, narrow, and oriented perpendicularly to migratory routes.

The selection of ice-covered waterbodies during long distance movements is likely due to a combination of factors such as snowpack and predation. For example, frozen lakes are windswept and, consequently, the snowpack is denser and shallower (Sturm and Liston, 2003), making them easier routes for caribou to travel than adjacent terrestrial habitats with deeper snow (Pruitt, Jr., 1959). Frozen lakes also provide large open areas which may help caribou detect and evade predators (Ferguson and Elkie, 2005) and avoid ambush hunters such as wolves. The unique physiology of caribou hooves provides further evidence that they are highly adapted to long-distance travel over ice. Specifically, the cusps of the hooves are equipped with micro-structures that provide exceptional adherence and abrasion resistance to hard and slippery surfaces (Zhang et al., 2017) and specialized tendons in the dewclaws help stabilize the hooves (Hull et al., 2021).

3.4.2 Breaking ice is strongly avoided by migrating caribou and avoidance increases with lake size

Our study demonstrates that breaking ice, the transition state between ice cover and open water, is the phenological state that is most strongly avoided by females from the Bathurst and Bluenose-East herds during spring migration (see Fig. 3.4C). This relative avoidance further increases when females encounter larger waterbodies. Throughout the study period, breakup conditions did occur in larger lakes in some parts of the Bathurst and Bluenose-East herds' ranges, most often in areas with stronger currents in long and narrow chain of lakes forming interconnected sections of larger rivers such as the Coppermine River, Burnside River, Camsell River, and Snare River. While many of these areas were typically avoided during migration, some migration paths did cross these areas even when breaking ice was present, presumably because they constitute strategic or obligatory crossing points. For example, observed migration paths in the Bathurst range encountered breaking ice conditions in lakes of the upper Burnside River system adjacent to the calving ground, such as the northernmost part of Contwoyto Lake and Kathawachaga Lake, and lakes of the Coppermine River such as Point Lake and the wide sections of the river between Desteffany Lake and Lac de Gras. Within the Bluenose-East range, observed migration paths most frequently encountered breaking ice conditions in crossings of the Dismal Lake system, and in larger lakes of the Calder River system such as Breadner Lake. Only a single female breaking ice conditions on a very large lake, and it was adjacent to the mouth of the Dease River on Great Bear Lake. The current rarity of encounters with breaking ice over very large lakes is likely attributable to: (i) the active avoidance of these lakes

regardless of their phenological state (see Fig. 3.4A) and (ii) that ice cover persists longer in larger/deeper lakes (Duguay et al., 2003; Giroux-Bougard et al., 2023).

Our inclusion of spring breakup conditions into a used-available study design is new, but migratory caribou responses to breaking ice have been well documented in other ways. The most complete account of caribou navigating breaking ice in the scientific literature is based on observations of the fall migration by Miller and Gunn (1986). In October of 1982, a year with delayed freeze-up due to warmer temperatures, the authors observed multiple groups of Beverly herd caribou venturing over smaller lakes and narrow channels, undeterred by the thin ice. Individuals that broke through ice did not seem immediately distressed, but the authors observed minor-to-severe injuries and mortality events from exposure or drowning as a direct consequence of difficult or failed extrications from the breaking ice. Indigenous hunters also reported numerous injuries to the anterior forelegs on caribou harvested that same fall (Miller and Gunn, 1986). Given that migrating caribou select ice but avoid breaking ice during spring migration, that the transition between these two states can be very rapid especially in moving waterbodies like rivers, and that thin or rotting ice is still sometimes crossed when it cannot be avoided, caribou encounters with breaking ice are inevitable. For example, migrating caribou are frequently observed drifting on ice floes during the spring breakup of arctic rivers (Lord, 2014) or stranded on sea ice floes (Thompson, 2017), presumably having been caught off-guard at the moment of breakup or when ice dams give away during obligatory crossings on their journey to the calving grounds.

3.4.3 Open water is avoided by migrating caribou but not as strongly as breaking ice

Once spring breakup is complete, migrating females avoid open water (see Fig. 3.3) but not as strongly as they avoid breaking ice. Because the spring migrations observed during our study period generally coincided with early phases of spring breakup (see Fig. 3.2), open water was only encountered over smaller waterbodies, which typically break up faster than larger lakes (Giroux-Bougard et al., 2023). While our results provide some evidence that avoidance of open water increases with waterbody size (see Fig. 3.4D), the scarcity of large lakes with open water during our study period constrains our ability to assess the relationship. Previous investigations of migratory caribou movements also indicate strong avoidance of open water. Using path selection analysis, Leclerc et al. (2021) found that caribou avoided all waterbodies altogether in favour of tundra habitats during spring migration, although they did not discern between water and ice. In contrast, using step selection analysis Leblond et al. (2016) found that, relative to ice, caribou avoided open water crossings during migration, a pattern which was accentuated in years when lake ice was available over a longer period. The authors noted that while most individuals circumvented large lakes with open water, some did initiate swimming crossings, and either turned around shortly after or progressed much more slowly than their counterparts. Caribou are agile and competent swimmers, assisted by their buoyant hollow-haired coats (Meeks and Cartwright, 2005) and large toes for propulsion, but sustained travel on land is much more energetically efficient than quadrupedal swimming (Fancy & White 1987). Despite avoidance of large open water expanses, caribou do not hesitate to swim when it is

strategic or obligatory. Barren-ground caribou undertake regular open water crossings of rivers and narrow lake channels during their seasonal migrations (Williams and Gunn, 1982). Peary caribou are known to swim across open sea channels between islands to access various parts of their range (~ 3 km; Miller, 1995). Woodland caribou undertake frequent water crossings between small islands to access forage and avoid predators (~ 1 km; Webber et al., 2021).

3.4.4 The ice phenology of small lakes and rivers

A major advance offered by our analysis of the effects of ice phenology on caribou migration is the capacity of the OPEN-ICE algorithm to assess the phenological state of small waterbodies. Small waterbodies are typically excluded from lake ice monitoring efforts (e.g., Du et al., 2017; Duguay et al., 2006; Latifovic & Pouliot, 2007) and caribou migration research (e.g., Gurarie et al., 2019; Le Corre et al., 2016; Leblond et al., 2016) due to constraints in spatial resolution, despite their abundance (Messenger et al., 2016), their important combined surface area relative to other lake size classes (Verpoorter et al., 2014), and their significance to caribou migration (Miller and Gunn, 1986; Williams and Gunn, 1982). While the freshwater ice phenology covariates in our study incorporated both lakes and rivers, a future challenge is to tease apart the unique effect of rivers. Rivers break up sooner in spring than lakes in the surrounding landscape, and their length and continuity impose obligatory crossings for caribou which cannot be circumvented like lakes. As such, natural river fords or narrows constitute important caribou crossing sites. The current of rivers, combined with laminar flow and depth heterogeneity, creates highly complex patterns of ice formation and breakup, including rapidly changing ice conditions in spring, on the scale of minutes and hours,

which are extremely difficult to observe (Floyd et al., 2014) and model (Das and Lindenschmidt, 2021). Specifically, in some years the breakup of Arctic rivers is characterized by a violent cycle of ice jams and floods, conditions which can injure or drown migrating caribou (Miller and Gunn, 1986; Nault and Le Hénaff, 1988). Even during less turbulent river breakup events, the mere presence of floating ice during crossings is hazardous to swimming caribou, especially younger ones (Williams and Gunn, 1982). Further research is needed to improve monitoring and assessment of river ice phenology and to better understand how these important, seasonally dynamic landscape bottlenecks impact caribou migration.

3.4.5 Ice phenology and the timing of spring migration

Because the timing of caribou migration and the timing of ice breakup varied annually (see Fig. 3.2A) and independently (see Fig. 3.2B) of each other throughout the nine-year study period, the proportion of observed migratory paths that encountered breakup conditions varied from more than 75% in 2015 and 2017 to 0% in 2020 and 2021 (see Fig. 3.2C). While spring migration start dates are variable across years and herds, females that depart late typically migrate faster, resulting in relatively consistent arrival and calving dates within each herd (Gurarie et al., 2019). However, the cues for the initiation of spring migration are decoupled from freshwater ice phenology (see Fig. 3.2B; Gurarie et al., 2019; Le Corre et al., 2016). Despite the plasticity in the timing of departure and arrival (Gurarie et al., 2019) and the selection/avoidance behaviours exhibited during migration (see Fig. 3.4), our research shows that interactions with breakup conditions during spring migration can significantly prolong the duration of migration (see Fig. 3.5) and, consequently, cause potential delays in arrival to the

calving ground. As the ice-free season progressively lengthens and the timing of spring ice melt advances throughout the northern hemisphere (Sharma et al., 2019), the severity of these effects on the duration of migration are likely to increase, potentially disrupting the timing of calving and calf survival.

Because it immediately precedes calving, the timing of spring migration constitutes a key period in the annual cycles of barren-ground caribou. The observed plasticity in the timing of migration constitutes a strategy to match up the parturition and lactation period with the fresh growth high-quality forage (Gurarie et al., 2019), which promotes calf health (Post and Forchhammer, 2008). This synchrony is so crucial that, in some migratory caribou herds (e.g., George and Leaf River herds), calving date has emerged as the single most important predictor of calf survival (Vuillaume et al., 2023). In light of the rapid environmental changes unfolding in the Arctic (Post et al., 2019), there is evidence that the timing of caribou migration and the synchronicity of calving with spring plant phenology may be disrupted (Post and Forchhammer, 2008). Indeed, in some herds migrating females have recently been observed calving before reaching their calving ground due to late departures from their wintering grounds (Couriot et al., 2023; Gurarie et al., 2019). Despite such concerns, multiple studies have highlighted the significant plasticity in the timing of spring migration (Gurarie et al., 2019; Laforge et al., 2023), and there is emerging evidence that migratory caribou can adapt the timing of their migration to avoid trophic mismatch in the post-calving period (Mallory et al., 2020). Although there remains a great deal of uncertainty surrounding the exact environmental cues that prompt the initiation of spring migration, research suggests that snow conditions in late winter are likely the main factor (Gurarie et al., 2019; Le Corre et

al., 2016; Mallory et al., 2020). In addition, snow conditions and specifically the timing of snowmelt is also the main determinant in the start of greening in tundra biomes (Kelsey et al., 2021), which is an important determinant for the timing of calving. However, the complex dynamics of freshwater ice formation and decay operate differently. Similarly to snowmelt, the beginning of the breakup period is mainly related to air temperature (Higgins et al., 2021), but the main determinants of the duration of the breakup period, and indeed the duration of the entire ice-on period, are air temperature and thermal inertia (i.e., heat storage as related to lake volume and depth) (Sharma et al., 2019; Warne et al., 2020). When the ice-free season is longer, more heat is stored in waterbodies which in turn leads to earlier and shorter breakup periods (Sharma et al., 2019). Because of this feedback, the ice-free period is increasing at a faster rate than the snow-free period throughout the Arctic (Dauginis and Brown, 2021). This suggests that even if caribou show continued plasticity in adapting the timing of their migrations based on environmental cues such as snow conditions, there will likely be a mismatch between the timing of migration and the availability of ice on lakes and rivers due to earlier breakup. In addition to experiencing more prevalent breakup conditions during spring migration, caribou will also need to navigate increased year-to-year variability in the timing of breakup (Weyhenmeyer et al., 2011). While individual spatial memory (Avgar et al., 2015) and emergent collective movement behaviours (Dalziel et al., 2016; Torney et al., 2018) may aid caribou to mitigate this increasing variability in the landscape, the rapidity of these environmental changes at a time when several large herds have experienced catastrophic declines casts some uncertainty on their ability to do so (Mallory and Boyce, 2018).

3.4.6 The connectivity of landscapes

As the pace of Arctic warming continues and freshwater ice availability declines during spring migration, our results suggest that caribou will increasingly rely on terrestrial corridors available in the landscape and limit their interactions with waterbodies to obligatory crossings of rivers or narrow channels. Based on their own findings, Leblond et al. (2016) concluded the same, and further estimated that 36% of the ice crossings observed in their study of the Leaf River herd could disappear as soon as 2041, effectively pushing migratory routes to adjacent terrestrial habitats and increasing the overall travel distance required for individuals to reach their destination. As migration routes become constrained to specific corridors and crossings, these areas will play an important role in conserving the connectivity of these northern landscapes. Due to the importance of these crossings and corridors for Indigenous hunters who have relied on caribou for thousands of years, these areas are already well documented through community-led traditional knowledge projects (Parlee et al., 2005; Zalatan et al., 2006). Notably, some of these important crossing sites, such as the Lockhart River outflow from Artillery Lake, are not presently used due to important range shifts that have occurred following recent drastic population declines (Dokis-Jansen et al., 2021). Within the Bluenose-East and Bathurst herd ranges, some of these corridors are already heavily impacted by industrial development and roads (Government of the Northwest Territories, 2019; Mueller and Gunn, 1996) which impact caribou movement behaviours (Boulanger et al., 2021; Wilson et al., 2016). As continued rapid warming is expected for the foreseeable future, comprehensive herd range and land use planning may be the only tools available to wildlife management agencies to reduce potential

disturbances to these crucial corridors and mitigate further impacts to spring migration routes.

3.5 Conclusion

As the Arctic continues to warm at a faster pace than the rest of the planet, it is clear that shifting freshwater ice phenology will bring about massive changes to the landscapes experienced by caribou during spring migrations. While previous studies have mainly focused on effects of ice and water on caribou movement, we have found that it is the transitional state during which ice is breaking up that actually constitutes the most avoided condition over freshwater features. Given the inherent difficulties and dangers of navigating thin or rotting ice, this is an intuitive result with important implications for the continued period of warming we are witnessing in the Arctic. Indeed, in the immediate future it is mainly breaking ice, not open water, that we expect caribou will encounter at a much higher rate. As avoidance of hydrological features increases, migratory routes will increasingly rely on terrestrial habitats, the depth and characteristics of snow cover, and the landscape structures and barriers imposed by lakes and breaking ice within each herd's range. In the immediate future, the increased prevalence of breaking ice will not only be a concern for landscape connectivity and the energetic costs involved in reaching calving grounds, but the increasing rapidity and unpredictability of breakup and the potential delayed arrival to the calving ground may impact recruitment through female survival during migration and calf survival following parturition.

3.6 References

- Aikens, E.O., Dwinnell, S.P.H., LaSharr, T.N., Jakopak, R.P., Fralick, G.L., Randall, J., Kaiser, R., Thonhoff, M., Kauffman, M.J., Monteith, K.L., 2021. Migration distance and maternal resource allocation determine timing of birth in a large herbivore. *Ecology* 102. <https://doi.org/10.1002/ecy.3334>
- Alerstam, T., Hedenstrom, A., Akesson, S., 2003. Long-distance migration: Evolution and determinants. *Oikos* 103, 247–260. <https://doi.org/10.1034/j.1600-0706.2003.12559.x>
- Bergerud, A.T., Luttich, S.N., Camps, L., 2008. The return of caribou to Ungava. McGill-Queen's University Press, Montreal, Canada.
- Berkes, F., 1988. The intrinsic difficulty of predicting impacts: Lessons from the James Bay hydro project. *Environ. Impact Assess. Rev.* 8, 201–220. [https://doi.org/10.1016/0195-9255\(88\)90067-4](https://doi.org/10.1016/0195-9255(88)90067-4)
- Betancourt, M., 2017. A conceptual introduction to Hamiltonian Monte Carlo. arXiv. <https://doi.org/10.48550/ARXIV.1701.02434>
- Bonfil, R., Meyer, M., Scholl, M.C., Johnson, R., O'Brien, S., Oosthuizen, H., Swanson, S., Kotze, D., Paterson, M., 2005. Transoceanic migration, spatial dynamics, and population linkages of white sharks. *Science* 310, 100–103. <https://doi.org/10.1126/science.1114898>
- Boulanger, J., Poole, K.G., Gunn, A., Adamczewski, J., Wierzchowski, J., 2021. Estimation of trends in zone of influence of mine sites on barren-ground caribou populations in the Northwest Territories, Canada, using new methods. *Wildl. Biol.* 2021. <https://doi.org/10.2981/wlb.00719>
- Bowers, E.K., Grindstaff, J.L., Soukup, S.S., Drilling, N.E., Eckerle, K.P., Sakaluk, S.K., Thompson, C.F., 2016. Spring temperatures influence selection on breeding date and the potential for phenological mismatch in a migratory bird. *Ecology* 97, 2880–2891. <https://doi.org/10.1002/ecy.1516>
- Bürkner, P.-C., 2017. brms: An R package for Bayesian multilevel models using Stan. *J. Stat. Softw.* 80, 1–28. <https://doi.org/10.18637/jss.v080.i01>
- Cattet, M., 2011. Standard operating procedure for the capture, handling & release of caribou. Wildlife Care Committee, Government of the Northwest Territories, Yellowknife, Canada.
- Checkley, D.M., Raman, S., Maillet, G.L., Mason, K.M., 1988. Winter storm effects on the spawning and larval drift of a pelagic fish. *Nature* 335, 346–348. <https://doi.org/10.1038/335346a0>
- Chmura, H.E., Kharouba, H.M., Ashander, J., Ehlman, S.M., Rivest, E.B., Yang, L.H., 2019. The mechanisms of phenology: The patterns and processes of phenological shifts. *Ecol. Monogr.* 89, e01337. <https://doi.org/10.1002/ecm.1337>
- Cotton, P.A., 2003. Avian migration phenology and global climate change. *Proc. Natl. Acad. Sci.* 100, 12219–12222. <https://doi.org/10.1073/pnas.1930548100>
- Couriot, O.H., Cameron, M.D., Joly, K., Adamczewski, J., Campbell, M.W., Davison, T., Gunn, A., Kelly, A.P., Leblond, M., Williams, J., Fagan, W.F., Brose, A., Gurarie, E., 2023. Continental synchrony and local responses: Climatic effects on spatiotemporal patterns of calving in a social ungulate. *Ecosphere* 14, e4399. <https://doi.org/10.1002/ecs2.4399>

- Dalziel, B.D., Corre, M.L., Côté, S.D., Ellner, S.P., 2016. Detecting collective behaviour in animal relocation data, with application to migrating caribou. *Methods Ecol. Evol.* 7, 30–41. <https://doi.org/10.1111/2041-210X.12437>
- Das, A., Lindenschmidt, K.-E., 2021. Modelling climatic impacts on ice-jam floods: A review of current models, modelling capabilities, challenges, and future prospects. *Environ. Rev.* 29, 378–390. <https://doi.org/10.1139/er-2020-0108>
- Dauginis, A.A., Brown, L.C., 2021. Recent changes in pan-Arctic sea ice, lake ice, and snow-on/off timing. *The Cryosphere* 15, 4781–4805. <https://doi.org/10.5194/tc-15-4781-2021>
- Dokis-Jansen, K.L., Parlee, B.L., Łutsël K'e Dëne First Nation, Hik, D.S., Gendreau-Berthiaume, B., Macdonald, E., Stinn, C., 2021. “These trees have stories to tell”: Linking Dënesǫłiné oral history of caribou use with trample scar frequency on black spruce roots at ǂedacho Kué. *Arctic* 74, 290–305. <https://doi.org/10.14430/arctic73160>
- Du, J., Kimball, J.S., Duguay, C., Kim, Y., Watts, J.D., 2017. Satellite microwave assessment of Northern Hemisphere lake ice phenology from 2002 to 2015. *The Cryosphere* 11, 47–63. <https://doi.org/10.5194/tc-11-47-2017>
- Duguay, C.R., Flato, G.M., Jeffries, M.O., Ménard, P., Morris, K., Rouse, W.R., 2003. Ice-cover variability on shallow lakes at high latitudes: Model simulations and observations. *Hydrol. Process.* 17, 3465–3483. <https://doi.org/10.1002/hyp.1394>
- Duguay, C.R., Prowse, T.D., Bonsal, B.R., Brown, R.D., Lacroix, M.P., Ménard, P., 2006. Recent trends in Canadian lake ice cover. *Hydrol. Process.* 20, 781–801. <https://doi.org/10.1002/hyp.6131>
- Ecological Stratification Working Group, 1995. A national ecological framework for Canada. Agriculture and Agri-Food Canada, Research Branch, Centre for Land and Biological Resources Research, and Environment Canada, State of the Environment Directorate, Ecozone Analysis Branch, Ottawa, Canada.
- Fancy, S.G., White, R.G., 1987. Energy expenditures for locomotion by barren-ground caribou. *Can. J. Zool.* 65, 122–128. <https://doi.org/10.1139/z87-018>
- Ferguson, S.H., Elkie, P.C., 2005. Use of lake areas in winter by woodland caribou. Northeast. *Nat.* 12, 45–66. [https://doi.org/10.1656/1092-6194\(2005\)012\[0045:UOLAIW\]2.0.CO;2](https://doi.org/10.1656/1092-6194(2005)012[0045:UOLAIW]2.0.CO;2)
- Floyd, A.L., Prakash, A., Meyer, F.J., Gens, R., Liljedahl, A., 2014. Using synthetic aperture radar to define spring breakup on the Kuparuk River, Northern Alaska. *Arctic* 67, 462. <https://doi.org/10.14430/arctic4426>
- Forester, J.D., Im, H.K., Rathouz, P.J., 2009. Accounting for animal movement in estimation of resource selection functions: Sampling and data analysis. *Ecology* 90, 3554–3565. <https://doi.org/10.1890/08-0874.1>
- Fortin, D., Beyer, H.L., Boyce, M.S., Smith, D.W., Duchesne, T., Mao, J.S., 2005. Wolves influence elk movements: Behavior shapes a trophic cascade in Yellowstone National Park. *Ecology* 86, 1320–1330. <https://doi.org/10.1890/04-0953>
- Fudickar, A.M., Jahn, A.E., Ketterson, E.D., 2021. Animal migration: An overview of one of nature’s great spectacles. *Annu. Rev. Ecol. Evol. Syst.* 52, 479–497. <https://doi.org/10.1146/annurev-ecolsys-012021-031035>

- Gabry, J., Simpson, D., Vehtari, A., Betancourt, M., Gelman, A., 2019. Visualization in Bayesian workflow. *J. R. Stat. Soc. Ser. A Stat. Soc.* 182, 389–402. <https://doi.org/10.1111/rssa.12378>
- Gelman, A., Vehtari, A., Simpson, D., Margossian, C.C., Carpenter, B., Yao, Y., Kennedy, L., Gabry, J., Bürkner, P.-C., Modrák, M., 2020. Bayesian workflow. *arXiv*. <https://doi.org/10.48550/ARXIV.2011.01808>
- Gillett, N.P., Weaver, A.J., Zwiers, F.W., Flannigan, M.D., 2004. Detecting the effect of climate change on Canadian forest fires. *Geophys. Res. Lett.* 31, 1–4. <https://doi.org/10.1029/2004GL020876>
- Gillies, C.S., Hebblewhite, M., Nielsen, S.E., Krawchuk, M.A., Aldridge, C.L., Frair, J.L., Saher, D.J., Stevens, C.E., Jerde, C.L., 2006. Application of random effects to the study of resource selection by animals: Random effects in resource selection. *J. Anim. Ecol.* 75, 887–898. <https://doi.org/10.1111/j.1365-2656.2006.01106.x>
- Giroux-Bougard, X., Fluet-Chouinard, E., Crowley, M.A., Cardille, J.A., Humphries, M.M., 2023. Multi-sensor detection of spring breakup phenology of Canada's lakes. *Remote Sens. Environ.* 295, 113656. <https://doi.org/10.1016/j.rse.2023.113656>
- Gorelick, N., Hancher, M., Dixon, M., Ilyushchenko, S., Thau, D., Moore, R., 2017. Google Earth Engine: Planetary-scale geospatial analysis for everyone. *Remote Sens. Environ.* 202, 18–27. <https://doi.org/10.1016/j.rse.2017.06.031>
- Government of the Northwest Territories, 2019. Bathurst caribou range plan. Environment and Natural Resources, Government of the Northwest Territories, Yellowknife, Canada.
- Government of the Northwest Territories, 2016. Technical report on the Cape Bathurst, Bluenose-West, and Bluenose-East barren-ground caribou herds. Environment and Natural Resources, Government of the Northwest Territories, Yellowknife, Canada.
- Gunn, A., D'Hont, A., Williams, J., Boulanger, J., 2013. Satellite collaring in the Bathurst herd of barren-ground caribou 1996-2005. Government of the Northwest Territories, Yellowknife, Canada.
- Gurarie, E., Hebblewhite, M., Joly, K., Kelly, A.P., Adamczewski, J., Davidson, S.C., Davison, T., Gunn, A., Sutor, M.J., Fagan, W.F., Boelman, N., 2019. Tactical departures and strategic arrivals: Divergent effects of climate and weather on caribou spring migrations. *Ecosphere* 10. <https://doi.org/10.1002/ecs2.2971>
- Haest, B., Hüppop, O., Bairlein, F., 2018. The influence of weather on avian spring migration phenology: What, where and when? *Glob. Change Biol.* 24, 5769–5788. <https://doi.org/10.1111/gcb.14450>
- Higgins, S.N., Desjardins, C.M., Drouin, H., Hrenchuk, L.E., van der Sanden, J.J., 2021. The role of climate and lake size in regulating the ice phenology of boreal lakes. *J. Geophys. Res. Biogeosciences* 126. <https://doi.org/10.1029/2020JG005898>
- Hoberg, E.P., Polley, L., Jenkins, E.J., Kutz, S.J., Veitch, A.M., Elkin, B.T., 2008. Integrated approaches and empirical models for investigation of parasitic diseases in northern wildlife. *Emerg. Infect. Dis.* 14, 10–17. <https://doi.org/10.3201/eid1401.071119>

- Hull, E., Semeniuk, M., Puolakka, H.-L., Kynkäänniemi, S.-M., Niinimäki, S., 2021. Tendons and ligaments of the *Rangifer tarandus* metapodial and hoof. *Polar Biol.* 44, 1803–1816. <https://doi.org/10.1007/s00300-021-02919-z>
- IPCC, 2014. Climate change 2014: Synthesis report. Intergovernmental Panel on Climate Change, Geneva, Switzerland.
- Johnson, C.J., Nielsen, S.E., Merrill, E.H., McDonald, T.L., Boyce, M.S., 2006. Resource selection functions based on use–availability data: Theoretical motivation and evaluation methods. *J. Wildl. Manag.* 70, 347–357. [https://doi.org/10.2193/0022-541X\(2006\)70\[347:RSFBOU\]2.0.CO;2](https://doi.org/10.2193/0022-541X(2006)70[347:RSFBOU]2.0.CO;2)
- Joly, K., 2013. Sea ice crossing by migrating caribou, *Rangifer tarandus*, in northwestern Alaska. *Can. Field-Nat.* 126, 217. <https://doi.org/10.22621/cfn.v126i3.1363>
- Kays, R., Davidson, S.C., Berger, M., Bohrer, G., Fiedler, W., Flack, A., Hirt, J., Hahn, C., Gauggel, D., Russell, B., Kölzsch, A., Lohr, A., Partecke, J., Quetting, M., Safi, K., Scharf, A., Schneider, G., Lang, I., Schaeuffelhut, F., Landwehr, M., Storhas, M., van Schalkwyk, L., Vinciguerra, C., Weinzierl, R., Wikelski, M., 2022. The Movebank system for studying global animal movement and demography. *Methods Ecol. Evol.* 13, 419–431. <https://doi.org/10.1111/2041-210X.13767>
- Kelsey, K.C., Pedersen, S.H., Leffler, A.J., Sexton, J.O., Feng, M., Welker, J.M., 2021. Winter snow and spring temperature have differential effects on vegetation phenology and productivity across Arctic plant communities. *Glob. Change Biol.* 27, 1572–1586. <https://doi.org/10.1111/gcb.15505>
- Knudsen, E., Lindén, A., Ergon, T., Jonzén, N., Vik, J., Knape, J., Røer, J., Stenseth, N., 2007. Characterizing bird migration phenology using data from standardized monitoring at bird observatories. *Clim. Res.* 35, 59–77. <https://doi.org/10.3354/cr00714>
- Laforge, M.P., Webber, Q.M.R., Vander Wal, E., 2023. Plasticity and repeatability in spring migration and parturition dates with implications for annual reproductive success. *J. Anim. Ecol.* 92, 1042–1054. <https://doi.org/10.1111/1365-2656.13911>
- Latifovic, R., Pouliot, D., 2007. Analysis of climate change impacts on lake ice phenology in Canada using the historical satellite data record. *Remote Sens. Environ.* 106, 492–507. <https://doi.org/10.1016/j.rse.2006.09.015>
- Le Corre, M., Dussault, C., Côté, S.D., 2016. Weather conditions and variation in timing of spring and fall migrations of migratory caribou. *J. Mammal.* gyw177. <https://doi.org/10.1093/jmammal/gyw177>
- Leblond, M., St-Laurent, M.-H., Côté, S.D., 2016. Caribou, water, and ice – Fine-scale movements of a migratory arctic ungulate in the context of climate change. *Mov. Ecol.* 4, 14. <https://doi.org/10.1186/s40462-016-0079-4>
- Leclerc, M., Leblond, M., Le Corre, M., Dussault, C., Côté, S.D., 2021. Determinants of migration trajectory and movement rate in a long-distance terrestrial mammal. *J. Mammal.* 102, 1342–1352. <https://doi.org/10.1093/jmammal/gyab081>
- Lemoine, N.P., 2019. Moving beyond noninformative priors: Why and how to choose weakly informative priors in Bayesian analyses. *Oikos* 128, 912–928. <https://doi.org/10.1111/oik.05985>
- Lord, D., 2014. Caribou adrift as ice breaks up near Old Crow, Yukon. *CBC News*.

- Mallory, C.D., Boyce, M.S., 2018. Observed and predicted effects of climate change on Arctic caribou and reindeer. *Environ. Rev.* 26, 13–25. <https://doi.org/10.1139/er-2017-0032>
- Mallory, C.D., Williamson, S.N., Campbell, M.W., Boyce, M.S., 2020. Response of barren-ground caribou to advancing spring phenology. *Oecologia* 192, 837–852. <https://doi.org/10.1007/s00442-020-04604-0>
- Mansfield, K.L., Mendilaharsu, M.L., Putman, N.F., dei Marcovaldi, M.A.G., Sacco, A.E., Lopez, G., Pires, T., Swimmer, Y., 2017. First satellite tracks of South Atlantic sea turtle 'lost years': Seasonal variation in trans-equatorial movement. *Proc. R. Soc. B Biol. Sci.* 284, 20171730. <https://doi.org/10.1098/rspb.2017.1730>
- Marra, P.P., Cohen, E.B., Loss, S.R., Rutter, J.E., Tonra, C.M., 2015. A call for full annual cycle research in animal ecology. *Biol. Lett.* 11, 20150552. <https://doi.org/10.1098/rsbl.2015.0552>
- Meeks, N.D., Cartwright, C.R., 2005. Caribou and seal hair: Examination by scanning electron microscopy, in: *Arctic Clothing of North America-Alaska, Canada, Greenland*. McGill-Queen's University Press, pp. 42–44.
- Messenger, M.L., Lehner, B., Grill, G., Nedeva, I., Schmitt, O., 2016. Estimating the volume and age of water stored in global lakes using a geo-statistical approach. *Nat. Commun.* 7, 13603. <https://doi.org/10/f9g5qg>
- Miller, F.L., 1995. Inter-island water crossings by Peary caribou, south-central Queen Elizabeth Islands. *Arctic* 48, 8–12. <https://doi.org/10.14430/arctic1219>
- Miller, F.L., Barry, S.J., Calvert, W.A., 2005. Sea-ice crossings by caribou in the south-central Canadian Arctic Archipelago and their ecological importance. *Rangifer* 25, 77. <https://doi.org/10.7557/2.25.4.1773>
- Miller, F.L., Gunn, A., 2003. Catastrophic die-off of Peary caribou on the western Queen Elizabeth Islands, Canadian High Arctic. *Arctic* 56, 381–390.
- Miller, F.L., Gunn, A., 1986. Observations of barren-ground caribou travelling on thin ice during autumn migration. *Arctic* 39, 85–88.
- Morisette, J.T., Richardson, A.D., Knapp, A.K., Fisher, J.I., Graham, E.A., Abatzoglou, J., Wilson, B.E., Breshears, D.D., Henebry, G.M., Hanes, J.M., Liang, L., 2009. Tracking the rhythm of the seasons in the face of global change: Phenological research in the 21st century. *Front. Ecol. Environ.* 7, 253–260. <https://doi.org/10.1890/070217>
- Mueller, F.P., Gunn, A., 1996. Caribou behaviour in the vicinity of Lupin gold mine Northwest Territories (Technical Report No. 91). Department of Resources, Wildlife and Economic Development, Government of the Northwest Territories, Yellowknife, Canada.
- Muff, S., Signer, J., Fieberg, J., 2020. Accounting for individual-specific variation in habitat-selection studies: Efficient estimation of mixed-effects models using Bayesian or frequentist computation. *J. Anim. Ecol.* 89, 80–92. <https://doi.org/10.1111/1365-2656.13087>
- Musolin, D.L., 2007. Insects in a warmer world: Ecological, physiological and life-history responses of true bugs (*Heteroptera*) to climate change. *Glob. Change Biol.* 13, 1565–1585. <https://doi.org/10.1111/j.1365-2486.2007.01395.x>
- Nagy, J.A., 2011. Use of space by caribou in Northern Canada (PhD Thesis). University of Alberta, Edmonton, Canada.

- Nault, R., Le Hénaff, D., 1988. Validation des sites potentiellement dangereux pour le caribou sur le territoire du Nouveau-Québec. Ministère du Loisir, de la Chasse et de la pêche du Gouvernement du Québec, Québec, Canada.
- Newton, I., 2007. Weather-related mass-mortality events in migrants: Weather-related mass-mortality events in migrants. *Ibis* 149, 453–467. <https://doi.org/10.1111/j.1474-919X.2007.00704.x>
- Parlee, B., Manseau, M., Łutsël K'e Dëne First Nation, 2005. Using traditional knowledge to adapt to ecological change: Denésłłné monitoring of caribou movements. *Arctic* 58, 26–37.
- Pedersen, E.J., Miller, D.L., Simpson, G.L., Ross, N., 2019. Hierarchical generalized additive models in ecology: An introduction with mgcv. *PeerJ* 7, e6876. <https://doi.org/10.7717/peerj.6876>
- Pekel, J.-F., Cottam, A., Gorelick, N., Belward, A.S., 2016. High-resolution mapping of global surface water and its long-term changes. *Nature* 540, 418–422. <https://doi.org/10.1038/nature20584>
- Piironen, J., Vehtari, A., 2017. Comparison of Bayesian predictive methods for model selection. *Stat. Comput.* 27, 711–735. <https://doi.org/10.1007/s11222-016-9649-y>
- Post, E., Alley, R.B., Christensen, T.R., Macias-Fauria, M., Forbes, B.C., Gooseff, M.N., Iler, A., Kerby, J.T., Laidre, K.L., Mann, M.E., Olofsson, J., Stroeve, J.C., Ulmer, F., Virginia, R.A., Wang, M., 2019. The polar regions in a 2°C warmer world. *Sci. Adv.* 5, eaaw9883. <https://doi.org/10.1126/sciadv.aaw9883>
- Post, E., Forchhammer, M.C., 2008. Climate change reduces reproductive success of an Arctic herbivore through trophic mismatch. *Philos. Trans. R. Soc. B Biol. Sci.* 363, 2367–2373. <https://doi.org/10.1098/rstb.2007.2207>
- Pruitt, Jr., W.O., 1959. Snow as a factor in the winter ecology of the barren ground caribou (*Rangifer arcticus*). *Arctic* 12, 158–179. <https://doi.org/10.14430/arctic3723>
- QGIS Development Team, 2022. QGIS Geographic Information System. Open Source Geospatial Foundation Project.
- R Core Team, 2023. R: A language and environment for statistical computing. R Foundation for Statistical Computing, Vienna, Austria.
- Rantanen, M., Karpechko, A.Yu., Lipponen, A., Nordling, K., Hyvärinen, O., Ruosteenoja, K., Vihma, T., Laaksonen, A., 2022. The Arctic has warmed nearly four times faster than the globe since 1979. *Commun. Earth Environ.* 3, 168. <https://doi.org/10.1038/s43247-022-00498-3>
- Reppert, S.M., de Roode, J.C., 2018. Demystifying monarch butterfly migration. *Curr. Biol.* 28, R1009–R1022. <https://doi.org/10.1016/j.cub.2018.02.067>
- Riekkola, L., Andrews-Goff, V., Friedlaender, A., Zerbini, A.N., Constantine, R., 2020. Longer migration not necessarily the costliest strategy for migrating humpback whales. *Aquat. Conserv. Mar. Freshw. Ecosyst.* 30, 937–948. <https://doi.org/10.1002/aqc.3295>
- Roberts, B.J., Catterall, C.P., Eby, P., Kanowski, J., 2012. Long-distance and frequent movements of the flying-fox *Pteropus poliocephalus*: Implications for management. *PLoS ONE* 7, e42532. <https://doi.org/10.1371/journal.pone.0042532>

- Rupp, T.S., Olson, M., Adams, L.G., Dale, B.W., Joly, K., Henkelman, J., Collins, W.B., Starfield, A.M., 2006. Simulating the influence of various fire regimens on caribou winter habitat. *Ecol. Appl.* 16, 1730–1743. [https://doi.org/10.1890/1051-0761\(2006\)016\[1730:stiovf\]2.0.co;2](https://doi.org/10.1890/1051-0761(2006)016[1730:stiovf]2.0.co;2)
- Schermer, É., Bel-Venner, M., Gaillard, J., Dray, S., Boulanger, V., Le Roncé, I., Oliver, G., Chuine, I., Delzon, S., Venner, S., 2020. Flower phenology as a disruptor of the fruiting dynamics in temperate oak species. *New Phytol.* 225, 1181–1192. <https://doi.org/10.1111/nph.16224>
- Schwartz, M.D. (Ed.), 2013. *Phenology: An integrative environmental science*. Springer Netherlands, Dordrecht. <https://doi.org/10.1007/978-94-007-6925-0>
- Sharma, S., Blagrove, K., O'Reilly, C.M., Samantha, O., Ryan, B., Magee, MR., Straile, D., Weyhenmeyer, GA., Winslow, L., Woolway, R., Magnuson, JJ., 2019. Widespread loss of lake ice around the Northern Hemisphere in a warming world. *Nat. Clim. Change*. <https://doi.org/10.1038/s41558-018-0393-5>
- Simpson, G.L., 2024. *gratia: Graceful ggplot-based graphics and other functions for GAMs fitted using mgcv*, R package version 0.9.0.
- Singh, N.J., Allen, A.M., Ericsson, G., 2016. Quantifying migration behaviour using net squared displacement approach: Clarifications and caveats. *PLoS ONE* 11, e0149594. <https://doi.org/10.1371/journal.pone.0149594>
- Stan Development Team, 2022. *Stan probabilistic programming language user's guide and reference manual, version 2.34*.
- Sturm, M., Liston, G.E., 2003. The snow cover on lakes of the Arctic Coastal Plain of Alaska, U.S.A. *J. Glaciol.* 49, 370–380. <https://doi.org/10.3189/172756503781830539>
- Thompson, J., 2017. Nunavut's Dolphin and Union caribou herd deemed endangered. *Nunatsiaq News*.
- Thurfjell, H., Ciuti, S., Boyce, M.S., 2014. Applications of step-selection functions in ecology and conservation. *Mov. Ecol.* 2, 1–12. <https://doi.org/10.1186/2051-3933-2-4>
- Torney, C.J., Lamont, M., Debell, L., Angohiatok, R.J., Leclerc, L.-M., Berdahl, A.M., 2018. Inferring the rules of social interaction in migrating caribou. *Philos. Trans. R. Soc. B Biol. Sci.* 373, 20170385. <https://doi.org/10.1098/rstb.2017.0385>
- Turunen, M., Soppela, P., Kinnunen, H., Sutinen, M.L., Martz, F., 2009. Does climate change influence the availability and quality of reindeer forage plants? *Polar Biol.* 32, 813–832. <https://doi.org/10.1007/s00300-009-0609-2>
- van Buskirk, J., Mulvihill, R.S., Leberman, R.C., 2009. Variable shifts in spring and autumn migration phenology in North American songbirds associated with climate change. *Glob. Change Biol.* 15, 760–771. <https://doi.org/10.1111/j.1365-2486.2008.01751.x>
- Vehtari, A., Gabry, J., Magnusson, M., Yao, Y., Bürkner, P.-C., Paananen, T., Gelman, A., 2022. *loo: Efficient leave-one-out cross-validation and WAIC for Bayesian models*.
- Vehtari, A., Gelman, A., Gabry, J., 2017. Practical Bayesian model evaluation using leave-one-out cross-validation and WAIC. *Stat. Comput.* 27, 1413–1432. <https://doi.org/10.1007/s11222-016-9696-4>

- Vuillaume, B., Richard, J.H., Hamel, S., Taillon, J., Festa-Bianchet, M., Côté, S.D., 2023. Birth date determines early calf survival in migratory caribou. *Oecologia* 202, 819–830. <https://doi.org/10.1007/s00442-023-05441-7>
- Warne, C.P.K., McCann, K.S., Rooney, N., Cazelles, K., Guzzo, M.M., 2020. Geography and morphology affect the ice duration dynamics of Northern Hemisphere lakes worldwide. *Geophys. Res. Lett.* 47. <https://doi.org/10.1029/2020GL087953>
- Watanabe, S., 2010. Asymptotic equivalence of Bayes cross validation and widely applicable information criterion in singular learning theory. *J. Mach. Learn. Res.* 11, 3571–3594.
- Webber, Q.M.R., Hendrix, J.G., Robitaille, A.L., Vander Wal, E., 2021. On the marginal value of swimming in woodland caribou. *Ecology* 102, e03491. <https://doi.org/10.1002/ecy.3491>
- Weyhenmeyer, G.A., Livingstone, D.M., Meili, M., Jensen, O., Benson, B., Magnuson, J.J., 2011. Large geographical differences in the sensitivity of ice-covered lakes and rivers in the Northern Hemisphere to temperature changes. *Glob. Change Biol.* 17, 268–275. <https://doi.org/10.1111/j.1365-2486.2010.02249.x>
- Williams, T.M., Gunn, A., 1982. Descriptions of water crossings and their use by migratory barren-ground caribou in the districts of Keewatin and MacKenzie, NWT. Northwest Territories Wildlife Service, Yellowknife, Canada.
- Wilson, R.R., Parrett, L.S., Joly, K., Dau, J.R., 2016. Effects of roads on individual caribou movements during migration. *Biol. Conserv.* 195, 2–8. <https://doi.org/10.1016/j.biocon.2015.12.035>
- Witter, L.A., Johnson, C.J., Croft, B., Gunn, A., Poirier, L.M., 2012. Gauging climate change effects at local scales: Weather-based indices to monitor insect harassment in caribou. *Ecol. Appl.* 22, 1838–1851. <https://doi.org/10.1890/11-0569.1>
- Wood, C.C., Bickham, J.W., John Nelson, R., Foote, C.J., Patton, J.C., 2008. Recurrent evolution of life history ecotypes in sockeye salmon: Implications for conservation and future evolution. *Evol. Appl.* 1, 207–221. <https://doi.org/10.1111/j.1752-4571.2008.00028.x>
- Wood, S.N., 2017. *Generalized Additive Models: An introduction with R*, 2nd ed. Chapman and Hall/CRC, New York, United States. <https://doi.org/10.1201/9781315370279>
- Wood, S.N., 2003. Thin-plate regression splines. *J. R. Stat. Soc. B* 65, 95–114.
- Wright, R.M., Piper, A.T., Aarestrup, K., Azevedo, J.M.N., Cowan, G., Don, A., Gollock, M., Rodriguez Ramallo, S., Velterop, R., Walker, A., Westerberg, H., Righton, D., 2022. First direct evidence of adult European eels migrating to their breeding place in the Sargasso Sea. *Sci. Rep.* 12, 15362. <https://doi.org/10.1038/s41598-022-19248-8>
- Yao, Y., Vehtari, A., Simpson, D., Gelman, A., 2018. Using stacking to average Bayesian predictive distributions (with discussion). *Bayesian Anal.* 13. <https://doi.org/10.1214/17-BA1091>
- Zalatan, R., Gunn, A., Henry, G.H.R., 2006. Long-term abundance patterns of barren-ground caribou using trampling scars on roots of *Picea mariana* in the Northwest Territories, Canada. *Arct. Antarct. Alp. Res.* 38, 624–630.

- Zeller, K.A., McGarigal, K., Cushman, S.A., Beier, P., Vickers, T.W., Boyce, W.M., 2015. Using step and path selection functions for estimating resistance to movement: Pumas as a case study. *Landsc. Ecol.* <https://doi.org/10.1007/s10980-015-0301-6>
- Zhang, R., Qiao, Y., Ji, Q., Ma, S., Li, J., 2017. Macro-microscopic research in reindeer (*Rangifer tarandus*) hoof suitable for efficient locomotion on complex grounds. *J. Vet. Res.* 61, 223–229. <https://doi.org/10.1515/jvetres-2017-0029>

3.7 Linking statement

In the previous chapter, I used GPS collar data from two migratory caribou herds to investigate how females respond to shifting lake ice phenology conditions during spring migration to reach calving grounds. To properly match the rapidity of their movements and the highly dynamic processes driving the breakup of lakes and rivers in spring, I relied on the high-resolution OPEN-ICE data product I developed in Chapter 2. I found that migrating females typically avoided exposed crossings over larger lakes and favoured regions of the landscape dominated by small ice-covered lakes. As they encountered more spring breakup conditions, they strongly avoided breaking ice and to a lesser extent, avoided open water, and this avoidance behaviour increased for larger lakes. The study of fine-scale movement patterns using the approaches described in the previous chapter is simply not possible without GPS collars, but while such devices are the cornerstone of many wildlife monitoring programs, they are not without impact on behaviour and, in some instances, survival.

In this next chapter, I focus on estimating the short-term impacts of capture and collaring on the movement and survival of barren-ground caribou. In the Northwest Territories, most caribou captures are conducted in late winter, at the end of a forage-limited season and prior to the limited window-of-opportunity and energetically expensive spring migration. In regions as remote and as difficult to access as the ranges of the Bluenose-East and Bathurst herds, monitoring programs typically rely on single-capture studies in which an individual is captured and fitted with a collar that is preprogrammed to drop-off at later date. Indeed, in such landscapes it is logistically and financially prohibitive: (i) to monitor an individual before a capture to establish baseline

behaviour with which to compare potential capture-related changes, (ii) to monitor the individual after release to identify potential capture-related illness, or (iii) to recapture a previously collared individual to compare recorded movement behaviour before and after a capture event. In this next chapter, I address the challenge of assessing capture impacts in single-capture biologging studies. Specifically, I develop and describe some statistical strategies: (i) to estimate the magnitude and duration of discrepancies in an individual's movement rate relative to population baselines, (ii) to estimate survival outcomes based on data that can be recorded and sampled during captures. This information can provide crucial assessment of capture impacts and help refine capture, immobilization, and collaring protocols to improve outcomes and reduce the period during which observations are biased by capture-related stress.

Chapter 4 - Post-capture survival and movements of barren-ground caribou (*Rangifer tarandus groenlandicus*)

4.0 Abstract

While biologging and telemetry technologies such as GPS-equipped collars have emerged as powerful tools for wildlife research, the stress experienced by individuals during capture and handling can lead to unforeseen short-term effects on movement behaviour and, in more extreme cases, capture myopathy. Visual observations of behaviour before and after capture or recapture studies can provide individual baselines that can highlight potential shifts in behaviour or onset of capture myopathy. However, in single-capture study designs and in remote regions where visual observations or recaptures are logistically unfeasible, establishing appropriate behavioural baselines remains particularly challenging. We describe statistical modelling strategies that allow comparisons of recently captured individuals to population baseline behaviours that account for seasonal patterns, sex, inter-annual and inter-individual differences. Using these models, we analyzed movement data collected through GPS-collars fitted on male and female barren-ground caribou (*Rangifer tarandus groenlandicus*) through a single-capture monitoring program for the Bluenose-East and Bathurst migratory tundra herds in the Northwest Territories and Nunavut in Canada. We further evaluated capture events for a subset of females from which stress-related blood serum indicators were sampled during handling and estimated the risks of suspected capture myopathy cases using survival analysis. Males and females from each herd exhibited, respectively, faster and slower movement rates over a period of 3-4 days post-capture before returning to baseline behaviours estimated from previously collared individuals. In the subset of

females from which blood was sampled, survival outcomes were mediated by the combined effects of the total duration of capture and handling and the individual-specific stress response as estimated by cortisol concentrations in blood serum. We also found evidence that blood indicators related to musculoskeletal stress (e.g., acetate aminotransferase) experienced prior to capture might be related to survival outcomes. Our study confirms that current capture guidelines are adequate for reducing short-term effects on movement behaviours and capture related risks in barren-ground caribou and provides statistical strategies to overcome limitations imposed by single-capture study designs, especially in remote regions.

4.1 Introduction

Biologging advancements, including GPS collars, have unlocked unparalleled insights into our understanding of animal behaviour and movement, especially in large mammals that travel great distances in remote regions (Hofman et al., 2019). However, the capture and immobilization procedures required to attach collars to free-ranging animals are invasive and not without risk of adverse effects (Arnemo et al., 2006; McMahon et al., 2012). Collaring requires immobilization, which can be accomplished by chemical anaesthetics delivered through darts (Kreeger et al., 2023) or net-gunning followed by physical restraints (Webb et al., 2008). Chemical or physical immobilization is typically preceded by either trapping (e.g., Rockhill et al., 2011), ambush or pursuit on foot (e.g., Brivio et al., 2015), water pursuit of swimming animals using a boat (e.g., Cumming and Beange, 1987; Miller and Robertson, 1967; Walker et al., 2012), snow pursuit using a snowmobile (e.g., Jingfors and Gunn, 1989), or most commonly and recently aerial pursuit using a helicopter (e.g., Baumgardt et al., 2023; Jacques et al.,

2009; Rode et al., 2014). These sequences of trapping or pursuit, followed by darting or physical restraint, and subsequent handling amount to a stressful event, which can impact the physiology, behaviour, and survival of collared wildlife. Biologging technologies and methods have continued to improve, for example by increasing battery life (Crabtree et al. 2015), reducing the size and weight of instruments, collecting a greater quantity and diversity of data (Kays et al., 2015; Williams et al., 2020), and developing passive deployment techniques that avoid the need for captures in some applications (e.g., bur-tagging; Wilson et al., 2023). To reduce the impacts of wildlife research, less invasive alternatives for studying wildlife populations, such as snow tracking, camera traps, and the genetic analysis of scat and fur, continue to be promoted and advanced (Barber-Meyer, 2022; Cooke et al., 2017; Soulsbury et al., 2020; Zemanova, 2020). Nonetheless, collaring animals remains an important and increasingly used technique for assessing the habitat use, movements, and survival of free-ranging wildlife, especially in large and remote landscapes. Biologging approaches have been promoted as a method to reduce observer effects on free-ranging wildlife (Brown et al., 2013), but determining whether this is in fact the case requires some method of assessing impacts of capture and collaring on behaviour and survival. Assessing and communicating the impacts of collaring methods on the physiology, behaviour, and survival of wildlife is an important component of all biologging research (McIntyre, 2015).

The impacts of capture and collaring on wildlife can range from immediate to long-term and from minor to lethal (Rachlow et al., 2014) and while all potential impacts are important, some are much easier to detect and assess than others. Injuries,

mortality, and stress indicators during the capture process can be directly observed and the incidence of these immediate impacts have been widely reported (Arnemo et al., 2006; Jacques et al., 2009). Assessing how capture and device attachment affect long-term survival and reproductive success requires longer-term observations and indirect inference, because less information is typically available for uncaptured, non-collared control groups. Specifically, potential behavioural and survival impacts of capture and collaring in the days to months immediately following the event are difficult to assess and are rarely reported, primarily because the baseline behaviours and survival of uncollared animals is unknown. To investigate long-term survival and reproductive impacts of handling and collaring, studies have typically leveraged comparisons between: population vital rates estimated from collared individuals and those estimated from aerial surveys (Haskell and Ballard, 2007), survival metrics of collared and non-collared individuals estimated from mark-recapture (LeTourneux et al., 2022), population trends across groups of individuals fitted with different types of collars (Rasiulis et al., 2014), or physiological and reproductive baselines of recaptured individuals relative to their initial capture (Cattet et al., 2008; Rode et al., 2014). However, in many wildlife biologging studies, there is no behavioural information available before or after a capture event, either because collars are removed and not replaced during recaptures or, increasingly, automatic collar drop-offs eliminate the need for recaptures. Assessing the behavioural and survival impacts of a single capture and collar event, under conditions where the behaviour and survival of uncollared individuals is not known, is difficult and an important knowledge gap.

Capture myopathy is an important example of the physiological stress and potential mortality arising from the capture and immobilization procedures required to collar wildlife. Analogous to exertional heatstroke in humans, capture myopathy is an often fatal disease caused by a metabolic shock typically originating from lactic acid buildup in the damaged muscle tissue (often skeletal muscles) of wildlife following extreme exertion and prolonged or intense bouts of stress caused by chase, capture, handling, and transport (Paterson, 2014). While we still lack a detailed understanding of the underlying stress-induced mechanisms (Breed et al., 2019), capture myopathy presents itself through a variety of visible and non-visible symptoms such as stiff limbs and neck (e.g., torticollis), shivering, panting, hyperthermia, and lethargy, all of which can lead to paralysis, unresponsiveness, and death (Breed et al., 2019; Paterson, 2014; Spraker, 1993). In larger mammals, capture myopathy related mortalities can occur as quickly as a few hours and as many as 30 days after capture (Beringer et al., 1996), but in many remote regions it often remains logistically impossible to closely monitor individuals after release or determine if and how handling and collaring may have caused or contributed to mortality. However, the stress-related mechanisms that initiate the cascade into capture myopathy (Breed et al., 2019) consist of: (i) stimuli in the form of an exogenous stressor (e.g., helicopter chase), (ii) the activation of the central nervous system (e.g., fight or flight response), (iii) the acute stress response activated by the hypothalamic–pituitary–adrenal axis (HPA; Herman et al., 2016), and (iv) the musculoskeletal activation. The analysis of blood samples collected during capture and handling can provide important insights into these initial mechanisms by assessing the relative magnitude of individual stress responses, early signs of muscle stress and

muscle damage incurred from exertion, and possible predisposing risk factors associated with capture myopathy. Specifically, cortisol can provide important information on both baseline or chronic stress in individuals (Ashley et al., 2011) as well as the magnitude of the acute stress response to stressors like capture events (Trondrud et al., 2022). Other serological indicators like creatine kinase (CK) and aspartate aminotransferase (AST) can inform us on preexisting muscle, liver, or heart damage or muscle damage from recent exertion (Cattet et al., 2008; Kock et al., 1987). GPS location data collected from recently fitted collars can also provide important insights into individual behaviour and possible cases of capture myopathy. Individuals that appear to recover quickly from capture-related stress can exhibit reduced movement rates in the days following capture (Dechen Quinn et al., 2012; Jung et al., 2019; Thiemann et al., 2013), although this remains difficult to detect without appropriate movement baselines. Within the logistical constraint of remote regions and single capture studies, while prolonged observation of individual behaviour or thorough investigations of suspect mortalities are unfeasible, it remains an important priority to identify and mitigate any capture-related factors associated with increased risks of capture myopathy.

Caribou and reindeer (*Rangifer tarandus*) are of great traditional, cultural, and economic importance throughout boreal and circumpolar regions. Due to the particular ecological and cultural importance of migratory caribou, the remoteness of the regions they occupy, the spatial extent of their migrations (Joly et al., 2019), the occurrence of significant population declines (Gunn, 2016; Uboni et al., 2016; Vors and Boyce, 2009), and the persisting uncertainties over primary drivers of their population dynamics

(COSEWIC, 2017, 2016), collar-based research on caribou and reindeer has been a major contributor to their research and management (Bergerud et al., 2008). Telemetry monitoring efforts began with VHF collars, first deployed on the Delta and Western Arctic caribou herds in Alaska in 1979 (Davis and Valkenburg, 1979), and accelerated after the advent of GPS collars (Rodgers et al., 1996), first deployed on the Leaf River caribou herd in northern Quebec in 1993 (Rodgers, 2001) and quickly adopted across other jurisdictions. The first generation of GPS collars were 3 times heavier than their VHF predecessors, and it was soon suspected that long-distance migrators such as caribou might incur important energetic penalties from carrying the additional mass (Dau, 1997; Haskell and Ballard, 2007). Indeed, early adopters found evidence of increased mortality in females of the Western Arctic (Dau, 1997) and George River (Rasiulis et al., 2014) herds equipped with these heavier collars. Population vital rates extrapolated from both VHF- and GPS-collared individuals of the Western Arctic herd were found to be negatively biased relative to population-wide vital rates estimated from aerial censuses (Haskell and Ballard, 2007). In contrast, no such long-term effects on mortality or even body condition were detected in the relatively sedentary Svalbard reindeer herd (Borquet, 2020). Early studies evaluating the immediate effects of caribou capture focused on the comparison of chemical immobilization protocols and the compilation of injuries directly caused by different darts and helicopter chase and net-gun methods (Valkenburg et al., 1999, 1983). Subsequent studies have carefully recorded cases of mortality occurring in the 30 days following the capture of caribou and reported them as suspected cases of capture myopathy (St-Laurent and Dussault, 2012; Wood, 1996). However, despite the fact that ungulates are particularly vulnerable

to capture myopathy (Paterson, 2014), investigations of potential risk factors for migratory caribou during and after capture and handling are lacking. While studies evaluating stress responses to multiple recaptures have assessed both short- and long-term effects of handling on activity levels, recovery rates, and reproductive success of Svalbard reindeer (Trondrud et al., 2022; Ugland, 2021), these approaches are not feasible for migratory caribou because their vast ranges constrain monitoring programs to single-capture study designs for which movement baselines are harder to define. Previous studies of post-capture movement in deer circumvented this problem by comparing the movement rates of recently collared animals to those of animals collared in previous years (e.g., Dechen Quinn et al., 2012). However, migratory caribou herds undertake the longest terrestrial migrations on Earth (Joly et al., 2019) and their movement rates follow pronounced seasonal cycles, which vary between herds (Nagy, 2011), sexes (Cameron and Whitten, 1979; Jakimchuk et al., 1987), and as a function of environmental conditions including snow depth and hardness (Gurarie et al., 2019), insect harassment (Joly et al., 2020), and plant phenology (Mallory et al., 2020). Individuals also exhibit unique movement behaviours which are influenced by personality traits (Spiegel et al., 2017), life history stage (Cameron et al., 2018), and social group dynamics (Torney et al., 2018). Defining baseline movements in migratory caribou herds requires methods to effectively describe these complex population- and individual-level effects.

Our objective is to evaluate the short-term effects of capture and handling on movement rates and survival of barren-ground caribou (*Rangifer tarandus groenlandicus*) using data that can be sampled within the constraints of single capture

collaring programs. Specifically, our study focuses on describing appropriate statistical methodologies to: (i) estimate how capture and collaring affect post-release movements, including estimates of the magnitude and duration of these capture effects, and (ii) elucidate the effects of stressors (e.g., handling time) and stress responses (e.g., glucocorticoids) during the capture event on movement rates and mortality within a 30-day post-capture window. As part of ongoing monitoring programs administered by the Government of the Northwest Territories, cows and more recently bulls of the Bluenose-East and Bathurst caribou herds have been fitted with GPS collars for almost 30 years. Once population baselines are appropriately estimated, we predict that, like other social ungulates (Jung et al., 2019), females and males will exhibit differences in movement rates and recovery times in the period immediately following release. We also predict that capture event duration and indicators of acute stress response (cortisol) will be important predictors of suspected cases of myopathy in the 30-day post-capture window, but not indicators of musculoskeletal stress (CK and AST) due to short handling period and the typically longer serum kinetics associated to these indicators.

4.2 Methods

4.2.1 Study area and caribou herds

Our study spans a period of 16 years (2006 to 2022) in the regions north of Yellowknife, Northwest Territories, Canada (62.4540° N, 114.3718° W) in the winter ranges of the Bathurst and Bluenose-East herds. The maximum known extents of the Bathurst and Bluenose-East herds' annual ranges cover thousands of square kilometres spanning the northern limits of the boreal forests and the barren-ground plains adjacent

to the seas of the Canadian Arctic Archipelago, including Coronation Gulf and Bathurst Inlet (see Fig. 4.1). Like many large migratory caribou herds, the Bathurst and Bluenose-East herds have shown large changes in abundance over time (NWT Species at Risk Committee, 2017). The Bathurst herd was estimated at 470,000 in 1986 but declined more than 98% to an estimate of 6,800 in 2022 (Adamczewski et al., 2023). The Bluenose-East herd declined from about 120,000 in 2010 to about 19,300 in 2018, then stabilized and was estimated at 39,500 in 2023 (Boulanger et al., 2024). As a result of these important population declines, the annual ranges of each herd have contracted towards their respective former cores. The Bathurst herd's annual range has contracted northward and now occupies a mere 20% of the range occupied at peak population numbers (Mennell 2021). Since 2015, the herd now overwinters mainly at or above treeline. While the population decline of the Bluenose-East herd has been less pronounced, their winter range has also contracted. All the captures were conducted on the winter ranges of the two herds, which are now situated in the region north of Yellowknife between Great Slave and Great Bear Lakes above and below treeline (Fig. 4.1). Their current winter ranges are located in the Taiga Plain and Taiga Shield ecozones, which are characterized by spruce forests (*Picea spp.*) in the Mackenzie River lowlands and on the Canadian Shield, respectively. In spring, barren-ground caribou migrate north far above the treeline to reach their coastal calving grounds on the tundra of the Southern Arctic ecozone.

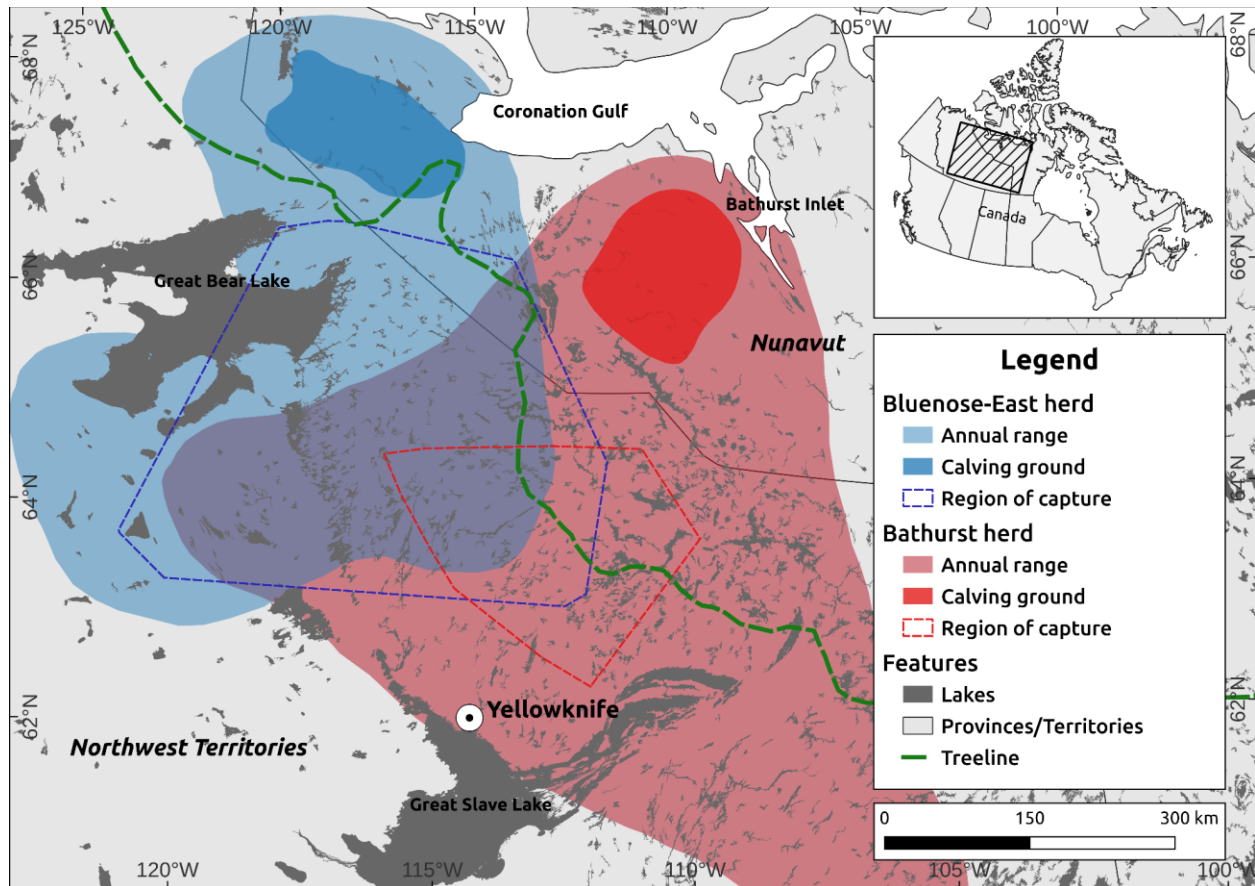


Figure 4.1 Map illustrating the region of each herd's range in which capture and collaring efforts were concentrated throughout the study period. Spatial data for annual and calving ranges were provided by the Government of the Northwest Territories. Regions of captures for each herd were drawn using a 95% minimum convex polygon around all capture locations. Projection: NWT Lambert, NAD83.

4.2.2 Capture and serology data

As part of ongoing caribou monitoring programs administered by the Wildlife Division of the Government of the Northwest Territories since 1996, handlers and net-gun capture specialists captured female and male barren-ground caribou from the Bluenose-East and Bathurst herds and fitted them with GPS satellite collars to track individual and population movements. Following standard operating procedures established by the NWT Wildlife Care Committee (Cattet, 2018), crews captured individual caribou by net-gunning from a helicopter then promptly applying a blindfold

and binding all four legs together to securely immobilize and reduce stress during handling without the use of chemical immobilization. Captures mostly occurred in March due to a combination of abundant snow cover to cushion the animal's contact with the ground, a suitable temperature range and extended daylight hours for field work.

Helicopter pilots initiated chases of caribou over sparsely covered or unforested terrain, typically over frozen lakes, to facilitate net-gunning and reduce the time required for landing and handling routines. Areas with rugged terrain or bare ice were avoided. Capture caribou were released as quickly as possible, generally within 15 minutes of initial capture. Each caribou was only captured once, and its fitted tracking collar was programmed to release and drop after a predetermined sampling period, usually 2.5 to 3 years. Collars on females were fitted relatively snugly, allowing for a hand to be fitted inside the collar. Collars on males were fitted more loosely, allowing for a fist to be fitted inside the collar, to allow for neck swelling during the rut. Field crews generally limited chasing a group of caribou more than once. In parallel to fitting of GPS collars (Lotek and Telonics), technicians recorded chase start time, net-gun deployment time, sex, and release time (see Appendix E in Cattet, 2018). Hereinafter, we refer to the time elapsed between the initiation of the helicopter chase and the final release of the individual as the “capture event duration”, which we used as an indicator of the relative stress of each capture event in our evaluation of capture myopathy risks (see Section 4.2.5).

Field crews took a number of samples during captures, including hair, feces, and blood for diverse monitoring and research applications. Blood was sampled from captured caribou prior to their release and assayed to evaluate diverse indicators of overall physiological health, including stress and musculoskeletal indicators that can be

used to evaluate risks of capture myopathy. The blood sampled during handling was stored either as whole blood or as serum spun from blood on the same day as captures. Serum was subsequently analyzed for several serological parameters following the procedure described by Johnson et al. (2010). We used the concentrations of cortisol in blood samples as an indicator of pre-existing and current (i.e., during capture and handling) stress levels in caribou. Additionally, we used the concentration of creatine kinase (CK) and aspartate aminotransferase (AST) in serum as indicators of pre-existing and current muscle stress that could potentially predispose individuals to capture myopathy. While the population-wide frequencies of serological indicator concentrations in blood samples are typically normally distributed, it is relatively common for the distribution of some indicators to be right-hand skewed (Feldman and Dickson, 2017). To address this in our own study, we applied a natural log-transformation on CK and AST concentration values.

4.2.3 Daily movement rates

To study movement behaviours in the days and weeks after capture, we computed daily movement rates (DMR) for each individual using location data recorded by their GPS collars throughout the study period. Since 1996, telemetry collars have been deployed on new individuals in barren-ground caribou herds using a staggered entry sampling design to facilitate herd population-level survival estimates (Pollock et al., 1989) and to keep the number of active collars relatively consistent (Gunn et al., 2013). Total deployments have increased considerably in the last decade (2015-2022), especially on males, as part of more intensive monitoring of the two herds associated with their low numbers and declining trend. We retrieved location data recorded by

collars equipped with GPS (i.e., no ARGOS data) for the Bathurst and Bluenose-East herds via a Movebank repository (Kays et al., 2022) preprocessed to filter out location errors and outliers. The resulting dataset spanned 16 years (2006 to 2022), a period during which sampling frequencies varied by collar, season, and year, typically ranging from 1 to as many as 24 locations recorded per day as technology improved and monitoring objectives evolved (e.g., increased sampling during calving/post-calving or geofencing near industrial development).

We screened individual tracks for duplicate records and unlikely movement speeds between two successive locations (e.g., extraordinarily rapid movement relative to population distribution and/or rapid round trips due to GPS errors). To reduce sampling frequency bias in speed estimates (Gunn et al., 2001; Prichard et al., 2014; Rowcliffe et al., 2012), we resampled one location per day for each individual to match the coarsest sampling rate across all collars (i.e., 1 fix/day). Specifically, for each individual each day we retained whichever observation was recorded closest to 09:00 hours (UTC-07:00), which constituted the most frequent GPS fix timestamp across all the deployed collars in the dataset. Finally, we computed the geographical distance travelled (i.e., Earth great-circle distance) between two successive latitude/longitude coordinates using the haversine law, and estimated DMR (km/h) over the elapsed period between the recorded daily locations. We square-root transformed DMR to reduce the right-hand skew in the distribution of residuals in downstream analyses. We conducted all collar location data inspection, visualization, manipulation, and computation of DMR estimates using the “dplyr” and “ggplot2” packages in R (R Core Team, 2023).

4.2.4 Post-capture daily movement rates

We evaluated patterns in movement speeds of barren-ground caribou throughout their annual cycle and in the post-capture period by parameterizing, fitting, and comparing candidate models nested in increasing order of complexity using hierarchical generalized additive models (HGAMs). We modelled seasonal patterns in DMR using smooth terms for day of year (“doy”, 1 to 366) and post-capture temporal patterns using days since capture (“dsc”, 1 to 30). We accounted for individual (“id”), annual (“year”), and social (“sex” and “herd”) differences in the shape of those smooth terms by using factor variables as interactions with smooth terms or as factor smooth terms. We used these covariates to build three candidate models representative of our *a priori* hypotheses:

- *Model 1: The daily movement rates of each sex and each herd follows distinct annual seasonal cycles that vary according to individual behavioural differences and annual environmental differences. We accounted for seasonal cycles in our baseline model by including a cyclic cubic regression spline for “doy” to constrain the start (0) of the spline to its end (366). We added a combined interaction of “herd” and “sex” to the cyclic smooth, effectively allowing the model to fit separate population-level (i.e., fixed effect) smooths and intercepts for the seasonal cycles within each group. To account for differences in movement speeds due to individual behavioural traits and annual variations in environmental conditions, we also included a factor smooth term whereby the shape of the smooth term for “doy” was further allowed to vary as a function of “id” and “year” combined as a single factor variable (hereinafter “id/year”), an*

approach that is analogous to random slopes in generalized linear mixed models (Pedersen et al., 2019). This model explains movement speed patterns using the most current knowledge of barren-ground caribou behaviours and movement ecology, effectively serving as a baseline model with which to compare the next two.

- *Model 2: The daily movement rates of recently captured caribou differ from the population baselines.* In this model we included all the same terms as Model 1, but we allowed for a continuous population-wide response in DMR over the post-capture period by adding a cubic regression spline for days since capture (“dsc”) up to 30 days.
- *Model 3: The responses of caribou to capture events are sex specific.* Following Model 2, we allowed for a continuous change in DMR in the post-capture period up to 30 days, but we allowed separate cubic regression splines of “dsc” for each sex by including an interaction with the “sex” factor variable.

We verified that smooth terms were fit with the appropriate degrees of freedom (i.e., “k” parameter allowing level of wiggleness) using the HGAM workflow described by (Simpson, 2018), and we fixed this parameter for smooth terms across models to allow comparisons (Pedersen et al., 2019) and reduce bias in likelihood ratio tests (Young et al., 2011). For models 2 and 3, we expected any movement rate differences in the post-capture window to gradually resolve over a 30-day period, so we specified low wiggleness ($k = 3$) for the smooth term of days since capture, effectively mimicking a low-order polynomial that returns to the seasonal baseline on day 30. Time series analyses with both population- (i.e., “doy” cyclic regression for “sex” and “herd”) and

group-level (i.e., “doy” factor smooth for “id/year”) smooth terms can be susceptible to concurvity, analogous to collinearity in linear models. Following Pedersen et al. (2019), we mitigated concurvity in the three models by: (i) carefully including appropriate combinations of continuous/factor variables within the same model, (ii) specifying higher wiggleness (i.e., parameter “k”) in the population-level smooths for seasonal cycles relative to group-level smooths and post-capture smooths, and (iii) penalizing pronounced departures from zero in the group-level smooths (i.e., parameter “m” set to 1). Following this approach, we did not include a separate population-level smooth term for “year” because it was highly concave with a factor smooth term of “doy” and “id” given the staggered entry sampling design for the GPS collars in this monitoring program. In addition to mitigating possible concurvity, attributing increased wiggleness to the population-level smooths versus group-level smooths constitutes an important requirement for proper inference given the gregarious nature of migratory caribou and the strong seasonal signal in each herd’s dataset. We fit the three models using square-root transformed daily movement rates as a response variable in order to normalize model residuals and conserve the true zero of the response variable.

We parameterized, fit, and inspected each model using the “mgcv” (Wood, 2017) and “gratia” (Simpson, 2024) packages implemented in R (R Core Team, 2023). To improve computation time, we used cubic regression or cubic cyclic splines (i.e. no thin plate regression splines), discretized model covariates (Li and Wood, 2020) and fit each model using fast Restricted Maximum Likelihood in the “mgcv::bam()” function (Wood et al., 2015) with parallel processing enabled (32 cores). To evaluate the trade-off between predictive ability and parsimony, we compared the three nested HGAMs using Akaike’s

Information Criterion (AIC) adapted to GAMs (Wood et al., 2016) and selected the best model based on the lowest AIC.

4.2.5 Capture myopathy survival analysis

We used survival analysis to evaluate how stress-related factors mediate the risk of capture myopathy related mortality in a subset of females included in the study (n = 143). Specifically, we used generalized additive model (GAM) implementations of the Cox proportional hazards model (Cox, 1972) to allow the fitting of non-linear and interacting smooth terms (Wood et al., 2016).

We used the number of days an individual survived after a capture event as the response variable in the survival analysis. In the post-capture period, deaths related to predation and capture myopathy can be conflated (Beringer et al., 1996) and it is often logistically unfeasible and cost-prohibitive to conduct immediate aerial investigations or perform field necropsies to determine the exact cause of any given mortality given the vast and remote study area. Despite helicopters being deployed in the NWT to investigate any stationary collars in the 4-6 week period after a capture since 2012, in the vast majority of cases there are no conclusive observations with regard to the cause of mortality due to scavengers and predators. Consequently, we considered all stationary collars within the first 30 days to be suspected cases of capture myopathy related mortalities (Baumgardt et al., 2023; Beringer et al., 1996) and we right-censored individuals that survived beyond that period.

To emulate frameworks describing the initial steps of capture myopathy (Breed et al., 2019), we included model covariates representative of exogenous stressors and the

resulting endogenous stress expressed in the form of increased nervous system activation and musculoskeletal activity. Specifically, we used the capture event duration as a proxy for the relative magnitude of the exogenous stressor experienced by each individual and incorporated it into our model as a smooth term. We also included the concentration of stress indicators in blood samples as measures of the endogenous stress responses in each female. We included the concentration of cortisol as an indicator of nervous system activation and CK and AST as indicators of the stress engendered by musculoskeletal exertion. In addition to variations in pre-existing baseline stress levels unrelated to the capture event (e.g., previous injury/exertion, nutritional stress), the concentration of these indicators can increase as a direct function of the duration of the capture and handling procedure (albeit at different rates) up to the moment blood is sampled prior to release. Therefore, they should be included in the model both as direct consequences of exogenous stress (capture event duration) and as predisposing risk factors. To account for this, we included each stress indicator in the model twice: (i) as a 1-dimensional smooth term (indicative of predisposing risk factors) and (ii) as a 2-dimensional anisotropic tensor smooth term in which the indicator interacts with capture event duration (indicative of capture event related stress). We modelled all covariates using smooth and tensor smooth terms using thin plate spline regressions with shrinkage, an approach analogous to variable selection whereby terms can be penalized toward 0 if they are not important predictors (Marra and Wood, 2011).

We parameterized, fit, and inspected the Cox proportional hazards model using the “mgcv” (Wood, 2017) and “gratia” (Simpson, 2024) packages implemented in R (R Core Team, 2023). We used scaled score plots (Klein and Moeschberger, 2003) to

verify that proportional hazard model assumptions were not violated by the model. We used the partial effects of significant covariates to estimate their effect on predicted survival at day 30 while fixing other covariates (including non-significant terms) at their mean value.

4.3 Results

4.3.1 Capture and collar data

In total, we analyzed data from 450 individuals fitted with GPS collars as part of monitoring programs in the NWT. Observations for the Bathurst herd are distributed among 151 and 54 collared females and males, respectively. For the Bluenose-East herd, there were collars fitted to 169 females and 76 males. Following recommendations by Cattet (2018), most captures (90%) occurred in barren-ground caribou's late winter season (*sensu* Nagy, 2011) between March 10th and April 10th, allowing more than one month of recovery prior to the calving season. This also corresponds to the period of the year when caribou are relatively sedentary and during which winter weather and snow conditions are the most favourable. Save 10 males captured during the spring migration or calving seasons, the remaining 10% of collared individuals were captured in early or mid winter (December to March). In the subset of 143 females included in the survival analysis (see Section 4.3.3), a total of 5 deaths were recorded in the first 30 days, a mortality rate of approximately 3.5%. While these are all treated as suspected cases of capture myopathy, only 2 of them occurred in the week following capture, while 3 of them occurred 20 days or more after.

4.3.2 Post-capture movements

Following our initial prediction, male and female migratory caribou exhibit different daily movement rate (DMR) patterns in the recovery period immediately following capture events. We successfully fit a baseline model (Model 1) that explains population-level DMR patterns throughout seasonal cycles between herds and sexes while accounting for group-level variability among years and individuals. Adding a smooth term for “days since capture” to investigate post-capture recovery (Model 2) does not improve predictions of DMR relative to the baseline model ($\Delta AIC < 2$, Table 4.1). However, when smooth terms for “days since capture” are fit separately for each sex (Model 3) we obtain important gains in predictive ability despite the added complexity, which results in the lowest AIC score among the three candidate HGAMs (Table 4.1). This best model’s explained deviance is 39.6% with an adjusted coefficient of determination of 0.387 (Table 4.2).

Table 4.1 Model comparison metrics for the three candidate hierarchical generalized additive models. The Akaike Information Criterion (AIC) for each model is presented along with the AIC difference (ΔAIC) relative to the best model.

Model	Terms	AIC	ΔAIC
1	s(day of year, by = herd/sex) + s(day of year, id/year) + herd + sex	-60,435.17	9.05
2	Model 1 + s(days since capture)	-60,434.35	9.87
3	Model 1 + s(days since capture, by = sex)	-60,444.22	0

Bold typeface indicates the model and associated terms with the most support.

The baseline component of the best model (Model 3) highlights important patterns in the movement rates between each herd and each sex, across each season in the annual cycle, and across individuals and years (see Table 4.2 & Fig. 4.2). The partial effects of the model's parametric terms describe four intercepts, one for each unique combination of sex and herd, that reveal statistically significant differences in the mean movement rates between groups. Specifically, based on the mean of all observed DMR values for Bluenose-East females (reference level), our model estimates they travelled 5078.40 metres each day. In contrast, each day males travelled on average 92.26 metres less (SE = 1.18, $p < 0.0001$) than females while individuals from the Bathurst herd travelled 5.40 metres more (SE = 0.25, $p < 0.0001$) than their counterparts from the Bluenose-East herd (Table 4.2). While the wiggleness of the model's seasonal components is the same, the partial effects of smooth terms for "day of year" (DOY) describe significantly distinct ($p < 0.0001$; see Table 4.2) shapes that are unique to each factor level. For example, females exhibit greater fluctuations in DMR throughout their annual cycle (see Fig. 4.2): (i) they are more sedentary than males in late winter, (ii) they travel faster than males during the spring migration and abruptly slow down again during the calving period, and (iii) they travel faster than males in late summer. The population-level movement rates of females peak during spring migration (DOY = 137) in the Bathurst herd and during early summer (DOY = 200) in the Bluenose-East herd (see Fig. 4.2A & C). The only period in which male DMR is higher than females of the same herd is during the rut, which typically peaks in mid to late October (DOY = 290, Fig. 4.2B & D). After the breeding season, DMR slowly declines across both herds and sexes throughout the duration of winter, hitting its annual

minimum just prior to spring migration (see Fig. 4.2) when most captures occur. The factor smooth allowing seasonal patterns to vary by individual and by year (i.e., “s(doy, id/year)”) provides a significant contribution to the model ($p < 0.0001$; Table 4.2), therefore improving estimates of population-level intercepts and smooth terms across sex and herd.

Table 4.2 Model summary output for parametric and smooth terms in the selected candidate model that best describes daily movement rates of barren-ground caribou. Model was fit using a hierarchical generalized additive model. Parametric terms include factor-level intercepts for combinations of sex and herd relative to the intercept for the model’s reference level (“Intercept”, Bluenose-East Female), in units of the response variable ($\sqrt{\text{km/h}}$). Smooth terms include cyclic cubic spline regressions for day of year (“s(doy)”), factor-level smooths for day of year for each individual each year (“s(doy, id/year)”), and thin-plate spline regressions for days since capture up to 30 days following a capture event (“s(dsc30)”).

Parametric terms	Estimate	Std. error	t-value	p-value
Intercept	0.460	0.004	118.663	0.0000 ***
sex.Male	-0.062	0.007	-9.163	0.0000 ***
herd.Bathurst	0.015	0.003	4.610	0.0000 ***
Smooth terms	edf	Ref. edf	F-value	p-value
s(doy):sex.Female/herd.Bluenose-East	21.932	22.000	1215.639	0.0000 ***
s(doy):sex.Male/herd.Bluenose-East	21.676	22.000	407.169	0.0000 ***
s(doy):sex.Female/herd.Bathurst	21.881	22.000	765.394	0.0000 ***
s(doy):sex.Male/herd.Bathurst	20.851	22.000	203.982	0.0000 ***
s(doy, id/year)	3769.497	5692.000	5.084	0.0000 ***
s(dsc30):sex.Female	1.840	1.971	3.583	0.0262 *
s(dsc30):sex.Male	1.884	1.984	4.047	0.0241 *

Significance codes: 0 <= **** < 0.001 < *** < 0.01 < ** < 0.05

R-sq.(adj) = 0.387, Deviance explained = 39.6%

REML = -26802, Scale est. = 0.046516, n = 279405

“.” denotes interaction, “.” indicates factor’s level, “/” indicates combination of two factors

The best model includes a statistically significant effect of “days since capture” when the associated smooth term is fit separately for males ($p = 0.0241$; Table 4.2) and females ($p = 0.0262$; Table 4.2), partially confirming our initial prediction that each sex would exhibit differences in movement rates in the post-capture period. Once we account for the additive effects of seasons, herd, sex, id, and year (i.e., baseline

movement rates), females typically exhibit lower movement rates in the days immediately following capture (see Fig. 4.2E) while males exhibit higher movement rates (see Fig. 4.2F). While male and female movement rates are affected differently (*i.e.*, increase vs. decrease), these differences gradually return to baseline movement rates over similar time frames, partially rejecting our initial prediction that recovery time would be different between sexes. The recovery period for females is approximately four days, at which point the differences in DMR are no longer distinct from baseline (*i.e.*, CI overlaps with 0). For males, we observe a return to baseline movement rates on the third day after capture.

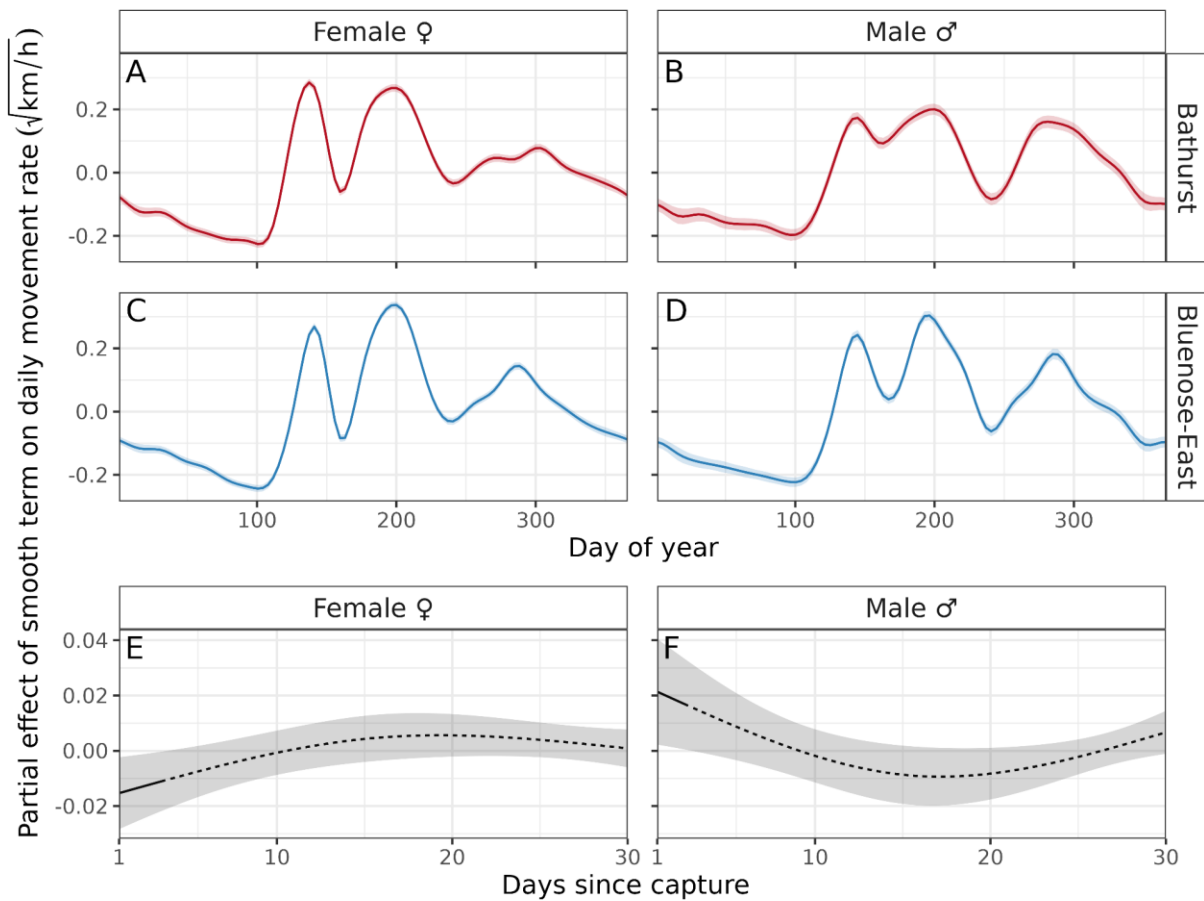


Figure 4.2 Partial effects of the smooth terms on daily movement rates of caribou fit with a hierarchical generalized additive model (HGAM). (ABCD) Seasonal patterns unique to

each sex and each herd are modelled by a cyclic cubic regression of caribou daily movement rates as a function of day of year. (EF) Post-capture movement behaviours are modelled by a cubic regression spline of daily movement rates as a function of days since capture. Solid lines and shaded ribbons represent smooth term estimates and their corresponding confidence intervals. Dotted lines indicate trends in which confidence intervals overlap with zero. Strips in the margin of each plot indicate distinct levels for interacting terms for sex and herd. Bathurst herd estimates are illustrated in red while Bluenose-East estimates are illustrated in blue. Y-axis scale is the square-root-transformed daily movement rate (km/h).

Comparing the best model's summed effects for recently captured individuals (≤ 30 days post capture) versus previously captured individuals (> 30 days post capture) highlights that recovery time is short (see Fig. 4.3), even when predicted differences in movement rates are relatively large. Most captures were performed when baseline movement rates are at or approaching their annual low. Consequently, while absolute divergences in DMR immediately following capture are small, they are proportionally high relative to seasonal baselines, especially for females. For example, on the 80th day of the year (the median capture date) the predicted movement rates of females immediately following capture are 13% to 14% lower than expected based on the seasonal behaviours of previously captured females, in the order of approximately 221 and 201 metres per day less than baseline for the Bathurst (see Fig. 4.3A) and Bluenose-East (see Fig. 4.3C) herds, respectively. The lower DMR predicted for recently captured females rapidly resolves and gradually increases until it intersects the baseline around the 10th day. From day 10 to day 30, the trajectory and the shape of the predicted DMR response for recently captured and habituated females are almost identical. In contrast, predicted male DMR gradually decreases post capture and the predicted trajectory and shape of DMR smooths for recently captured and habituated males is similar throughout the 30-day post-capture period. The predicted movement

rates of males immediately following capture are approximately 14% to 16% higher than expected based on the seasonal behaviours of previously captured males of the same herd (see Fig. 4.3B & D), a difference of approximately 218 and 175 metres per day more than baseline for the Bathurst and Bluenose-East herds, respectively.

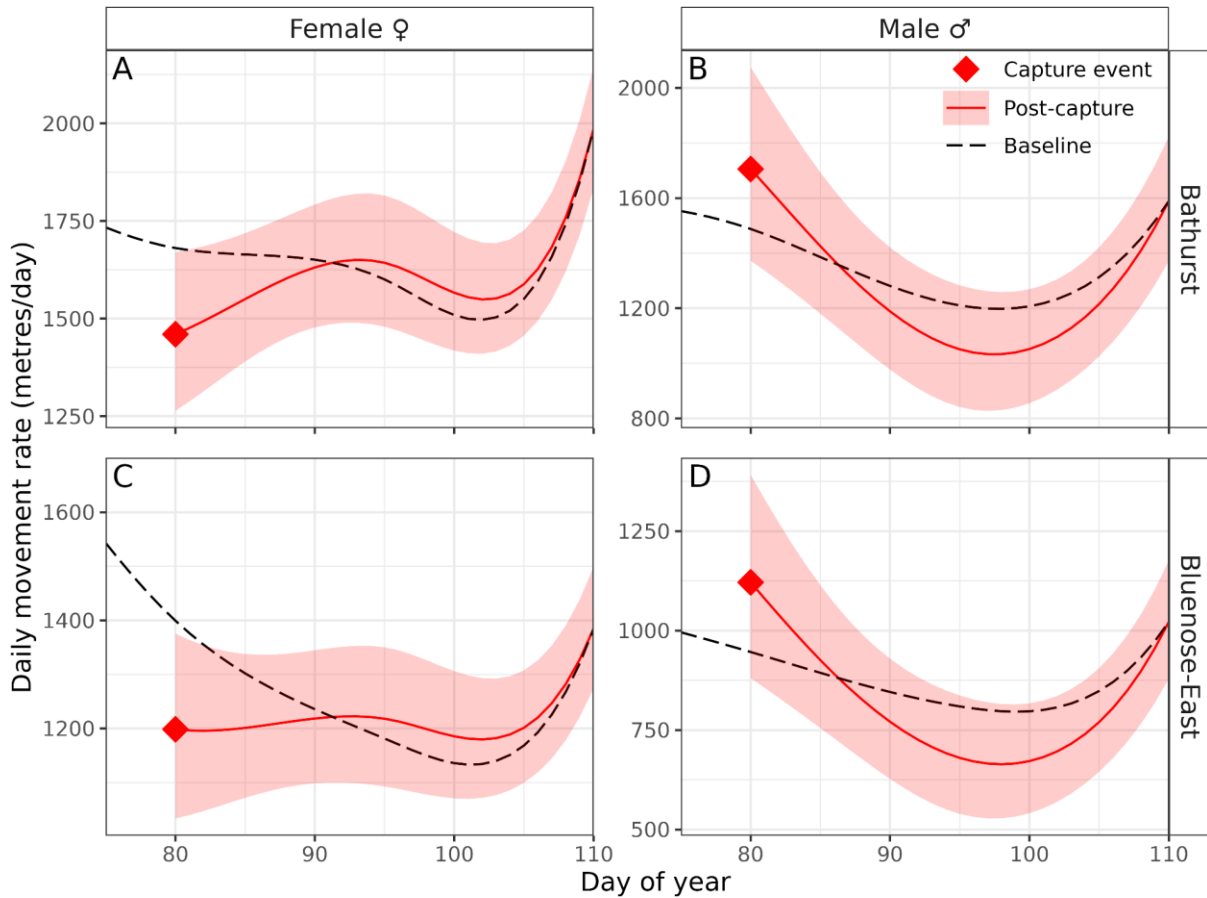


Figure 4.3 Comparison of predicted daily movement rates (DMR) of caribou in the 30-day period following capture and handling (i.e., post capture) relative to population baseline. DMR for both female (AC) and male (BD) caribou in the Bathurst (AB) and Bluenose-East (CD) herds as predicted by a hierarchical generalized additive model (see Fig. 4.2). Capture events (red diamonds) are evaluated as having occurred on the 80th day of the year (~ March 20th), the mean capture date. Predicted post-capture DMR (solid red line, \pm 95% confidence interval) and baseline DMR (black dashed line) are evaluated for the 30-day period thereafter.

4.3.3 Post-capture survival

Capture event duration and the concentration of cortisol and aspartate aminotransferase (AST) in blood samples are important predictors of suspected cases of capture myopathy in females in the 30-day period following capture (Table 4.3). The tensor smooth combining the effects of cortisol and capture event duration is the most significant term in the model ($p = 0.0016$; Table 4.2), while the smooth term for $\log(\text{AST})$ is marginally significant ($p = 0.0926$; Table 4.2). Together, these two terms explain 35.5% of the deviance in the dataset of 143 females (Table 4.2). As a result of the shrinkage splines used to estimate smooths, all other terms in the model effectively shrank towards 0 (see Table 4.2 & Suppl. Fig. 4.1). The predicted probability of surviving the 30-day post-capture period decreases gradually following a gradient of increasing capture event duration and increasing cortisol concentration (see Fig. 4.3A). When capture event duration is below 10 minutes, the predicted probability of survival is very high (between 100% and 98%), even for females with an above average cortisol concentration (> 110 mmol/L). When capture event duration increases to 15 minutes, the predicted probability of survival is similar for individuals with below average cortisol concentration (< 110 mmol/L), but it decreases to between 95% and 98% for females with above higher cortisol concentrations. After 20 minutes the predicted probability of survival remains above 90% even for females with higher cortisol levels, but between 20 and 25 minutes the predicted survival decreases below 80% then precipitously drops regardless of cortisol levels. Independently of capture event duration, the rising concentration of AST in blood samples is associated with a decline in the predicted probability of survival (see Fig. 4.3B). While $\log(\text{AST})$ provides some contribution to the

model, the confidence intervals of the predicted relationship overlap with 1 (see Fig. 4.3B) and the confidence intervals of corresponding partial effects on the log-hazard function overlap with 0 (see Suppl. Fig. 4.1D). The predicted probability of survival remains above 98% until the log(AST) reaches approximately 4.55 ([AST] = 95 U/L), at which point it gradually declines towards 92.5% when the maximum observed log(AST) is reached at 5.16 ([AST] = 175 U/L).

Table 4.3 Model summary output for generalized additive Cox proportional hazard model implemented with shrinkage on thin plate regression smooth and tensor terms.

Smooth/tensor terms with shrinkage	edf	Ref. edf	Chi. sq	p-value
s(capture event duration)	0.000	2	0.000	0.3849
s(cortisol)	0.000	2	0.000	0.3233
s(aspartate aminotransferase)	0.6614	2	1.790	0.0926 .
s(creatine kinase)	0.000	2	0.000	0.7533
te(capture event duration, cortisol)	2.4459	11	9.933	0.0016 **
te(capture event duration, aspartate aminotransferase)	0.2799	10	0.371	0.1803
te(capture event duration, creatine kinase)	0.000	10	0.000	0.3795

Significance codes: 0.001 < '***' < 0.01 < '**' < 0.05 < '.' < 0.1

Deviance explained = 35.5%

-REML = 21.476, Scale est. = 1, n = 143

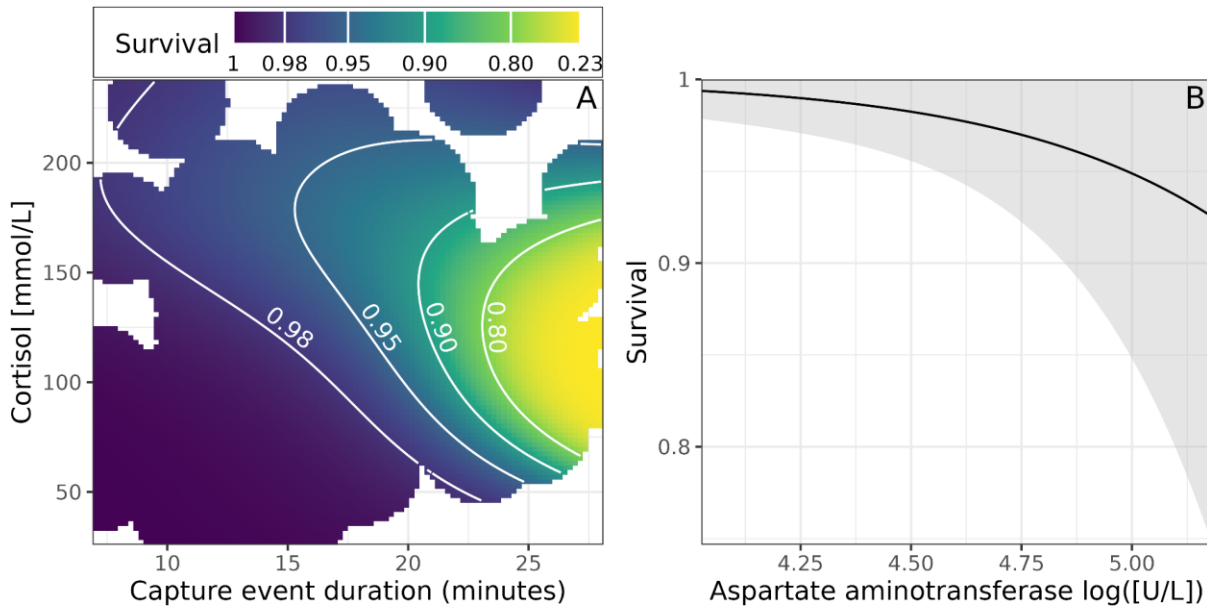


Figure 4.4 Predicted probability of female caribou survival 30 days post-capture as a function of significant capture and stress indicators. The probability of survival is predicted by: (A) the combined effects of capture event duration (minutes) and cortisol concentration (mmol/L) modelled by a tensor smooth (2-dimensional response surface illustrated with stretched colour scale) and (B) the effects of natural log-transformed aspartate aminotransferase concentration (units/L) modelled using a thin-plate regression smooth (black line, grey ribbon for \pm 95% confidence intervals). The probability of survival was predicted using a generalized additive Cox proportional hazards model implemented with shrinkage smooths to identify important predictors. See Table 4.3 and Supplementary Figure 4.1 for all model terms and corresponding partial effects. Note that colour scale is bound by the limits of predicted values for survival (0.23 to 1).

4.4 Discussion

The short-term impacts of capture on the movement rates and survival of barren-ground caribou can be assessed, within the constraints imposed by single-capture GPS-collar study designs and monitoring programs, using statistical routines that model baseline movement behaviours to compare recently captured individuals with previously collared individuals. Our assessment suggests that, across both herds, captures of females conducted in late winter reduce movement rates by less than 300 metres per day for approximately three days before returning to population baselines. We also

found that longer capture and handling times and the magnitude of a female's stress response are associated with a small decrease in the probability of survival in the 30-day period following release. We have demonstrated how, beyond reporting the incidence of capture-related mortality, data commonly collected within the constraints of single-capture collaring programs (i.e., GPS location data, blood serum analysis) can be used to evaluate and communicate the impacts of capture and to inform strategies to reduce them. Using these methodologies, our study further improves our understanding of the effects of capture and handling on migratory caribou.

4.4.1 Short-term effects on movement rates

At a population level, there is a discernible effect of capture and collaring events on the movement rates of barren-ground caribou in the days following release, but our results suggest that this effect is relatively limited, and that recovery is swift. Specifically, female movement rates were lower than seasonal baselines for up to three days after release. During this three-day period, females typically moved 220 meters less than baseline (see Fig. 4.3). However, given that most captures are conducted when movement rates are at their annual minimum (i.e., late winter), this difference represents an approximately 15% reduction relative to the baseline rate for females of each herd. Males also returned to baseline movement rates within three days of being released, but in contrast to females, males travelled more during the three-day period, typically up to 220 meters more per day than expected (see Fig. 4.3B & D), an approximately 15% increase over the male seasonal baseline for each herd. However, recovery time is essentially identical between sexes (see Fig. 4.2F). To our knowledge, no other studies have estimated capture effects on the movement behaviours of caribou in the period

following an initial capture event. Trondrud et al. (2022) compared activity data recorded by subcutaneous accelerometers before and after the recapture and chemical immobilization of female Svalbard reindeer, estimating that activity levels decreased by approximately 10% and returned to baseline within approximately 11 hours, on average. The authors observed that when females were recaptured multiple times a year, activity levels increased at each subsequent recapture but returned to baseline faster, although the time required for heart rate to decrease back to a normal range was much longer (Trondrud et al., 2022; Ugland, 2021). Other studies have investigated potential changes in behaviours of wild caribou after longer interventions such as capture and translocation for maternal penning or reintroduction. In a study of mountain caribou, Ford et al. (2023) found that the movement rates of females following their release from maternal pens were undifferentiated from their non-penned counterparts. Mathieu et al. (2022) found that habitat selection of recently released translocated female mountain caribou was identical to that of resident individuals. Post-capture effects in movement behaviours are well documented in closely related cervids. For example, female white-tailed deer (*Odocoileus virginianus*) exhibit lower movement rates, and their recovery period extends to 14 days post-capture (Dechen Quinn et al., 2012). In contrast, female mule deer (*Odocoileus hemionus*) exhibit elevated movement rates and displacement following capture and translocation, and recover much faster, typically returning to baseline behaviours within 24 hours. Like mule deer, female moose (*Alces alces*) also increase their movement rates and displacement, and discrepancies in these behaviours are detectable up to five days post-capture (Northrup et al., 2014).

The contrast in movement behaviour between male and female caribou immediately following capture could be attributed to: (i) physiological and energetic differences between sexes, especially for pregnant females, and (ii) a higher affinity of females to their immediate social group in a season when they are already highly sedentary. Late winter represents an important seasonal energetic bottleneck due to the low availability of high-quality food and the increased effort required to move around and crater in deep snow (Bergerud et al., 2008). Pregnant females incur higher energetic costs than other females during this period because they are diverting more resources toward gestation (Barboza et al., 2020; Barboza and Parker, 2008) and because they are heavier (Gerhart et al., 1997), which increases the cost of locomotion through snow (Fancy and White, 1986). As a result of these additional energetic and metabolic requirements, pregnant cows have higher heart rates than non-pregnant females during the active phases of their daily cycle in late winter (Trondrud et al., 2021). Recent research also suggests that hair cortisol concentration, an indicator of chronic stress levels, is slightly higher in females than males of the Bluenose-East herd and increases throughout late winter to reach its annual peak during migration and calving (Rakic et al., 2023). The post-release decrease in movement observed in females is likely driven by shifts in behaviours to promote rest and recovery from the additional stress and energy expenditures associated with capture events. Social dynamics may also play an important role. For example, Jung et al. (2019) studied bison (*Bison bison*), another social ungulate, and observed that the movement rates of females increased in the period following recaptures conducted by helicopter chase and chemical immobilization, a pattern the authors attribute to the drive to regain their social

group and dependent calves. Unlike bison, who are sexually segregated throughout most of their annual cycle, migratory caribou occur partially in mixed sex groups during the late winter season (Jakimchuk et al., 1987) when captures are conducted although mature bulls still tend to congregate together. Late winter is the most sedentary phase of caribou's annual cycle, so it is unlikely that a captured individual's social group has ventured far from the site of capture once the helicopter pursuit ends. We speculate that the post-capture increase in movement for males could be due to a stronger flight response following release and a looser affinity to their immediate social group relative to females.

Overall, our study demonstrated that the effects of capture on movement rates for both sexes are limited, and the latency period required for behaviours to return to population baselines are short. It remains possible that these population-level patterns may mask some individual variation. Given the duration of the movement effects we detected, researchers could censor the first week of location data associated with each collar to reduce capture-effect biases if their research focuses on the late winter season. However, given that (i) potential biases related to acclimation behaviours decrease when longer time series are considered (Dechen Quinn et al., 2012) and (ii) the spring migration period is characterized by some of the highest movement rates observed throughout migratory caribou's annual cycle, censoring data is unlikely to change the outcomes of analyses conducted over the weeks and months following the capture period.

4.4.2 Statistical tools for estimating baselines and divergences from baselines

We demonstrated how hierarchical generalized additive models can be used to estimate capture effects in single capture studies. We accomplished this assessment by estimating population-level baseline movement rates, which are compared to recently captured individuals to estimate the magnitude and duration of deviations. In recapture studies, an individual can be compared to itself, but this precludes the evaluation of the effects of the first capture. Alternatively, where possible, direct visual observation of uncaptured and recently captured individuals can provide a powerful means to compare their respective behaviours (Arzamendia and Vilá, 2012; Nussberger and Ingold, 2006; Stabach et al., 2020). However, in most cases where direct observation is not possible and capture events occur only once, establishing a baseline requires control groups of previously captured and collared individuals. For example, studies have compared post-capture movement metrics or spatial distributions to those of previously captured groups of individuals over the same period, employing methods such as individual-based comparisons to daily summary statistics computed from groups of previously captured individuals (Dechen Quinn et al., 2012), ad hoc comparisons of separate models fit to recently and previously captured individuals (Northrup et al., 2014), and randomization tests to detect differences between groups of recently and previously captured individuals (Prichard et al., 2023). Some studies have forgone the use of control groups entirely, opting to model post-capture time series with sigmoidal curves based on the assumption that movement metrics for groups of recently captured individuals should regress toward the unknown uncaptured population mean over a specified period (Bengsen et al., 2021). In essence, the strategy we employed combines this last

approach with those based on control groups, whereby we include model terms to describe population baselines (i.e., cyclic smooths for day of year) while accounting for annual and individual variation (i.e., factor smooths for id and year) then test for any divergences from this baseline in the post-capture period by adding an additional term (i.e., smooths for days since capture) with low wiggleness (i.e., low order polynomial) emulating a return to baseline over the 30 days since capture. The main advantage of this method is that a single model can be parameterized with all the covariates of interest, avoiding the need to fit multiple models for individual covariates which would likely violate model assumptions (Zuur and Ieno, 2016). Specifically, we were able to examine the magnitude and duration of divergences from population baselines in the post-capture period without the need for multiple individual statistical comparisons, multiple single-covariate models with structured residual patterns, or visual inspection of descriptive statistics.

The modelling strategy described herein demonstrates the power of cyclic cubic spline regressions as a tool to account for the highly non-linear and cyclical daily and seasonal movement patterns that can be especially pronounced in migratory species. In ungulates, it is generally recommended to monitor for movement behaviour discrepancies for up to 30 days post capture because this is a typical window within which physiological effects of stress and capture myopathy may present themselves (Arnemo et al., 2006; Beringer et al., 1996; Dechen Quinn et al., 2014). In many studies, captures are conducted at different periods of the year, either opportunistically or by design, posing an important challenge as comparisons of post-capture responses across seasons with different baseline behaviours can introduce bias and uncertainty

into estimates of the strength and duration of effects (Northrup et al., 2014; Trondrud et al., 2022). Even when capture efforts are focused in a narrow period of the year, the seasonal shifts in movement behaviours over the 30-day window can introduce important biases into estimates of post-capture behavioural differences and recovery periods. Our own study perfectly illustrates this challenge because the 30-day period following the median capture date overlaps both the late winter and spring migration seasons which are characterized, respectively, by some of the lowest and highest movement rates (see Fig. 4.3) observed throughout migratory caribou's annual cycle (Nagy, 2011). By including cyclic cubic spline regressions to describe baseline seasonal movements, researchers can control for these important variations and reduce the potential biases they introduce into comparisons of post-capture effects across different periods of the year. Similarly, they can be used to account for daily cycles when sampling frequencies are high.

Researchers must carefully consider which hierarchical model structure may be most suitable for their own study species. For example, migratory caribou are highly gregarious and individual movements closely match herd-wide patterns (Nagy, 2011). As such, the baseline components of the HGAMs are parameterized using population-level smooths (i.e., one for each combination of herd and sex) and group-level smooths (i.e., id/year) with similar wiggleness between groups (*sensu* Model GS, Pedersen et al., 2019). However, in some species inter-individual differences in movement behaviours may be the only pattern present or may completely eclipse any population-level patterns (Shaw, 2020). When a population-level pattern is still present but inter-individual differences in movement patterns are a stronger driver of variability, HGAMs can also be

parameterized with a global smooth and group-level smoothers with a different wiggleness for each group (*sensu* Model G1, Pedersen et al., 2019). Researchers must carefully consider the benefits of this approach, with particular attention to the greater risks of introducing concurvity and inflating uncertainty around global-level smooths, and the increased computational costs required to estimate penalties separately for each group of observations (Pedersen et al., 2019).

4.4.3 Stress response and post-capture survival

While the incidence of post-capture female mortality was very low, our analysis reveals that the risk of suspected cases of capture myopathy increases through the combined effects of the total duration of the capture event (including helicopter chase, physical immobilization, and handling) and the individual-specific stress response (as indicated by cortisol and aspartate aminotransferase concentrations in blood samples). A term combining the effects of cortisol and capture event duration was the most significant term in the model and a term indicating AST concentration was marginally significant. Creatinine kinase was also measured but was not found to be predictive of post-capture survival.

While cortisol levels can indicate an individual stress response, their concentration in wildlife blood samples can fluctuate with capture method, species, sex, age, and habituation (Morton et al., 1995). The cortisol concentrations we observed were typically between 27 and 237 nmol/L, which is lower than the 64 to 363 nmol/L reported for 139 female boreal caribou blood sampled following a single capture by helicopter using only physical restraints (no chemical immobilization) (Johnson et al., 2010). This difference may be explained by shorter capture and handling times when

conducting helicopter captures in tundra versus forested habitats. Levels in our study are more similar to the 8 to 266 nmol/L cortisol ranges reported for female Svalbard reindeer recaptured by snowmobile chases using both physical restraints and chemical immobilization (Trondrud et al., 2022), although the Svalbard study's handling times were notably longer than ours, frequently lasting more than 25 minutes and sometimes over an hour. In our study, we avoided chemical immobilization due to the susceptibility of caribou to thermal stress when sedated in the cold temperature of late winter in our study area and, consequently, all efforts were made to keep handling time below the recommended 15 minutes (Cattet, 2018). In addition, barren-ground caribou are a hunted species in the NWT and some hunters expressed concern about residual drugs in caribou they might harvest. While numerous reindeer and caribou studies have reported on baseline serological indicators of stress (e.g., Johnson et al., 2010) or on the incidence of short-term capture/handling related mortalities (e.g., Mathieu et al., 2022), to our knowledge none have related serological indicators to survival.

Endogenous responses to exogenous stressors initiate the metabolic mechanisms that lead to capture myopathy in many species (Breed et al., 2019), and previous studies have confirmed that increased handling time is the most important determinant of cortisol levels in the blood samples of captured reindeer (Trondrud et al., 2022). By including capture event duration and cortisol concentration into our survival model as a tensor smooth term, our modelling approach accounts for their interdependence and confirms that their interaction is an important determinant of survival outcomes.

Specifically, our results show that the predicted probability of survival declines as capture events lengthen and cortisol concentrations elevate (see Fig. 4.4). Previous

survival analyses conducted on caribou have focused on estimating population-wide mortality rates and therefore have typically removed capture-related mortalities to avoid potential biases (e.g., Hervieux et al., 2013). Focusing survival analyses on mortalities occurring at capture or in the 30-day post-capture period can provide valuable insights into the factors that mitigate or increase stress and risks to different ungulates. For example, Baumgardt et al. (2023) found that neither sex nor age class influenced nilgai antelope (*Boselaphus tragocamelus*) survival outcomes, but that overall mortality risk was greatest in the first five days immediately following release. Van De Kerk et al. (2020) found that mule deer (*Odocoileus hemionus*) mortality doubled relative to population baselines for up to four weeks after capture and that younger deer were generally more vulnerable. Jacques et al. (2009) used logistic regression to show that relocation distances following capture were directly related to capture-related mortality for pronghorn (*Antilocapra americana*), an effect that was not observed for the white-tailed deer (*Odocoileus virginianus*) in the same study. In addition to species and age, baseline stress or pre-existing musculoskeletal stress may also increase an individual's susceptibility to capture myopathy (Breed et al., 2019).

Our results suggest that aspartate aminotransferase (AST) concentration in blood samples is related to post-capture survival outcomes in migratory caribou, although the source of detectable AST in our study is attributable to pre-capture musculoskeletal stress. Blood indicators can provide a trove of information on the nutritional and physiological health of individuals prior to capture. In particular, musculoskeletal stress indices such as creatine phosphokinase (CK) and AST can provide direct evidence of the physical exertion and muscle injury which may lead to

capture myopathy (Breed et al., 2019). However, when capture events are short (< 15 minutes) it is unlikely that CK and AST would be produced and released into the bloodstream quickly enough to be detected in samples collected prior to release. Serum kinetics are poorly understood in wildlife species, and lacking species-specific rates of AST and CK release from muscle cells and subsequent removal from the bloodstream may limit our ability to discern indications of the onset of capture myopathy (i.e., muscle damage) from pre-existing musculoskeletal stress as a result of prior injury, exertion, or predator evasion. The modelling strategy we have described can account for this uncertainty, whereby the inclusion of CK and AST in the survival analysis both as independent terms and as terms that interact with capture event duration can help discern if their concentration in the blood serum were are likely related to pre-capture stress or a direct consequence of capture-related stress, respectively. Indeed, because there was no evidence that AST or CK interact with capture event duration, we attribute their variation to population baseline levels and pre-existing musculo-skeletal stress. In domestic mammals there is evidence that serum concentrations of AST remain elevated up to a week after muscle stress, while for CK only increases in the first day or two before dropping (Latimer et al., 2003). In our own study, we speculate that because of its longer detection window, AST provides a better indicator than CK for pre-capture muscle stress and exertion, which likely explains why it was favoured as a covariate within the survival model. Although no capture-related deaths were included in their analysis, Trondrud et al. (2022) reported that recapturing female Svalbard reindeer multiple times in the same year was linked to increased stress indices including longer heart rate recovery time, higher cortisol concentration, and lower body mass relative to

females capture once annually, results which suggest that baseline health and stress levels further mediate stress responses.

4.4.4 Overall implications and recommendations

The results of this study indicate that post-capture movement rates of female and male caribou return to baseline within four days of capture when assessed at a population level, but the recovery time of some individuals may be considerably longer. Given the importance of spring migration to caribou's reproductive strategy, we recommend allowing at least double and ideally triple this four-day population average of post-capture recovery and acclimation prior to the start of spring migration. Because the initiation of spring migration varies across years and between individuals, we acknowledge that ensuring this post-capture and pre-migration recovery window can prove difficult to balance with other important considerations such as temperature, wind chill, and visibility (Cattet, 2018). Overall winter and spring snow conditions are likely the best indicators for inferring the likely timing of migration, as shallow and/or compact snow conditions may motivate earlier departures while deep snow may retard them (Gurarie et al., 2019; Laforge et al., 2021; Le Corre et al., 2016).

While the varied acute stress responses of each individual to capture-related stressors present an important confounding factor, the duration of capture events is the primary variable that wildlife managers can control to reduce the risk of capture myopathy. Current capture guidelines for barren-ground caribou suggest limiting the total duration of capture and handling to 15 minutes (Cattet, 2018). Our results support this limit on duration, and suggest it is adequate to mitigate the risks of capture myopathy in the majority of captured females given the distribution of observed stress

responses. Our analysis also suggests that when females exhibit a more pronounced acute stress response relative to their peers, limiting capture event duration to 10 minutes can improve their probability of survival by almost 3%. While reducing capture event duration by an additional five minutes is difficult even with experience and optimal conditions, crews conducting migratory caribou captures should continuously strive to minimize all handling time. In addition, although we did not investigate this specifically, avoiding repeated helicopter chases of the same group of individuals may reduce potential stressors and improve survival outcomes.

4.5 Conclusion

To minimize the impacts on individuals and maximize the benefits of collaring, each wildlife monitoring program must carefully reconcile unique logistical constraints and species-specific vulnerabilities. This can prove particularly challenging in remote areas, where evaluating short-term and long-term impacts of captures and collars on behaviour and survival is constrained by the lack of information from uncollared individuals. In single-capture study designs, the types of analyses presented herein may constitute one of the only sources of information to understand the relationships between capture procedures and observed survival outcomes, especially in previously unstudied or understudied species where physiological and veterinary knowledge is limited. The rarity of immediate or short-term mortalities following caribou captures in our own study is encouraging and highlights important advances in our understanding of stress in ungulates and improvements of protocols and procedures to reduce potential harm.

4.6 References

- Adamczewski, J., Boulanger, J., Williams, J., Cluff, D., Clark, K., 2023. June 2022 calving ground surveys: Bathurst and Bluenose-East barren-ground caribou herds (No. 308). Environment and Climate Change, Government of the Northwest Territories, Yellowknife, Canada.
- Arnemo, J.M., Ahlqvist, P., Andersen, R., Berntsen, F., Ericsson, G., Odden, J., Brunberg, S., Segerström, P., Swenson, J.E., 2006. Risk of capture-related mortality in large free-ranging mammals: Experiences from Scandinavia. *Wildl. Biol.* 12, 109–113. [https://doi.org/10.2981/0909-6396\(2006\)12\[109:ROCMIL\]2.0.CO;2](https://doi.org/10.2981/0909-6396(2006)12[109:ROCMIL]2.0.CO;2)
- Arzamendia, Y., Vilá, B., 2012. Effects of capture, shearing, and release on the ecology and behavior of wild vicuñas. *J. Wildl. Manag.* 76, 57–64. <https://doi.org/10.1002/jwmg.242>
- Ashley, N.T., Barboza, P.S., Macbeth, B.J., Janz, D.M., Cattet, M.R.L., Booth, R.K., Wasser, S.K., 2011. Glucocorticosteroid concentrations in feces and hair of captive caribou and reindeer following adrenocorticotrophic hormone challenge. *Gen. Comp. Endocrinol.* 172, 382–391. <https://doi.org/10.1016/j.ygcen.2011.03.029>
- Barber-Meyer, S.M., 2022. Can non-invasive methods replace radiocollar-based winter counts in a 50-year wolf study? Lessons learned from a three-winter trial. *Wildl. Res.* 50, 451–464. <https://doi.org/10.1071/WR22001>
- Barboza, P.S., Parker, K.L., 2008. Allocating protein to reproduction in arctic reindeer and caribou. *Physiol. Biochem. Zool.* 81, 835–855. <https://doi.org/10.1086/590414>
- Barboza, P.S., Shively, R.D., Gustine, D.D., Addison, J.A., 2020. Winter is coming: Conserving body protein in female reindeer, caribou, and muskoxen. *Front. Ecol. Evol.* 8, 150. <https://doi.org/10.3389/fevo.2020.00150>
- Baumgardt, J.A., Foley, A.M., Sliwa, K.M., DeYoung, R.W., Ortega-S., J.A., Hewitt, D.G., Campbell, T.A., Goolsby, J.A., Lohmeyer, K.H., 2023. Effects of helicopter net gunning on the survival and movement behaviour of nilgai antelope. *Wildl. Res.* 50, 890–898. <https://doi.org/10.1071/WR22049>
- Bengsen, A.J., Hampton, J.O., Comte, S., Freney, S., Forsyth, D.M., 2021. Evaluation of helicopter net-gunning to capture wild fallow deer (*Dama dama*). *Wildl. Res.* 48, 722–729. <https://doi.org/10.1071/WR21007>
- Bergerud, A.T., Luttich, S.N., Camps, L., 2008. The return of caribou to Ungava. McGill-Queen's University Press, Montreal, Canada.
- Beringer, J., Hansen, L.P., Wilding, W., Fischer, J., Sheriff, S.L., 1996. Factors affecting capture myopathy in white-tailed deer. *J. Wildl. Manag.* 60, 373–380.
- Borquet, G., 2020. Effects of GPS-collars on Svalbard reindeer survival and body condition (MSc Thesis). Inland Norway University of Applied Sciences, Innlandet, Norway.
- Boulanger, J., Adamczewski, J., Williams, J., Goodman, S., Clark, K., Abernethy, R., Leclerc, L.-M., 2024. June 2023 calving ground surveys: Bluenose-East and Bathurst barren-ground caribou herds (No. 319). Environment and Climate Change, Government of the Northwest Territories, Yellowknife, Canada.

- Breed, D., Meyer, L.C.R., Steyl, J.C.A., Goddard, A., Burroughs, R., Kohn, T.A., 2019. Conserving wildlife in a changing world: Understanding capture myopathy—a malignant outcome of stress during capture and translocation. *Conserv. Physiol.* 7, coz027. <https://doi.org/10.1093/conphys/coz027>
- Brivio, F., Grignolio, S., Sica, N., Cerise, S., Bassano, B., 2015. Assessing the impact of capture on wild animals: The case study of chemical immobilisation on Alpine ibex. *PLoS ONE* 10, 1–18. <https://doi.org/10.1371/journal.pone.0130957>
- Brown, D.D., Kays, R., Wikelski, M., Wilson, R., Klimley, A., 2013. Observing the unwatchable through acceleration logging of animal behavior. *Anim. Biotelemetry* 1, 20. <https://doi.org/10.1186/2050-3385-1-20>
- Cameron, M.D., Joly, K., Breed, G.A., Parrett, L.S., Kielland, K., 2018. Movement-based methods to infer parturition events in migratory ungulates. *Can. J. Zool.* 96, 1187–1195. <https://doi.org/10.1139/cjz-2017-0314>
- Cameron, R.D., Whitten, K.R., 1979. Seasonal movements and sexual segregation of caribou determined by aerial survey. *J. Wildl. Manag.* 43, 626–633.
- Cattet, M., 2018. Capture, handling and release of caribou standard operating procedure. Wildlife Care Committee, Government of the Northwest Territories, Yellowknife, Northwest Territories, Canada.
- Cattet, M., Boulanger, J., Stenhouse, G., Powell, R.A., Reynolds-Hogland, M.J., 2008. An evaluation of long-term capture effects in ursids: Implications for wildlife welfare and research. *J. Mammal.* 89, 973–990. <https://doi.org/10.1644/08-MAMM-A-095.1>
- Cooke, S.J., Nguyen, V.M., Kessel, S.T., Hussey, N.E., Young, N., Ford, A.T., 2017. Troubling issues at the frontier of animal tracking for conservation and management. *Conserv. Biol.* 31, 1205–1207. <https://doi.org/10.1111/cobi.12895>
- COSEWIC, 2017. COSEWIC assessment and status report on the Caribou *Rangifer tarandus*, Eastern Migratory population and Torngat Mountains population, in Canada. Committee on the Status of Endangered Wildlife in Canada, Ottawa, Canada.
- COSEWIC, 2016. COSEWIC assessment and status report on the Caribou *Rangifer tarandus*, Barren-ground population, in Canada. Committee on the Status of Endangered Wildlife in Canada, Ottawa, Canada.
- Cox, D.R., 1972. Regression models and life-tables. *J. R. Stat. Soc. Ser. B Methodol.* 34, 187–202. <https://doi.org/10.1111/j.2517-6161.1972.tb00899.x>
- Crabtree, G., Kócs, E., Trahey, L., 2015. The energy-storage frontier: Lithium-ion batteries and beyond. *MRS Bull.* 40, 1067–1078. <https://doi.org/10.1557/mrs.2015.259>
- Cumming, H.G., Beange, D.B., 1987. Dispersion and movements of woodland caribou near Lake Nipigon, Ontario. *J. Wildl. Manag.* 51, 69. <https://doi.org/10.2307/3801634>
- Dau, J., 1997. Western Arctic Caribou Herd - Units 21D, 22A, 22B, 23, 24, and 26A, Caribou. Federal aid in wildlife restoration management report of survey-inventory activities 1 July 1994-30 June 1996. Alaska Department of Fish and Game, Juneau, Alaska, United States.

- Davis, J.L., Valkenburg, P., 1979. Natural Mortality of Western Arctic Caribou, Federal Aid in Wildlife Restoration. State of Alaska, Department of Fish and Game, Division of Game, Juneau, Alaska, United States.
- Dechen Quinn, A.C., Williams, D.M., Porter, W.F., 2012. Postcapture movement rates can inform data-censoring protocols for GPS-collared animals. *J. Mammal.* 93, 456–463. <https://doi.org/10.1644/10-MAMM-A-422.1>
- Dechen Quinn, A.C., Williams, D.M., Porter, W.F., Fitzgerald, S.D., Hynes, K., 2014. Effects of capture-related injury on postcapture movement of white-tailed deer. *J. Wildl. Dis.* 50, 250–258. <https://doi.org/10.7589/2012-07-174>
- Fancy, S.G., White, R.G., 1986. Predicting energy expenditures for activities of caribou from heart rates. *Rangifer* 6, 123. <https://doi.org/10.7557/2.6.2.636>
- Feldman, M., Dickson, B., 2017. Plasma electrolyte distributions in humans—normal or skewed? *Am. J. Med. Sci.* 354, 453–457. <https://doi.org/10.1016/j.amjms.2017.07.012>
- Ford, A.T., Noonan, M.J., Bollefer, K., Gill, R., Legebokow, C., Serrouya, R., 2023. The effects of maternal penning on the movement ecology of mountain caribou. *Anim. Conserv.* 26, 72–85. <https://doi.org/10.1111/acv.12801>
- Gerhart, K.L., Ruussell, D.E., Wetering, D.V.D., White, R.G., Cameron, R.D., 1997. Pregnancy of adult caribou (*Rangifer tarandus*): Evidence for lactational infertility. *J. Zool.* 242, 17–30. <https://doi.org/10.1111/j.1469-7998.1997.tb02926.x>
- Gunn, A., 2016. *Rangifer tarandus*. The IUCN Red List of Threatened Species 2016: e.T29742A22167140. <https://doi.org/10.2305/IUCN.UK.2016-1.RLTS.T29742A22167140.en>
- Gunn, A., D'Hont, A., Williams, J., Boulanger, J., 2013. Satellite collaring in the Bathurst herd of barren-ground caribou 1996–2005. Government of the Northwest Territories, Yellowknife, Canada.
- Gunn, A., Dragon, J., Boulanger, J., 2001. Seasonal movements of satellite-collared caribou from the Bathurst herd, Final report to the West Kitikmeot Slave Study Society. Yellowknife, Canada.
- Gurarie, E., Hebblewhite, M., Joly, K., Kelly, A.P., Adamczewski, J., Davidson, S.C., Davison, T., Gunn, A., Sutor, M.J., Fagan, W.F., Boelman, N., 2019. Tactical departures and strategic arrivals: Divergent effects of climate and weather on caribou spring migrations. *Ecosphere* 10. <https://doi.org/10.1002/ecs2.2971>
- Haskell, S.P., Ballard, W.B., 2007. Modeling the Western Arctic caribou herd during a positive growth phase: Potential effects of wolves and radiocollars. *J. Wildl. Manag.* 71, 619–627. <https://doi.org/10.2193/2006-349>
- Herman, J.P., McKlveen, J.M., Ghosal, S., Kopp, B., Wulsin, A., Makinson, R., Scheimann, J., Myers, B., 2016. Regulation of the hypothalamic-pituitary-adrenocortical stress response, in: Prakash, Y.S. (Ed.), *Comprehensive Physiology*. Wiley, pp. 603–621. <https://doi.org/10.1002/cphy.c150015>
- Hervieux, D., Hebblewhite, M., DeCesare, N.J., Russell, M., Smith, K., Robertson, S., Boutin, S., 2013. Widespread declines in woodland caribou (*Rangifer tarandus caribou*) continue in Alberta. *Can. J. Zool.* 91, 872–882. <https://doi.org/10.1139/cjz-2013-0123>
- Hofman, M.P.G., Hayward, M.W., Heim, M., Marchand, P., Rolandsen, C.M., Mattisson, J., Urbano, F., Heurich, M., Mysterud, A., Melzheimer, J., Morellet, N., Voigt, U.,

- Allen, B.L., Gehr, B., Rouco, C., Ullmann, W., Holand, Ø., Jørgensen, N.H., Steinheim, G., Cagnacci, F., Kroeschel, M., Kaczensky, P., Buuveibaatar, B., Payne, J.C., Palmegiani, I., Jerina, K., Kjellander, P., Johansson, Ö., LaPoint, S., Bayrakcismith, R., Linnell, J.D.C., Zaccaroni, M., Jorge, M.L.S., Oshima, J.E.F., Songhurst, A., Fischer, C., Mc Bride, R.T., Thompson, J.J., Streif, S., Sandfort, R., Bonenfant, C., Drouilly, M., Klapproth, M., Zinner, D., Yarnell, R., Stronza, A., Wilmott, L., Meisingset, E., Thaker, M., Vanak, A.T., Nicoloso, S., Graeber, R., Said, S., Boudreau, M.R., Devlin, A., Hoogesteijn, R., May-Junior, J.A., Nifong, J.C., Odden, J., Quigley, H.B., Tortato, F., Parker, D.M., Caso, A., Perrine, J., Tellaeche, C., Zieba, F., Zwijacz-Kozica, T., Appel, C.L., Axsom, I., Bean, W.T., Cristescu, B., Périquet, S., Teichman, K.J., Karpanty, S., Licoppe, A., Menges, V., Black, K., Scheppers, T.L., Schai-Braun, S.C., Azevedo, F.C., Lemos, F.G., Payne, A., Swanepoel, L.H., Weckworth, B.V., Berger, A., Bertassoni, A., McCulloch, G., Šustr, P., Athreya, V., Bockmuhl, D., Casaer, J., Ekori, A., Melovski, D., Richard-Hansen, C., Van De Vyver, D., Reyna-Hurtado, R., Robardet, E., Selva, N., Sergiel, A., Farhadinia, M.S., Sunde, P., Portas, R., Ambarli, H., Berzins, R., Kappeler, P.M., Mann, G.K., Pyritz, L., Bissett, C., Grant, T., Steinmetz, R., Swedell, L., Welch, R.J., Armenteras, D., Bidder, O.R., González, T.M., Rosenblatt, A., Kachel, S., Balkenhol, N., 2019. Right on track? Performance of satellite telemetry in terrestrial wildlife research. *PLoS ONE* 14, e0216223. <https://doi.org/10.1371/journal.pone.0216223>
- Jacques, C.N., Jenks, J.A., Deperno, C.S., Sievers, J.D., Grovenburg, T.W., Brinkman, T.J., Swanson, C.C., Stillings, B.A., 2009. Evaluating ungulate mortality associated with helicopter net-gun captures in the Northern Great Plains. *J. Wildl. Manag.* 73, 1282–1291. <https://doi.org/10.2193/2009-039>
- Jakimchuk, R.D., Ferguson, S.H., Sopuck, L.G., 1987. Differential habitat use and sexual segregation in the Central Arctic caribou herd. *Can. J. Zool.* 65, 534–541. <https://doi.org/10.1139/z87-083>
- Jingfors, K., Gunn, A., 1989. The use of snowmobiles in the drug immobilization of muskoxen. *Can. J. Zool.* 67, 1120–1121. <https://doi.org/10.1139/z89-160>
- Johnson, D., Harms, N.J., Larter, N.C., Elkin, B.T., Tabel, H., Wei, G., 2010. Serum biochemistry, serology, and parasitology of boreal caribou (*Rangifer tarandus caribou*) in the Northwest Territories, Canada. *J. Wildl. Dis.* 46, 1096–1107. <https://doi.org/10.7589/0090-3558-46.4.1096>
- Joly, K., Couriot, O., Cameron, M.D., Gurarie, E., 2020. Behavioral, physiological, demographic and ecological impacts of hematophagous and endoparasitic insects on an Arctic ungulate. *Toxins* 12, 334. <https://doi.org/10.3390/toxins12050334>
- Joly, K., Gurarie, E., Sorum, M.S., Kaczensky, P., Cameron, M.D., Jakes, A.F., Borg, B.L., Nandintsetseg, D., Hopcraft, J.G.C., Buuveibaatar, B., Jones, P.F., Mueller, T., Walzer, C., Olson, K.A., Payne, J.C., Yadamsuren, A., Hebblewhite, M., 2019. Longest terrestrial migrations and movements around the world. *Sci. Rep.* 9, 15333. <https://doi.org/10/ggccp4>
- Jung, T.S., Konkolics, S.M., Kukka, P.M., Majchrzak, Y.N., Menzies, A.K., Oakley, M.P., Peers, M.J.L., Studd, E.K., 2019. Short-term effect of helicopter-based capture

- on movements of a social ungulate. *J. Wildl. Manag.* 83, 830–837.
<https://doi.org/10.1002/jwmg.21640>
- Kays, R., Crofoot, M.C., Jetz, W., Wikelski, M., 2015. Terrestrial animal tracking as an eye on life and planet. *Science* 348, aaa2478.
<https://doi.org/10.1126/science.aaa2478>
- Kays, R., Davidson, S.C., Berger, M., Bohrer, G., Fiedler, W., Flack, A., Hirt, J., Hahn, C., Gauggel, D., Russell, B., Kölzsch, A., Lohr, A., Partecke, J., Quetting, M., Safi, K., Scharf, A., Schneider, G., Lang, I., Schaeuffelhut, F., Landwehr, M., Storhas, M., van Schalkwyk, L., Vinciguerra, C., Weinzierl, R., Wikelski, M., 2022. The Movebank system for studying global animal movement and demography. *Methods Ecol. Evol.* 13, 419–431. <https://doi.org/10.1111/2041-210X.13767>
- Klein, J.P., Moeschberger, M.L., 2003. Survival analysis: Techniques for censored and truncated data, *Statistics for Biology and Health*. Springer, New York, United States. <https://doi.org/10.1007/b97377>
- Kock, M.D., Jessup, D.A., Clark, R.K., Franti, C.E., 1987. Effects of capture on biological parameters in free-ranging bighorn sheep (*Ovis canadensis*): Evaluation of drop-net, drive-net, chemical immobilization and the net-gun. *J. Wildl. Dis.* 23, 641–651. <https://doi.org/10.7589/0090-3558-23.4.652>
- Kreeger, T.J., Arnemo, J.M., Caulkett, N.A., Hampton, J.O., Meyer, L.C.R., 2023. Handbook of wildlife chemical immobilization, 6th edition.
- Latimer, K.S., Mahaffey, E.A., Prasse, K.W., Duncan, J.R., 2003. Duncan and Prasse's veterinary laboratory medicine: Clinical pathology, 4th ed. Iowa State Press, Ames, United States.
- LeTourneux, F., Gauthier, G., Pradel, R., Lefebvre, J., Legagneux, P., 2022. Evidence for synergistic cumulative impacts of marking and hunting in a wildlife species. *J. Appl. Ecol.* 59, 2705–2715. <https://doi.org/10.1111/1365-2664.14268>
- Li, Z., Wood, S.N., 2020. Faster model matrix crossproducts for large generalized linear models with discretized covariates. *Stat. Comput.* 30, 19–25.
<https://doi.org/10.1007/s11222-019-09864-2>
- Mallory, C.D., Williamson, S.N., Campbell, M.W., Boyce, M.S., 2020. Response of barren-ground caribou to advancing spring phenology. *Oecologia* 192, 837–852.
<https://doi.org/10.1007/s00442-020-04604-0>
- Marra, G., Wood, S.N., 2011. Practical variable selection for generalized additive models. *Comput. Stat. Data Anal.* 55, 2372–2387.
<https://doi.org/10.1016/j.csda.2011.02.004>
- Mathieu, A., Vander Vennen, L.M., Ried, A., Legebokow, C., Schwantje, H.M., 2022. Translocation of southern mountain caribou using a soft-release technique. *Rangifer* 42, 1–16. <https://doi.org/10.7557/2.42.1.5930>
- McIntyre, T., 2015. Animal telemetry: Tagging effects. *Science* 349, 596–597.
<https://doi.org/10.1126/science.349.6248.596-b>
- McMahon, C.R., Hindell, M.A., Harcourt, R.G., 2012. Publish or perish: why it's important to publicise how, and if, research activities affect animals. *Wildl. Res.* 39, 375. <https://doi.org/10.1071/WR12014>
- Mennell, R., 2021. Spatial and temporal trends in range-use by the Bathurst caribou during a population decline, 1997-2019 (MSc Thesis). Queen's University, Kingston, Canada.

- Miller, D.R., Robertson, J.D., 1967. Results of tagging caribou at Little Duck Lake, Manitoba. *J. Wildl. Manag.* 31, 150. <https://doi.org/10.2307/3798370>
- Morton, D., Anderson, E., Foggin, C., Kock, M., Tiran, E., 1995. Plasma cortisol as an indicator of stress due to capture and translocation in wildlife species. *Vet. Rec.* 136, 60–63. <https://doi.org/10.1136/vr.136.3.60>
- Nagy, J.A., 2011. Use of space by caribou in Northern Canada. University of Alberta, Edmonton, Canada.
- Northrup, J.M., Anderson, C.R., Wittemyer, G., 2014. Effects of helicopter capture and handling on movement behavior of mule deer. *J. Wildl. Manag.* 78, 731–738. <https://doi.org/10.1002/jwmg.705>
- Nussberger, B., Ingold, P., 2006. Effects of radio-collars on behaviour of alpine chamois *Rupicapra rupicapra rupicapra*. *Wildl. Biol.* 12, 339–343. [https://doi.org/10.2981/0909-6396\(2006\)12\[339:EROBO\]2.0.CO;2](https://doi.org/10.2981/0909-6396(2006)12[339:EROBO]2.0.CO;2)
- NWT Species at Risk Committee, 2017. Species status report for Porcupine caribou and barren-ground caribou (Tuktoyaktuk Peninsula, Cape Bathurst, Bluenose-West, Bluenose-East, Bathurst, Beverly, Ahiak, and Qamanirjuaq herds) (*Rangifer tarandus groenlandicus*) in the Northwest Territories. Government of the Northwest Territories, Yellowknife, Canada.
- Paterson, J., 2014. Capture myopathy, in: West, G., Heard, D., Caulkett, N. (Eds.), *Zoo Animal and Wildlife Immobilization and Anesthesia*, 2nd Edition. John Wiley & Sons, Inc., Ames, United States, pp. 171–179.
- Pedersen, E.J., Miller, D.L., Simpson, G.L., Ross, N., 2019. Hierarchical generalized additive models in ecology: An introduction with mgcv. *PeerJ* 7, e6876. <https://doi.org/10.7717/peerj.6876>
- Pollock, K.H., Winterstein, S.R., Bunck, C.M., Curtis, P.D., 1989. Survival analysis in telemetry studies: The staggered entry design. *J. Wildl. Manag.* 53, 7. <https://doi.org/10.2307/3801296>
- Prichard, A.K., Joly, K., Parrett, L.S., Cameron, M.D., Hansen, D.A., Person, B.T., 2023. Achieving a representative sample of marked animals: A spatial approach to evaluating post-capture randomization. *Wildl. Soc. Bull.* 47, e1398. <https://doi.org/10.1002/wsb.1398>
- Prichard, A.K., Yokel, D.A., Rea, C.L., Person, B.T., Parrett, L.S., 2014. The effect of frequency of telemetry locations on movement-rate calculations in arctic caribou. *Wildl. Soc. Bull.* 38, 78–88. <https://doi.org/10.1002/wsb.357>
- R Core Team, 2023. *R: A language and environment for statistical computing*. R Foundation for Statistical Computing, Vienna, Austria.
- Rachlow, J.L., Peter, R.M., Shipley, L.A., Johnson, T.R., 2014. Sub-lethal effects of capture and collaring on wildlife: Experimental and field evidence. *Wildl. Soc. Bull.* 38, 458–465. <https://doi.org/10.1002/wsb.444>
- Rakic, F., Fernandez-Aguilar, X., Pruvot, M., Whiteside, D.P., Mastro Monaco, G.F., Leclerc, L.M., Jutha, N., Kutz, S.J., 2023. Variation of hair cortisol in two herds of migratory caribou (*Rangifer tarandus*): Implications for health monitoring. *Conserv. Physiol.* 11, coad030. <https://doi.org/10.1093/conphys/coad030>
- Rasiulis, A.L., Festa-Bianchet, M., Couturier, S., Côté, S.D., 2014. The effect of radio-collar weight on survival of migratory caribou. *J. Wildl. Manag.* 78, 953–956. <https://doi.org/10.1002/jwmg.722>

- Rockhill, A.P., Chinnadurai, S.K., Powell, R.A., DePerno, C.S., 2011. A comparison of two field chemical immobilization techniques for bobcats (*Lynx rufus*). *J. Zoo Wildl. Med.* 42, 580–585. <https://doi.org/10.1638/2010-0152.1>
- Rode, K.D., Pagano, A.M., Bromaghin, J.F., Atwood, T.C., Durner, G.M., Simac, K.S., Amstrup, S.C., 2014. Effects of capturing and collaring on polar bears: Findings from long-term research on the southern Beaufort Sea population. *Wildl. Res.* 41, 311–322. <https://doi.org/10.1071/WR13225>
- Rodgers, A.R., 2001. Tracking animals with GPS: The first 10 years, in: *Proceedings of the Conference on Tracking Animals with GPS*. The Macaulay Land Use Research Institute, Aberdeen, United Kingdom, pp. 1–10.
- Rodgers, A.R., Rempel, R.S., Abraham, K.F., 1996. A GPS-based telemetry system. *Wildl. Soc. Bull.* 24, 559–568.
- Rowcliffe, J.M., Carbone, C., Kays, R., Kranstauber, B., Jansen, P.A., 2012. Bias in estimating animal travel distance: The effect of sampling frequency. *Methods Ecol. Evol.* 3, 653–662. <https://doi.org/10.1111/j.2041-210X.2012.00197.x>
- Shaw, A.K., 2020. Causes and consequences of individual variation in animal movement. *Mov. Ecol.* 8, 12. <https://doi.org/10.1186/s40462-020-0197-x>
- Simpson, G.L., 2024. gratia: Graceful ggplot-based graphics and other functions for GAMs fitted using mgcv, R package version 0.9.0.
- Simpson, G.L., 2018. Modelling palaeoecological time series using generalised additive models. *Front. Ecol. Evol.* 6, 149. <https://doi.org/10.3389/fevo.2018.00149>
- Soulsbury, C.D., Gray, H.E., Smith, L.M., Braithwaite, V., Cotter, S.C., Elwood, R.W., Wilkinson, A., Collins, L.M., 2020. The welfare and ethics of research involving wild animals: A primer. *Methods Ecol. Evol.* 11, 1164–1181. <https://doi.org/10.1111/2041-210X.13435>
- Spiegel, O., Leu, S.T., Bull, C.M., Sih, A., 2017. What's your move? Movement as a link between personality and spatial dynamics in animal populations. *Ecol. Lett.* 20, 3–18. <https://doi.org/10.1111/ele.12708>
- Spraker, T.R., 1993. Stress and capture myopathy in artiodactylids, in: Fowler, M.E. (Ed.), *Zoo and Wild Animal Medicine: Current Therapy 3*. WB Saunders Company, pp. 481–488.
- Stabach, J.A., Cunningham, S.A., Connette, G., Mota, J.L., Reed, D., Byron, M., Songer, M., Wacher, T., Mertes, K., Brown, J.L., Comizzoli, P., Newby, J., Monfort, S., Leimgruber, P., 2020. Short-term effects of GPS collars on the activity, behavior, and adrenal response of scimitar-horned oryx (*Oryx dammah*). *PLoS ONE* 15, e0221843. <https://doi.org/10.1371/journal.pone.0221843>
- St-Laurent, M.-H., Dussault, C., 2012. The reintroduction of boreal caribou as a conservation strategy: A long-term assessment at the southern range limit. *Rangifer* 32, 127. <https://doi.org/10.7557/2.32.2.2261>
- Thiemann, G.W., Derocher, A.E., Cherry, S.G., Lunn, N.J., Peacock, E., Sahanatien, V., 2013. Effects of chemical immobilization on the movement rates of free-ranging polar bears. *J. Mammal.* 94, 386–397. <https://doi.org/10.1644/12-MAMM-A-230.1>
- Torney, C.J., Lamont, M., Debell, L., Angohiatok, R.J., Leclerc, L.-M., Berdahl, A.M., 2018. Inferring the rules of social interaction in migrating caribou. *Philos. Trans. R. Soc. B Biol. Sci.* 373, 20170385. <https://doi.org/10.1098/rstb.2017.0385>

- Trondrud, L.M., Pigeon, G., Albon, S., Arnold, W., Evans, A.L., Irvine, R.J., Król, E., Ropstad, E., Stien, A., Veiberg, V., Speakman, J.R., Loe, L.E., 2021. Determinants of heart rate in Svalbard reindeer reveal mechanisms of seasonal energy management. *Philos. Trans. R. Soc. B Biol. Sci.* 376, 20200215. <https://doi.org/10.1098/rstb.2020.0215>
- Trondrud, L.M., Ugland, C., Ropstad, E., Loe, L.E., Albon, S., Stien, A., Evans, A.L., Thorsby, P.M., Veiberg, V., Irvine, R.J., Pigeon, G., 2022. Stress responses to repeated captures in a wild ungulate. *Sci. Rep.* 12, 16289. <https://doi.org/10.1038/s41598-022-20270-z>
- Uboni, A., Horstkotte, T., Kaarlejärvi, E., Sévêque, A., Stammler, F., Olofsson, J., Forbes, B.C., Moen, J., 2016. Long-term trends and role of climate in the population dynamics of Eurasian reindeer. *PLoS ONE* 11, e0158359. <https://doi.org/10.1371/journal.pone.0158359>
- Ugland, C., 2021. Effects of repeated captures on Svalbard reindeer (*Rangifer tarandus platyrhynchus*): Implications for animal welfare and scientific bias (MSc Thesis). Norwegian University of Life Sciences, Ås, Norway.
- Valkenburg, P., Boertje, R.D., Davis, J.L., 1983. Effects of darting and netting on caribou in Alaska. *J. Wildl. Manag.* 47, 1233–1237.
- Valkenburg, P., Tobey, R.W., Kirk, D., 1999. Velocity of tranquilizer darts and capture mortality of caribou calves. *Wildl. Soc. Bull.* 27, 894–896.
- Van De Kerk, M., McMillan, B.R., Hersey, K.R., Roug, A., Larsen, R.T., 2020. Effect of net-gun capture on survival of mule deer. *J. Wildl. Manag.* 84, 813–820. <https://doi.org/10.1002/jwmg.21838>
- Vors, L.S., Boyce, M.S., 2009. Global declines of caribou and reindeer. *Glob. Change Biol.* 15, 2626–2633. <https://doi.org/10.1111/j.1365-2486.2009.01974.x>
- Walker, K.A., Trites, A.W., Haulena, M., Weary, D.M., 2012. A review of the effects of different marking and tagging techniques on marine mammals. *Wildl. Res.* 39, 15. <https://doi.org/10.1071/WR10177>
- Webb, S.L., Lewis, J.S., Hewitt, D.G., Hellickson, M.W., Bryant, F.C., 2008. Assessing the helicopter and net gun as a capture technique for white-tailed deer. *J. Wildl. Manag.* 72, 310–314. <https://doi.org/10.2193/2007-101>
- Williams, H.J., Taylor, L.A., Benhamou, S., Bijleveld, A.I., Clay, T.A., De Grissac, S., Demšar, U., English, H.M., Franconi, N., Gómez-Laich, A., Griffiths, R.C., Kay, W.P., Morales, J.M., Potts, J.R., Rogerson, K.F., Rutz, C., Spelt, A., Trevail, A.M., Wilson, R.P., Börger, L., 2020. Optimizing the use of biologgers for movement ecology research. *Journal of Animal Ecology* 89, 186–206. <https://doi.org/10.1111/1365-2656.13094>
- Wilson, R., Redcliffe, J., Holton, M., Thomas, V., Gunner, R., Silovski, V., Jezek, M., English, H., Shott, O., Bambridge, K., Dee, E., Nichols, H., Quintana, F., Fahlman, A., Larsson, J., Scantlebury, D.M., Siebert, U., 2023. Why catch when you can throw? A framework for tagging animals without capture or restraint. *Res. Sq.* <https://doi.org/10.21203/rs.3.rs-3415966/v1>
- Wood, M.D., 1996. Seasonal habitat use and movements of woodland caribou in the Omineca Mountains, north central British Columbia, 1991-1993. *Rangifer* 16, 365. <https://doi.org/10.7557/2.16.4.1279>

- Wood, S.N., 2017. *Generalized Additive Models: An introduction with R*, 2nd ed. Chapman and Hall/CRC, New York, United States.
<https://doi.org/10.1201/9781315370279>
- Wood, S.N., Goude, Y., Shaw, S., 2015. Generalized additive models for large data sets. *J. R. Stat. Soc. Ser. C Appl. Stat.* 64, 139–155.
<https://doi.org/10.1111/rssc.12068>
- Wood, S.N., Pya, N., Säfken, B., 2016. Smoothing parameter and model selection for general smooth models. *J. Am. Stat. Assoc.* 111, 1548–1563.
<https://doi.org/10.1080/01621459.2016.1180986>
- Young, R.L., Weinberg, J., Vieira, V., Ozonoff, A., Webster, T.F., 2011. Generalized additive models and inflated type I error rates of smoother significance tests. *Comput. Stat. Data Anal.* 55, 366–374.
<https://doi.org/10.1016/j.csda.2010.05.004>
- Zemanova, M.A., 2020. Towards more compassionate wildlife research through the 3Rs principles: Moving from invasive to non-invasive methods. *Wildl. Biol.* 2020.
<https://doi.org/10.2981/wlb.00607>
- Zuur, A.F., Ieno, E.N., 2016. A protocol for conducting and presenting results of regression-type analyses. *Methods Ecol. Evol.* 7, 636–645.
<https://doi.org/10.1111/2041-210X.12577>

5. General discussion

In this thesis, I have provided unique insights into the migratory movements of barren-ground caribou in response to the rapid phenological shifts in lake ice occurring throughout their circumpolar distribution. I have also analyzed how captures required for current tracking and monitoring approaches affect caribou behaviour and survival. By developing a new remote sensing algorithm named OPEN-ICE, I successfully processed large quantities of satellite imagery from the open-access archives of multiple optical sensors, fused them into a single times series of ice and water observations, and produced the first high-resolution map of spring freshwater ice phenology events that can accurately provide breakup dates for both very small ($< 0.01 \text{ km}^2$) and very large lakes ($> 10,000 \text{ km}^2$) lakes over entire continents (Chapter 2). Capitalizing on the spatial resolution and broad coverage of the OPEN-ICE data product, I was able to investigate the full breadth of freshwater ice phenology conditions in the thousands of waterbodies encountered by female caribou during spring migration, and found that females from Bluenose-East and Bathurst herds selected routes through areas of the landscape dominated by small ice-covered lakes, generally avoided larger waterbodies, and strongly avoided areas with breaking ice (Chapter 3). I further investigated caribou movement and survival in the period immediately following their capture, and found that: (i) movement rates of males increased in the days after capture while those of females decreased, but that both sexes typically returned to their respective population means within three to four days of release, and (ii) female mortality in the post-capture period was rare, though its probability increased with the duration of capture events and higher blood cortisol (Chapter 4). As a whole, this thesis

provides unique contributions to our understanding of the seasonality and phenology of the Arctic and its most abundant and widely-distributed large mammal, migratory caribou, and sheds light on how its behaviour is shaped by spatio-temporal variation in its environment and by the very methods we employ to monitor them.

5.1 Big data approaches to remote sensing and wildlife ecology

By distilling massive quantities of data into useful and easily interpretable aggregate products, visualizations, and results, this thesis has contributed to developing and describing analytical tools and methodologies that contribute to big data approaches in the fields of remote sensing and movement ecology (Chapter 2, 3, and 4). Key scientific discoveries emerge from both experimental and observational study designs, but as the complexity and the spatio-temporal scales of the systems being studied increase, sampling large collections of observations across the different nodes and links of a system informing ad hoc analysis is often the only avenue of investigation (McCleery et al., 2023). Indeed, in disciplines like climatology or landscape ecology, experimental manipulations at broad spatial scales are often impossible. The recent explosion of both Earth observations (Chi et al., 2016; Wulder et al., 2019) and biologging (Nathan et al., 2022) has provided unprecedented opportunity to dissect complex spatio-temporal relationships between the environment and wildlife, including investigations of nutrition and energetics (English et al., 2024), individual and population behaviours (Gurarie et al., 2019), emergent collective behaviour (Dalziel et al., 2016), and population dynamics (Johnson et al., 2022). However, traditional statistical and computational methods may be insufficient or incapable of handling such large quantities of data. As the low hanging fruits of ecology have been mostly picked dry

(Low-Décarie et al., 2014), many disciplines have increasingly devoted efforts to developing novel methods that can analyze and condense exponentially large datasets to extract metrics with which to investigate and explore new questions in ecology.

In developing the OPEN-ICE algorithm and deploying it over all of Canada between 2013 and 2021, I estimate that approximately 1.5 million distinct images were accessed, classified, temporally filtered, and analyzed to identify temporal transitions from ice to water in each 30-metre freshwater pixel (Chapter 2). Together, these images have a combined footprint of approximately 22 billion square kilometres and contain approximately 0.898 petabytes of information, an amount of data which would take centuries to analyze even on most modern computers. The OPEN-ICE algorithm successfully summarized all this information to extract an annual spring breakup date for each freshwater pixel of Canada, which along with 3 other bands containing QA/QC is approximately 10 gigabytes of information for each year.

While the collection of GPS observations collected by the collaring programs for the Bathurst and Bluenose-East herds is several orders of magnitude smaller than the image collections used to produce the OPEN-ICE data product, they nonetheless form large databases that present challenging characteristics such as the hierarchical structures and interdependence imposed by groups of observations tied to each individual (Chapter 3 and 4). Furthermore, spatial analyses that estimate selection/avoidance based on used-available study designs (i.e., path selection analysis) can be extremely challenging to implement at these spatial scales especially when some of the covariates of interest are in a rapid state of flux. For example, to investigate the influence of lake ice on spring migration, we sampled ice phenology

conditions by aggregating the frequencies of pixel breakup dates in the landscape immediately surrounding each step (i.e., observed and random steps), requiring over 2 million distinct operations cumulatively summarizing all the 30-metre freshwater pixels in an area over 100 million square kilometres. None of these operations would have been possible without a cloud-computing platform such as GEE, which explains why such tools are an increasingly essential part of the movement ecologist's toolbox, and indeed for any discipline investigating questions at such broad spatial scales.

5.2 Broad-scale high-resolution freshwater ice phenology data product

The OPEN-ICE algorithm and data product delivers the first high-resolution (30-metre) freshwater ice phenology product with North American coverage, providing an unprecedented level of detail for the more than 880,000 Canadian lakes larger than 0.1 km² (Messenger et al., 2016), and countless smaller ones (Cael and Seekell, 2016), distributed throughout regions undergoing some of the fastest warming on Earth (Rantanen et al., 2022). Beyond its utilization for migratory caribou research in this thesis, the potential applications for the OPEN-ICE data product are diverse and impactful, ranging from safety and transportation to limnology, aquatic and terrestrial ecology, global biogeochemistry and climatology. Smaller lakes are more numerous than larger ones (Messenger et al., 2016), their combined area likely occupies a greater proportion of the Earth's surface than large lakes (Cael and Seekell, 2016; Verpoorter et al., 2014), and, relative to their size, they are disproportionately large contributors to atmospheric gas exchanges and geochemical cycles, including greenhouse gases (Downing, 2010; Holgerson and Raymond, 2016; Pi et al., 2022). Despite ice cover

playing such a central role in their interface to global cycles, a broad-scale understanding of their ice phenology characteristics and feedback with regional climate systems has been lacking. The thermal inertia of large lakes attenuates some of the inter-annual variability in phenological events and, as such, they are and will continue to be extremely important sentinels of long-term changes in climate (Sharma et al., 2022). In contrast, small lakes exhibit much more interannual variation in ice-on/ice-off dates, and monitoring breakup over thousands of lakes spanning many orders of magnitude in size may help isolate the effects of thermal inertia in order to refine our understanding of the climate drivers of that interannual variability, their relative contributions, and how their local and regional differences may emerge into global trends. The OPEN-ICE data product can also contribute to transportation safety and economic development, and though it lacks the real-time capabilities for logistical and operational deployments, it can be used to identify areas of lakes that are consistently first or last to thaw as an indication of areas with thinner or thicker ice-cover, a crucial piece of information for winter ice road networks or access to traplines and traditional territories (Mullan et al., 2017; Prowse et al., 2009).

In its current form, OPEN-ICE has two main avenues for improvement: (i) extending the algorithm to the fall freeze-up period, and (ii) accessibility of the product for non-experts. Because freeze-up occurs when the duration of daylight decreases throughout northern latitudes, the quantity and quality of the images captured by optical sensors are lower during fall freeze-up than during spring thaw, a problem which is further compounded by more prevalent autumn cloud cover (Sudmanns et al., 2020). As a result, developing broad-scale models of freeze-up is a more difficult problem that is

more prone to poor accuracy. Since the deployment of the Sentinel-1 SAR satellite constellation (Torres et al., 2012), there has been a rapid increase in the availability of open-access high-resolution radar imagery which is particularly well suited to detecting ice conditions through clouds or in the darkness of night. This thesis would be incomplete without a brief mention of the trials and tribulations I experienced trying to classify Sentinel-1 imagery to integrate them into OPEN-ICE, efforts which I eventually abandoned. While water and ice have distinct backscatter signatures in radar imagery, during periods of transition between both states it can be quite challenging to discern them (Geldsetzer et al., 2010). Researchers have demonstrated how Otsu thresholding (Otsu, 1979) can be applied to Sentinel-1 imagery to accurately detect ice phenology events like freeze-up in High Arctic lakes (Murfitt and Duguay, 2020). This methodology requires building large frequency histograms of backscatter signatures in groups of pixels over a region or through time. This is a powerful approach, but one that remains difficult to adapt to broad-scale automated analyses due to memory limitations even on cloud-computing platforms like Google Earth Engine. While easily scalable threshold-based methods do exist for Sentinel 1 imagery, they are much less accurate. For example, the Copernicus Land Monitoring Service's ARLIE data product has integrated Sentinel-1 ice classification in its current offering, but the designers of the underlying algorithm report it only achieves 76.7% accuracy (CLMS, 2023). While freeze-up remains unavailable within the OPEN-ICE data product, its algorithm is modular to facilitate future integrations of other sources of ice-water classifications such as Sentinel-1 imagery. The code base for the OPEN-ICE algorithm is open-source and freely accessible through GitHub, but the data product itself remains difficult to share

with non-experts because: (i) it is stored in 10 gigabyte rasters (one raster per spring), (ii) it requires GIS software with a powerful computer or a Google Earth Engine (GEE) account to visualize, and (iii) it does not provide lake-based or local regional statistics without further processing. While it is possible to build web-apps on the GEE platform and deploy some simple tools that would allow users to analyze or extract information from lakes of interest, it does require some investment to cover the fees of hosting large datasets. Such a platform could contribute valuable resources for citizen science projects like IceWatch (naturewatch.ca/icewatch/) and Fresh Eyes on Ice (fresheyesonice.org), helping drive engagement and integrate local and global scales of observations.

5.3 The spatio-temporal dynamics of caribou spring migration in a warming Arctic

This thesis provides significant insights into the migratory behaviour of female caribou, specifically their avoidance or selection of paths in response to the size of waterbodies and the phenological conditions of ice in the thousands of lakes they encounter on their journey to calving grounds in spring. Because the timing of calving is so crucial to calf survival (Vuillaume et al., 2023), a better understanding of the factors that can facilitate or impede the arrival of females to the calving ground informs understanding of caribou adaptability to the increased variability of conditions in a rapidly warming Arctic. While emerging research has highlighted the roles of snow and lake ice conditions during migration (Gurarie et al., 2019; Joly et al., 2021; Le Corre et al., 2016; Leblond et al., 2016), only the presence or absence of ice has been considered, usually in exceptionally large lakes over the landscape due to limitations in

resolution. Using the OPEN-ICE high-resolution ice phenology product, I was able to discern the phenological states of lakes to study how caribou not only respond to ice and water, but how they respond to the transition between them, breaking ice, in both small and large lakes in the landscape. I found that migrating females select migration paths through areas of the landscape dominated by smaller ice-covered lakes and typically avoid exposed crossings over large ice-covered lakes (see Fig. 3.4). While females avoided areas with open water, they exhibited stronger avoidance of areas with breaking ice, especially in larger lakes (see Fig. 3.4).

The research in this thesis has also demonstrated that the cues for the initiation of migration by caribou are decoupled from spring ice phenology, which indicates that migrating females will encounter breakup conditions more frequently as the Arctic continues to warm. Recent broad-scale investigations of the timing of spring migration suggests that females can adapt the timing of their migration to spring snow conditions in anticipation of snowmelt and spring green-up at their calving grounds (Couriot et al., 2023; Gurarie et al., 2019; Laforge et al., 2021; Mallory et al., 2020). However, the thermal inertia of lakes and the additional heat stored during longer ice-free seasons has resulted in a more rapid advance of break-up relative to snowmelt (Dauginis and Brown, 2021), indicating that migrating females will encounter breaking ice more frequently even as they advance the timing of their migration to earlier spring snowmelt and green-up. While breakup conditions were still relatively uncommon during the study period, observed migratory paths that encountered breaking ice more frequently incurred important delays (see Fig. 3.5). Given that the migration routes of many migratory caribou herds traverse some of the most lake-rich landscapes on Earth, these

findings have profound implications for the future of caribou migrations. As breaking ice is encountered more frequently in the coming years, it is likely that caribou will rely more heavily on water-free corridors and land bridges during migration. Protecting these movement corridors from industrial development or human disturbance will become essential to conserve landscape connectivity and mitigate further disruptions to migration. Spring snow conditions are and will continue to be a highly important determinant of not only the timing, but also the duration of spring migration (Gurarie et al., 2019). Indeed, while we understand that snow depth increases the energetic costs of caribou movement (Fancy and White, 1987), we currently lack adequately detailed remote sensing products to investigate snowscapes (Boelman et al., 2019) and their broader impact on females, the energetic costs of their migration, and the inter-annual variability of their arrival to the calving ground. While these constitute important research priorities, identifying and protecting spring migratory corridors from human disturbance through herd range planning is not only crucial but, save slowing the pace of climate change, it is perhaps the only measure that is entirely within our power.

5.4 Estimating short-term effects on behaviour and survival in single-capture studies

This research has contributed to our understanding of the short-term impacts of capture and collaring events on the movement rates and survival of barren-ground caribou and, more broadly, has described statistical strategies that enable researchers to estimate capture effects in caribou and other species using data that can be collected within the constraints of single-capture study designs (e.g., GPS location data, handling

times, individual stress indicators). Estimating the effects of capture on movement behaviour generally requires prior knowledge of an individual's baseline behaviour as a unit of comparison. However, directly observing behaviour prior to a capture or conducting recaptures to compare behaviour before and after a capture (e.g., Stabach et al., 2020) is unfeasible in many regions, especially those as large and remote as the ranges of migratory caribou. Instead, researchers can compare a recently captured individual's behaviour with baselines established by previously collared individuals that are presumably habituated (Dechen Quinn et al., 2014). In this thesis, I describe a strategy based on Hierarchical Generalized Additive Models (HGAM) that allows researchers to estimate both the magnitude and duration of differences in post-capture behaviour while controlling for important sources of variability such as the capture period and the seasonal, inter-annual, and inter-individual fluctuations in movement behaviour across herds. By controlling for herd, sex, year, and day of year, I found that both male and female caribou exhibited different movement rates relative to population baselines for approximately 3 to 4 days after capture (see Fig. 4.2E & F). But, contrary to our initial expectations, the direction of that divergence differed between sexes. Specifically, relative to the movement rates of their previously captured counterparts, females moved less while males moved more following captures, a difference which we speculate may relate to females experiencing higher energetic costs due to pregnancy requiring them to reduce rather than increase movement following a stressful, energy-demanding event. Indeed, captures were predominantly conducted in late winter, a food-limited season that immediately precedes an urgent and expensive long-distance migration.

In this thesis, I demonstrated how survival analysis models can be used to evaluate relative risks of capture myopathy and identify associated risk factors to help improve capture methodologies. Capture myopathy is more common in ungulates relative to other mammals and can occur within hours and up to 30 days after capture (Breed et al., 2019; Paterson, 2014; Spraker, 1993). In the absence of visual monitoring of potential symptoms after release or confirmation by a necropsy of muscle tissue, it is often impossible to diagnose capture myopathy in remote areas where it is often conflated with predation even if inspection of a carcass is possible (Beringer et al., 1996; Flueck et al., 2005). As a result, unless a mortality occurs during capture and handling, it can be extremely difficult to include post-release survival outcomes in the evaluation of the short-term impacts of capture methodologies. However, using post-capture movement and survival data from GPS-collars, we can flag suspected cases of capture myopathy (Dechen Quinn et al., 2012) and use survival analysis to estimate if characteristics of a particular capture event (e.g., handling time) or an individual response to capture (e.g., combativeness, stress) correlates with survival outcomes. In our study, we used this approach to analyze the survival outcomes of females in the 30-day post-capture period and found that, while mortality was extremely low, the total duration of the capture event (i.e., helicopter chase and handling time) and individual-specific indicators of the relative intensity of current stress response (i.e., cortisol) and pre-existing muscle stress response (i.e., aspartate aminotransferase) were predictive of suspected cases of capture myopathy. Indeed, the concentration of stress indicators in blood samples collected from individuals prior to release can provide a powerful tool to evaluate capture-related or baseline stress (Cattet et al., 2008; Kock et al., 1987;

Morton et al., 1995; Trondrud et al., 2022) and, to our knowledge, our study provides the first evidence linking these stress indicators to post-capture survival outcomes in caribou or reindeer.

6. Conclusion

The future of migratory caribou is uncertain, but the emergence of new big data applications and their importance to the future of wildlife science and conservation seems clear. Combining Earth observations and biologging information is full of promise and challenges, and this thesis has attempted to navigate both to advance knowledge regarding lake ice phenology and caribou movement ecology. Future work can refine and extend the big data and movement analysis approaches described here to remaining knowledge gap, which include the fall freeze-up, winter and spring snow conditions, and the applicability of these findings to other migratory caribou herds. Regardless of the potential conservation value of biologging research, we must continuously strive to reduce the impacts of biologging methods on the well-being of wildlife and be wary of the potential for stress-related biases in observations. This thesis has helped describe statistical strategies to evaluate these potential impacts. Future work should focus on the development of less invasive technologies that require little to no handling. While biologging and telemetry will likely remain important contributors to many wildlife monitoring programs, researchers must carefully consider their impacts, their associated research questions, and their potential for real and actionable conservation outcomes.

7. Supplementary materials

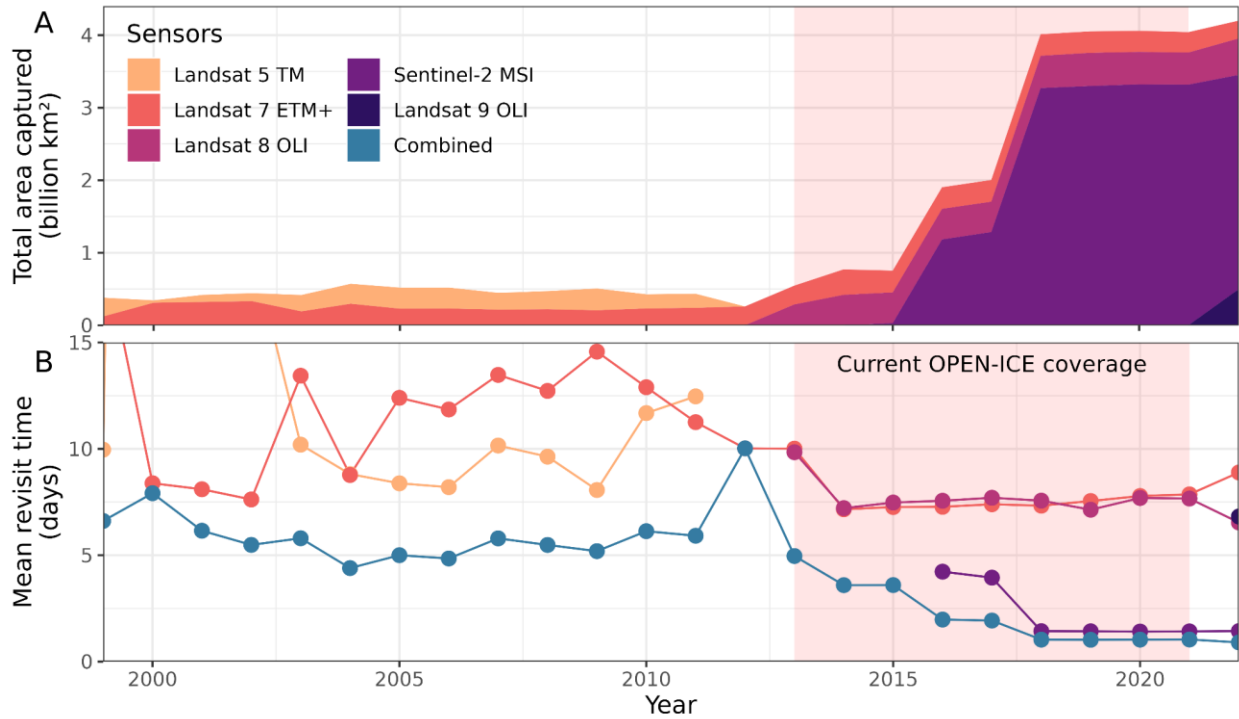
7.1 Supplementary materials for Chapter 2

Supplementary Table 2.1 Names, HydroLAKES IDs, surface area, and centroid geographical coordinates of the 24 lakes from which spectral data was randomly sampled from scenes captured by Landsat 7, Landsat 8, and Sentinel-2.

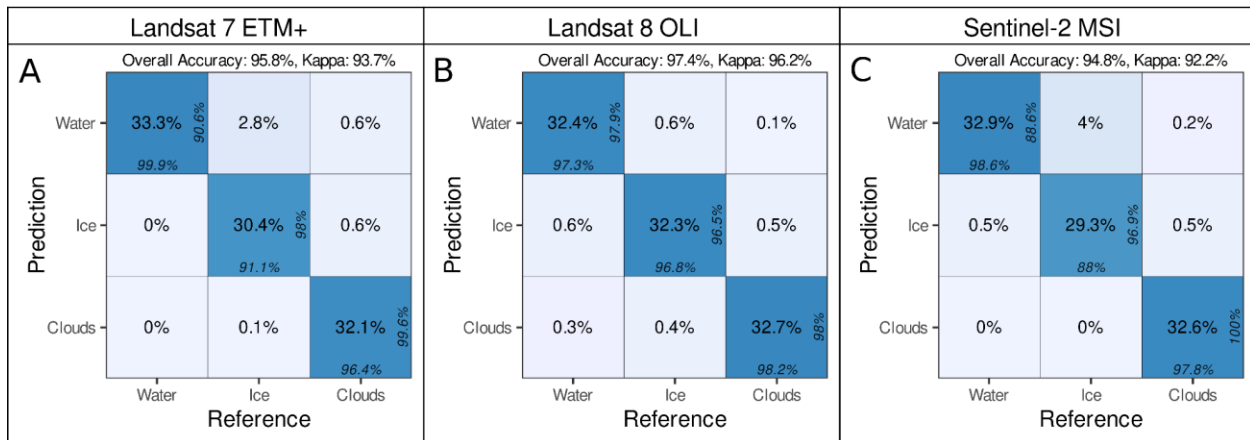
Lake Name	ID	Surface Area (km ²)	Latitude	Longitude
Napaktulik Lake	21	1031.69	66.304	-113.089
Baker Lake	25	1664.70	64.162	-95.281
Dubawnt Lake	26	3583.21	63.111	-101.403
Lake Claire	34	1332.93	58.584	-112.089
Cedar Lake	51	2504.26	53.327	-100.134
Manicouagan Reservoir	55	1795.64	51.389	-68.648
Lake Nipigon	58	4505.95	49.822	-88.515
Red Lake Reservoir	61	1141.61	48.032	-94.916
Bluenose Lake	218	425.67	68.454	-119.717
MacAlpine Lake	234	392.01	66.558	-102.748
Nose Lake	255	155.19	65.411	-108.923
Artillery Lake	327	516.24	63.177	-107.867
Buffalo Lake	397	553.24	60.228	-115.446
Payne Lake	423	487.93	59.435	-74.103
Black Lake	425	443.84	59.183	-105.296
Peter Pond Lake	498	827.51	55.948	-108.817
Molson Lake	565	394.73	54.215	-96.815
La Grande 4 Reservoir	585	805.72	53.956	-73.266
Big Trout Lake	587	644.10	53.760	-89.993
Missisa Lake	622	182.80	52.312	-85.197
Trout Lake	646	347.42	51.204	-93.303
Kesagami Lake	665	175.21	50.347	-80.243
Lake Abitibi	707	946.77	48.750	-79.800
Duncan Lake	3890	69.27	62.872	-113.961

Supplementary Table 2.2 Currently available large-scale data products used for monitoring sea ice, snow cover, and lake ice.

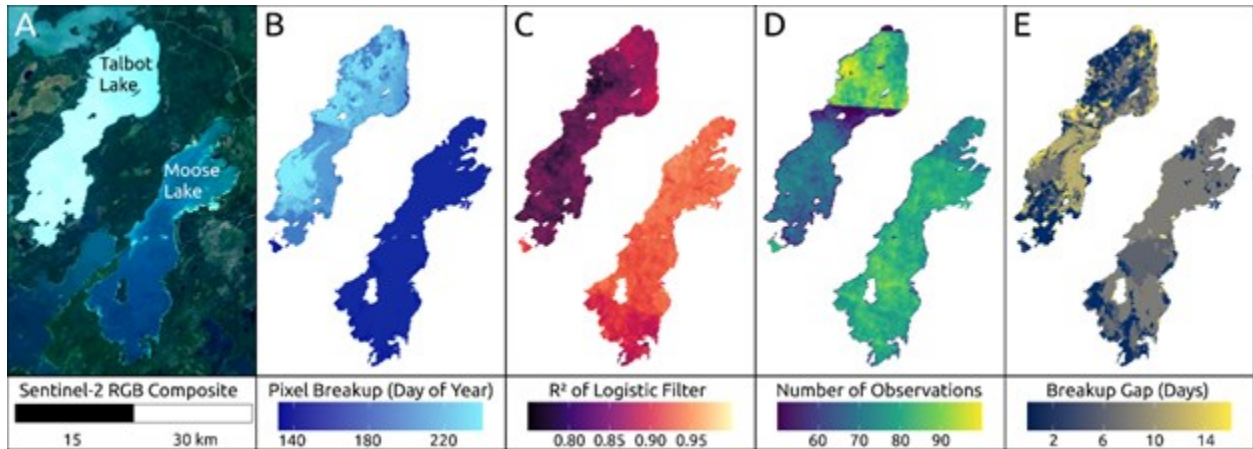
Data product	Sensor(s)	Spatial resolution	Revisit time	Method	Area covered	Years covered
IMS Daily Northern Hemisphere Snow and Ice Analysis (USNIC, 2008)	AMSU-A, ATMS, AVHRR, GOES I-M IMAGER, MODIS, MTSAT 1R Imager, MTSAT 2 Imager, MVIRI, SAR, SEVIRI, SSM/I, SSMIS, VIIRS	1 kilometre	1 day	Analyst-informed interactive decision tree	Northern Hemisphere	1997 - present
MODIS Snow/Ice Products (Hall et al., 2023)	MODIS Terra/Aqua	250/500 metre	1 day	Threshold-based classification	Global coverage	2000 - present
Copernicus Global Land Service Lake Ice Extent (LIE-NH; CGLS, 2023)	Sentinel-3 SLSTR	500 metre	1 day	Gaussian mixture model	Northern Hemisphere (~13,000 lakes)	2021 - present
ESA Lakes Climate Change Initiative data product (Lakes_cci; Crétaux et al., 2021)	MODIS Terra/Aqua	250/500 metre	2 days	Threshold-based retrieval algorithm	Global (~2,000 lakes)	2000 - 2020
Aggregated River and Lake Ice Extent (ARLIE; CLMS, 2023a)	Sentinel-1 SAR, Sentinel-2 MSI+	20 metre	2 days	Threshold-based classification	Europe freshwater	2015 - present



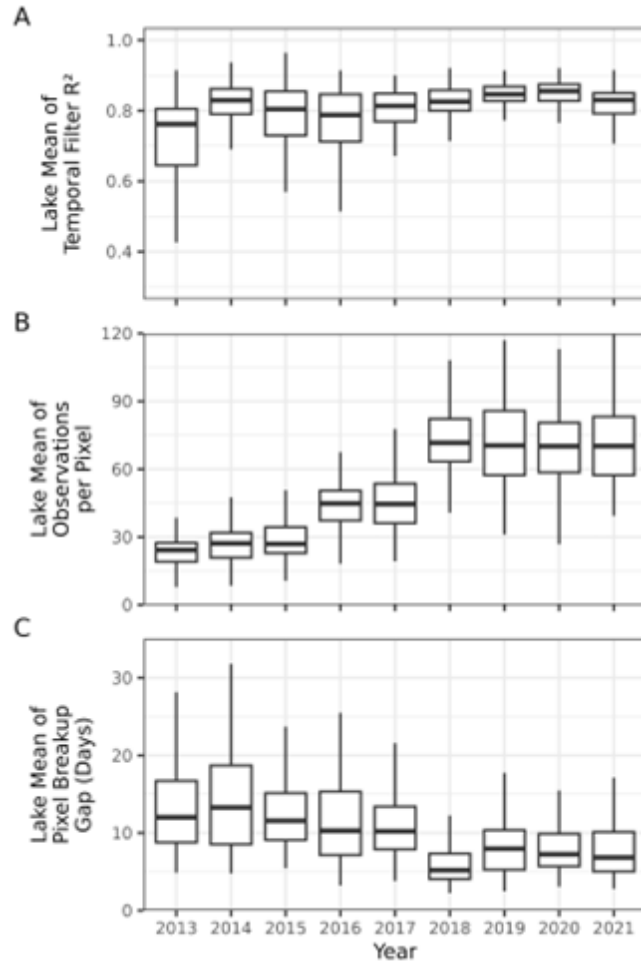
Supplementary Figure 2.1 Individual and combined coverage of top-of-atmosphere reflectance image collections captured by open-access high-resolution optical sensors over Canada between 1999 and 2022. Coverage is illustrated by (A) the total area of all scenes captured by each sensor and (B) the mean revisit time of each sensor over 10,000 randomly selected water pixels across Canada. Coverage was assessed annually specifically within the window used by OPEN-ICE to estimate spring breakup (February 15th to September 30th). The area of the timeline highlighted in red corresponds to the period currently covered by the OPEN-ICE data product. Coverage was assessed using Collection 2 Tier 1 images for Landsat sensors and Level 1-C for Sentinel-2.



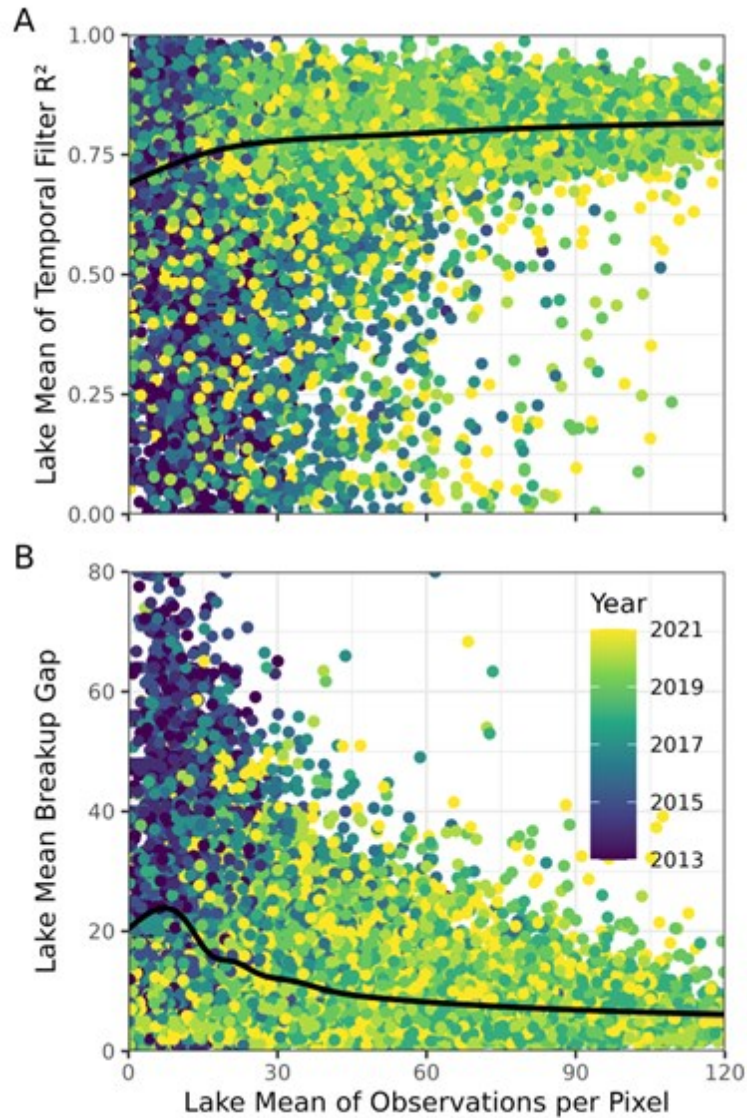
Supplementary Figure 2.2 Individual and combined coverage of top-of-atmosphere reflectance image collections captured by open-access high-resolution optical sensors over Canada between 1999 and 2022. Coverage is illustrated by (A) the total area of all scenes captured by each sensor and (B) the mean revisit time of each sensor over 10,000 randomly selected water pixels across Canada. Coverage was assessed annually specifically within the window used by OPEN-ICE to estimate spring breakup (February 15th to September 30th). The area of the timeline highlighted in red corresponds to the period currently covered by the OPEN-ICE data product. Coverage was assessed using Collection 2 Tier 1 images for Landsat sensors and Level 1-C for Sentinel-2.



Supplementary Figure 2.3 Maps illustrating a (A) Sentinel-2 RGB composite of two lakes alongside the four layers provided by the OPEN-ICE data product for the year 2020. For each pixel, OPEN-ICE provides (B) the breakup date (day of year), (C) the R^2 of the logistic temporal filter (see Fig. 2.2E), (D) the total number of observations used to detect the breakup sequence, and (E) the breakup gap (in days) between the last observed ice and the first observed water (see Fig. 2.2F). Talbot Lake (54.02° N, 99.92° W) was chosen to illustrate a case of extreme turbidity where OPEN-ICE performs poorly. In this case, OPEN-ICE quality metrics indicate that the logistic filter's R^2 is low, that the number of observations is low, and that the breakup gaps are large relative to the neighbouring Moose Lake (53.91° N, 99.76° W).



Supplementary Figure 2.4 Distribution of per lake means of pixel quality metrics associated with OPEN-ICE breakup estimates between 2013 and 2021. For each of the 105 lakes monitored by the Canadian Ice Service (see Fig. 2.1), per lake means were computed for (A) the R^2 of the logistic temporal filter (see Fig. 2.2E), (B) the total number of observations used to detect the breakup sequence (between February 15th and September 30th), and (C) the breakup gap (in days) between the last observed ice and the first observed water (see Fig. 2.2F).



Supplementary Figure 2.5 Trends of OPEN-ICE quality metrics extracted from 4000 random lakes annually between 2013 and 2021. Per lake means were computed for (A) the R^2 of the logistic temporal filter (see Fig. 2.2E) and (B) the breakup gap (in days) between the last observed ice and the first observed water (see Fig. 2.2F). These two metrics are presented as a function of the mean lake observations per pixel to assess their trends as the data density of time series increases. The presented trends are fit using a generalized additive model.

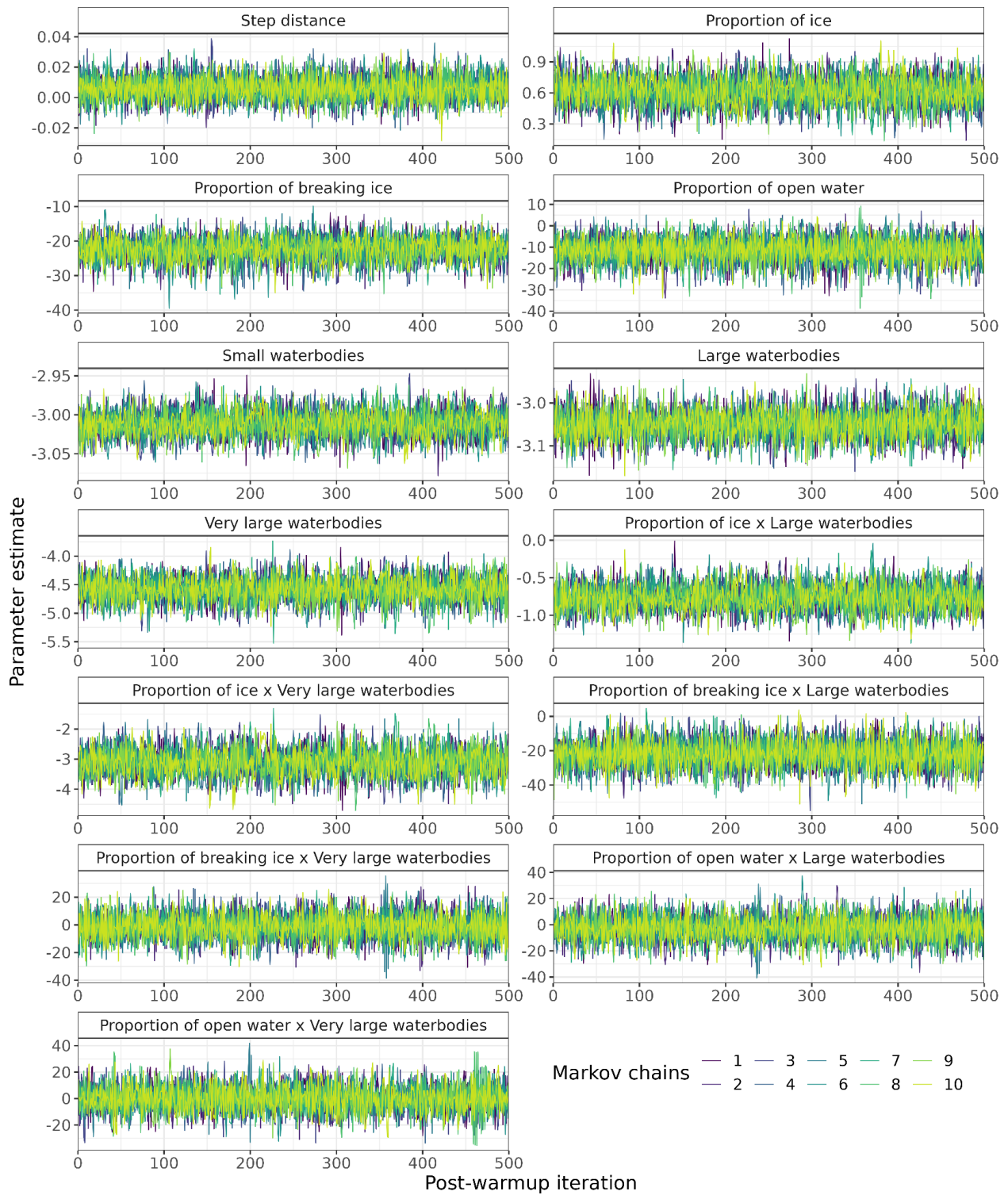
7.2 Supplementary materials for Chapter 3

Supplementary Table 3.1 Model comparison metrics for the three candidate path selection models. The environmental covariates of interest for each model are indicated along with their relative support by the data as estimated by the widely-applicable information criterion (WAIC \pm standard error), the corresponding expected log predictive densities (ELPD \pm standard error), and the differences in ELPD (Δ ELPD \pm standard error) relative to the best model.

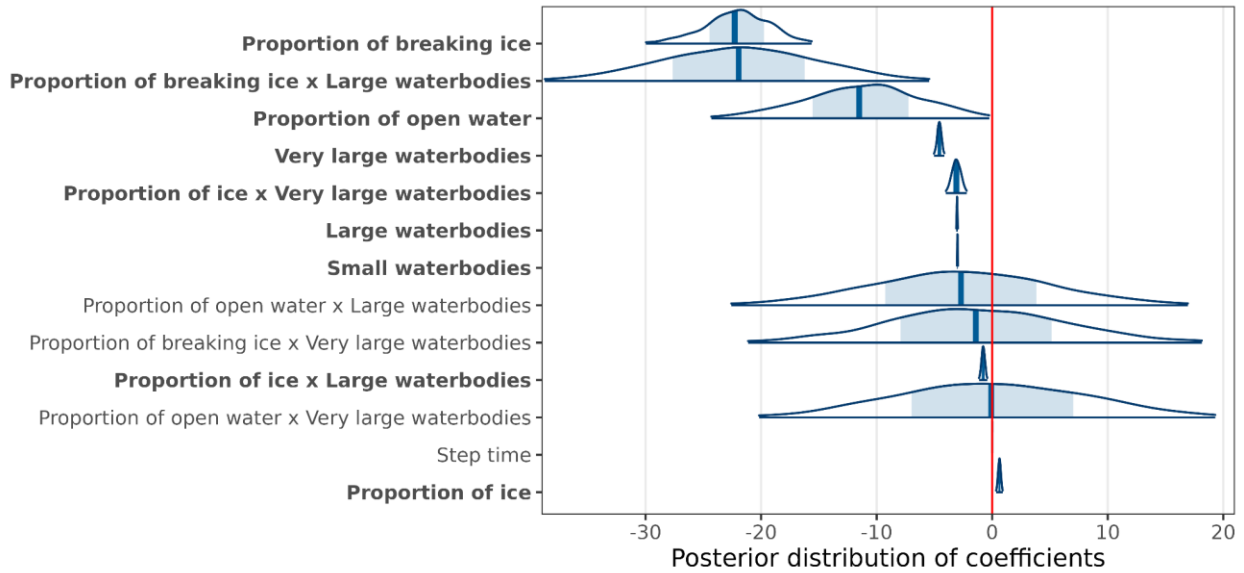
Model	Environmental covariates	WAIC (\pm SE)	ELPD (\pm SE)	Δ ELPD (\pm SE)
3	Mean lake size (Small, Large, Very Large) Proportion of ice x Mean lake size Proportion of breaking ice x Mean lake size Proportion of open water x Mean lake size	157,395.7 (814.7)	-78,697.8 (407.3)	0 (0)
2	Proportion of ice Proportion of breaking ice Proportion of open water	194,741.0 (979.1)	-97,370.5 (489.6)	-18,672.7 (113.1)
1	Proportion of hydrological features	195,181.4 (982.2)	-97,590.7 (491.1)	-18,892.9 (114.0)

x Denotes interactions between variables

Bold typeface indicates the model and associated variables with the most support.

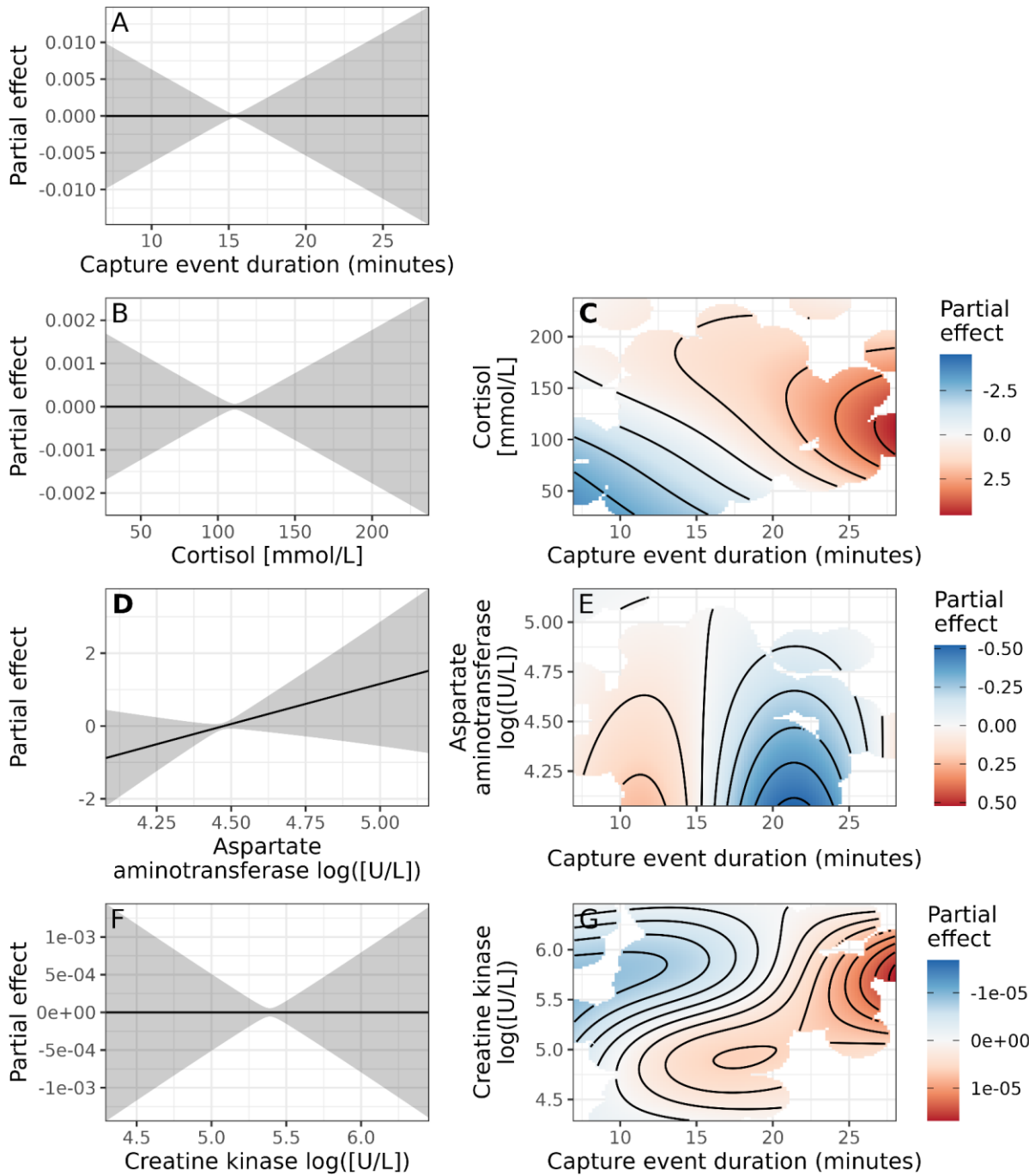


Supplementary Figure 3.1 Bayesian estimate trace plots depicting the estimated values of each population-level parameter included in model 3 (most supported model) sampled over 500 post-warmup iterations in each of the 10 Markov chains.



Supplementary Figure 3.2 Distribution of posterior estimates for each coefficient in the path selection model with the most support, where step time was included to reduce bias associated to sampling frequency. The vertical band illustrates each distribution's median value along with a shaded area representing 50% of the posterior distribution. The distributions are truncated at 95% and bold typeface indicates covariates and interactions that do not overlap with zero, illustrated in red. Interactions between terms are denoted by "x".

7.3 Supplementary materials for Chapter 4



Supplementary Figure 4.1 Partial effects of stress-related covariates on the log-hazards function of a Cox proportional hazards model. Panel lettering in bold typeface indicates terms with significant (C) and marginally significant (D) contributions to the survival model (see Table 4.3 and Fig. 4.4).

8. Literature cited

- Adamczewski, J.Z., Boulanger, J., Williams, J., Cluff, H.D., Clark, K., Nishi, J.S., Goodman, S., Chan, K., Abernethy, R., 2022. Estimates of breeding females and adult herd size and analyses of demographics for the Bathurst herd of barren-ground caribou: 2021 calving ground photographic survey (No. 326). Government of the Northwest Territories, Yellowknife, Northwest Territories, Canada.
- Adamczewski, J., Gunn, A., Poole, K.G., Hall, A., Nishi, J., Boulanger, J., 2015. What happened to the Beverly caribou herd after 1994? *Arctic* 68, 407. <https://doi.org/10.14430/arctic4523>
- Adrian, R., O'Reilly, C.M., Zagarese, H., Baines, S.B., Hessen, D.O., Keller, W., Livingstone, D.M., Sommaruga, R., Straile, D., Van Donk, E., Weyhenmeyer, G.A., Winder, M., 2009. Lakes as sentinels of climate change. *Limnol. Oceanogr.* 54, 2283–2297. https://doi.org/10.4319/lo.2009.54.6_part_2.2283
- Adrian, R., Wilhelm, S., Gerten, D., 2006. Life-history traits of lake plankton species may govern their phenological response to climate warming. *Glob. Change Biol.* 12, 652–661. <https://doi.org/10.1111/j.1365-2486.2006.01125.x>
- Albon, S.D., Irvine, R.J., Halvorsen, O., Langvatn, R., Loe, L.E., Ropstad, E., Veiberg, V., Van Der Wal, R., Bjørkvoll, E.M., Duff, E.I., Hansen, B.B., Lee, A.M., Tveraa, T., Stien, A., 2017. Contrasting effects of summer and winter warming on body mass explain population dynamics in a food-limited Arctic herbivore. *Glob. Change Biol.* 23, 1374–1389. <https://doi.org/10.1111/gcb.13435>
- Alerstam, T., Hedenstrom, A., Akesson, S., 2003. Long-distance migration: Evolution and determinants. *Oikos* 103, 247–260. <https://doi.org/10.1034/j.1600-0706.2003.12559.x>
- Arnemo, J.M., Ahlqvist, P., Andersen, R., Berntsen, F., Ericsson, G., Odden, J., Brunberg, S., Segerström, P., Swenson, J.E., 2006. Risk of capture-related mortality in large free-ranging mammals: Experiences from Scandinavia. *Wildl. Biol.* 12, 109–113. [https://doi.org/10.2981/0909-6396\(2006\)12\[109:ROCMIL\]2.0.CO;2](https://doi.org/10.2981/0909-6396(2006)12[109:ROCMIL]2.0.CO;2)
- Arnold, W., Ruf, T., Loe, L.E., Irvine, R.J., Ropstad, E., Veiberg, V., Albon, S.D., 2018. Circadian rhythmicity persists through the Polar night and midnight sun in Svalbard reindeer. *Sci. Rep.* 8, 14466. <https://doi.org/10.1038/s41598-018-32778-4>
- Banfield, A.W.F., 1961. A revision of the reindeer and caribou, genus *Rangifer*, Bulletin of the National Museum of Canada. Department of Northern Affairs and National Resources, Ottawa, Canada.
- Béland, S., Vuillaume, B., Leclerc, M., Bernier, M., Côté, S.D., 2023. Selection of summer feeding sites and food resources by female migratory caribou (*Rangifer tarandus*) determined using camera collars. *PLoS ONE* 18, e0294846. <https://doi.org/10.1371/journal.pone.0294846>
- Bergerud, A.T., 1996. Evolving perspectives on caribou population dynamics, have we got it right yet? *Rangifer* 16, 96–116. <https://doi.org/10.7557/2.16.4.1225>

- Bergerud, A.T., Luttich, S.N., Camps, L., 2008. The return of caribou to Ungava. McGill-Queen's University Press, Montreal, Canada.
- Beringer, J., Hansen, L.P., Wilding, W., Fischer, J., Sheriff, S.L., 1996. Factors affecting capture myopathy in white-tailed deer. *J. Wildl. Manag.* 60, 373–380.
- Boelman, N.T., Liston, G.E., Gurarie, E., Meddens, A.J.H., Mahoney, P.J., Kirchner, P.B., Bohrer, G., Brinkman, T.J., Cosgrove, C.L., Eitel, J.U.H., Hebblewhite, M., Kimball, J.S., LaPoint, S., Nolin, A.W., Pedersen, S.H., Prugh, L.R., Reinking, A.K., Vierling, L.A., 2019. Integrating snow science and wildlife ecology in Arctic-boreal North America. *Environ. Res. Lett.* 14, 010401. <https://doi.org/10.1088/1748-9326/aaec1>
- Bongelli, E., Orman, L., Adamczewski, J., Campbell, M., Cluff, H.D., Guile, A., Pellissey, J., Qaqqutaq, E., Ray, J., Russell, D., Schmelzer, I., Suitor, M., Taillon, J., 2022. Caribou – Heartbeat of the tundra. Polar Knowledge: Aqhaliat Report, Volume 4. Polar Knowledge Canada.
- Borquet, G., 2020. Effects of GPS-collars on Svalbard reindeer survival and body condition (MSc Thesis). Inland Norway University of Applied Sciences, Innlandet, Norway.
- Boulanger, J., Adamczewski, J., Williams, J., Cluff, D., Clark, K., Goodman, S., Chan, K., Abernethy, R., 2022. Estimates of breeding females & adult herd size and analyses of demographics for the Bluenose-East herd of barren-ground caribou: 2021 calving ground photographic survey (No. 325). Environment and Natural Resources, Government of the Northwest Territories, Yellowknife, Canada.
- Boulanger, J., Kite, R., Campbell, M., Shaw, J., Lee, D.S., 2020. Kivalliq caribou monitoring program - analysis of caribou movements relative to Meadowbank mine and roads during spring migration, Technical Report Series. Government of Nunavut Department of Environment, Iqaluit, Nunavut, Canada.
- Boulanger, J., Poole, K.G., Gunn, A., Adamczewski, J., Wierzchowski, J., 2021. Estimation of trends in zone of influence of mine sites on barren-ground caribou populations in the Northwest Territories, Canada, using new methods. *Wildl. Biol.* 2021. <https://doi.org/10.2981/wlb.00719>
- Bourgeon, L., Burke, A., Higham, T., 2017. Earliest human presence in North America dated to the last glacial maximum: New radiocarbon dates from Bluefish Caves, Canada. *PLoS ONE* 12, e0169486. <https://doi.org/10.1371/journal.pone.0169486>
- Breed, D., Meyer, L.C.R., Steyl, J.C.A., Goddard, A., Burroughs, R., Kohn, T.A., 2019. Conserving wildlife in a changing world: Understanding capture myopathy—a malignant outcome of stress during capture and translocation. *Conserv. Physiol.* 7, coz027. <https://doi.org/10.1093/conphys/coz027>
- Brodeur, V., Rivard, S., Taillon, J., 2021. Inventaire aérien du troupeau de caribous migrants de la rivière George en juillet 2020. Ministère des Forêts, de la Faune et des Parcs & Department of Fisheries, Forestry, and Agriculture, Québec, Canada.
- Brooks, C., Bonyongo, C., Harris, S., 2008. Effects of global positioning system collar weight on zebra behavior and location error. *J. Wildl. Manag.* 72, 527–534. <https://doi.org/10.2193/2007-061>

- Brown, D.D., Kays, R., Wikelski, M., Wilson, R., Klimley, A., 2013. Observing the unwatchable through acceleration logging of animal behavior. *Anim. Biotelemetry* 1, 20. <https://doi.org/10.1186/2050-3385-1-20>
- Bryant, J.P., Joly, K., Chapin, F.S., DeAngelis, D.L., Kielland, K., 2014. Can antibrowsing defense regulate the spread of woody vegetation in arctic tundra? *Ecography* 37, 204–211. <https://doi.org/10.1111/j.1600-0587.2013.00436.x>
- Cael, B.B., Seekell, D.A., 2016. The size-distribution of Earth's lakes. *Sci. Rep.* 6, 29633. <https://doi.org/10.1038/srep29633>
- Campeau, A.B., Rickbeil, G.J.M., Coops, N.C., Côté, S.D., 2019. Long-term changes in the primary productivity of migratory caribou (*Rangifer tarandus*) calving grounds and summer pasture on the Quebec-Labrador Peninsula (Northeastern Canada): The mixed influences of climate change and caribou herbivory. *Polar Biol.* 42, 1005–1023. <https://doi.org/10.1007/s00300-019-02492-6>
- Case, R., Buckland, L., Williams, M., 1996. The status and management of the Bathurst caribou herd, Northwest Territories, Canada (No. 116). Department of Renewable Resources, Government of the Northwest Territories, Yellowknife, Canada.
- Cattet, M., 2018. Capture, handling and release of caribou standard operating procedure. Wildlife Care Committee, Government of the Northwest Territories, Yellowknife, Canada.
- Cattet, M., 2011. Standard operating procedure for the capture, handling & release of caribou. Wildlife Care Committee, Government of the Northwest Territories, Yellowknife, Canada.
- Cattet, M., Boulanger, J., Stenhouse, G., Powell, R.A., Reynolds-Hogland, M.J., 2008. An evaluation of long-term capture effects in ursids: Implications for wildlife welfare and research. *J. Mammal.* 89, 973–990. <https://doi.org/10.1644/08-MAMM-A-095.1>
- Chi, M., Plaza, A., Benediktsson, J.A., Sun, Z., Shen, J., Zhu, Y., 2016. Big data for remote sensing: Challenges and opportunities. *Proc. IEEE* 104, 2207–2219. <https://doi.org/10.1109/JPROC.2016.2598228>
- Chisana Caribou Recovery Team, 2010. Recovery of the Chisana caribou herd in the Alaska/Yukon borderlands: Captive-rearing trials (No. TR-10-02). Yukon Department of Environment Fish and Wildlife Branch, Whitehorse, Canada.
- Compton, B.B., Zager, P., Servheen, G., 1995. Survival and mortality of translocated woodland caribou. *Wildl. Soc. Bull.* 23, 490–496.
- Copernicus Global Land Service, 2023. Lake Ice Extent - Northern Hemisphere (LIE-NH): 500 metre version 1 product.
- Copernicus Land Monitoring Service, 2023a. Pan-European high-resolution snow & ice monitoring of the Copernicus Land Monitoring Service: Quality assessment report for ice products based on Sentinel-1 and Sentinel-2.
- Copernicus Land Monitoring Service, 2023b. Pan-European high-resolution snow & ice monitoring of the Copernicus Land Monitoring Service.
- COSEWIC, 2016. COSEWIC assessment and status report on the Caribou *Rangifer tarandus*, Barren-ground population, in Canada. Committee on the Status of Endangered Wildlife in Canada, Ottawa, Canada.
- COSEWIC, 2011. Designatable units for caribou (*Rangifer tarandus*) in Canada. Committee on the Status of Endangered Wildlife in Canada, Ottawa, Canada.

- COSEWIC, 2002. COSEWIC assessment and update status report on the woodland caribou *Rangifer tarandus caribou* in Canada. Committee on the Status of Endangered Wildlife in Canada, Ottawa, Canada.
- Couriot, O.H., Cameron, M.D., Joly, K., Adamczewski, J., Campbell, M.W., Davison, T., Gunn, A., Kelly, A.P., Leblond, M., Williams, J., Fagan, W.F., Brose, A., Gurarie, E., 2023. Continental synchrony and local responses: Climatic effects on spatiotemporal patterns of calving in a social ungulate. *Ecosphere* 14, e4399. <https://doi.org/10.1002/ecs2.4399>
- Couturier, S., Courtois, R., Crépeau, H., Rivest, L.-P., Luttich, S., 1996. Calving photocensus of the Rivière George caribou herd and comparison with an independent census. *Rangifer* 16, 283. <https://doi.org/10.7557/2.16.4.1268>
- Créteaux, J.-F., Merchant, C.J., Duguay, C., Simis, S., Calmettes, B., Bergé-Nguyen, M., Wu, Y., Zhang, D., Carrea, L., Liu, X., Selmes, N., Warren, M., 2021. ESA Lakes Climate Change Initiative (Lakes_cci): Lake products, version 1.1. <https://doi.org/10.5285/EF1627F523764EAE8BBB6B81BF1F7A0A>
- Dalziel, B.D., Corre, M.L., Côté, S.D., Ellner, S.P., 2016. Detecting collective behaviour in animal relocation data, with application to migrating caribou. *Methods Ecol. Evol.* 7, 30–41. <https://doi.org/10.1111/2041-210X.12437>
- Dau, J., 1997. Western Arctic caribou herd - Units 21D, 22A, 22B, 23, 24, and 26A, Caribou. Federal aid in wildlife restoration management report of survey-inventory activities 1 July 1994-30 June 1996. Alaska Department of Fish and Game, Juneau, United States.
- Dauginis, A.A., Brown, L.C., 2021. Recent changes in pan-Arctic sea ice, lake ice, and snow-on/off timing. *The Cryosphere* 15, 4781–4805. <https://doi.org/10.5194/tc-15-4781-2021>
- Davis, J.L., Valkenburg, P., 1979. Natural mortality of Western Arctic caribou, Federal aid in wildlife restoration. State of Alaska, Department of Fish and Game, Division of Game, Juneau, United States.
- Dearborn, K.D., Danby, R.K., 2022. Remotely sensed trends in vegetation productivity and phenology during population decline of the Bathurst caribou (*Rangifer tarandus groenlandicus*) herd. *Arct. Sci.* 8, 228–251. <https://doi.org/10.1139/as-2021-0003>
- Dechen Quinn, A.C., Williams, D.M., Porter, W.F., 2012. Postcapture movement rates can inform data-censoring protocols for GPS-collared animals. *J. Mammal.* 93, 456–463. <https://doi.org/10.1644/10-MAMM-A-422.1>
- Dechen Quinn, A.C., Williams, D.M., Porter, W.F., Fitzgerald, S.D., Hynes, K., 2014. Effects of capture-related injury on postcapture movement of white-tailed deer. *J. Wildl. Dis.* 50, 250–258. <https://doi.org/10.7589/2012-07-174>
- Descals, A., Verger, A., Yin, G., Peñuelas, J., 2020. Improved estimates of Arctic land surface phenology using Sentinel-2 time series. *Remote Sens.* 12, 3738. <https://doi.org/10.3390/rs12223738>
- Doiron, M., Legagneux, P., Gauthier, G., Lévesque, E., 2013. Broad-scale satellite Normalized Difference Vegetation Index data predict plant biomass and peak date of nitrogen concentration in Arctic tundra vegetation. *Appl. Veg. Sci.* 16, 343–351. <https://doi.org/10.1111/j.1654-109X.2012.01219.x>

- Dokis-Jansen, K.L., Parlee, B.L., Łutsël K'e Dëne First Nation, Hik, D.S., Gendreau-Berthiaume, B., Macdonald, E., Stinn, C., 2021. "These trees have stories to tell": Linking Dënesǫ́łiné oral history of caribou use with trample scar frequency on black spruce roots at ʔedacho Kué. *Arctic* 74, 290–305. <https://doi.org/10.14430/arctic73160>
- Dolant, C., Langlois, A., Brucker, L., Royer, A., Roy, A., Montpetit, B., 2018. Meteorological inventory of rain-on-snow events in the Canadian Arctic Archipelago and satellite detection assessment using passive microwave data. *Phys. Geogr.* 39, 428–444. <https://doi.org/10.1080/02723646.2017.1400339>
- Downing, J.A., 2010. Emerging global role of small lakes and ponds: Little things mean a lot. *Limnetica* 29, 9–24. <https://doi.org/10.23818/limn.29.02>
- Du, J., Kimball, J.S., Duguay, C., Kim, Y., Watts, J.D., 2017. Satellite microwave assessment of Northern Hemisphere lake ice phenology from 2002 to 2015. *The Cryosphere* 11, 47–63. <https://doi.org/10.5194/tc-11-47-2017>
- Duguay, C.R., Flato, G.M., Jeffries, M.O., Ménard, P., Morris, K., Rouse, W.R., 2003. Ice-cover variability on shallow lakes at high latitudes: Model simulations and observations. *Hydrol. Process.* 17, 3465–3483. <https://doi.org/10.1002/hyp.1394>
- Eikelenboom, M., Higgins, R.C., John, C., Kerby, J., Forchhammer, M.C., Post, E., 2021. Contrasting dynamical responses of sympatric caribou and muskoxen to winter weather and earlier spring green-up in the Arctic. *Food Webs* 27, e00196. <https://doi.org/10.1016/j.fooweb.2021.e00196>
- Elton, C.S., 1924. Periodic fluctuations in the numbers of animals: Their causes and effects. *J. Exp. Biol.* 2, 119–163. <https://doi.org/10.1242/jeb.2.1.119>
- English, H.M., Börger, L., Kane, A., Ciuti, S., 2024. Advances in biologging can identify nuanced energetic costs and gains in predators. *Mov. Ecol.* 12, 7. <https://doi.org/10.1186/s40462-024-00448-y>
- ESA, 2023. SNAP - European Space Agency Sentinel Application Platform v9.0.3, <http://step.esa.int>.
- Fancy, S.G., Pank, L.F., Whitten, K.R., Regelin, W.L., 1989. Seasonal movements of caribou in arctic Alaska as determined by satellite. *Can. J. Zool.* 67, 644–650. <https://doi.org/10.1139/z89-093>
- Fancy, S.G., White, R.G., 1987. Energy expenditures for locomotion by barren-ground caribou. *Can. J. Zool.* 65, 122–128. <https://doi.org/10.1139/z87-018>
- Fancy, S.G., White, R.G., 1985. Energy expenditures by caribou while cratering in snow. *J. Wildl. Manag.* 49, 987. <https://doi.org/10.2307/3801384>
- Ferguson, M.A.D., Williamson, R.G., Messier, F., 1998. Inuit knowledge of long-term changes in a population of Arctic tundra caribou. *Arctic* 51, 201–219. <https://doi.org/10.14430/arctic1062>
- Ferguson, S.H., Elkie, P.C., 2005. Use of lake areas in winter by woodland caribou. Northeast. *Nat.* 12, 45–66. [https://doi.org/10.1656/1092-6194\(2005\)012\[0045:UOLAIW\]2.0.CO;2](https://doi.org/10.1656/1092-6194(2005)012[0045:UOLAIW]2.0.CO;2)
- Flueck, W.T., Smith-Flueck, J.A.M., Bonino, N.A., 2005. A preliminary analysis of death cause, capture-related mortality and survival of adult red deer in northwestern Patagonia. *Ecol. Austral* 15, 23–30.

- Frison, G., 1970. The Glenrock buffalo jump, 48c0304: Late prehistoric period buffalo procurement and butchering. *Plains Anthropol.* 15, 1–45.
<https://doi.org/10.1080/2052546.1970.11908592>
- Garibaldi, A., Turner, N., 2004. Cultural keystone species: Implications for ecological conservation and restoration. *Ecol. Soc.* 9, 1. <https://doi.org/10.5751/ES-00669-090301>
- Geldsetzer, T., van der Sanden, J., Brisco, B., 2010. Monitoring lake ice during spring melt using RADARSAT-2 SAR. *Can. J. Remote Sens.* 36, 391–400.
<https://doi.org/10.5589/m11-001>
- Gerhart, K.L., White, R.G., Cameron, R.D., Russell, D.E., 1996. Body composition and nutrient reserves of arctic caribou. *Can. J. Zool.* 74, 136–146.
<https://doi.org/10.1139/z96-018>
- Gorelick, N., Hancher, M., Dixon, M., Ilyushchenko, S., Thau, D., Moore, R., 2017. Google Earth Engine: Planetary-scale geospatial analysis for everyone. *Remote Sens. Environ.* 202, 18–27. <https://doi.org/10.1016/j.rse.2017.06.031>
- Government of the Northwest Territories, 2019. Bathurst caribou range plan. Environment and Natural Resources, Government of the Northwest Territories, Yellowknife, Canada.
- Gunn, A., 2016. *Rangifer tarandus*. The IUCN red list of threatened species 2016.
<https://doi.org/10.2305/IUCN.UK.2016-1.RLTS.T29742A22167140.en>
- Gunn, A., 2003. Voles, lemmings and caribou - Population cycles revisited? *Rangifer* 23, 105. <https://doi.org/10.7557/2.23.5.1689>
- Gunn, A., Johnson, C.J., Nishi, J.S., Daniel, C.J., Russell, D.E., Carlson, M., Adamczewski, J.Z., 2011a. Understanding the cumulative effects of human activities of barren-ground caribou reserved, in: Krausman, P.R., Harris, L.K. (Eds.), *Cumulative Effects in Wildlife Management : Impact Mitigation*. CRC Press, Boca Raton, United States, pp. 113–133.
- Gunn, A., Miller, F.L., 1986. Traditional behaviour and fidelity to caribou calving grounds by barren-ground caribou. *Rangifer* 6, 151. <https://doi.org/10.7557/2.6.2.640>
- Gunn, A., Poole, K.G., Wierzchowski, J., Nishi, J.S., Adamczewski, J., Russell, D.E., D'Hont, A., 2011b. Have geographical influences and changing abundance led to sub-population structure in the Ahiak caribou herd, Nunavut, Canada? *Rangifer* 33, 35–58.
- Gurarie, E., Hebblewhite, M., Joly, K., Kelly, A.P., Adamczewski, J., Davidson, S.C., Davison, T., Gunn, A., Sutor, M.J., Fagan, W.F., Boelman, N., 2019. Tactical departures and strategic arrivals: Divergent effects of climate and weather on caribou spring migrations. *Ecosphere* 10. <https://doi.org/10.1002/ecs2.2971>
- Hall, D.K., Riggs, G.A., Salomonson, V.V., 1995. Development of methods for mapping global snow cover using moderate resolution imaging spectroradiometer data. *Remote Sens. Environ.* 54, 127–140. [https://doi.org/10.1016/0034-4257\(95\)00137-P](https://doi.org/10.1016/0034-4257(95)00137-P)
- Hall, D.K., Riggs, G.A., Solomonson, V., 2023. MODIS Terra/Aqua Snow Cover and Ice Extent data products. <https://doi.org/10.5067/MODIS/MOD10A1.006>
- Hansen, B.B., Grøtan, V., Herfindal, I., Lee, A.M., 2020. The Moran effect revisited: Spatial population synchrony under global warming. *Ecography* 43, 1591–1602.
<https://doi.org/10.1111/ecog.04962>

- Harding, L.E., 2022. Available names for *Rangifer* (*Mammalia*, *Artiodactyla*, *Cervidae*) species and subspecies. *ZooKeys* 1119, 117–151. <https://doi.org/10.3897/zookeys.1119.80233>
- Haskell, S.P., Ballard, W.B., 2007. Modeling the Western Arctic caribou herd during a positive growth phase: Potential effects of wolves and radiocollars. *J. Wildl. Manag.* 71, 619–627. <https://doi.org/10.2193/2006-349>
- Helfricht, K., Hartl, L., Koch, R., Marty, C., Olefs, M., 2018. Obtaining sub-daily new snow density from automated measurements in high mountain regions. *Hydrol. Earth Syst. Sci.* 22, 2655–2668. <https://doi.org/10.5194/hess-22-2655-2018>
- Henry, G.H.R., Gunn, A., 1991. Recovery of tundra vegetation after overgrazing by caribou in Arctic Canada. *Arctic* 44, 38–42. <https://doi.org/10.14430/arctic1516>
- Hervieux, D., Hebblewhite, M., DeCesare, N.J., Russell, M., Smith, K., Robertson, S., Boutin, S., 2013. Widespread declines in woodland caribou (*Rangifer tarandus caribou*) continue in Alberta. *Can. J. Zool.* 91, 872–882. <https://doi.org/10.1139/cjz-2013-0123>
- Hofman, M.P.G., Hayward, M.W., Heim, M., Marchand, P., Rolandsen, C.M., Mattisson, J., Urbano, F., Heurich, M., Mysterud, A., Melzheimer, J., Morellet, N., Voigt, U., Allen, B.L., Gehr, B., Rouco, C., Ullmann, W., Holand, Ø., Jørgensen, N.H., Steinheim, G., Cagnacci, F., Kroeschel, M., Kaczensky, P., Buuveibaatar, B., Payne, J.C., Palmegiani, I., Jerina, K., Kjellander, P., Johansson, Ö., LaPoint, S., Bayrakcismith, R., Linnell, J.D.C., Zaccaroni, M., Jorge, M.L.S., Oshima, J.E.F., Songhurst, A., Fischer, C., Mc Bride, R.T., Thompson, J.J., Streif, S., Sandfort, R., Bonenfant, C., Drouilly, M., Klapproth, M., Zinner, D., Yarnell, R., Stronza, A., Wilmott, L., Meisingset, E., Thaker, M., Vanak, A.T., Nicoloso, S., Graeber, R., Said, S., Boudreau, M.R., Devlin, A., Hoogesteijn, R., May-Junior, J.A., Nifong, J.C., Odden, J., Quigley, H.B., Tortato, F., Parker, D.M., Caso, A., Perrine, J., Tellaeche, C., Zieba, F., Zwijacz-Kozica, T., Appel, C.L., Axsom, I., Bean, W.T., Cristescu, B., Périquet, S., Teichman, K.J., Karpanty, S., Licoppe, A., Menges, V., Black, K., Scheppers, T.L., Schai-Braun, S.C., Azevedo, F.C., Lemos, F.G., Payne, A., Swanepoel, L.H., Weckworth, B.V., Berger, A., Bertassoni, A., McCulloch, G., Šustr, P., Athreya, V., Bockmuhl, D., Casaer, J., Ekori, A., Melovski, D., Richard-Hansen, C., Van De Vyver, D., Reyna-Hurtado, R., Robardet, E., Selva, N., Sergiel, A., Farhadinia, M.S., Sunde, P., Portas, R., Ambarli, H., Berzins, R., Kappeler, P.M., Mann, G.K., Pyritz, L., Bissett, C., Grant, T., Steinmetz, R., Swedell, L., Welch, R.J., Armenteras, D., Bidder, O.R., González, T.M., Rosenblatt, A., Kachel, S., Balkenhol, N., 2019. Right on track? Performance of satellite telemetry in terrestrial wildlife research. *PLoS ONE* 14, e0216223. <https://doi.org/10.1371/journal.pone.0216223>
- Holgerson, M.A., Raymond, P.A., 2016. Large contribution to inland water CO₂ and CH₄ emissions from very small ponds. *Nat. Geosci.* 9, 222–226. <https://doi.org/10.1038/ngeo2654>
- Høye, T.T., Post, E., Meltofte, H., Schmidt, N.M., Forchhammer, M.C., 2007. Rapid advancement of spring in the High Arctic. *Curr. Biol.* 17, R449–R451. <https://doi.org/10.1016/j.cub.2007.04.047>
- Hummel, M., Ray, J.C., 2008. Caribou and the North: A shared future. Dundurn, Toronto, Canada.

- Jacobsen, P., 2011. "With a connection to the land, our spirit is strong" Tłı̨cẖ traditional knowledge of climate change and impacts for caribou hunting: Implication for traditional knowledge research (MA Thesis). University of Northern British Columbia, Prince George, British Columbia, Canada.
- Jenkins, D.A., Lecomte, N., Schaefer, J.A., Olsen, S.M., Swingedouw, D., Co, S.D., Yannic, G., 2016. Loss of connectivity among island-dwelling Peary caribou following sea ice decline. *Biol. Lett.* 3–7. <https://doi.org/10.1098/rsbl.2016.0235>
- John, C., Miller, D., Post, E., 2020. Regional variation in green-up timing along a caribou migratory corridor: Spatial associations with snowmelt and temperature. *Arct. Antarct. Alp. Res.* 52, 416–423. <https://doi.org/10.1080/15230430.2020.1796009>
- Johnson, C.J., Russell, D.E., 2014. Long-term distribution responses of a migratory caribou herd to human disturbance. *Biol. Conserv.* 177, 52–63. <https://doi.org/10.1016/j.biocon.2014.06.007>
- Johnson, H.E., Lenart, E.A., Gustine, D.D., Adams, L.G., Barboza, P.S., 2022. Survival and reproduction in arctic caribou are associated with summer forage and insect harassment. *Front. Ecol. Evol.* 10, 899585. <https://doi.org/10.3389/fevo.2022.899585>
- Joly, K., Couriot, O., Cameron, M.D., Gurarie, E., 2020. Behavioral, physiological, demographic and ecological impacts of hematophagous and endoparasitic insects on an arctic ungulate. *Toxins* 12, 334. <https://doi.org/10.3390/toxins12050334>
- Joly, K., Duffy, P.A., Rupp, T.S., 2012. Simulating the effects of climate change on fire regimes in Arctic biomes: Implications for caribou and moose habitat. *Ecosphere* 3, 1–18. <https://doi.org/10.1890/ES12-00012.1>
- Joly, K., Gunn, A., Côté, S.D., Panzacchi, M., Adamczewski, J., Sutor, M.J., Gurarie, E., 2021. Caribou and reindeer migrations in the changing Arctic. *Anim. Migr.* 8, 156–167. <https://doi.org/10.1515/ami-2020-0110>
- Joly, K., Gurarie, E., Sorum, M.S., Kaczensky, P., Cameron, M.D., Jakes, A.F., Borg, B.L., Nandintsetseg, D., Hopcraft, J.G.C., Buuveibaatar, B., Jones, P.F., Mueller, T., Walzer, C., Olson, K.A., Payne, J.C., Yadamsuren, A., Hebblewhite, M., 2019. Longest terrestrial migrations and movements around the world. *Sci. Rep.* 9, 15333. <https://doi.org/10/ggccc4>
- Joly, K., Jandt, R.R., Meyers, C.R., Cole, M.J., 2007. Changes in vegetative cover on Western Arctic herd winter range from 1981 to 2005: Potential effects of grazing and climate change. *Rangifer* 27, 199. <https://doi.org/10.7557/2.27.4.345>
- Joo, R., Picardi, S., Boone, M.E., Clay, T.A., Patrick, S.C., Romero-Romero, V.S., Basille, M., 2022. Recent trends in movement ecology of animals and human mobility. *Mov. Ecol.* 10, 26. <https://doi.org/10.1186/s40462-022-00322-9>
- Jung, T.S., Konkolics, S.M., Kukka, P.M., Majchrzak, Y.N., Menzies, A.K., Oakley, M.P., Peers, M.J.L., Studd, E.K., 2019. Short-term effect of helicopter-based capture on movements of a social ungulate. *J. Wildl. Manag.* 83, 830–837. <https://doi.org/10.1002/jwmg.21640>
- Kelsey, K.C., Pedersen, S.H., Leffler, A.J., Sexton, J.O., Feng, M., Welker, J.M., 2021. Winter snow and spring temperature have differential effects on vegetation phenology and productivity across Arctic plant communities. *Glob. Change Biol.* 27, 1572–1586. <https://doi.org/10.1111/gcb.15505>

- Kenny, T.-A., Fillion, M., Simpkin, S., Wesche, S.D., Chan, H.M., 2018. Caribou (*Rangifer tarandus*) and Inuit nutrition security in Canada. *EcoHealth* 15, 590–607. <https://doi.org/10.1007/s10393-018-1348-z>
- Klüttsch, C.F.C., Manseau, M., Trim, V., Polfus, J., Wilson, P.J., 2016. The eastern migratory caribou: The role of genetic introgression in ecotype evolution. *R. Soc. Open Sci.* 3, 150469. <https://doi.org/10.1098/rsos.150469>
- Kock, M.D., Jessup, D.A., Clark, R.K., Franti, C.E., 1987. Effects of capture on biological parameters in free-ranging bighorn sheep (*Ovis canadensis*): Evaluation of drop-net, drive-net, chemical immobilization and the net-gun. *J. Wildl. Dis.* 23, 641–651. <https://doi.org/10.7589/0090-3558-23.4.652>
- Koltz, A.M., Culler, L.E., 2021. Biting insects in a rapidly changing Arctic. *Curr. Opin. Insect Sci.* 47, 75–81. <https://doi.org/10.1016/j.cois.2021.04.009>
- Konkolics, S., Dickie, M., Serrouya, R., Hervieux, D., Boutin, S., 2021. A burning question: What are the implications of forest fires for woodland caribou? *J. Wildl. Manag.* 85, 1685–1698. <https://doi.org/10.1002/jwmg.22111>
- Kreeger, T.J., Arnemo, J.M., Caulkett, N.A., Hampton, J.O., Meyer, L.C.R., 2023. Handbook of wildlife chemical immobilization, 6th edition, 6th ed.
- Kubelka, V., Sandercock, B.K., Székely, T., Freckleton, R.P., 2022. Animal migration to northern latitudes: Environmental changes and increasing threats. *Trends Ecol. Evol.* 37, 30–41. <https://doi.org/10.1016/j.tree.2021.08.010>
- Laforge, M.P., Bonar, M., Vander Wal, E., 2021. Tracking snowmelt to jump the green wave: Phenological drivers of migration in a northern ungulate. *Ecology* 102, e03268. <https://doi.org/10.1002/ecy.3268>
- Laforge, M.P., Webber, Q.M.R., Vander Wal, E., 2023. Plasticity and repeatability in spring migration and parturition dates with implications for annual reproductive success. *J. Anim. Ecol.* 92, 1042–1054. <https://doi.org/10.1111/1365-2656.13911>
- Lam, H.M., Geldsetzer, T., Howell, S.E.L., Yackel, J., 2023. Snow depth on sea ice and on land in the Canadian Arctic from long-term observations. *Atmosphere-Ocean* 61, 217–233. <https://doi.org/10.1080/07055900.2022.2060178>
- Latifovic, R., Pouliot, D., 2007. Analysis of climate change impacts on lake ice phenology in Canada using the historical satellite data record. *Remote Sens. Environ.* 106, 492–507. <https://doi.org/10.1016/j.rse.2006.09.015>
- Le Corre, M., Dussault, C., Côté, S.D., 2016. Weather conditions and variation in timing of spring and fall migrations of migratory caribou. *J. Mammal.* gyw177. <https://doi.org/10.1093/jmammal/gyw177>
- Leblond, M., St-Laurent, M.-H., Côté, S.D., 2016. Caribou, water, and ice – Fine-scale movements of a migratory arctic ungulate in the context of climate change. *Mov. Ecol.* 4, 14. <https://doi.org/10.1186/s40462-016-0079-4>
- Leclerc, M., Leblond, M., Le Corre, M., Dussault, C., Côté, S.D., 2021. Determinants of migration trajectory and movement rate in a long-distance terrestrial mammal. *J. Mammal.* 102, 1342–1352. <https://doi.org/10.1093/jmammal/gyab081>
- Lemmetyinen, J., Cohen, J., Kontu, A., Vehviläinen, J., Hannula, H.-R., Merkouridi, I., Scheiblauer, S., Rott, H., Nagler, T., Ripper, E., Elder, K., Marshall, H.-P., Fromm, R., Adams, M., Derksen, C., King, J., Meta, A., Coccia, A., Rutter, N., Sandells, M., Macelloni, G., Santi, E., Leduc-Leballeur, M., Essery, R., Menard, C., Kern, M., 2022. Airborne SnowSAR data at X and Ku bands over boreal forest, alpine

- and tundra snow cover. *Earth Syst. Sci. Data* 14, 3915–3945.
<https://doi.org/10.5194/essd-14-3915-2022>
- Lenormand, F., Duguay, C.R., Gauthier, R., 2002. Development of a historical ice database for the study of climate change in Canada. *Hydrol. Process.* 16, 3707–3722. <https://doi.org/10.1002/hyp.1235>
- Liu, P., Di, L., Du, Q., Wang, L., 2018. Remote sensing big data: Theory, methods and applications. *Remote Sens.* 10, 711. <https://doi.org/10.3390/rs10050711>
- Low-Décarie, E., Chivers, C., Granados, M., 2014. Rising complexity and falling explanatory power in ecology. *Front. Ecol. Environ.* 12, 412–418.
<https://doi.org/10.1890/130230>
- Luojus, K., Pulliainen, J., Takala, M., Lemmetyinen, J., Mortimer, C., Derksen, C., Mudryk, L., Moisaner, M., Hiltunen, M., Smolander, T., Ikonen, J., Cohen, J., Salminen, M., Norberg, J., Veijola, K., Venäläinen, P., 2021. GlobSnow v3.0 Northern Hemisphere snow water equivalent dataset. *Sci. Data* 8, 163.
<https://doi.org/10.1038/s41597-021-00939-2>
- Macander, M.J., Palm, E.C., Frost, G.V., Herriges, J.D., Nelson, P.R., Roland, C., Russell, K.L.M., Sutor, M.J., Bentzen, T.W., Joly, K., Goetz, S.J., Hebblewhite, M., 2020. Lichen cover mapping for caribou ranges in interior Alaska and Yukon. *Environ. Res. Lett.* 15, 055001. <https://doi.org/10.1088/1748-9326/ab6d38>
- Magnuson, J.J., Robertson, D.M., Benson, B.J., Wynne, R.H., Livingstone, D.M., Arai, T., Assel, R.A., Barry, R.G., Card, V., Kuusisto, E., Granin, N.G., Prowse, T.D., Stewart, K.M., Vuglinski, V.S., 2000. Historical trends in lake and river ice cover in the Northern Hemisphere. *Science* 289, 1743–1746.
<https://doi.org/10.1126/science.289.5485.1743>
- Malenovsky, Z., Rott, H., Cihlar, J., Schaepman, M.E., García-Santos, G., Fernandes, R., Berger, M., 2012. Sentinels for science: Potential of Sentinel-1, -2, and -3 missions for scientific observations of ocean, cryosphere, and land. *Remote Sens. Environ.* 120, 91–101. <https://doi.org/10.1016/j.rse.2011.09.026>
- Mallory, C.D., Williamson, S.N., Campbell, M.W., Boyce, M.S., 2020. Response of barren-ground caribou to advancing spring phenology. *Oecologia* 192, 837–852.
<https://doi.org/10.1007/s00442-020-04604-0>
- Mallory, F.F., Hillis, T.L., 1998. Demographic characteristics of circumpolar caribou populations: Ecotypes, ecological constraints, releases, and population dynamics. *Rangifer* 18, 49. <https://doi.org/10.7557/2.18.5.1541>
- Mathieu, A., Vander Vennen, L.M., Ried, A., Legebokow, C., Schwantje, H.M., 2022. Translocation of southern mountain caribou using a soft-release technique. *Rangifer* 42, 1–16. <https://doi.org/10.7557/2.42.1.5930>
- McCarthy, F.M., Patterson, R.T., Head, M.J., Riddick, N.L., Cumming, B.F., Hamilton, P.B., Pisaric, M.F., Gushulak, A.C., Leavitt, P.R., Lafond, K.M., Llew-Williams, B., Marshall, M., Heyde, A., Pilkington, P.M., Moraal, J., Boyce, J.I., Nasser, N.A., Walsh, C., Garvie, M., Roberts, S., Rose, N.L., Cundy, A.B., Gaca, P., Milton, A., Hajdas, I., Crann, C.A., Boom, A., Finkelstein, S.A., McAndrews, J.H., 2023. The varved succession of Crawford Lake, Milton, Ontario, Canada as a candidate Global boundary Stratotype Section and Point for the Anthropocene series. *Anthr. Rev.* 10, 146–176. <https://doi.org/10.1177/20530196221149281>

- McCleery, R., Guralnick, R., Beatty, M., Belitz, M., Campbell, C.J., Idec, J., Jones, M., Kang, Y., Potash, A., Fletcher, R.J., 2023. Uniting experiments and big data to advance ecology and conservation. *Trends Ecol. Evol.* 38, 970–979. <https://doi.org/10.1016/j.tree.2023.05.010>
- McCrystall, M.R., Stroeve, J., Serreze, M., Forbes, B.C., Screen, J.A., 2021. New climate models reveal faster and larger increases in Arctic precipitation than previously projected. *Nat. Commun.* 12, 6765. <https://doi.org/10.1038/s41467-021-27031-y>
- McGrath, D., Webb, R., Shean, D., Bonnell, R., Marshall, H., Painter, T.H., Molotch, N.P., Elder, K., Hiemstra, C., Brucker, L., 2019. Spatially extensive ground-penetrating radar snow depth observations during NASA's 2017 SnowEx campaign: Comparison with in situ, airborne, and satellite observations. *Water Resour. Res.* 55, 10026–10036. <https://doi.org/10.1029/2019WR024907>
- McIntyre, T., 2015. Animal telemetry: Tagging effects. *Science* 349, 596–597. <https://doi.org/10.1126/science.349.6248.596-b>
- McKinnon, L., Smith, P.A., Nol, E., Martin, J.L., Doyle, F.I., Abraham, K.F., Gilchrist, H.G., Morrison, R.I.G., Bêty, J., 2010. Lower predation risk for migratory birds at high latitudes. *Science* 327, 326–327. <https://doi.org/10.1126/science.1183010>
- Messenger, M.L., Lehner, B., Grill, G., Nedeva, I., Schmitt, O., 2016. Estimating the volume and age of water stored in global lakes using a geo-statistical approach. *Nat. Commun.* 7, 13603. <https://doi.org/10/f9g5qg>
- Messier, F., Huot, J., Le Henaff, D., Luttich, S., 1988. Demography of the George River caribou herd: Evidence of population regulation by forage exploitation and range expansion. *Arctic* 41, 279–287. <https://doi.org/10.14430/arctic1733>
- Miller, F.L., 1995. Inter-island water crossings by Peary caribou, south-central Queen Elizabeth Islands. *Arctic* 48, 8–12. <https://doi.org/10.14430/arctic1219>
- Miller, F.L., Barry, S.J., Calvert, W.A., 2005. Sea-ice crossings by caribou in the south-central Canadian Arctic Archipelago and their ecological importance. *Rangifer* 25, 77. <https://doi.org/10.7557/2.25.4.1773>
- Miller, F.L., Gunn, A., 1986. Observations of barren-ground caribou travelling on thin ice during autumn migration. *Arctic* 39, 85–88.
- Mills, L.S., Soulé, M.A., Doak, D.F., 1993. The keystone-species concept in ecology and conservation. *BioScience* 43, 219–224. <https://doi.org/10.2307/1312122>
- Moran, P., 1953. The statistical analysis of the Canadian lynx cycle. *Aust. J. Zool.* 1, 291. <https://doi.org/10.1071/ZO9530291>
- Morneau, C., Payette, S., 2000. Long-term fluctuations of a caribou population revealed by tree-ring data. *Can. J. Zool.* 78, 1784–1790. <https://doi.org/10.1139/z00-122>
- Morton, D., Anderson, E., Foggin, C., Kock, M., Tiran, E., 1995. Plasma cortisol as an indicator of stress due to capture and translocation in wildlife species. *Vet. Rec.* 136, 60–63. <https://doi.org/10.1136/vr.136.3.60>
- Mullan, D., Swindles, G., Patterson, T., Galloway, J., Macumber, A., Falck, H., Crossley, L., Chen, J., Pisaric, M., 2017. Climate change and the long-term viability of the World's busiest heavy haul ice road. *Theor. Appl. Climatol.* 129, 1089–1108. <https://doi.org/10.1007/s00704-016-1830-x>
- Murfitt, J., Duguay, C.R., 2020. Assessing the performance of methods for monitoring ice phenology of the world's largest High Arctic lake using high-density time

- series analysis of Sentinel-1 data. *Remote Sens.* 12, 382.
<https://doi.org/10.3390/rs12030382>
- Mysterud, A., 2013. Ungulate migration, plant phenology, and large carnivores: The times they are a-changin. *Ecology* 94, 1257–1261. <https://doi.org/10.1890/12-0505.1>
- Nagy, J.A., 2011. Use of space by caribou in Northern Canada (PhD Thesis). University of Alberta, Edmonton, Canada.
- Nagy, J.A., Johnson, D.L., Larter, N.C., Campbell, M.W., Derocher, A.E., Kelly, A., Dumond, M., Allaire, D., Croft, B., 2011. Subpopulation structure of caribou (*Rangifer tarandus* L.) in Arctic and Subarctic Canada. *Ecol. Appl.* 21, 2334–2348. <https://doi.org/10.1890/10-1410.1>
- Nathan, R., Getz, W.M., Revilla, E., Holyoak, M., Kadmon, R., Saltz, D., Smouse, P.E., 2008. A movement ecology paradigm for unifying organismal movement research. *Proc. Natl. Acad. Sci. U. S. A.* 105, 19052–19059.
<https://doi.org/10.1073/pnas.0800375105>
- Nathan, R., Monk, C.T., Arlinghaus, R., Adam, T., Alós, J., Assaf, M., Baktoft, H., Beardsworth, C.E., Bertram, M.G., Bijleveld, A.I., Brodin, T., Brooks, J.L., Campos-Candela, A., Cooke, S.J., Gjelland, K.Ø., Gupte, P.R., Harel, R., Hellström, G., Jeltsch, F., Killen, S.S., Klefoth, T., Langrock, R., Lennox, R.J., Lourie, E., Madden, J.R., Orchan, Y., Pauwels, I.S., Říha, M., Roeleke, M., Schlägel, U.E., Shohami, D., Signer, J., Toledo, S., Vilck, O., Westrelin, S., Whiteside, M.A., Jarić, I., 2022. Big-data approaches lead to an increased understanding of the ecology of animal movement. *Science* 375, eabg1780.
<https://doi.org/10.1126/science.abg1780>
- NWT Species at Risk Committee, 2017. Species status report for Porcupine caribou and barren-ground caribou (Tuktoyaktuk Peninsula, Cape Bathurst, Bluenose-West, Bluenose-East, Bathurst, Beverly, Ahiak, and Qamanirjuaq herds) (*Rangifer tarandus groenlandicus*) in the Northwest Territories. Government of the Northwest Territories, Yellowknife, Canada.
- Olofsson, J., Kitti, H., Rautiainen, P., Stark, S., Oksanen, L., 2001. Effects of summer grazing by reindeer on composition of vegetation, productivity and nitrogen cycling. *Ecography* 24, 13–24. <https://doi.org/10.1034/j.1600-0587.2001.240103.x>
- Otsu, N., 1979. A threshold selection method from gray-level histograms. *IEEE Trans. Syst. Man Cybern.* 9, 62–66. <https://doi.org/10.1109/TSMC.1979.4310076>
- Pajunen, A., Virtanen, R., Roininen, H., 2012. Browsing-mediated shrub canopy changes drive composition and species richness in forest-tundra ecosystems. *Oikos* 121, 1544–1552. <https://doi.org/10.1111/j.1600-0706.2011.20115.x>
- Panzacchi, M., Van Moorter, B., Strand, O., 2013. A road in the middle of one of the last wild reindeer migration routes in Norway: Crossing behaviour and threats to conservation. *Rangifer* 15–26. <https://doi.org/10.7557/2.33.2.2521>
- Paoli, A., Weladji, R.B., Holand, Ø., Kumpula, J., 2018. Winter and spring climatic conditions influence timing and synchrony of calving in reindeer. *PLoS ONE* 13, e0195603. <https://doi.org/10.1371/journal.pone.0195603>

- Park, H., Walsh, J.E., Kim, Y., Nakai, T., Ohata, T., 2013. The role of declining Arctic sea ice in recent decreasing terrestrial Arctic snow depths. *Polar Sci.* 7, 174–187. <https://doi.org/10.1016/j.polar.2012.10.002>
- Paterson, J., 2014. Capture myopathy, in: West, G., Heard, D., Caulkett, N. (Eds.), *Zoo Animal and Wildlife Immobilization and Anesthesia*, 2nd Edition. John Wiley & Sons, Inc., Ames, United States, pp. 171–179.
- Pi, X., Luo, Q., Feng, L., Xu, Y., Tang, J., Liang, X., Ma, E., Cheng, R., Fensholt, R., Brandt, M., Cai, X., Gibson, L., Liu, J., Zheng, C., Li, W., Bryan, B.A., 2022. Mapping global lake dynamics reveals the emerging roles of small lakes. *Nat. Commun.* 13, 5777. <https://doi.org/10.1038/s41467-022-33239-3>
- Poole, K.G., Gunn, A., Patterson, B.R., Dumond, M., 2010. Sea ice and migration of the Dolphin and Union caribou herd in the Canadian Arctic: An uncertain future. *Arctic* 63, 414–428. <https://doi.org/10.14430/arctic3331>
- Porcupine Caribou Technical Committee, 2022. Porcupine caribou annual summary report 2021-2022. Porcupine Caribou Management Board.
- Post, E., Forchhammer, M.C., 2008. Climate change reduces reproductive success of an Arctic herbivore through trophic mismatch. *Philos. Trans. R. Soc. B Biol. Sci.* 363, 2367–2373. <https://doi.org/10.1098/rstb.2007.2207>
- Prince, P., 2005. Fish weirs, salmon productivity, and village settlement in an Upper Skeena River tributary, British Columbia. *Can. J. Archaeol.* 68–87.
- Prowse, T., Alfredsen, K., Beltaos, S., Bonsal, B., Duguay, C., Korhola, A., McNamara, J., Vincent, W.F., Vuglinsky, V., Weyhenmeyer, G.A., 2011. Arctic freshwater ice and its climatic role. *Ambio* 40, 46–52. <https://doi.org/10.1007/s13280-011-0214-9>
- Prowse, T.D., Furgal, C., Chouinard, R., Melling, H., Milburn, D., Smith, S.L., 2009. Implications of climate change for economic development in Northern Canada: Energy, resource, and transportation sectors. *Ambio* 38, 272–281. <https://doi.org/10.1579/0044-7447-38.5.272>
- Rachlow, J.L., Peter, R.M., Shipley, L.A., Johnson, T.R., 2014. Sub-lethal effects of capture and collaring on wildlife: Experimental and field evidence. *Wildl. Soc. Bull.* 38, 458–465. <https://doi.org/10.1002/wsb.444>
- Rantanen, M., Karpechko, A.Yu., Lipponen, A., Nordling, K., Hyvärinen, O., Ruosteenoja, K., Vihma, T., Laaksonen, A., 2022. The Arctic has warmed nearly four times faster than the globe since 1979. *Commun. Earth Environ.* 3, 168. <https://doi.org/10.1038/s43247-022-00498-3>
- Rasiulis, A.L., Festa-Bianchet, M., Couturier, S., Côté, S.D., 2014. The effect of radio-collar weight on survival of migratory caribou. *J. Wildl. Manag.* 78, 953–956. <https://doi.org/10.1002/jwmg.722>
- Reist, J.D., Wrona, F.J., Prowse, T.D., Power, M., Dempson, J.B., King, J.R., Beamish, R.J., 2006. An overview of effects of climate change on selected Arctic freshwater and anadromous fishes. *Ambio* 35, 381–387. [https://doi.org/10.1579/0044-7447\(2006\)35](https://doi.org/10.1579/0044-7447(2006)35)
- Rickbeil, G.J.M., Hermosilla, T., Coops, N.C., White, J.C., Wulder, M.A., 2017. Estimating changes in lichen mat volume through time and related effects on barren-ground caribou (*Rangifer tarandus groenlandicus*) movement. *PLoS ONE* 12, e0172669. <https://doi.org/10.1371/journal.pone.0172669>

- Rickbeil, G.J.M., Hermosilla, T., Coops, N.C., White, J.C., Wulder, M.A., Lantz, T.C., 2018. Changing northern vegetation conditions are influencing barren ground caribou (*Rangifer tarandus groenlandicus*) post-calving movement rates. *J. Biogeogr.* 1–11. <https://doi.org/10.1111/jbi.13161>
- Rienecker, M.M., Suarez, M.J., Gelaro, R., Todling, R., Bacmeister, J., Liu, E., Bosilovich, M.G., Schubert, S.D., Takacs, L., Kim, G.-K., Bloom, S., Chen, J., Collins, D., Conaty, A., Da Silva, A., Gu, W., Joiner, J., Koster, R.D., Lucchesi, R., Molod, A., Owens, T., Pawson, S., Pegion, P., Redder, C.R., Reichle, R., Robertson, F.R., Ruddick, A.G., Sienkiewicz, M., Woollen, J., 2011. MERRA: NASA's modern-era retrospective analysis for research and applications. *J. Clim.* 24, 3624–3648. <https://doi.org/10.1175/JCLI-D-11-00015.1>
- Rivest, L.-P., Couturier, S., Crepeau, H., 1998. Statistical methods for estimating caribou abundance using postcalving aggregations detected by radio telemetry. *Biometrics* 54, 865. <https://doi.org/10.2307/2533841>
- Rodgers, A.R., 2001. Tracking animals with GPS: The first 10 years, in: *Proceedings of the Conference on Tracking Animals with GPS*. The Macaulay Land Use Research Institute, Aberdeen, United Kingdom, pp. 1–10.
- Rott, H., Cline, D.W., Duguay, C., Essery, R., Etchevers, P., Hajnsek, I., Kern, M., Macelloni, G., Malnes, E., Pulliainen, J., Yueh, S.H., 2012. CoReH2O, a dual frequency radar mission for snow and ice observations, in: *2012 IEEE International Geoscience and Remote Sensing Symposium*. Presented at the IGARSS 2012 - 2012 IEEE International Geoscience and Remote Sensing Symposium, IEEE, Munich, Germany, pp. 5550–5553. <https://doi.org/10.1109/IGARSS.2012.6352348>
- Rouse Jr, J., Haas, R., Schell, J., Deering, D., 1974. Monitoring vegetation systems in the Great Plains with ERTS, in: *Third Earth Resources Technology Satellite-1 Symposium: The Proceedings of a Symposium Held by Goddard Space Flight Center at Washington, DC on December 10-14, 1973: Prepared at Goddard Space Flight Center*. Scientific and Technical Information Office, National Aeronautics and Space Administration, pp. 309–317.
- Russell, D.E., Whit, P.H., Cai, J., Gunn, A., White, R.G., Poole, K., 2013. CARMA's MERRA-based caribou range climate database. *Rangifer* 33, 145–152.
- Schmidt, N.M., Kankaanpää, T., Tiusanen, M., Reneerkens, J., Versluijs, T.S.L., Hansen, L.H., Hansen, J., Gerlich, H.S., Høye, T.T., Cirtwill, A.R., Zhemchuzhnikov, M.K., Peña-Aguilera, P., Roslin, T., 2023. Little directional change in the timing of Arctic spring phenology over the past 25 years. *Curr. Biol.* 33, 3244-3249.e3. <https://doi.org/10.1016/j.cub.2023.06.038>
- Schuster, R.C., Wein, E.E., Dickson, C., Chan, H.M., 2011. Importance of traditional foods for the food security of two First Nations communities in the Yukon, Canada. *Int. J. Circumpolar Health* 70, 286–300. <https://doi.org/10.3402/ijch.v70i3.17833>
- Serrouya, R., Seip, D.R., Hervieux, D., McLellan, B.N., McNay, R.S., Steenweg, R., Heard, D.C., Hebblewhite, M., Gillingham, M., Boutin, S., 2019. Saving endangered species using adaptive management. *Proc. Natl. Acad. Sci.* 116, 6181–6186. <https://doi.org/10.1073/pnas.1816923116>

- Sharma, S., Blagrove, K., O'Reilly, C.M., Samantha, O., Ryan, B., Magee, MR., Straile, D., Weyhenmeyer, GA., Winslow, L., Woolway, R., Magnuson, JJ., 2019. Widespread loss of lake ice around the Northern Hemisphere in a warming world. *Nat. Clim. Change*. <https://doi.org/10.1038/s41558-018-0393-5>
- Sharma, S., Couturier, S., Côté, S.D., 2009. Impacts of climate change on the seasonal distribution of migratory caribou. *Glob. Change Biol.* 15, 2549–2562. <https://doi.org/10.1111/j.1365-2486.2009.01945.x>
- Sharma, S., Filazzola, A., Nguyen, T., Imrit, M.A., Blagrove, K., Bouffard, D., Daly, J., Feldman, H., Feldsine, N., Hendricks-Franssen, H.-J., Granin, N., Hecock, R., L'Abée-Lund, J.H., Hopkins, E., Howk, N., Iacono, M., Knoll, L.B., Korhonen, J., Malmquist, H.J., Marszelewski, W., Matsuzaki, S.-I.S., Miyabara, Y., Miyasaka, K., Mills, A., Olson, L., Peters, T.W., Richardson, D.C., Robertson, D.M., Rudstam, L., Wain, D., Waterfield, H., Weyhenmeyer, G.A., Wiltse, B., Yao, H., Zhdanov, A., Magnuson, J.J., 2022. Long-term ice phenology records spanning up to 578 years for 78 lakes around the Northern Hemisphere. *Sci. Data* 9, 318. <https://doi.org/10.1038/s41597-022-01391-6>
- Skoog, R.O., 1968. Ecology of the caribou (*Rangifer tarandus granti*) in Alaska (PhD Thesis). University of California, Berkely, California, United States.
- Spraker, T.R., 1993. Stress and capture myopathy in artiodactylids, in: Fowler, M.E. (Ed.), *Zoo and Wild Animal Medicine: Current Therapy*. WB Saunders Company, pp. 481–488.
- Stabach, J.A., Cunningham, S.A., Connette, G., Mota, J.L., Reed, D., Byron, M., Songer, M., Wachter, T., Mertes, K., Brown, J.L., Comizzoli, P., Newby, J., Monfort, S., Leimgruber, P., 2020. Short-term effects of GPS collars on the activity, behavior, and adrenal response of scimitar-horned oryx (*Oryx dammah*). *PLoS ONE* 15, e0221843. <https://doi.org/10.1371/journal.pone.0221843>
- St-Laurent, M.-H., Dussault, C., 2012. The reintroduction of boreal caribou as a conservation strategy: A long-term assessment at the southern range limit. *Rangifer* 32, 127. <https://doi.org/10.7557/2.32.2.2261>
- Sudmanns, M., Tiede, D., Augustin, H., Lang, S., 2020. Assessing global Sentinel-2 coverage dynamics and data availability for operational Earth observation (EO) applications using the EO-Compass. *Int. J. Digit. Earth* 13, 768–784. <https://doi.org/10.1080/17538947.2019.1572799>
- Taillon, J., Barboza, P.S., Côté, S.D., 2013. Nitrogen allocation to offspring and milk production in a capital breeder. *Ecology* 94, 1815–1827. <https://doi.org/10.1890/12-1424.1>
- Taillon, J., Brodeur, V., Festa-Bianchet, M., Côté, S.D., 2012. Is mother condition related to offspring condition in migratory caribou (*Rangifer tarandus*) at calving and weaning? *Can. J. Zool.* 90, 393–402. <https://doi.org/10.1139/z2012-001>
- Tape, K., Sturm, M., Racine, C., 2006. The evidence for shrub expansion in Northern Alaska and the Pan-Arctic. *Glob. Change Biol.* 12, 686–702. <https://doi.org/10.1111/j.1365-2486.2006.01128.x>
- Thompson, D.P., Barboza, P.S., 2014. Nutritional implications of increased shrub cover for caribou (*Rangifer tarandus*) in the Arctic. *Can. J. Zool.* 92, 339–351. <https://doi.org/10.1139/cjz-2013-0265>

- Torres, R., Snoeij, P., Geudtner, D., Bibby, D., Davidson, M., Attema, E., Potin, P., Rommen, B., Floury, N., Brown, M., Traver, I.N., Deghaye, P., Duesmann, B., Rosich, B., Miranda, N., Bruno, C., L'Abbate, M., Croci, R., Pietropaolo, A., Huchler, M., Rostan, F., 2012. GMES Sentinel-1 mission. *Remote Sens. Environ.* 120, 9–24. <https://doi.org/10.1016/j.rse.2011.05.028>
- Tremblay, B., Lévesque, E., Boudreau, S., 2012. Recent expansion of erect shrubs in the Low Arctic: Evidence from Eastern Nunavik. *Environ. Res. Lett.* 7, 035501. <https://doi.org/10.1088/1748-9326/7/3/035501>
- Trondrud, L.M., Pigeon, G., Albon, S., Arnold, W., Evans, A.L., Irvine, R.J., Król, E., Ropstad, E., Stien, A., Veiberg, V., Speakman, J.R., Loe, L.E., 2021. Determinants of heart rate in Svalbard reindeer reveal mechanisms of seasonal energy management. *Philos. Trans. R. Soc. B Biol. Sci.* 376, 20200215. <https://doi.org/10.1098/rstb.2020.0215>
- Trondrud, L.M., Ugland, C., Ropstad, E., Loe, L.E., Albon, S., Stien, A., Evans, A.L., Thorsby, P.M., Veiberg, V., Irvine, R.J., Pigeon, G., 2022. Stress responses to repeated captures in a wild ungulate. *Sci. Rep.* 12, 16289. <https://doi.org/10.1038/s41598-022-20270-z>
- Tsang, L., Durand, M., Derksen, C., Barros, A.P., Kang, D.-H., Lievens, H., Marshall, H.-P., Zhu, J., Johnson, J., King, J., Lemmetyinen, J., Sandells, M., Rutter, N., Siqueira, P., Nolin, A., Osmanoglu, B., Vuyovich, C., Kim, E., Taylor, D., Merkouriadi, I., Brucker, L., Navari, M., Dumont, M., Kelly, R., Kim, R.S., Liao, T.-H., Borah, F., Xu, X., 2022. Review article: Global monitoring of snow water equivalent using high-frequency radar remote sensing. *The Cryosphere* 16, 3531–3573. <https://doi.org/10.5194/tc-16-3531-2022>
- Uboni, A., Horstkotte, T., Kaarlejärvi, E., Sévêque, A., Stammler, F., Olofsson, J., Forbes, B.C., Moen, J., 2016. Long-term trends and role of climate in the population dynamics of Eurasian reindeer. *PLoS ONE* 11, e0158359. <https://doi.org/10.1371/journal.pone.0158359>
- Ugland, C., 2021. Effects of repeated captures on Svalbard reindeer (*Rangifer tarandus platyrhynchus*): Implications for animal welfare and scientific bias (MSc Thesis). Norwegian University of Life Sciences, Ås, Norway.
- Valkenburg, P., Boertje, R.D., Davis, J.L., 1983. Effects of darting and netting on caribou in Alaska. *J. Wildl. Manag.* 47, 1233–1237.
- Valkenburg, P., Tobey, R.W., Kirk, D., 1999. Velocity of tranquilizer darts and capture mortality of caribou calves. *Wildl. Soc. Bull.* 27, 894–896.
- Van Der Sluijs, J., MacKay, G., Andrew, L., Smethurst, N., Andrews, T.D., 2020. Archaeological documentation of wood caribou fences using unmanned aerial vehicle and very high-resolution satellite imagery in the Mackenzie Mountains, Northwest Territories. *J. Unmanned Veh. Syst.* 8, 186–206. <https://doi.org/10.1139/juvs-2020-0007>
- van der Wal, R., Stien, A., 2014. High-Arctic plants like it hot: A long-term investigation of between-year variability in plant biomass. *Ecology* 95, 3414–3427. <https://doi.org/10.1890/14-0533.1>
- Verpoorter, C., Kutser, T., Seekell, D.A., Tranvik, L.J., 2014. A global inventory of lakes based on high-resolution satellite imagery. *Geophys. Res. Lett.* 41, 6396–6402. <https://doi.org/10.1002/2014GL060641>

- Vors, L.S., Boyce, M.S., 2009. Global declines of caribou and reindeer. *Glob. Change Biol.* 15, 2626–2633. <https://doi.org/10.1111/j.1365-2486.2009.01974.x>
- Vuillaume, B., Richard, J.H., Côté, S.D., 2021. Using camera collars to study survival of migratory caribou calves. *Wildl. Soc. Bull.* 45, 325–332. <https://doi.org/10.1002/wsb.1193>
- Vuillaume, B., Richard, J.H., Hamel, S., Taillon, J., Festa-Bianchet, M., Côté, S.D., 2023. Birth date determines early calf survival in migratory caribou. *Oecologia* 202, 819–830. <https://doi.org/10.1007/s00442-023-05441-7>
- Webber, Q.M.R., Ferraro, K.M., Hendrix, J.G., Vander Wal, E., 2022. What do caribou eat? A review of the literature on caribou diet. *Can. J. Zool.* 100, 197–207. <https://doi.org/10.1139/cjz-2021-0162>
- Williams, C.T., Klaassen, M., Barnes, B.M., Buck, C.L., Arnold, W., Giroud, S., Vetter, S.G., Ruf, T., 2017. Seasonal reproductive tactics: Annual timing and the capital-to-income breeder continuum. *Philos. Trans. R. Soc. B Biol. Sci.* 372, 20160250. <https://doi.org/10.1098/rstb.2016.0250>
- Wilmers, C.C., Nickel, B., Bryce, C.M., Smith, J.A., Wheat, R.E., Yovovich, V., 2015. The golden age of bio-logging: How animal-borne sensors are advancing the frontiers of ecology. *Ecology* 96, 1741–1753. <https://doi.org/10.1890/14-1401.1>
- Wilson, R.R., Parrett, L.S., Joly, K., Dau, J.R., 2016. Effects of roads on individual caribou movements during migration. *Biol. Conserv.* 195, 2–8. <https://doi.org/10.1016/j.biocon.2015.12.035>
- Witter, L.A., Johnson, C.J., Croft, B., Gunn, A., Poirier, L.M., 2012. Gauging climate change effects at local scales: Weather-based indices to monitor insect harassment in caribou. *Ecol. Appl.* 22, 1838–1851. <https://doi.org/10.1890/11-0569.1>
- Wood, H.B., 1945. The history of bird banding. *The Auk* 62, 256–265.
- Wulder, M.A., Loveland, T.R., Roy, D.P., Crawford, C.J., Masek, J.G., Woodcock, C.E., Allen, R.G., Anderson, M.C., Belward, A.S., Cohen, W.B., Dwyer, J., Erb, A., Gao, F., Griffiths, P., Helder, D., Hermosilla, T., Hipple, J.D., Hostert, P., Hughes, M.J., Huntington, J., Johnson, D.M., Kennedy, R., Kilic, A., Li, Z., Lyburner, L., McCorkel, J., Pahlevan, N., Scambos, T.A., Schaaf, C., Schott, J.R., Sheng, Y., Storey, J., Vermote, E., Vogelmann, J., White, J.C., Wynne, R.H., Zhu, Z., 2019. Current status of Landsat program, science, and applications. *Remote Sens. Environ.* 225, 127–147. <https://doi.org/10.1016/j.rse.2019.02.015>
- Yu, Q., Epstein, H., Engstrom, R., Walker, D., 2017. Circumpolar Arctic tundra biomass and productivity dynamics in response to projected climate change and herbivory. *Glob. Change Biol.* 23, 3895–3907. <https://doi.org/10.1111/gcb.13632>
- Zalatan, R., Gunn, A., Henry, G.H.R., 2006. Long-term abundance patterns of barren-ground caribou using trampling scars on roots of *Picea mariana* in the Northwest Territories, Canada. *Arct. Antarct. Alp. Res.* 38, 624–630.
- Zoe, J.B., 2012. Ekwò , and Tłıchọ Nàowo / Caribou and Tłıchọ language, culture and way of life: An evolving relationship and shared history. *Rangifer Spec. Issue* 69–74.